Density functional theory for transition metals and transition metal chemistry

Christopher J. Cramer* and Donald G. Truhlar*

Received 8th April 2009, Accepted 20th August 2009
First published as an Advance Article on the web 21st October 2009
DOI: 10.1039/b907148b

We introduce density functional theory and review recent progress in its application to transition metal chemistry. Topics covered include local, meta, hybrid, hybrid meta, and range-separated functionals, band theory, software, validation tests, and applications to spin states, magnetic exchange coupling, spectra, structure, reactivity, and catalysis, including molecules, clusters, nanoparticles, surfaces, and solids.

1. Introduction

Density functional theory (DFT) describes the electronic states of atoms, molecules, and materials in terms of the three-dimensional electronic density of the system, which is a great simplification over wave function theory (WFT), which involves a $3N$-dimensional antisymmetric wave function for a system with N electrons.[1] Although DFT is sometimes considered the "new kid on the block", it is now ~45 years old in its modern formulation[2] (more than half as old as quantum mechanics itself), and it has roots[3,4] that are almost as ancient as the Schrödinger equation. In practical work, DFT is almost always applied in the form introduced by Kohn and Sham,[5] including its spin-polarized extension.[6,7] The basic quantity in DFT is the many-electron spin density, ρ. The spin-polarized Kohn–Sham formalism involves a determinant formed from a set of N fictitious single-particle spin-orbitals corresponding to a non-interacting system of electrons with the same spin densities, ρ_α and ρ_β, as the real system, where ρ is the sum of ρ_α and ρ_β, the spin density ρ_α is the 3-dimensional electron density of all spin-up electrons, and ρ_β is the same for spin-down electrons. In the original Kohn–Sham formalism (applicable to closed-shell molecules and nonmagnetic solids), ρ_α equals ρ_β. (The original Kohn–Sham formalism may also be labeled spin-restricted Kohn–Sham or restricted Kohn–Sham, and the spin-polarized version may be called spin-unrestricted or unrestricted.) We note that "spin density" is a generic term for the density associated with the subset of electrons characterized by the same definite value of S_z, *i.e.*, either α or β (thus one might say "spin-up density and spin-down density" rather than "spin densities"). In a many-electron system comprised of *both* spin-up and spin-down electrons, the term spin-density is also sometimes used to refer to the position-dependent *difference* between the up and down spin densities, or to the vector analog of this quantity. To avoid confusion, in this article we will refer to the difference density as the spin polarization density.

Density functional theory (DFT) has now become the preferred method for electronic structure theory for complex chemical systems, in part because its cost scales more favorably with system size than does the cost of correlated WFT, and yet it competes well in accuracy except for very small systems. This is true even in organic chemistry, but the advantages of DFT are still greater for metals, especially transition metals. The reason for this added advantage is static electron correlation.

It is now well appreciated that quantitatively accurate electronic structure calculations must include electron correlation. It is convenient to recognize two types of electron correlation, the first called dynamical electron correlation and the second called static correlation, near-degeneracy correlation, or non-dynamical correlation. Dynamical correlation is a short-range effect by which electrons avoid one another to reduce electron repulsion. It is a very general effect for all finite systems containing two or more electrons. Accounting for dynamical correlation by a configuration interaction wave function is very slowly convergent and requires a very large number of configurations. Other correlation effects, which are very system specific and can be either medium ranged or long ranged, can be accounted for to a large extent by mixing a small number (sometimes two, sometimes more) of configurations that are "nearly" degenerate.[8,9] Such correlation effects are called static or near-degeneracy correlation and systems exhibiting significant static correlation effects are often called multi-reference systems;[10] likewise, WFT methods based on multi-configurational zero-order states are often called multi-reference methods. Due to partially filled d subshells, and nearly degenerate $(n + 1)s$ and nd subshells, systems containing transition metals often have a plethora of low-lying nearly degenerate states, and near-degeneracy correlation effects on the ground-state structure, electron distribution, and energy of transition metal systems can be very large. Even though static correlation can often be accounted for to a zero-order approximation by a small number of configurations, it is often very difficult to include correlation effects in a well balanced way in WFT calculations on multi-reference systems.[11,12] DFT, however, remains simple for such systems and is often surprisingly accurate. This empirical fact adds to the advantage of computational efficiency in making DFT a preferred method for transition metal chemistry.

The subject of transition-metal DFT is too large for any single review to be complete. We selected recent papers that

Department of Chemistry and Supercomputing Institute, University of Minnesota, Minneapolis, MN 55455-0431, USA. E-mail: cramer@umn.edu, truhlar@umn.edu

best illustrate the promise of DFT in a number of very active areas of transition-metal chemistry, and we also include some older references that help to put them in perspective. We largely exclude biological applications, which deserve and receive[13–17] their own reviews.

Section 2 reviews the theory, section 3 contains some comments on methodology, and section 4 reviews validation studies. Section 5 reviews recent applications and section 6 contains concluding remarks.

2. Overview of DFT and functionals

2.1 Fundamental background

Kohn–Sham spin-orbitals, $\psi_{j\sigma}$ where σ is α or β and j denotes the other quantum numbers, are obtained by a self-consistent field (SCF) calculation and are formally functions of the exact density of the system. Then

$$\rho_\sigma = \sum_j^{\text{occ}} |\psi_{j\sigma}|^2 \qquad (1)$$

where σ is the spin component (α or β), the spin-orbitals are normalized, and the sum is over occupied orbitals of a given spin component. The electronic energy of the system is approximated as a sum of four terms, T_n, ε_{ne}, ε_{ee}, and ε_{xc}. T_n is the kinetic energy of a system of noninteracting electrons with the same spin densities as the real system; ε_{ne} is the interaction of the electron distribution with the nuclear framework; ε_{ee} is the classical Coulomb energy of the spin densities interacting with each other and with themselves; and ε_{xc}, called the exchange–correlation energy, is everything else (everything except T_n, ε_{ne}, and ε_{ee}). Therefore ε_{xc} includes the interaction correction to T_n, the correction to V_{ee} for the fact that real electrons do not interact with themselves, the exchange energy (due to the indistinguishability of electrons exchanging their space and spin variables), and the correlation energy (due to the fact that the many-electron spin densities are not uncorrelated products of spin-orbital densities). ε_{xc} is written as a functional, called the spin-density functional, of the spin densities. Since the Kohn–Sham spin-orbitals are functions of the spin-densities, ε_{xc} can depend explicitly on the spin densities and also implicitly on them by depending on the spin-orbitals. Direct dependence on the spin-densities can also include a dependence on their derivatives (*e.g.*, the magnitudes of their gradients, their Laplacians, *etc.*). The Hohenberg–Kohn theorem[2] shows that the density functional exists; but a closed-form expression for the exact spin-density functional does not exist, and there are no systematic routes to improving an approximate functional. Nevertheless useful approximations have been obtained, and—by a series of fits and starts—they keep getting better.

The effective potential corresponding to ε_{xc} is generated from a functional of the spin densities. The spin-polarized Kohn–Sham formalism and the spin-density functional are usually just called Kohn–Sham theory and the density functional, and approximations to the latter are also called density functionals. The density functional is usually written as the sum of an "exchange" part and a "correlation" part. One should be careful though because the meaning of these terms is different in DFT and in WFT. In particular, DFT correlation includes only dynamic correlation, and DFT exchange includes not only exchange but also some static correlation, although the latter is present in an unspecified and uncontrolled way.[18,19] In subsection 2.2 we introduce some exchange and correlation density functionals, and in subsections 2.4 and 2.5 we describe a greater number of them.

Transition metal chemistry often involves open-shell systems and excited states. Kohn–Sham theory is not general enough to treat all open-shell systems or excited states.[20–22] Although generalized Kohn–Sham theories have been advanced to overcome this limitation, they are not in widespread use. Thus one encounters difficulties not just due to inaccurate density functionals but due to Kohn–Sham theory itself. There is a rich theoretical literature on these questions, but it contains more than one point of view, and much practical work in DFT involves using approximate functionals in a rough-and-ready way (see, *e.g.*, section 5.1). Despite such issues, Kohn–Sham theory, even with approximate functionals, is often the most accurate available approach for practical work on a given system, especially for complex systems.

One type of generalized Kohn–Sham theory that *is* in widespread use is often called hybrid DFT, and it involves combining Hartree–Fock exchange, which is orbital-dependent, with explicit functions of local spin densities and their gradients. (Note that one can also treat Hartree–Fock exchange within the ungeneralized Kohn–Sham framework by using the "optimized effective potential" (OEP) method,[23,24] but we shall not consider this formalism in detail within the present review.) Further generalizing hybrid functionals to include dependences on the local Laplacians of the spin densities or on the local spin kinetic energies computed from the spin-orbitals yields what are called hybrid meta functionals, and these are the most powerful functionals now available. Although one should distinguish between Kohn–Sham and generalized Kohn–Sham methods, and making fundamental progress at extending DFT to arbitrarily complex systems certainly will require careful attention to the fundamentals of the theory,[25] especially for magnetic properties,[26] most practical algorithms in popular use ignore such issues and address the theory from a computational perspective with approximate methods and procedures being accepted or abandoned based on their success or failure for practical predictions, *i.e.*, empirically. Since the present review is application oriented, we will concentrate on such practical aspects and put these fundamental issues aside for now. We note that extended coverage of applications, as opposed to the theory, *is* included in this review and can be found in section 5.

One should be careful not to overinterpret the Kohn–Sham orbitals. They correspond to a fictitious noninteracting system with the same electron density as the correct many-body function. They are introduced primarily to get an approximation for the kinetic energy, which equals

$$T = \tfrac{1}{2}\tau_\alpha + \tfrac{1}{2}\tau_\beta \qquad (2)$$

where

$$\tau_\sigma = \frac{\hbar^2}{m_e}\sum_j^{\text{occ}} |\nabla\psi_{j\sigma}|^2 \qquad (3)$$

where $\hbar$ is Planck's constant divided by 2π, and m_e is the mass of an electron. Since the density computed from the Kohn–Sham orbitals is an approximation to the exact density (it is inexact only because we do not know the true density functional), one-electron properties like dipole moments are meaningful. But most properties that depend on individual orbitals should be interpreted with care. One important exception is the orbital energy of the HOMO. This is correctly interpreted[27] as the negative of the lowest ionization potential (for solids that would be the work function). Nevertheless many studies, including a large number of those cited in this review, do employ DFT molecular orbitals to interpret the electronic origins of chemical bonding and reactivity.

An issue of great concern in many cases is the proper treatment of noncovalent interactions. For two ground-state closed-shell spherical atoms (for example, Zn and Ne), the interaction potential at long distances decreases as R^{-6}, where R is the distance between the atoms. In the region where the electron densities of the interacting monomers do not overlap, the long-range forces can be expressed in an asymptotic series in powers of $1/R$ by using WFT, a multipole expansion, and perturbation theory, and the forces in this region of R are called dispersion forces. The asymptotic series diverges at smaller R,[28] and this is sometimes modeled by truncating the asymptotic series and adding damping factors to the retained terms.[29,30] Semiempirical analytic functions for potential energies are usually called molecular mechanics (MM), and MM terms of this form are sometimes added to DFT to improve the interaction potentials at large R, but this is not a fully satisfactory method for several reasons. First of all, the semiempirical damping functions are somewhat arbitrary and must be readjusted when the underlying DFT method is improved. Secondly, the usual functional forms are not uniformly valid, failing, for example, for metallic nanostructures.[31] A completely satisfactory solution to including long-range noncovalent interactions in DFT will probably ultimately be based on the random phase approximation for correlation energy,[32,33] but in chemistry we are usually more interested in noncovalent interactions at medium range, for example at the distances typical of van der Waals molecules or of 1,3 interactions (geminal interactions). At such distances, overlap of the change distributions of the interacting moieties cannot be neglected (for example, at the van der Waals minimum the gradient of the sum of the repulsive interactions is equal in magnitude to the gradient of the sum of the attractive interactions), and some recent density functionals, especially those involving kinetic energy density that were developed with special attention to medium-range exchange and correlation energy (see section 2.2), do already seem to provide very useful estimates of the medium-range correlation energy in such interactions.[34–40] The best way to include medium-range correlation energy in DFT is not understood in satisfactory detail, just as it is not understood in satisfactory detail how correlation functionals include other kinds of dynamical correlation energy.

There are so many reviews of DFT that even a review of the reviews would be very long, but it is still useful to point the reader to some previous reviews. For fundamental background we mention only a few particularly lucid expositions.[1,41–49] We also mention two recent papers by Perdew and coworkers that give useful perspective on various aspects of DFT.[50,51]

2.2 Introduction to functionals

(We consider only collinear functionals in this section, that is, functionals for collinear DFT—see section 3.2 for a definition of collinear DFT.)

The oldest approximation to a density functional is the Dirac–Slater approximation[52,53] to exchange. This must be renormalized for use with Kohn–Sham theory.[5] This is now usually called the local spin density approximation (LSDA) since it depends only on spin densities (not their derivatives or orbitals). It can be derived from the exact exchange energy of a uniform electron gas (UEG), which is a somewhat unphysical system in which a constant electron density is neutralized by a constant background positive charge (rather than by discrete nuclear charges). The UEG correlation energy can be calculated numerically[54] and fit in various ways[55,56] and that leads to the LSDA for correlation, which has recently been thoroughly reviewed.[57]

The next level of complexity in density functionals is to add a dependence on the gradients of the spin densities; in particular the functional depends on the unitless reduced spin-density gradients, s_σ, which are proportional to $|\nabla\rho_\sigma|/\rho_\sigma^{4/3}$. (Usually, though, we just say it depends on $\nabla\rho_\sigma$.) Such functionals are called generalized gradient approximations (GGAs). Popular GGAs include BP86, where B denotes Becke's 1988 exchange functional (usually abbreviated as B88 or just B),[58] and P86 denotes Perdew's 1986 correlation functional;[59] BLYP, where LYP denotes the Lee–Yang–Parr correlation functional;[60] PW91, from Perdew and Wang in 1991;[61] and a functional of Perdew, Burke, and Ernzerhof (PBE).[62] The modified Perdew–Wang functional of Adamo and Barone,[63] called *m*PWPW, is very similar to PBE. Notice that GGAs may combine an exchange functional from one source with a correlation functional from another, or they may both be from the same source. Thus BP86 and BLYP combine B88 exchange with P86 or LYP correlation, respectively; PW91 combines PW91 exchange with PW91 correlation; PBE combines PBE exchange with PBE correlation; *m*PWPW combines *m*PW exchange with PW91 correlation; SLYP combines the Slater LSDA exchange with LYP correlation; and PBELYP combines PBE exchange with LYP correlation.

Density functional theory with LSDA or GGA functionals includes self-exchange and self-correlation, both of which are unphysical. As a consequence such functions tend to predict too small a HOMO–LUMO gap in molecules or too small a band gap in solids. Furthermore they tend to underestimate the relative stability of high-spin states in molecules or of high magnetic moments in solids. An important consequence of the error in LSDA and GGA exchange functionals is that an electron interacts with its own charge density; this unphysically raises the energy of localized states and causes DFT to produce excessively delocalized charge distributions[64–73] and to incorrectly predict some materials to be metals rather than insulators. Systems for which these errors are especially severe are sometimes called strongly correlated systems because delocalization is associated with the dominance of kinetic energy terms, and localization is associated with dominance by screened Coulomb potentials,[74] and electron correlation is important for electron localization because correlation

minimizes the interatomic repulsion of electrons near the same center. The connection between covalency and an insulator gap has been especially well studied in the metal oxide insulators like MnO, FeO, CoO, and NiO.[75–92] By including partial or full Hartree–Fock exchange one can decrease or eliminate, respectively, self-exchange, and by including kinetic energy density one can eliminate self-correlation[50,79] and decrease the sensitivity to the percentage of Hartree–Fock exchange.[39] Hartree–Fock exchange and kinetic energy density thus reduce some of the inaccuracies of the LSDA and GGA functionals while retaining many of the computational advantages of GGAs as compared to WFT.

The density functionals that perform best for main-group chemistry are not the same as those that perform best for transition metals.[93–95] Whereas in solid-state chemistry local functionals are often chosen, partly because they are easier to apply to extended systems, in organic chemistry hybrid functionals are the more typical choice because of their demonstrated superior predictions of energetics; by far the most popular such hybrid functional is B3LYP, which is a hybrid GGA put together by Stephens *et al.*[96] on the basis of earlier work by Becke and others,[58,60,97] especially a hybrid GGA called B3PW91.[97] The correlation functionals of B3PW91 and B3LYP are based on PW91 and LYP, respectively but are optimized specifically for use in a hybrid functional,[97,98] whereas the most straightforward hybrid functionals result from simply replacing a percentage (here called X) of local density functional exchange by Hartree–Fock exchange. Such functionals often have a "1" in their name to denote this one parameter (although there are usually other parameters in the local part of the exchange–correlation functional). Examples include B1LYP[99] (BLYP with $X = 25$), *m*PW1PW[63] (*m*PWPW with $X = 25$), PBE1PBE[99,100] (PBE with $X = 25$, also called PBEh [but it is not the only functional called PBEh] and here called PBE0, which is its most common name), and MPW1K[101] (*m*PWPW with $X = 42.8$). One occasionally sees a functional, *e.g.*, BH&HLYP, with $X = 50$. In comparison, B3LYP and B3PW91 both have $X = 20$ (and each has two other new parameters as well). Reiher *et al.*,[102] on the basis of predicting the relative energetics of various spin states of Fe^{II} complexes, suggested adjusting X to 15 in B3LYP; they called the resulting functional B3LYP*. Later, Brewer *et al.*[103] found that $X = 13$ works best for a set of iron(II) and iron(III) complexes. Bredow and Gerson[81] proposed a PW91-based hybrid functional, called HF + PWGGA[81] or PW1PW,[104] with $X = 20$, which was optimized to the band gaps and thermodynamic and geometric properties of MgO, CoO, and NiO.

In further related work, Radon *et al.*[105] performed CASPT2 calculations, a method that uses second-order WFT perturbation theory to add dynamical correlation to the complete active space self-consistent-field WFT method, CASSCF, which is a multi-configurational method that includes only a small fraction of the dynamical correlation. They assumed the CASPT2 calculations on single molecules of bis(acetylacetonate) cobalt(II), usually abbreviated $Co(acac)_2$, to be of benchmark quality, and they found a tetrahedral quartet ground state. They then found that BP86, PBE, and TPSS (all with $X = 0$) predict the ground state to be a planar doublet, whereas B3LYP, PBE0, and TPSSh (with $X = 20$, 25, and 10, respectively) predict a tetrahedral quartet. The crystal is known experimentally to involve planar $Co(acac)_2$, where the difference from the single-molecule case is apparently due to π–π stacking interactions.

Mixing in Hartree–Fock exchange is not the only way to include nonlocality. The nonlocal character of the true density functional is more general and can be summarized by noting that the exchange–correlation energy density at a given point in space depends not just on the local properties of the density at that point but rather on the density everywhere. The Kohn–Sham orbitals also depend on the density everywhere. Some methods of including nonlocality that are even older than hybrid DFT are the weighted density approximation[106–111] (WDA), the self-interaction correction (SIC) method,[112,113] the average-density SIC method,[114,115] and the screened exchange (sX) approximation of Bylander and Kleinman.[110,111,116] The WDA is particularly interesting in that it is based on approximating the exchange–correlation charge density in a way that conserves the total exchange charge and the depth of the exchange hole.

An approximate version of the SIC method based on the premise that most of the self-interaction error arises from localized regions has been introduced,[117,118] variously called atomic SIC (ASIC) and pseudo-SIC. Pemmaraju *et al.*[119] further developed the ASIC method and suggested it for use in modeling quantum transport. Although ASIC accomplishes some of its goals in correcting self interaction, it still suffers from the inadequacy of being built on the LSDA.[120]

Another approach to reducing these inaccuracies is to invoke the so called DFT + U approximation,[76,121,122] which becomes LSDA + U or GGA + U, depending on the type of density functional employed. The +U modification ameliorates self-interaction by using system-dependent parameters (for solids, the parameters should probably also depend on pressure or molar volume and on phase, and for molecules on geometry). The +U modification takes one out of the realm of DFT and into a less rigorous model Hamiltonian approach, but it is instructive in the way it corrects DFT. The method is approximate and not uniquely defined[123] and is employed in a variety of inequivalent ways by different researchers, but the various versions attempt to enforce the same physical corrections by adding a Hubbard-like[124] term to the DFT energy; this term has the form (in the version[78,85] of DFT + U employed in the VASP program):

$$E^{\mathrm{DFT+U}} - E^{\mathrm{DFT}} = \frac{U - J}{2} \sum_{\sigma} \mathrm{Tr}(\rho^{\sigma} - \rho^{\sigma}\rho^{\sigma}) \qquad (4)$$

where $U - J$ (sometimes called U) is an empirical constant, and ρ^{σ} is the one-electron density matrix of metal d electrons (sometimes metal f electrons) for spin σ. A key issue in essentially all implementations is the inclusion of the Hubbard-like term only in a basis of localized d electrons (or f electrons). The Hubbard-like term adds a penalty for non-idempotent density matrices in this subspace and therefore it favors filling d orbitals that are localized on one particular atom[78] (a "correlation" effect), which sometimes also favors high-spin states on each atom and therefore less covalent

bonding in molecules or antiferromagnetic coupling in solids. The +U correction would be expected to be smaller for a GGA than for LSDA, and smaller yet or not needed for a well balanced hybrid functional; for accurate results, the +U correction should depend on the structure.[125]

In some cases, for example solid MnO,[87,126,127] FeO,[88,126,127] and Co,[88,126,127] the +U approach and the inclusion of partial Hartree–Fock exchange lead to similar results, which are much better than GGA, and one anticipates that the methods would be even more similar if the Hubbard-like term were included for the entire electronic space rather than just the metal *d* space.[85]

As just one example, we note that LSDA,[128–130] BLYP,[131] PW91,[129] and PBE[130] predict that FeO is a metal (no band gap), whereas LSDA with SIC,[126,127] LSDA + U[84] and hybrid DFT (BLYP with $X \geq 10$, from ref. 131) correctly predict it to be an insulator. However, the detailed nature of the crystal orbitals is predicted differently by the various methods.[131]

A key issue in +U methods is that they approximate the energy not only in terms of the electron density but more generally in terms of the density matrix. Further development of this line of approach includes LDA + DMFT[132] (in which the LSDA approximation is combined with dynamical mean-field theory). We will not include DFT + U or LDA + DMFT in the rest of this review, but the reader is directed to a few particularly relevant references for further reading.[85,132–149] A related approach that attempts to improve on LDA + U is the recent Gutzwiller DFT[150,151] (LDA + G).

2.3 Introduction to band theory

Since DFT saw its initial development in the physics community but has since become an essential tool in chemistry, there is a certain difficulty in reconciling the conceptual frameworks used in the two disciplines. This is especially true for the language developed around the important application of band theory, and this language now occurs in many contexts in the DFT literature.

As in many areas of chemical physics, a useful first step is defining terms, and that is especially important for chemists reading the solid-state physics literature where many applications of density functional theory to systems containing transition metals have been reported. One key quantity associated with a solid is its "gap", but there is more than one way in which this is defined; alternatively one can say that there is more than one gap. First, one can define the gap by using quasielectrons and holes, sometimes called quasiparticles.[152] The energy to remove an electron from a system is called the ionization potential (for metals it is called the work function), I, and it is equal to $E_{N-1} - E_N$ where N is the number of electrons in the material or molecule under study. Experimentally, I can be measured by photoelectron spectroscopy (PES) [which is also called photoemission spectroscopy and which could be ultraviolet photoelectron spectroscopy (UPS) or X-ray photoelectron spectroscopy (XPS)] or by inverse photoemission spectroscopy (IPES). The energy to add an electron is called the electron affinity, A, equal to $E_N - E_{N+1}$. One definition of the gap is $I - A$.[153] This is sometimes called the physical gap, the quasiparticle gap, or the fundamental gap.

The gap is also sometimes associated with excitation energies, as in optical spectroscopy. This may be called the optical gap, and it is defined by the onset energy of absorption. An optical excitation does not change N. In quasiparticle language, the calculation of optical properties requires calculating the interaction between a quasielectron (also called an electron or a particle) and a hole (and their exchange counterparts).[154–157] The optical spectrum of a solid is the frequency-dependent imaginary part of the macroscopic dielectric function, and the spectrum is sometimes calculated using this equivalence.

Thirdly, the gap may be associated with the difference between the energy of the highest occupied molecular orbital (HOMO) or highest occupied crystal orbital (HOCO) and the lowest unoccupied molecular orbital (LUMO) or lowest unoccupied crystal orbital (LUCO). This orbital-energy gap is sometimes called the independent-particle gap, the single-particle gap, or the one-electron gap. Strictly speaking, the orbital-energy gap is only an approximation to the physical quasiparticle gap or the optical gap. Thus, orbital-energy band gaps are often 30–100% below the quasiparticle band gaps in semiconductors and insulators.[158,159] The correction of the orbital energy gap to the quasiparticle one is sometimes called a quasiparticle shift[160] or a quasiparticle correction,[159] and the correction of the physical gap to the optical one, due to electron–hole interaction,[161] is sometimes called an exciton shift or a local-field effect. In practice there is typically some cancellation between the quasiparticle shift and the exciton shift because the former increases the gap, and electron–hole attraction lowers it (just as electron–nucleus interactions in atoms lower the bound states below the ionization potential). The electron–hole unit is a two-body quasiparticle, and it is called an exciton. In semiconductors and other high-dielectric materials, the electron–hole interaction is often weak (~0.1 eV), and the exciton is spread out over several unit cells (this is called a Mott–Wannier exciton). In insulators the exciton may be localized and can be thought of as a mobile electronically excited state of a molecule or formula unit (such an exciton is called a Frenkel exciton); the exciton shift of a Frenkel exciton can be very significant, 1 eV or more.

Note that the expression "band gap" is itself ambiguous since the word "band" is used to describe not only the quasiparticle energies as a function of momentum $\hbar\boldsymbol{k}$ but also the independent-particle approximation to those curves.

The quasiparticle shifts may be approximated by the GW approximation[159,162–165] for the self energy operator (also called the mass operator or effective mass operator), where G is a one-particle Green's function, and W is the dynamically screened Coulomb interaction. The quasiparticle shift calculated this way is sometimes called the GW shift. The GW approximation is a many-body perturbative solution of the exact equation, called the Dyson equation, for the self-energy operator, and the calculations often begin with a DFT calculation[160,166–169] (just as perturbative solutions for molecules often begin with a Hartree–Fock calculation). The non-self-consistent version of the GW method is called G_0W_0.[160,170] The solution to the Dyson equation may also be approximated by uniform electron gas considerations.[171] At a higher level one would solve the Dyson equation without

approximations. Exciton effects may be calculated by the Bethe–Salpeter equation involving the two-particle Green's function.[159,163]

Onida *et al.*[159] have provided a comparison of the *GW* and Bethe–Salpeter approaches commonly used in solid-state physics to the TD-DFT approach commonly used for optical spectra in chemical physics. Whereas the Bethe–Salpter equation starts with the quasiparticle states corresponding to $(N-1)$- and $(N+1)$-electron systems, as calculated for example by the *GW* approximation, TD-DFT works directly with the *N*-electron systems.[172] TD-DFT is based on the response of a system to a time-dependent perturbation, and Onida *et al.*[159] point out that "the system's response is directly related to the *N*-particle excited states of an *N*-particle system similar[ly] to the way the one-particle Green's function is related to the $(N+1)$- and $(N-1)$-particle excited states of the same system". Both approaches are exact in principle but subject to inevitable error due to the practical approximations, such as approximate density functionals or the truncation[173] of TD-DFT response at linear terms. The exchange–correlation potential of a TD-DFT calculation must provide the same physics as self-energy corrections and electron–hole interactions in the *GW* and Bethe–Salpeter calculations.[159]

In principle, the exchange–correlation functional of TD-DFT is time-dependent and depends on the entire past history of the density. If the time-dependent potential changes slowly, the system adjusts adiabatically, and one can approximate the time-dependent exchange–correlation functional by the time-independent (local-in-time, frequency-independent) ground-state exchange–correlation functional. This is called the adiabatic approximation.[174] Most TD-DFT calculations employ this approximation.

A complication with the traditional physics-literature hierarchy described above is that hybrid functionals, which until recently were the starting point for most chemistry applications but very few physics ones, include some of the interactions often included in the physics community by the *GW* perturbative approach to the exchange–correlation functional. In particular, Hartree–Fock exchange is similar to the screened exchange interaction in *GW* theory. Therefore hybrid functionals can be a better starting point than local functionals for *GW* calculations; this leads to smaller quasiparticle shifts.[160] Hybrid functionals can also be very useful without *GW* shifts because they are less expensive than the *GW* method and permit economical self-consistent calculations of electronic eigenfunctions;[83] the same can be said for the sX approximation.[175] The poor accuracy of band gaps computed with local functionals may ultimately be attributed to the nonanalytic dependence of the effective potential on the density due to the derivative discontinuity at integer numbers of electrons.[153,176–179]

2.4 More types of functionals

Let's again start with language. Many chemists label any functional that depends only on local properties, *e.g.*, LSDA or GGA, as "local"[79,180–184] and other functionals, such as hybrid GGAs, are called nonlocal. This language focuses on the algorithmically important consideration of whether the effective potential in the generalized Kohn–Sham equations can be applied as a multiplicative operator or requires an integral operator (rather than focusing on the strict locality of the functional relationship). We will follow this usage in the present review. In the older literature, GGAs are sometimes called nonlocal or gradient-corrected, but this usage is now becoming uncommon. Some chemists call local functionals "pure" but we deprecate this usage because it could imply to nonspecialists that the unknown exact functional is local, which is untrue. Some physicists separate local functionals into strictly local, as in the LSDA, and "semilocal", which is used to describe GGAs (and meta functionals, which are described in the next paragraph). We will not use the "semilocal" language. Although we distinguished the Kohn–Sham equations from the generalized Kohn–Sham equations in section 2.1, in the rest of this article we will call them both the Kohn–Sham equations.

Local functionals may involve more than just spin densities and reduced spin density gradients. The next level of complexity is to introduce either $\nabla^2\rho_\alpha$ or the magnitude of the spin kinetic energy density. The latter is given by $\frac{1}{2}\tau_\sigma$. For a one-electron system, ρ_α is equal to $|\psi_{1\alpha}|^2$ and τ_α becomes $\hbar^2|\nabla\rho_\alpha|^2/4m_e\rho_\alpha$. Thus the deviation of τ_α from this quantity may be used to "detect" one-electron regions and eliminate spurious self-interactions and self-correlation in such regions.[79,185]

Functionals that depend on the spin kinetic energy density or $\nabla^2\rho_\alpha$ are called meta functionals. The only established meta functionals are meta GGAs, which depend on ρ_α, $\nabla\rho_\alpha$, and $\nabla^2\rho_\alpha$ or on ρ_α, $\nabla\rho_\alpha$, and τ_α. Adding Hartree–Fock exchange to meta GGAs yields hybrid meta GGAs, which were already mentioned in section 2.1.

Some early examples of meta GGAs are Becke95[186] (usually abbreviated B95) for correlation and TPSS[187] for exchange and correlation. The B95 correlation functional was originally combined with B88 exchange, yielding BB95. Adding an optimized amount of Hartree–Fock exchange to BB95 yields B1B95 where the "1" stands for the one optimized parameter, *X*. Optimizing *X* for TPSS yields a functional called TPSSh where "h" denotes hybrid.

Notice that hybrid GGAs, meta GGAs, and hybrid meta GGAs depend explicitly on the occupied spin orbitals as well as on the spin densities and their derivatives. The next level of complexity is to introduce a dependence on the unoccupied spin orbitals. This allows one to model correlation energy in a way analogous to how it is modeled in WFT. Functionals depending on unoccupied orbitals are called fifth-rung functionals. Hybrid functionals depending on unoccupied orbitals are sometimes called doubly hybrid functionals. Such functionals have not yet been widely applied to transition metals.

A very promising approach, also not yet applied widely to transition metals, involves range-separated hybrid functionals and local hybrid functionals. Range-separated functionals[188–196] involve separating the electron–electron interaction into a short-range and a long-range part,[188–195] or even into three parts[196] (short-, middle-, and long-range) and treating the contribution of one part of the exchange energy by the Hartree–Fock method and the other part or parts by a local exchange functional. In local hybrid functionals,[197–201] the

percentage of Hartree–Fock exchange that is mixed with density functional exchange depends on the point in space. The percentage could depend on any local function of the point in space; for example, τ_α[197,198] or the reduced spin density gradient, s_σ.[199–201] A particularly successful range-separated functional is that of Heyd, Scuseria, and Ernzerhof (HSE).[191]

2.5 Still more functionals

So far we have introduced the following functional types and functionals:

1. *local*: *LSDA approximation*. Various approximations or fits to UEG exchange and correlation energies. (All LSDA functionals are very similar, and in the present review we will not distinguish them.)
2. *local*: *GGAs*. BP86, SLYP, BLYP, PW91, PBE, PBELYP, *m*PWPW, *m*PWLYP.
3. *nonlocal*: *hybrid GGAs*. B3PW91, B3LYP, B1LYP, PBE0, MPW1K, B3LYP*, HSE.
4. *local*: *meta GGAs*. BB95, TPSS.
5. *nonlocal*: *hybrid meta GGAs*. B1B95, TPSSh.

In this section we introduce additional functionals of types 2–5.

GGAs. GGAs for exchange are defined by a single curve corresponding to the enhancement of exchange as a function of s_σ. For larger s_σ, addressing the GGA exchange functionals mentioned in section 2.2, B88 has the largest enhancement, PW91 has the lowest, and PBE and *m*PW are in between these two. Other functional forms for this curve have also been proposed, or sometimes the curve is found by multiparameter optimization. In the former category we mention ten particularly interesting exchange functionals. In 1996, Gill[202] introduced a functional now called G96 with the goal of finding an exchange functional that performs as well as B88 but has a simpler form. In 1998, Zhang and Yang[203] introduced a revised PBE functional called revPBE, with the goal of obtaining more accurate atomic absolute energies and molecular atomization energies; then in 1999, Hammer *et al.*[204] introduced another (closely related) revision usually called RPBE, with the goal of obtaining improved chemisorption energies for small molecules on metal surfaces. In 2000, Vitos *et al.*[205] parameterized an exchange functional, called LAG, against the local Airy gas model[206] in an attempt to improve the predictions for bulk properties of late transition metals and semiconductors and the exchange energies of surfaces. The local Airy gas is an "edge" electron gas, designed to mimic electronic properties near an edge, such as a solid surface (that is, a solid/vacuum interface) or the periphery of a molecule. In 2001, Handy and Cohen[207] introduced an exchange functional called OPTX, usually abbreviated O. This exchange functional was designed to predict more accurate exchange energies of atoms, but it does not satisfy the UEG limit. In 2004, Xu and Goddard[208] introduced an exchange functional called X. This X exchange functional was designed to improve non-covalent interaction energies; it is very similar to *m*PW. In 2005, Armiento and Mattsson[209] presented a functional, now called AM05, optimized against the jellium-surface exchange–correlation energy (which has recently been clarified[210]) and designed to give improved lattice constants, bulk moduli, and vacancy formation energies. In 2006 Wu and Cohen[211] designed a new exchange functional, now called WC, with the goal of improving lattice constants, crystal structures, and metal surface energies. Their derivation was based on attempting to enforce the expansion about the UEG limit through fourth order in s_σ. However, due to an error in their derivation, the claimed accuracy through fourth order does not hold;[212] their functional must therefore be judged on empirical grounds rather than on the basis of the gradient expansion. In 2008, Perdew *et al.*[213] empirically modified the PBE functional to improve the predicted lattice constants. Their functional design strategy involved fitting the jellium surface exchange–correlation energies, as done previously for a GGA by Armiento and Mattsson. Also in 2008, Zhao and Truhlar[214] derived a functional, called SOGGA, that precisely satisfies the gradient expansion through second order for both exchange and correlation (none of the other functionals discussed so far does this). The G96, OPTX, and X exchange functionals are usually combined with the LYP correlation functional yielding G96LYP, OLYP, and XLYP, respectively. OPTX is also used with PBE correlation, yielding OPBE. The LAG exchange functional is used with the LSDA for correlation. The AM05, PBEsol, and SOGGA functionals have corresponding correlation functionals designed to complement them. The revPBE, RPBE, and WC functionals are used with the PBE correlation functional.

The above functionals are not unrelated. None of them satisfies all the known exact constraints on the density functional, and they involve different choices of which constraints to satisfy. Extensive discussion of the constraints satisfied and not satisfied by these functionals, the relationships between the functionals, and how the functionals' characteristics affect their performance has been provided by Zhang and Yang,[203] Perdew and coworkers,[213,215,216] Mattsson and coworkers,[217] and Zhao and Truhlar.[214] Mattsson *et al.*[218,219] have also provided further discussion of the importance of surface energy. The bottom line of these discussions is that different choices for the behavior of the density functionals determine whether a functional will be more accurate for interatomic spacings in lattices and small-molecule bonds or for solid-state cohesive energies and small-molecule energetics.[214] The surface energy provides a third dimension to this discussion.[216]

Hybrid GGAs. The very successful hybrid GGA called B3LYP has already been mentioned in section 2.2. Sousa *et al.*[220] analyzed the number of occurrences of various functional names in article titles and abstracts in the Web of Science over the 1990–2006 period and found that 80% of the references were to B3LYP, with a slightly higher percentage over the 2002–2006 period. For the 1990–2006 period the second most popular functional by this measure was the local BLYP (5%), followed by the hybrid GGA called B3PW91 (4%) and the local BP86 (3%). Another hybrid GGA, B3P86, which is similar to B3PW91 and B3LYP but with a different correlation functional, was fifth (2%). Hybrid density functionals, however, are still very expensive for periodic calculations on extended systems.[221]

Other hybrid functionals that occur in this review are X3LYP, which is like B3LYP but with the X exchange functional replacing B88, and MPWLYP1M, which is like *m*PWLYP, but with a nonzero percentage X of Hartree–Fock exchange, optimized for metals.[94]

A number of more sophisticated hybrid GGAs have been developed that go beyond combining separate GGAs for exchange and correlation with an optimized value of X. These include a sequence of multiparameter functionals from Becke, Handy, and Tozer and their coworkers: B98,[222] B97-1,[223] B97-2,[224] and B97-3.[225] By some measures B97-3 is the most accurate hybrid GGA for main-group chemistry, but, like B3LYP, it is inaccurate in general for transition metal chemistry.[39]

Meta GGAs and hybrid meta GGAs. Becke, Boese, Perdew, and Savin and their collaborators and Zhao and Truhlar developed functionals including τ_σ in the correlation,[186,226] the exchange,[185,227–229] or both.[79,187,230,231] Most of these density functionals can be used in either local or hybrid form. The τ-HCTH,[207] BMK,[208] and PW6B95[205] functionals have been especially widely tested, as have the M05 and M06 families discussed below. Prior to 2005, no available density functional was among the better functionals for both transition metal chemistry and main group barrier heights. Good accuracy for both is important for studying, for example, organometallic catalysis or organic reactions. The former seemed to require zero or low Hartree–Fock exchange ($X \gtrsim 15$), while the latter seemed to require high Hartree–Fock exchange ($X \lesssim 40$). Furthermore, no available functional predicted realistic noncovalent interactions for weakly interacting systems. The Minnesota 2005 hybrid meta functional,[34] called M05, overcame both of these difficulties, with $X = 28$, by incorporating τ_σ into exchange and correlation in a balanced way, removing self-interaction errors in exchange and self-correlation errors in correlation, enforcing the UEG limit, and including a diverse set of data in the parameterization, in particular main-group atomization energies, ionization potentials, electron affinities, barrier heights, noncovalent interactions, and absolute atomic energies and transition metal ionization potentials and bond energies. The functional was parameterized against 35 data and initially tested against 231 data. A key parameterization strategy was to optimize X simultaneously with the other parameters in the density functional to reduce the reliance on compensating errors in the local component of exchange with errors in the correlation functional. The resulting M05 functional showed, for the first time, uniformly good results for main-group thermochemistry, kinetics, and noncovalent interactions and transition metal bond energies. No previous functional was accurate for more than two of these four categories.

In a subsequent effort, Zhao and Truhlar[38] attempted to find the best functional with $X = 0$. The motivations for this were twofold: (i) to learn more about the best functional form and (ii) to develop a functional with lower cost for large and extended systems. To obtain good results with $X = 0$ they required a more general form for the local exchange functional. Great care was taken to be sure that flexibility afforded by the parameterization procedure was not too large for the size and diversity of the chosen training sets. The resulting functional, called M06-L, had the best overall performance of any functional for a combination of thermochemistry, thermochemical kinetics, metallochemical and noncovalent interactions, bond lengths, and vibrational frequencies. The worst performance area was barrier heights, although these were predicted more accurately than by any other local functional and with about the same accuracy as the popular B3LYP functional.

In later work, Zhao and Truhlar designed a functional with $X = 100$;[232] this functional, called M06-HF, completely removed one-electron self-interaction error, but it is not recommended in general for transition metals or transition-metal compounds because they often have multi-reference character. Based on what was learned by designing M06-L and M06-HF, Zhao and Truhlar redesigned and re-optimized M05, yielding M06,[39] which has $X = 27$, whereas M05 had $X = 28$.

Zhao and Truhlar doubled the percentage of Hartree–Fock exchange in M05 and M06, yielding M05-2X[233] and M06-2X,[39] respectively, and they made two slightly improved versions of M06-2X, called M08-HX and M08-SO.[234] These functionals are not recommended for transition metal chemistry, except for Zn, which Amin and Truhlar[235] found to have density-functional requirements more like a main-group metal than a transition metal. (The Minnesota functionals have not been tested for Cd and Hg.) We called M08-HX a "high exchange" functional because there is no M08 functional whose exchange can be doubled. In this language, low exchange would be X in the 5–15 range, "standard exchange" would be X in the approximately 20–30 range, and high-exchange would be X in the 40–60 range.

One advantage of M06-HF, as compared to most other functionals, is that it eliminates the long-range self-interaction error that has a disastrous effect on calculated charge transfer excitation energies.[39,232] Another way to eliminate the long-range self-interaction error is with range-separated functionals that use Hartree–Fock exchange for the long-range part[188,190] (unlike HSE,[191] which uses it for the middle range). An example of such a functional is CAM-B3LYP.[236]

Other general functionals encountered in this review are VSXC[237] (also called VS98), a meta functional, MPW1B95,[238] a hybrid meta functional formed from *m*PW exchange and B95 correlation, with $X = 31$, and OLAP3, a combination of OPTX with the LAP3[239] correlation functional.

Functionals with specific reaction parameters. Another type of functional is one in which the parameters are adjusted not in a general way for a broad range of systems, but rather to be as accurate as possible for a specific reaction or a small range of systems. Such a parametrization yields a function with specific reaction parameters (SRP). The SRP approach was first developed for small-molecule reactions in the gas phase,[240,241] and it has recently[242] been extended to predict a potential energy surface for H_2 chemisorbing on Cu(111).

3. Methodology and software

3.1 Methodology: nonrelativistic aspects

Most applications of DFT in chemistry are carried out using large electronic structure packages, and one way to understand the available methodology is to review the capabilities of these packages. Many of these packages are updated frequently, and many of them have web pages where new versions and added capabilities can be monitored. In addition in many cases the capabilities of the packages have been summarized in journal articles. This section includes some of those references.

One can distinguish various categories of calculations, *e.g.*, molecules *vs.* solids, calculations with Gaussian basis sets *vs.* those based on plane waves or both[243,244] Gaussians and plane waves, and all-electron calculations *vs.* those with effective core potentials[245–265] (ECPs, also called pseudopotentials) to replace some or all of the core electrons. The options for treating core electrons are even more diverse when one includes methods like the projector augmented-wave (PAW) method,[266–271] which is a frozen-core all-electron method. Some programs can carry out more than one kind of calculation; others can carry out only one kind. Programs employing periodic boundary conditions can include solid-state symmetry by sampling[272–274] many **k** points in the Brillouin zone; they can be applied to crystalline systems with nonperiodic defects or surfaces by the supercell method,[273,275,276] and they can be applied to liquids[277] or isolated molecules[278,279] by evaluating only the Γ point in the Brillouin zone. Several of the electronic structure packages also include dynamics modules.[280]

For calculations on molecules, some programs employ or can employ a procedure[281–284] called density fitting or resolution of the identity (RI) in which an auxiliary basis set is used to fit the electron density. In some cases this provides large savings in computer time for calculations on large molecules. For studying solids, a key procedure employed by several codes is variable-cell-shape molecular dynamics,[285,286] which can be used to optimize structures as a function of pressure.

Another methodological element that is becoming increasingly important is the combined quantum mechanical and molecular mechanical (QM/MM) method, in which the electronic structure of a primary subsystem is treated by explicit quantum mechanics (QM) whereas the effect on the energy of the secondary subsystem (the rest of the entire system) is included by molecular mechanics. A key issue in such methods is how to treat the boundary when it passes through one or more bonds. The QM/MM method is widely used, for example in enzyme chemistry,[287] but the QM/MM boundary is not usually placed through a bond to a transition metal. Ohnishi *et al.*[288] have considered the question of how to truncate the QM system at a bond between a transition metal and a phosphorus. A long-term goal would be to develop a QM/MM method defined for boundaries passing through any kinds of bond.[289]

3.2 Methodology: relativistic

Relativistic effects are non-negligible for late 3*d* transition metals, important for 4*d* transition metals, and so important for 5*d* transition metals that they must be included for even a zero-order description.[290] A fully relativistic calculation involves the four-component Dirac spinor operator, but this is seldom employed for transition metal chemistry, where, at least until recently, at most a two-component formalism has tended to be employed. A review from the point of view of DFT is available.[291]

The reduction of the four-component formulation to a useful two-component one can be accomplished by transformations developed by Foldy and Wouthuysen,[292] Douglas and Kroll,[293] and Hess[294–298] and van Lenthe[299] and their coworkers, with the former work leading to the Douglas–Kroll–Hess (DKH) Hamiltonian and the latter to the zero-order-regular approximation[299] (ZORA). Practical two-component formulations of the DKH and ZORA Hamiltonians suitable for use with DFT were reported by Malkin *et al.*[297] and Mayer *et al.*[300] and by van Lenthe *et al.*[301] and Wang *et al.*,[302] respectively. The reduction to two components eliminates the so-called small components associated with positrons (although these are usually called the small components, a more specific name is charge conjugation components). In two-component calculations, an atomic orbital is sometimes expressed as linear combination of spin-up and spin-down orbitals associated, respectively, with angular momentum $j = l \pm \frac{1}{2}$. A further reduction to a one-component formulation is also possible; this yields the spin–orbit operator in its familiar form,[303] as well as a spin–spin term. In the one-component formulation, the spin direction is fixed along an arbitrary axis (the *z* axis). This is sometimes called the collinear approximation or the spin-free formulation, even when the orbitals depend on the spin. In the collinear approximation, the spin polarization density is simply the difference of the spin-up density and the spin-down density. (Note that the spin polarization density is usually called the spin density, but the term "spin density" is also used to refer to the spin-up and spin-down densities in the collinear approximation, so there is a possible source of confusion.)

In two-component calculations—in contrast to a collinear calculation, in which every electron at every point in space is either spin-up or spin-down along the same axis—one has the flexibility for each one-electron orbital to have a spin pointing along any axis and, furthermore, the spin associated with a given orbital need not point in the same direction at all points in space. A formulation with this flexibility is called a non-collinear treatment.[7,297,300] This is accomplished by writing each orbital as a general spinor, that is, as a linear combination of a spin-up orbital times a spin-up spin function and a spin-down orbital times a spin-down spin function.

The relativistic formulation leads to a more satisfactory definition of the spin polarization density.[304] In particular the spin polarization density is defined using the length of the spin magnetization vector rather than *z* component of the spin magnetization vector, which means that the spin polarization vector has the desirable property of being invariant to rotations in spin space.[7] When we refer to a noncollinear treatment, we imply this improved definition of the spin polarization density.

In a spin-restricted DFT calculation, all spin orbitals have the form of a product of a spatial ket and spin ket, all spin kets have the same fixed quantization axis, and every occupied spin-up spin orbital is paired with a spin-down spin orbital

having the same spatial part. In a "spin-polarized" or "spin-unrestricted" DFT calculation, the spin orbitals still have the form of a space-spin product with a single quantization axis of the spin parts, but now the spatial orbitals are not doubly occupied; for example the spatial part of a spin-up 1*s* orbital need not be the same as the spatial part of a corresponding 1*s* spin-down orbital. In a noncollinear calculation, every orbital is a general spinor, with complex spatial parts. (As mentioned in section 1, it is common to say "restricted" or "unrestricted" rather than spin-restricted or spin-unrestricted. Furthermore, the noncollinear formalism is sometimes called the generalized spin orbital[305] or general spin orbital[306] description.) One can use general spinors not only in two-component relativistic calculations, but also in nonrelativistic SCF calculations; for Hartree–Fock theory this is called general Hartree–Fock theory (more general than spin-unrestricted Hartree–Fock theory),[307–309] and as a generalization of Kohn–Sham theory it is called generalized spin density functional theory[310] or noncollinear spin density functional theory.[311] These nonrelativistic formulations are useful for treating biradicals and certain magnetic problems.

The spin-dependent version of DFT developed by von Barth and Hedin[6] and Rajagopal and Callaway[7] was originally formulated for a general noncollinear system, but until recently it has usually been applied only to spin-polarized systems in the collinear approximation. The key distinction is that a noncollinear density functional depends on the off-diagonal elements of the spin density matrix as well as the diagonal elements.

An illustrative example of a system requiring a noncollinear treatment is provided by a spin frustrated Cr monolayer on a face-centered-cubic Cu(111) substrate[312] or an unsupported Cr(111) monolayer.[313,314] However, noncollinear magnetism can also be important in molecules as small as Fe_3,[315–317] Fe_5,[315–319] Cr_3,[314,320,321] and Cr_5.[320–322]

Relativistic effects may be classified into scalar effects and vector effects; the former are due to mass–velocity and Darwin terms in the relativistic kinetic energy, and the latter arise from magnetic interactions involving the operators associated with spin and orbital angular momentum.[290] Spin–orbit effects can be included by treating the spin–orbit terms by perturbation theory or variationally in one-component calculations or by a two-component calculation.[290]

The main effect of the scalar relativistic terms is to shrink the *s* orbitals and, to a lesser extent,[290,323–325] the *p* orbitals. This effect can be added to a nonrelativistic formulation by using ECPs determined in relativistic calculations on atoms. Such relativistic ECPs were recently tested for calculations on PdCO, where the relativistic effects are scalar in nature, and were found[326] to perform excellently in reproducing calculations[327] carried out with a relativistic Hamiltonian based on the regular approximation. When relativistic effects are to be treated explicitly, all-electron basis sets optimized for such calculations are required for good accuracy.[328–332]

3.3 Software

The *Gaussian* program[333] is based on Gaussian basis sets. It is the most widely used program for isolated molecules, but it also supports periodic boundary conditions, as well as calculations with continuum solvation. Molecular calculations with local functionals can employ density fitting. It includes TD-DFT as well as DFT. It is very flexible in the choice of basis sets, effective core potentials, and density functionals, and it has excellent geometry optimizers and initial guesses for the self-consistent-field iterations. It supports analytic Hessians[334] for all functionals (even meta and hybrid meta functionals), and it has classical dynamics capabilities and a very useful interface to external programs. An external interface to the POLYRATE[335,336] variational transition state theory code is available.

The Vienna *Ab initio* Simulation Package[278,337,338] (VASP) is the most widely used program for calculations on solids and surfaces. (The name is confusing since most implementations of density functional theory are not *ab initio* in the sense that "*ab initio*" is used by chemists. However, many physicists and materials scientists label all DFT methods as *ab initio* or "first principles" methods.) VASP employs plane waves with either pseudopotentials or the PAW method. It includes DFT + U and *GW* capabilities and has a dynamics module. VASP has especially powerful algorithms for converging the self-consistent-field iterations even for systems with near degeneracy of HOCO and LUCO.

The WIEN2k code[339,340] is another well established code. It uses the full-potential linearized augmented plane wave (FP-LAPW) method, which uses a spherical harmonic basis set inside of atomic spheres and a plane wave expansion in the interstices.

In a pair of landmark papers, Kresse and coworkers used the above three programs to demonstrate that if one converges the results with respect to basis set, one can obtain the same results with plane waves and Gaussians for molecules[279] and in some cases for solids.[341] For molecules the Gaussian and plane wave approaches were shown to become equivalent when the Gaussian basis set was increased to augmented correlation-consistent polarized valence quintuple-ζ and the plane wave cutoff for PAW calculations was increased to 60–70 Ry; the equivalence was demonstrated for both local and hybrid density functionals.[279] For solids,[193,341] reasonably good agreement was obtained between plane wave and Gaussian calculations with the range-separated HSE hybrid functional for most insulators, semiconductors, and simple metals, but not for open-shell transition metals. (Gaussian calculations with full-range hybrids (also called global hybrids) like PBE0 are still prohibitively costly because of the slow convergence for the long-range part of the exchange interaction.[341]) For both solids[341] and surfaces[342] the VASP-PAW and WIEN2k-FP-LAPW calculations agreed well.

The Amsterdam Density Functional (ADF) program,[343–345] somewhat uniquely, uses Slater-type orbitals rather than Gaussians. SCF calculations are performed only for local functionals, but post-SCF energies can be evaluated for hybrid functionals. ADF uses density fitting to reduce computational cost, and it treats scalar and vector relativistic effects by the ZORA method. For LSDA and GGA functionals, analytic Hessians are available. A companion program, called BAND,[346–348] carries out periodic calculations for bulk crystals, polymers, and surfaces; various tools, such as a search program for transition states in heterogeneous catalysis, are available.

The *NWChem* package[349,350] contains both a Gaussian module and an independent pseudopotential plane wave module. The program is especially designed for massively parallel calculations. Both internal (DRDY module) and external interfaces to the POLYRATE[335,336] variational transition state theory code are available.

The General Atomic and Molecular Electronic Structure System (GAMESS) package[351,352] has a broad range of Gaussian-based electronic structure capabilities, many of which are parallelized. Solvent effects can be modeled by effective fragment models. GAMESSPLUS[353] allows one to apply a well validated continuum solvation model.[354]

Jaguar is the electronic-structure program in the suite of computational chemistry and drug design program offered by Schrödinger, Inc. *Jaguar* carries out calculations with Gaussians for both isolated molecules and molecules in continuum solvent.[355] An external interface to the POLYRATE[335,336] variational transition state theory code is available.

MOLCAS is also a Gaussian-based electronic structure program for studying molecules.[356] Methods are included for modeling effects of solvents, embedding in ionic solids, or macromolecular environments.

QChem[357] is a modern quantum chemistry package available either as a stand-alone code or integrated with the *Spartan* '08 package from Wavefunction, Inc. It employs Gaussian basis sets and includes a well validated continuum solvation model.[354] *QChem* has been integrated with the CHARMM molecular mechanics and classical dynamics program.[358]

TURBOMOLE[359] is a Gaussian-based program with a fast RI algorithm, a TD-DFT option, and analytic Hessians. Density fitting and RI methods use an auxiliary Gaussian basis set to describe the electron density, in addition to the primary Gaussian basis set used to describe the orbitals.

DALTON 2.0[360] is a Gaussian-based program including linear, quadratic, and cubic[361] response functions for both singlet and triplet perturbing operators; the properties section is especially complete.

QUICKSTEP[244] is the electronic structure module of the CP2K program. It is a pseudopotential program that uses Gaussian basis functions to describe the orbitals and an auxiliary plane wave basis to describe the electron density. The CP2K package provides molecular dynamics capability.[362]

MOLPRO[363] is an electronic structure program with very fast post-Hartree–Fock capabilities, such as coupled cluster calculations. It includes a DFT module, and DFT orbitals can be used in coupled cluster calculations.

ORCA[364] is a Gaussian-based quantum chemistry program with special emphasis on spectroscopic properties of open-shell molecules. It includes hybrid, meta, and hyper functionals.

The Spanish Initiative for Electronic Simulations with Thousands of Atoms (SIESTA)[365–367] is a program designed for linear-scaling calculations on materials by employing a basis set of numerical finite-support atomic orbitals. It employs periodic boundary conditions.

The density of Montreal package[368] (*deMon*) carries out DFT calculations in a Gaussian basis with density fitting. It includes TD-DFT. It was merged with the ALLCHEM program,[369,370] and the merged code is called *deMon2k*.[371]

DMol^3 is a program that uses numerical functions on an atom-centered grid as basis functions and can be used for calculations in the gas phase, solvent, or solid state. Only local functionals are supported.[372–374]

The *Octopus* program[375,376] carries out DFT calculations including the influence of time-dependent electromagnetic fields. It can be used to calculate linear and non-linear absorption spectra, harmonic spectra, laser-induced fragmentation, and electron–ion dynamics of systems, from small clusters to medium-sized quantum dots.

PWSCF[377] (see also http://www.pwscf.org/) is the electronic structure module of the opEn Source Package for Research in Electronic Structure, Simulation and Optimization (*Quantum Espresso*) package, which adds capabilities for classical dynamics, geometry optimization, and transition state searches. PWSCF is a plane wave pseudopotential code for solid-state calculations. A linear scaling algorithm for hybrid functionals has recently been developed for *Quantum Espresso*.[378]

The CRYSTAL electronic structure code[379,380] forms Bloch orbitals for periodic calculations as linear combinations of Gaussians. Some examples of its usage are cited to illustrate its capabilities.[131,381,382] The tutorial article[380] by the authors of CRYSTAL is an excellent introduction to solid-state calculations in chemistry. Whereas CRYSTAL, *Quantum Espresso*, and VASP support hybrid calculations, most solid-state codes do not support nonlocal functionals.

We also mention four other plane wave codes and examples of their usage: ABINIT,[383–386] CASTEP,[387–391] *Dacapo*,[271,392–394] FLEUR,[395] LMTART,[396,397] and *ParaGauss*.[300,398]

Although we have emphasized computer programs based on Gaussian basis functions and/or plane waves, we note that some DFT calculations are instead accomplished by finite difference methods.[399–401]

Examples of codes that can carry out noncollinear DFT calculations are ABINIT, *deMon2k*, FLEUR, LMTART, *Paragauss*, SIESTA, VASP, and Wien2k.

4. Validation studies

There are a large number of papers devoted to validating density functional theory or containing a large validation component. The benchmark data used for validation can be either from experiment or, for simple enough systems, from high-level WFT. (One must be cautious about WFT results, even high-level ones, for transition-metal chemistry because if multi-reference character is too large, WFT may not be reliable.) In this section we briefly review some recent validation studies, beginning with those restricted to 3*d* metals and then lifting this restriction, in each case summarizing in approximately chronological order. (Additional validation studies are included in section 5.) Most validation studies are discussed in this section, but some solid-state validation is discussed in section 5.3.2. Furthermore, some of the papers considered in the application section (5.3.1) may be viewed as also contributing to the validation effort.

Barden *et al.*[402] considered the LSDA, BP86, BLYP, B3P86, and B3LYP functionals applied to nine homonuclear 3*d* dimers (they also considered LSDA and a functional called BHLYP that both performed very poorly and will not be

included in this summary). For bond energies, the mean unsigned error (MUE) ranged from 19 kcal mol^{-1} (BLYP) to 30 kcal mol^{-1} (B3P86). For bond distances the MUE ranged from 0.020 Å (BP86) to 0.053 Å (B3LYP). For vibrational frequencies the MUE ranged from 98 cm^{-1} (BLYP) to 122 cm^{-1} (B3P86). They characterized the performance of DFT as "surprisingly plausible," with BLYP and BP86 rated best. Already in this study we see a trend emerging. Whereas previous studies showed that hybrid functionals usually perform better for main-group chemistry, local functionals perform better for transition metal chemistry.

Diedrich *et al.*[403] tested BP86 against the first bond dissociation energy of four 3*d* transition metal carbonyls. The MUE was only 4 kcal mol^{-1}. First-row transition metal monocarbonyls were also studied by Adamo and Lelj,[40] who concluded that inclusion of HF character in B3LYP was important for the accurate calculation of vibrational frequencies and metal-carbonyl dissociation energies.

Holthausen[404] considered *s*/*d* excitation energies in 3*d*-series atomic cations. A number of subtle issues such as choosing orbital occupancies and artificial mixing of 3*d* and 4*s* orbitals were discussed. Unfortunately this study did not include scalar relativistic effects, and it was pointed out[405] that the conclusions are quite different if these are included. The revised conclusion is that local functionals are more accurate than hybrid functionals for these intershell excitation energies. The most accurate functionals, of 38 tested, are SLYP, PBE, BP86, PBELYP, and PW91, with MUEs for these five functionals ranging from 2.8 to 3.7 kcal mol^{-1}. B3LYP had an MUE of 4.4 kcal mol^{-1}, and HCTH had an MUE of 15.1 kcal mol^{-1}. It would be interesting to extend this study to more modern functionals.

Furche and Perdew[95] made a benchmark suite of 18 3*d* transition metal reaction energies, twelve of which are bond energies. They tested the LSDA, BP86, PBE, TPSS, B3LYP, and TPSSh functionals. Excluding LSDA, which has an MUE of 29 kcal mol^{-1}, the MUEs ranged from 10 kcal mol^{-1} for TPSSh to 12 kcal mol^{-1} for B3LYP. In later work, this benchmark test was extended to several more functionals, with the following MUEs in kcal mol^{-1}: 8 for M05 and B97-2, 9.5 for MPWLYP1M, and 11 for BLYP in the first extension,[406] 7 for M06-L, 8 for HCTH, 9 for VSXC and OLYP, 10 for G96LYP and *m*PWPW, 12 for τ-HCTH, and 12.5 for BB95 in the second,[38] and 7 for M06, 9 for B97-3, 10 for B98, and 13 for BMK and PBE0 in the third.[39]

Furche and Perdew[95] also examined the *s*/*d* excitation energies of the neutral 3*d*-series atoms, plus Ca. They used a procedure involving averaging non-self-consistent energies over multiplet components. MUEs ranged from 8.3 kcal mol^{-1} for B3LYP to 18–20 kcal mol^{-1} for PBE, BP86, and LSDA, with TPSSh and TPSS at 14 and 17 kcal mol^{-1}, respectively. Köster *et al.*[370] found that GGA calculations of *s*/*d* excitation energies of the neutral 3*d* atoms reproduce the experimental sawtooth behavior as a function of atomic number, but quantitative errors can be 15 kcal mol^{-1} or more.

Zhao and Truhlar[35] tested 18 density functionals for ZnNe, ZnAr, ZnKr, and Zn_2; these are all weakly bound complexes with accurate binding energies in the range from 0.07 to 0.80 kcal mol^{-1}. B97-1, M05-2X, and PWB6K were the most accurate functionals tested for the binding energies of Zn-rare gas dimers, and MPW1K, M05-2X, and PWB6K were the most accurate for Zn_2. Tests were also presented for geometries.

Karttunen *et al.*[407] tested B3LYP against WFT, in particular, Hartree–Fock theory and second-order perturbation theory (MP2) for geometry predictions on 80 hafnocenes in the Cambridge structural database. They found MP2 is most accurate, followed by Hartree–Fock theory, with B3LYP least accurate. This somewhat surprising result was attributed to low multi-reference character in the molecules studied.

Jensen *et al.*[408] tested the performance of BP86, BLYP, PBE, B3LYP, and PBE0 for 62 3*d*-series coordinatively unsaturated diatomics with bonds to H, C, N, O, F, S, Cl, and Br. Scalar relativistic effects were not included. Root-mean-square errors (RMSEs) in bond energies range from 13 kcal mol^{-1} (B3LYP and PBE0) to 17 kcal mol^{-1} (PBE). The poor performance was attributed mainly to inaccurate *s* to *d* promotion energies. The study also included dipole moments, and it was found that hybrid functionals lead to more ionic (less covalent) bonding character than local functionals; on average a PBE0 dipole moment is 0.7 D larger than a BLYP or PBE dipole moment. The spin densities on the metal were found to be widely different in several cases, with FeC the most extreme. BP86 and PBE were found to give the most accurate bond distances, with MUEs of ~0.02 Å. B3LYP gave the most accurate ionization potentials (RMSE = 2 kcal mol^{-1}) and BP86 and PBE0 the least accurate (RMSE = 5.5 kcal mol^{-1}).

Goel and Masunov[409] tested the BLYP, TPSS, B3LYP, and BMK functionals for hydrides and hydride cations of the 3*d*-series. The authors took special care with the SCF process to find broken-symmetry solutions that provide continuous potential energy curves. BMK gave the most accurate bond energies and TPSS the least accurate. Scalar relativistic effects were included and led to more accurate bond lengths. They found MUEs in ionization potentials of 3 kcal mol^{-1} for BMK and 6 kcal mol^{-1} for TPSS.

Legge *et al.*[410] tested the LSDA, BLYP, BPW91, B3PW91, and B3LYP density functionals against dissociation energies, geometries, and vibrational frequencies of 15 diatomic molecules containing Cu, Ag, and Au. Excluding LSDA, they got the most accurate results with BPW91 and the least accurate with B3LYP. They also tested vibrational frequencies for larger molecules.

Wang and Li[411] tested bond energies, geometries, and vibrational frequencies of 17 functionals against 6 diatomics containing Ag and 2 containing Au. Mean errors for the various functionals are not tabulated or discussed.

Schultz *et al.*[93] created databases of 9 bond energies and 8 bond lengths for transition metal dimers that contain only the data for which the experiments are judged to be especially reliable. The transition elements represented are Zr, V, Cr, Mo, Ni, Cu, and Ag. They used these databases to test 42 different density functionals, including two LSDA functionals, 12 GGAs, 13 hybrid GGAs, 7 meta GGAs, and 8 hybrid meta GGAs. The differences between double-ζ and triple-ζ basis sets are often quite large (greater than 10 kcal mol^{-1}), so double-ζ basis sets are not recommended

for transition metals. The bond energy MUEs (in kcal mol^{-1}) averaged across these classes of functionals are 7 for GGAs, 8 for meta GGAs, 19 for hybrid GGAs, 20 for hybrid meta GGAs, and 30 for LSDAs. The most accurate functional in each of these classes (and its MUE in kcal mol^{-1}) is respectively G96LYP and BLYP (5), TPSSKCIS (6), B97-1 (5), TPSSh (11), and SPWL (28), and the least accurate is respectively HCTH (12), *m*PWB95 (13), MPW1K (32), BB1K (28), and SVWN3 (33). The errors are much smaller if one limits attention to dimers with small amounts of multi-reference character, although even here the trends are different from main-group chemistry. This study shows very clearly that the methods that perform well for transition metal bonds are not the same ones that perform best for main-group chemistry. This study identified a key anticorrelation: none of the methods (*e.g.*, MPW1K or BB1K) that did well for barrier heights also did well for transition metal bond energies. This was shortly before the design of the M05 functional, which would be the first to overcome this limitation.

In a second paper, Schultz *et al.*,[94] again following the guideline of using only the most reliable data for validation, made databases of 21 metal–ligand bond energies and 13 metal–ligand bond distances. Of the 21 and 13 molecules in these sets, respectively 17 and 9 contain transition metals. The transition metals represented are V, Cr, Mn, Fe, Co, Rh, Ni, Cu, and Ag. A total of 57 density functionals were tested. A composite MUE was created based on main group atomization energies per bond, transition metal dimer bond energies, metal–ligand bond energies, atomic ionization energies (including metals), transition metal dimer bond lengths, and metal–ligand bond lengths. Based on this composite MUE the most accurate density functionals are, in order, G96LYP (a GGA), MPWLYP1M (a hybrid GGA), and XLYP, BLYP, MoHLYP and *m*PWLYP (four more GGAs). These tests preceded the creation of several more successful modern functionals such as B97-3, PW6B95, M05, M06-L, and M06.

In the process of analyzing the data in the two papers just discussed,[93,94] Schultz *et al.* created smaller representative databases, the first containing a subset of four transition-metal dimers and the second containing four metal–ligand complexes. Mean errors computed with these small databases reproduce the mean errors of the full databases remarkably well and allow one to gauge the accuracy of new density functionals very conveniently by comparing the results on the small databases to those for the very large number of functionals already tested against these databases.

The tests conducted with the databases of Furche and Perdew and of Schultz *et al.* are overall reasonably consistent.[38,93–95,406,412] They have been reviewed in detail by Harvey[413] in an excellent review that provides very useful general comments about testing DFT.

de Jong and Bickelhaupt[414] tested 26 density functionals for reaction energies and saddle point energies of oxidative addition of the C–Cl bond of CH3Cl to Pd atom. The best performing functionals, excluding HCTH, and their mean unsigned errors in kcal mol^{-1} were found to be X3LYP (1.4), RPBE (1.7), B3LYP (1.8), RevPBE (2.0), and BLYP (2.9). Three different parametrizations of the HCTH functional were tested with mean unsigned errors of 0.8, 1.0, and 4.2. Quintal *et al.*[415] tested 25 functionals for Pd oxidative addition reactions, the mechanism of the Heck reaction (which involves Pd in the 0, II, and IV oxidation states), the reduction of acetone by hydrogenation with a Rh complex, and other data. They found the best performance by hybrid meta functionals in particular B1B95 and PW6B95, followed by the hybrid PBE0, the hybrid meta TPSS25B95 (which is TPSS plus B95 with $X = 25$), and the hybrid B97-1 and B97-2.

Li *et al.*[416] tested 27 functionals (unfortunately, these were mainly old ones—25 from 2001 or earlier and one each from 2003 (TPSS) and 2004 (BMK)) against benchmark-quality WFT data for atomization energies and clustering energies of $(MO_2)_n$ (M = Ti, Zr, and Hf) and $(MO_3)_n$ (M = Cr, Mo, and W) transition metal oxide clusters with $n = 1$–4. Among the functionals tested, PBE0 performed best. In another recent study that tested only older density functionals, Mayhall *et al.*[417] tested PW91, B3LYP, and PBE for heats of formation of a test set of twenty small molecules (eighteen of which have 2–4 atoms) containing 3*d* transition metals and found mean unsigned errors of 5–22 kcal mol^{-1}, with B3LYP being the best.

Schultz *et al.*[326] obtained benchmark values and studied bond energies, geometries, and dipole moments of PdCO and Pd_2CO with 27 density functionals. They defined a mean percent unsigned error in three bond energies, two dipole moments, and five bond lengths. Both triple-ζ and quadruple-ζ basis sets were employed. The most accurate results were obtained with O3LYP (2%) and OLYP and PW6B95 (both 3%), followed by B97-1, B98, and MPW1K (all 4%). The least accurate methods were BMK (18%) and PBE, TPSS, BP86, and *m*PWPW (all 14%). This paper was published too soon to test M05, M06, or M06-L. Ge *et al.*[418] used PW91 to study CO adsorption on Pt and Au nanoparticles. (PW91 was not included in the study of Schultz *et al.*[326] because it is usually less accurate than its successors, PBE and *m*PWPW.) A similar strategy for testing DFT by comparing to coupled cluster calculations for MCO and M_2CO has been applied by Schwerdtfeger *et al.*,[419] who applied it for M = Au as compared to M = Pd here; their work is discussed in section 5.3.1.9.

de Jong *et al.*[420] tested 24 density functionals against a CCSD(T) benchmark for the energies along the reaction path for the oxidative addition reaction of Pd atom with methane, in particular, the relative energies of the separated reactants, the reaction complex, the saddle point, and the products. Their assessment includes the LSDA, 14 GGAs, 2 hybrid GGAs, and 7 meta functionals, but it did not include any of the six functionals mentioned above as having performed best in the later study of Quintal *et al.*[415] for Pd oxidative addition reactions. This study involved post-SCF calculations with the BLYP density, and the VS98 and TPSSh functionals performed best, with MUEs below 2 kcal mol^{-1}. The least accurate functionals and their MUEs in kcal mol^{-1} were LSDA, ~16; OLAP3, ~10; and PW91, PBE, and BP86, each ~6.

Ikeda *et al.*[421] calculated coupled cluster-quality binding energies of d^6, d^8, and d^{10} transition metals with π-conjugated systems with up to ten carbon atoms, and they used these results to test the B3LYP, B3PW91, BLYP, BP86,

BH&HLYP, mPW1PW, and LSDA functionals. They found that LSDA overestimates the binding energies and the other functionals significantly (*e.g.*, 25 kcal mol^{-1}) underestimate them when the π-conjugated system has four or more carbon atoms.

Li and Dixon[422] used experimental electron detachment energies for MO_6^- (M = Cr, Mo, and W) and $M_2O_6^-$ (M = Cr and W) to test the predictions of CCSD(T) and 28 functionals. They found that BP86 performed best, with a maximum error of 0.29 eV and second largest absolute error of 0.07 eV; CCSD(T) had a maximum and second largest absolute error of 0.31 and 0.12 eV respectively. DFT was found to be more accurate than CCSD(T) for systems with large multi-reference character. For heats of formation of MO_6 and M_2O_6, CCSD(T) was more accurate than DFT, and among functionals tested (only three were tested for heats of formation), B3LYP was most accurate, although the largest absolute error was 44 kcal mol^{-1}.

S. Zhao *et al.*[423] applied 23 density functionals to relative energies of different structures, ionization potentials, bond distances, and vibrational frequencies of neutral and ionic clusters containing up to four Ag atoms. PBE0 was found to be the most satisfactory functional. Functionals that tend to the correct limit for a uniform electron gas (UEG) were judged to be more satisfactory than those that do not.

Stevens *et al.*[424] applied two LSDAs, seven GGAs, seven meta GGAs, and four hybrid GGAs to bond distances, vibrational frequencies, and dipole moments of diatomics of Cr, Mo, and W with C, N, and O. The BP86 functional was judged to be the most satisfactory.

Rogal *et al.*[425] compared the LSDA, PBE, and RPBE functionals against experiment for the heat of formation of bulk PdO and the binding energies of O_2, CO, and CO_2 on Pd(110). The mean unsigned errors in these four quantities are 0.3 eV for RPBE, 0.6 eV for PBE, and 1.9 eV for LSDA, with 9 of the 12 values being overestimates.

Song *et al.*[426] applied one LSDA, three GGAs, and five hybrid GGAs to bond energies, bond lengths, and vibrational frequencies of 20 4*d*-series neutral and cationic monoxides. The main conclusions about performance were based on bond energies of neutrals, and the local BP86, BLYP, and BPW91 functionals were deemed to have best performance.

Sears and Sherrill[427,428] assessed the performance of the BP86, BPW91, and B3LYP functionals for Sc, Ti, V, Nb, Cr, Mo, and Mn complexes of bis(salicylaldehyde)ethylenediamine. The accuracy for relative energies was found to be poor, which was attributed to multi-reference character.

Ghosh *et al.*[429] provided multi-reference WFT calculations of the low-energy states of Fe^{III}, Co^{III}, and Ni^{III} diiminato complexes to serve as standards against which to evaluate the spin-state predictions of various density functionals. In particular they tested BP86, BLYP, PW91, OLYP, OPBE, B3LYP, and B3LYP*. The found that B3LYP performed best in these cases but cautioned that previous work by Ghosh and Taylor[430] showed opposite trends in functional performance for some bis(salicylaldehyde)ethylenediamine compounds.

In the first full benchmark study published after the hybrid meta M05 functional[34] became available, Zhao *et al.*[233] tested 14 functionals against 234 data in several databases including the two representative metal databases of Schultz *et al.*[93,94] For the latter, they found the best performance by BLYP and M05 (MUE = 6 kcal mol^{-1}), and the least accurate performance by BMK (MUE = 27 kcal mol^{-1}). M05 was found to have the advantage of working well both for systems with low multi-reference character and systems with high multi-reference character and to give much more accurate barrier heights, noncovalent interaction energies, and main-group bond energies than any previous functional with relatively good performance for transition metals. Zhao *et al.* concluded that designing the dependence of the exchange–correlation functional to take full advantage of the dependence on kinetic energy density and to be consistent with a reasonably high percentage of Hartree–Fock exchange was the key to this breakthrough.

Sousa *et al.*[220] reviewed the status of DFT and assessed the performance of many functionals for a variety of chemical properties. The review is very thorough up to mid 2006.

Zhao and Truhlar[38] carried out additional validation studies when the local meta M06-L functional became available. Nine GGAs, three meta GGAs, two hybrid GGAs, and one hybrid meta GGA were tested against 22 energetic databases plus main-group and metal–ligand bond lengths and main-group vibrational frequencies. Three of the energetic databases (all discussed above: two of Schultz *et al.*[93,94] and one of Furche and Perdew[95]) contain compounds containing transition metals. The composite MUE for these three metal databases ranged from 6 kcal mol^{-1} (M06-L) to 14 kcal mol^{-1} (τ-HCTH). The best performances following M06-L were: 7 kcal mol^{-1} for M05 and 8 kcal mol^{-1} for G96LYP, OLYP, and TPSS. BLYP and B3LYP had MUEs of 8.5 and 12 kcal mol^{-1}, respectively. A broader composite including main-group thermochemistry (atomization energies per bond and bond energies, ionization potentials, electron affinities, proton affinities, and π isomerization energies), barrier heights, noncovalent interactions, the metal databases mentioned above, and metal atom excitation energies yielded the following MUEs in kcal mol^{-1}: 3 for M06-L and M05, 5 for B3LYP, 5.5 for TPSSh, 6 for eight functionals, 7 for two others, and 7.5 for G96LYP. M06-L and M05 can be strongly recommended.

Yet another extensive evaluation was carried out when M06 became available.[39] Two GGAs, five hybrid GGAs, two meta GGAs, and seven hybrid meta GGAs were tested against 29 energetic databases, three bond length databases, one vibrational frequency database, and one zero point energy database (496 data). The M06 functional was recommended as the best for organometallic and inorganometallic chemistry. It also predicts accurate noncovalent interactions. A review is available.[412]

Amin and Truhlar[235] tested 39 density functionals against 12 bond energies, 10 bond lengths, and 8 dipole moments in Zn coordination compounds with H, NH_3, O, OH, H_2O, S, and SCH_3 ligands. It was found to be important to include scalar relativistic effects. The three best performing functionals overall were found to be M05-2X, PW6B95, and B97-2, in that order. A follow-up study[431] involved a larger dataset that also included binding energies and dipole moments of Zn centers in coordination environments taken from metalloenzymes, for

which bond lengths can be quite different than in small compounds. M05-2X continued to perform well, and B3LYP was found to have some large errors.

Paier *et al.*[432] published a study entitled "Why does the B3LYP hybrid functional fail for metals?" This study contains tests of the PBE, B3PW91, B3LYP, PBE0, and HSE functionals for lattice constants, bulk moduli, and cohesive energies of various metallic and nonmetallic systems. Transition metals are represented by bulk Rh, Pd, Cu, and Ag, and some aspects of the conclusions apply to all metals. In particular they conclude that the B3LYP functional "fails to describe the transition from localized electrons (atoms) to delocalized electrons (metals)". This failure is ascribed about 2/3 to the LYP correlation functional and about 1/3 to the B88 exchange functional. Behavior for extended systems with large gaps (*e.g.*, LiF, NaF, MgO, and diamond) was quite different from that for bulk metals. The authors concluded, as had many (but not all) workers before them, that it is important to incorporate the UEG limit.

Stroppa and Kresse[433] followed up by testing the accuracy of the BLYP, PBE, RPBE, B3LYP, HSE, AM05, and PBEsol functionals for the adsorption site and adsorption energy of CO on the (111) surfaces of Ru, Os, Rh, Ir, Pd, Pt, and Ag. They found that BLYP and B3LYP are the "overall best" choices for these adsorption properties among the functionals tested, but they were simultaneously dismayed that these functionals perform poorly for the properties of the metal itself, as discussed in the previous paragraph.

When the RPBE functional was originally developed,[204] it was tested for adsorption energies of O, CO, and NO on Rh(100), Ni(100), Pd(100), and Pd(111). RPBE and revPBE gave similar results, with noticeable improvement over PBE. In tests on molecules, Matveev *et al.*[434] found that revPBE and RPBE were more accurate than BP86, PW91, and PBE both for atomization energies of small molecules and for dissociation energies of $Cr(CO)_6$ and $Fe(CO)_5$. Deeth and Fey[435] tested the BLYP, PW91, PBE, revPBE, and RPBE functionals for geometries and energies of homoleptic $Fe^{II}L_6$ and $Fe^{III}L_6$ complexes, where L denotes a ligand. When solvation effects were included, the best performance was obtained with RPBE. However, the preference for low-spin states in iron complexes was overestimated by $\sim$13 kcal mol^{-1}. More recently, Mattsson *et al.*[219] tested the LSDA, BLYP, PBE, RPBE, PBE0, AM05, and HSE functionals for lattice constants and bulk moduli of 23 solids, seven of which (W, Rh, Pd, Pt, Cu, Ag, and Au) were transition metals. AM05, PBE0, and HSE outperformed LSDA and PBE, which in turn outperformed RPBE and BLYP. These trends (*e.g.*, RPBE better than PBE for energies but worse than PBE and AM05 for lattice constants) can seemingly be understood from the principles that emerged from the benchmarks of Zhao and Truhlar.[214] Zhao and Truhlar tested PBE, PBEsol, SOGGA, TPSS, and M06-L for lattice constants of 21 solids, including Rh, Pd, Cu, Ag, and $PbTiO_3$, cohesive energies of eight main-group solids, six representative atomization energies of main-group molecules, six representative barrier heights, the dissociation energy of SF_6, 20 main-group bond lengths, and the exchange energy and total energy of the He atom. For three lattice constants the comparisons also included LSDA, BLYP, PW91, BPW91, *m*PWPW, and RPBE. For lattice constants, SOGGA and M06-L were usually most accurate, followed by PBEsol, with RPBE and BLYP least accurate. For energies, M06-L was most accurate followed by RPBE. Again we see RPBE more accurate than PBE for energies and less accurate for interatomic distances. This, along with several other trends, was rationalized by examining the second-order term in the gradient expansion of the exchange functional. The results are also consistent with the analysis of Perdew *et al.*,[215] and they extend that analysis. Perdew *et al.*[216] have made the point that fitting to the jellium surface exchange–correlation energy is not a possible explanation of the relative performance of various functionals for the lattice constants of solids, and Csonka *et al.*[436] have recently tested selected density functionals for lattice constants, bulk moduli, and cohesive energies of nonmolecular solids (metals and nonmetals, including Rh, Pd, Cu, and Ag) and provided further discussion of the tradeoffs one must make in GGAs such that it may be impossible to develop a single GGA that can accurately predict solid-state cohesive energies, surface energies, lattice constants, and bulk moduli. Yet another test of functionals for surface properties has been provided recently by Haas *et al.*,[437] who found the best performance for lattice constants for 60 solids with PBEsol and SOGGA, which outperformed LSDA, PBE, TPSS, WC, and AM05. Unfortunately, neither the Csonka *et al.* paper[436] nor the Haas *et al.* paper[437] considers the M06-L functional.

Ropo *et al.*[438] tested the LSDA, PBE, LAG, AM05, and PBEsol functionals against exchange energies of five rare gas atoms, atomization energies of six main group diatomic molecules, and lattice constants and bulk moduli of eight metals (including Fe, W, Pd, Pt, Cu, and Au), three semiconductors, and NaCl (an insulator). They suggested that AM05 and PBEsol are superior to PBE and LAG.

Tran *et al.*[439] compared the performance of the LSDA and the PW91, PBE, and WC GGAs for main-group bond lengths and noncovalent interactions, for the surface formation energies and cohesive energies of ten bulk transition metals, and for the lattice constants and bulk moduli of 76 solids, including 14 bulk transition metals and 22 binary solids containing one transition metal and one main-group element. They found that the WC functional gives the most accurate lattice constants (MUE of 0.03 Å *vs.* 0.04 for PBE and 0.07 for LSDA) but that none of the functionals tested was uniformly better than the others for all properties. Many interesting systematic trends were observed such as how the errors change as one proceeds across a transition row.

Rinaldo *et al.*[440] evaluated the errors in B3LYP thermochemical predictions for 56 transition metal atomic energies and 71 bond energies of transition metal compounds and found MUEs of 7.7 and 5.3 kcal mol^{-1} respectively. They developed an empirical scheme to correct these errors.

Bühl *et al.*[441] tested 14 density functionals against 41 transition metal–ligand bond distances in 25 5*d*-series molecules. They found the best results for PBE0. They also updated previous tests for the 3*d* and 4*d* series, and for the combined test set comprising all three transition rows they obtained the best results with PBE0, B3P86, and B3PW91. They found that BLYP, VSXC, and LSDA "cannot be recommended". It would be interesting to extend these tests to M06-L and B98.

Handzlik[442] evaluated 22 density functionals against experimental data and CCSD(T) calculations for the thermochemistry of molybdenum compounds. The best performance was obtained with TPSS, PW91, PBE, and M05. M05 was the only functional with nonzero Hartree–Fock exchange to show good performance. The M06 and M06-L functionals were not included in the tests.

Although the study does not include transition metals, the work of Mosch *et al.*[443] on the interaction of O_2 with Al clusters and Al(111) is very relevant. They found, just as for nonmetallic reactions,[444] that GGAs (for example, they studied PBE) systematically underestimate barrier heights for reactions of metal clusters and at metal surfaces.

5. Applications

We now consider applications of particular interest that have appeared in the recent literature.

5.1 Spin state and magnetic properties

Spin and associated magnetic interactions in transition-metal-containing systems are often discussed within the context of considering the molecular system to be composed of one or more subsystems over which unpaired spin is localized, *e.g.*, the various transition-metal atoms in a cluster (for an interesting discussion of the physical meaning of spin localization in the context of various electronic structure theories, including DFT, see Reiher[445]). It is convenient to use a spin-labeled model Hamiltonian to describe such localized spins as if they interact as coupled angular momenta, as proposed by Heisenberg[446] and Dirac[447] and later elaborated by Van Vleck[448] and Slater.[449] This model has been used extensively in conjunction with DFT to explain magnetic properties in coordination compounds.[450–452]

If we restrict ourselves here, for simplicity, to two interacting centers A and B, the Heisenberg–Dirac Hamiltonian takes the form

$$H = -2J_{AB}S_A\cdot S_B \qquad (5)$$

where S_X is the local spin on center X, J_{AB} is the coupling constant between the two centers, and the dot product between the spins is considered only for antiparallel (antiferromagnetic, low-spin) or parallel (ferromagnetic, high-spin) vectors. It is important to keep in mind that eqn (5) is a shorthand description and should not be taken as an indication that magnetic interactions are involved; they are not. Rather the parameter J_{AB} results from exchange integrals involving electron repulsion. When the S^2 values for the pure spin states of the full system and the two fragments are well defined, the eigenvalues of the operator $S_A\cdot S_B$ for alternative total spin states may be determined from the relationship

$$S^2 = (S_A + S_B)^2 = S_A{}^2 + S_B{}^2 + 2S_A\cdot S_B \qquad (6)$$

If there is a single unpaired electron on each center A and B, the eigenvalues of $S_A{}^2$ and $S_B{}^2$ are each 3/4; therefore $\langle S_A\cdot S_B\rangle$ is −3/4 for singlet coupling (for which $\langle S^2\rangle = 0$) and 1/4 for triplet coupling (for which $\langle S^2\rangle = 2$). With such definitions of $S_A\cdot S_B$, eigenvalues of the Heisenberg–Dirac Hamiltonian are given by

$$E_S = -J_{AB}S(S+1) \qquad (7)$$

where S takes on whole or half-integer values ranging from $|S_A - S_B|$ to $|S_A + S_B|$, and where $-S_A(S_A+1) - S_B(S_B+1)$ has been moved into the zero of energy.

For a single unpaired electron on each center A and B, a linear combination of atomic orbitals (LCAO) wave function for the high-spin triplet state is typically well represented by a single determinant and in that respect is well suited for treatment by DFT within the Kohn–Sham formalism. In another respect though, it may be less well suited than the singlet because DFT is a ground-state theory and the triplet state might not be the ground state. The wave function for the low-spin singlet state, however, in the limit of weak coupling requires at least two determinants for a balanced description and is thus problematic for Kohn–Sham DFT if the goal is to compute directly the energy difference between the two states (the same problem holds for direct calculation of the $M_S = 0$ triplet).[453–456] This discussion may be generalized to multiple spins on each center, where the high-spin case (in which S is equal to the highest possible value of M_S) continues to be single determinantal. As originally discussed by Ziegler *et al.*[457] and Noodleman,[458] a non-physical broken-spin-symmetry state can be useful for predicting the proper state-energy difference in such instances. Cohen *et al.*[459] have recently noted that the broken-symmetry approach provides a formal way to circumvent static correlation errors in existing functionals by avoiding fractional spins in, say, stretched two-electron bonds.

The broken-symmetry state is constructed by permitting the system to localize antiparallel, unpaired spins separately on the two centers A and B. Such a situation is clearly non-physical, since, for instance, an antiferromagnetically coupled singlet would have up density on one center and down density on the other but a true singlet has zero spin polarization density at every position in space.[452,454] In the weakly interacting limit, however, this wave function is formally a weighted average of pure spin states, and Noodleman[458] has shown that the coupling constant J_{AB} may be estimated from it as[460,461]

$$J_{AB} = -\frac{^{HS}E - {}^{BS}E}{4|S_A||S_B|} \qquad (8)$$

where HS and BS denote high-spin and broken-symmetry, respectively. When the high-spin state has low multi-reference character, its Kohn–Sham DFT energy is sometimes taken (as a working hypothesis) as accurate (within the accuracy of the chosen functional) and the energies of other spin states are then computed relative to it using eqn (7) with the value of J_{AB} determined from a broken-symmetry calculation according to eqn (8).

In the limit of strong coupling, Ruiz *et al.*[462] have proposed that it is more appropriate to consider the broken-symmetry state to represent the true low-spin state (*e.g.*, the singlet state for an even number of electrons). This is equivalent to modifying eqn (8) as

$$J_{AB} = -\frac{^{HS}E - {}^{BS}E}{4|S_A||S_B| + 2|S_B|} \qquad (9)$$

where center B has the smaller of the two spins if the spins on A and B are not the same. In effect, eqn (9) simply expresses the energy difference from a ΔSCF calculation (that is, the difference in energy of separate SCF calculations on each state) of the two spin states in the J coupling notation of the Heisenberg–Dirac formalism.

Alternatively, Yamaguchi and co-workers[463,464] have suggested an approach designed to be valid over the full range from the weak to strong coupling limits

$$J_{AB} = -\frac{^{HS}E - {}^{BS}E}{^{HS}\langle S^2\rangle - {}^{BS}\langle S^2\rangle} \qquad (10)$$

where the expectation values of S^2 are evaluated for high-spin and broken-symmetry Kohn–Sham determinants, *i.e.*, they are treated as trial wave functions of this many-electron operator. Since the Kohn–Sham determinant is *not* the variational wave function for the electronic Hamiltonian, use of eqn (10) is necessarily empirical for DFT, but practical experience suggests that it can be effective. More recently Shoji *et al.*[465] have generalized the approach underlying eqn (10) in order to permit its application to systems having more than two interacting spin sites.

From a fundamental standpoint, there has been substantial discussion in the literature with respect to the meaning of $\langle S^2\rangle$ as determined from the Kohn–Sham determinant. Although the Kohn–Sham determinant has (for the unknown exact density functional) the same density as the exact wave function (and therefore provides a convenient parameterization of the density), its relationship to the actual wave function is not formally defined in DFT, and there has been lively debate with respect to the interpretation of the expectation value of the many-electron operator S^2. In 1995, Pople *et al.*[466] argued that restricted open-shell Kohn–Sham procedures were inappropriate for DFT as they would not properly predict negative spin densities in open-shell systems (the same can be said of restricted open-shell Hartree–Fock methods), and suggested—based on empirical observation—that spin contamination was not as significant a problem in DFT as in wave-function theories (which was first pointed out by Baker *et al.*[467] and others[64,468–471]), emphasizing, though, that one cannot be certain that $\langle S^2\rangle_{KS}$ is necessarily a quantitative *measure* of spin contamination (where $\langle\ldots\rangle_{KS}$ denotes an expectation value over the Kohn–Sham determinant). Wang *et al.*[472] pointed out that $\langle S^2\rangle$ can be computed from one- and two-particle density matrix elements, and examined $\langle S^2\rangle$ as a function of various approximations for the two-particle matrix elements that are not strictly available from a DFT calculation. A deeper analysis of the relationship between $\langle S^2\rangle_{KS}$ and spin contamination was provided by Cremer and co-workers[473–475] based on analysis of the total and on-top pair densities for a variety of systems having open-shell biradical character, following an approach first suggested by Perdew *et al.*[21] Cremer and co-workers noted that $\langle S^2\rangle_{KS}$ is not necessarily in good quantitative agreement with $\langle S^2\rangle$ as evaluated by other means for the Kohn–Sham density, but that $\langle S^2\rangle_{KS}$ is qualitatively useful in terms of its description of the degree to which mixing of spin states is present in the Kohn–Sham determinant. A number of subsequent works have explored the relationship between the spin properties of the Kohn–Sham determinant and the true wave function, in general emphasizing that the former need not satisfy the same restrictions as the latter.[51,476–479]

Returning to applications, the relative utility of eqn (8) [or its generalization eqn (10)] *vs.* eqn (9) for predicting magnetic coupling has been debated in the literature, but no clear consensus has emerged because results have been variable depending on the chemical system studied and the functional employed. For example, Valero *et al.*[480] recently compared results from eqn (8) and (9) for a number of functionals, including those in the M06 family,[39] for several binuclear copper complexes as well as other non-metallic biradicals, and observed that M06-L, M06, and B3LYP were more accurate with eqn (8), while M06-2X was more accurate with eqn (9), and PBE0 showed no preference for eqn (8) *vs.* eqn (9). One of the earliest studies employing the broken-symmetry approach was also to binuclear copper complexes, in particular 2-azido bridged compounds, where Adamo *et al.* observed that predicted exchange interactions using the *m*PW1PW functional were extremely sensitive to geometry.[481] Ruiz and co-workers[482] compared eqn (8) to eqn (9) for a binuclear copper complex and found that while the latter worked better with standard functionals, the former was better when self-interaction error was removed explicitly following the Perdew–Zunger approach.[112] They concluded that self-interaction error effectively cancelled the error associated with the non-dynamical correlation not captured by the single-determinant Kohn–Sham model, thereby eliminating the need to employ eqn (8) to correct for the latter error. This interpretation was, however, challenged by Adamo *et al.*,[483] who asserted that in general spin symmetry must be restored to broken-symmetry wave functions [*e.g.*, by the mapping associated with eqn (8)] in order to provide proper estimates of the energy.

In a different study also focusing on binuclear copper complexes, Lewin *et al.*[484] considered singlet–triplet splittings in various supported dicopper–dioxygen complexes in both their isomeric bis(μ-oxo) and μ-η^2:η^2-peroxo structural forms. These species provide a particularly interesting test set because the instability of their singlet Kohn–Sham orbital representations to spin-symmetry breaking is highly dependent on the choice of functional. Thus, with local functionals like BLYP or *m*PWPW, restricted closed-shell singlets are predicted to be stable or metastable in Kohn–Sham calculations, while the incorporation of Hartree–Fock exchange tends to lead to instability to symmetry breaking. In this case, six different functionals (BLYP, *m*PWPW, TPSS, TPSSh, B3LYP, and *m*PW1PW) are in reasonable agreement with one another for singlet–triplet splittings of the μ-η^2:η^2-peroxo isomers, where $\langle S^2\rangle$ values range from 0.00 to 0.95 depending on ligand and functional, but only when eqn (10) is used—use of eqn (9) leads to quite poor results for those cases having the greatest biradicaloid character (the importance of using eqn (10) to compute the singlet energies was also inferred from analysis of bis(μ-oxo)/μ-η^2:η^2-peroxo isomerization energies[484–486]). Interestingly, in the bis(μ-oxo) isomers, all functionals predicted rather similar singlet–triplet splittings when closed-shell singlets were assumed, even in those cases where a

broken-symmetry instability existed. Similar observation have been made for a number of monocopper complexes of dioxygen.[487,488] In all of these cases, it appears that substantial degrees of covalency in Cu–O interactions, as judged from explicitly multi-reference calculations,[489] can lead to improved predictions with restricted DFT calculations that would otherwise be inappropriate in more weakly coupled systems. In a very recent contribution, Rivero *et al.* also considered exchange coupling in binuclear copper compounds, but examined the performance of range-separated hybrid functionals for this task;[490] they concluded that such functionals might have utility for the study of magnetic interactions in metal oxides and other challenging solids. A study by Roth *et al.*[491] on a trinuclear copper complex supported by aminosugar Schiff base ligands found B3LYP* to give reasonable agreement with experiment for a small doublet–quartet splitting (-91 cm^{-1} *vs.* -24 cm^{-1}), with some of the discrepancy being attributed to delocalization of the spin on one of the coppers over adjacent coordinating heteroatoms, thereby limiting the applicability of the Heisenberg–Dirac model.

Another set of systems showing great sensitivity of the ground electronic state and symmetry breaking to the choice of functional are the intermediate-spin systems MnPc and FePc molecules, where Pc is phthalocyanine. Marom and Kronik[492] studied these systems with B3LYP, PBE, PBE0, and M06.

Another study comparing DFT to multi-reference calculations has been carried out by Batista and Martin,[493] who examined the binuclear ruthenium blue dimer $[(bpy)_2(OH_2)RuORu(OH_2)(bpy)_2]^{4+}$. In two prior publications, Yang and Baik[494,495] had initially reported a singlet ground state for this species and then a triplet ground state based on B3LYP calculations and a broken-symmetry formalism. Batista and Martin employed CASSCF. They had difficulty converging certain of the states reported by Yang and Baik, but noted that their CASSCF calculations predict a singlet ground state consistent with magnetic susceptibility measurements[496] and inconsistent with the B3LYP results. As the active space employed for the CAS wave function included only 10 electrons in 6 orbitals and dynamical correlation effects were not subsequently estimated, the CASSCF result is not quantitatively accurate, but the overestimation of the triplet stability by B3LYP is noteworthy and additional studies to assess the influence of Hartree–Fock exchange in the functional would be interesting.

A comparison of DFT to much more highly correlated multi-reference results has been reported by Pierloot and Vancoillie for the singlet–quintet energy splittings in [Fe(L)(NHS_4)], where NHS_4 is 2,2′-bis(2-mercaptophenylthio)diethylamine dianion and L = NH_3, N_2H_4, PMe_3, CO, and NO^+.[497] On the basis of comparison to extended-basis-set CASPT2 calculations, these authors noted that DFT functionals incorporating increased Hartree–Fock exchange did better in more ionic systems, but the opposite was true for more covalent systems (*cf.* the discussion of copper–dioxygen systems above). They found that OLYP offered the best quantitative performance for computing the spin-state energy splittings compared to other functionals that they tested, but noted that this functional did a poor job of predicting geometries and that its extensibility to other systems was suspect. Swart reported that the O exchange functional, when combined with PBE correlation, also gave good results for the ground spin states and geometries of a number of iron halide ions and spin crossover compounds.[498] Rong *et al.*[499] compared various functionals for state-energy splittings in supported iron complexes and suggested that the bias towards low-spin states observed for local as opposed to hybrid functionals could be attributed to a more localized frontier orbital that was placed at higher energy in the orbital manifold for the local functionals than for the hybrids. Carreon-Macedo and Harvey have emphasized the significant challenges associated with accurately computing the very small spin-state splittings in iron carbonyls, even with very large basis set CCSD(T) calculations,[500] where CCSD denotes coupled cluster theory (a single-reference WFT approach) with single and double excitations, and CCSD(T) denotes CCSD with a quasi-perturbative treatment of connected triple excitations. We note that CCSD(T) is usually reasonably reliable for single-reference systems but is of unknown validity for multi-reference systems, as illustrated by the following example.

The difficulty of evaluating the accuracy of DFT for spin-state orderings is well illustrated by a study of NiO_2. In main-group chemistry, a high-level WFT calculation is often used to provide a benchmark, and the most widely used method for this purpose is CCSD(T). Song *et al.*[501] employed CCSD, conventional CCSD(T), and four versions of locally renormalized CCSD(T), abbreviated as LR-CCSD(T), to calculate the singlet–triplet splitting (Δ, defined as energy of singlet minus energy of triplet) in the cyclic form of NiO_2. For the same problem, they also employed other WFT methods, namely multi-reference configuration interaction, without (MRCI) and with (MRCI + Q) a Davidson correction, CASSCF, and generalized Van Vleck perturbation theory (GVVPT2, a form of multi-reference perturbation theory), as well as two GGAs, including PBE, and two hybrid functionals, PBE0 and TPSSh. Conventional CCSD(T), one of the four LR-CCSD(T) methods, and GVVPT2 predicted negative Δ of -7, -5, and -8 kcal mol^{-1}, respectively, whereas CCSD, the other three LR-CCSD(T) calculations, CASSCF, MRCI, and all four DFT calculations predicted positive Δ, with the DFT predictions in the range 7–11 kcal mol^{-1}. Their best estimate was that Δ is positive and equal to about 4 kcal mol^{-1}. The MRCI and MRCI + D calculations predicted +12 and +13, respectively, significantly higher than their best estimate and also higher than DFT (of course MRCI would become exact if enough configurations were included, but this is impractical even for this triatomic system). Although the argument for what is the best value of Δ is not completely convincing, this study shows the danger and uncertainties associated with using either conventional CCSD(T) or MRCI as a benchmark for transition-metal systems. We also note the work of Neese examining the triplet and quintet states of $[FeO(NH_3)_5]^{2+}$ and comparing DFT to multi-reference WFT.[502]

A thorough comparison of methods including B3LYP was undertaken by Matxain *et al.*[503] for the scandium dimer. Based on many prior DFT calculations and an unclear experimental

situation, the ground state of Sc_2 came to be accepted as $^5\Sigma_u$, and indeed at the B3LYP level this state is predicted to be lowest by 0.08 eV. However, large CASPT2 calculations and diffusion quantum Monte Carlo calculations both predict that the $^3\Sigma_u$ state is 0.16 eV below the $^5\Sigma_u$ state and that the other properties of the $^3\Sigma_u$ state, namely the vibrational frequency and the dissociation energy, are in equally good agreement with experiment as those predicted for the $^5\Sigma_u$ state. Sorkin *et al.*[479] also considered state-energy splittings in diatomic cases, in particular Fe_2, Fe_2^-, and FeO^+. They highlighted the accuracy of predicted state-energy splittings from Kulik *et al.*[138] employing the PBE + U approach, although they noted that the U potentials employed in such calculations tend to be system-specific, and found that within the uncertainty in experimental values, B3LYP, M05, and M06 also gave reasonable results, but without system-dependent parameters. Sorkin *et al.* interpreted all of their broken-symmetry results as corresponding to $S = M_S$, *i.e.*, without resorting to spin purification, and additionally noted the importance of permitting *spatial* symmetry breaking. In particular, in the case of FeO^+, they observed a monotonic decrease in computed electronic energies for the $^4\Phi$ state upon reducing the imposed symmetry from C_{6v} to C_{4v} to C_{2v}, and the predicted energy relative to the $^6\Sigma^+$ ground state was found to improve with reduced symmetry.

Returning to spin-purified calculations, a particularly interesting variation on the use of the broken-symmetry approach to compute state-energy splitting has been reported by Herrmann *et al.*[504] for a study of the spin-state energetics ranging from $S = 0$ to $S = 4$ in the $[Fe_2O_2]$ core of methane monooxygenase. In this case, the use of eqn (10) was compared to an alternative[505]

$$J_{AB} = -\frac{^{HS}E - {}^{BS}E}{2(^{HS}\langle S_A \cdot S_B\rangle - {}^{BS}\langle S_A \cdot S_B\rangle)} \qquad (11)$$

where the expectation value of the $S_A{\cdot}S_B$ operator is computed using local projector techniques as described either by Clark and Davidson[506] or by Mayer.[507] The primarily methodological study of Herrmann *et al.* indicated substantial quantitative dependence of predicted J values on the amount of Hartree–Fock exchange in the functional employed (a similar sensitivity for a different bridged diiron core was observed by Hübner *et al.*[508]), and found that predictions from eqn (11) using Clark and Davidson's $S_A{\cdot}S_B$ operator differed from eqn (10) by 223 cm^{-1} (about a factor of 2) for a representative geometry, with eqn (10) being closer to the experimental value of less than 30 cm^{-1}. Podewitz *et al.*[509] later compared results from Clark and Davidson's approach to that obtained using Mayer's alternative for a set of supported iron and manganese clusters; they concluded that Mayer's method provided more physically meaningful measures of spin population on individual atoms (*i.e.*, when evaluating $S_A{\cdot}S_B$), but the two approaches give nearly identical results for $S_A{\cdot}S_B$ so that coupling constants computed using eqn (11) are insensitive to this choice.

Another new development that has begun to see application is the use of constrained DFT[510–512] (cDFT) to generate broken-symmetry Kohn–Sham determinants having their uncoupled spins localized by the chosen constraints, as opposed to determined only by the variational energy. As the energy of the broken-symmetry state does not correspond to a true spin state, including additional constraints need not be regarded as unphysical. Thus, Difley *et al.*[513] have used cDFT to study the singlet–triplet splittings of geminate electron-hole pairs in the charge-transfer configurations of zinc–organic light emitting devices, and Rudra *et al.*[514] have adopted the approach to study spin-frustrated iron and chromium clusters. In the latter case, Rudra *et al.* emphasize that optimal results can be obtained by associating each constrained Kohn–Sham determinant and its energy with an individual spin-coupling scheme in the Heisenberg–Dirac Hamiltonian. Using these energies the relevant coupling constants in multisite magnetic systems can be easily computed from the Heisenberg–Dirac Hamiltonian itself rather than by invoking a broken-symmetry projection scheme. Schmidt *et al.*[515] have recently described an extension of the cDFT approach that in addition to constraining spin localization constrains the magnitude of spin contamination computed from the Kohn–Sham orbitals. Schmidt *et al.* observe that the additional inclusion of the spin-contamination restraint is essential for the accurate computation of hyperfine couplings in doublet $[Mn(CN)_5NO]^{2-}$. In other work focused on multisite systems, Fliegl compared broken-symmetry approaches to CASCI models in order to examine magnetic couplings in a structural model for the tetramanganese-containing oxygen evolving complex in photosystem II and noted that BS DFT approaches tended to overestimate ferromagnetic couplings between centers.[516]

In the context of solid-state calculations, Ciofini *et al.* have observed that τ-dependent local functionals provide good accuracy for the prediction of exchange coupling constants in $KNiF_3$ and K_2NiF_4 insulators by broken-symmetry approaches.[517] Avoiding hybrid functionals and the costly computation of their HF exchange component speeds the solid-state calculation.

The use of broken-symmetry approaches in computing magnetic exchange is motivated by the poor performance of standard Kohn–Sham DFT for states that are not well represented by single determinants, like singlet-coupled diradicals. An alternative approach explored for cases of two unpaired electrons is to abandon the single determinantal formalism of the Kohn–Sham model and adopt the restricted ensemble-referenced Kohn–Sham (REKS) approach of Filatov and Shaik.[518–520] In this case the singlet density is constructed from two closed-shell Kohn–Sham determinants differing from one another by a single orbital, *i.e.*,

$$\rho^{REKS}(\mathbf{r}) = 2\sum_{i=1}^{N/2-1} |\phi_i(\mathbf{r})|^2 + n_r|\phi_i(\mathbf{r})|^2 + n_s|\phi_i(\mathbf{r})|^2 \qquad (12)$$

where N is the total number of electrons and n_r and n_s are fractional occupation numbers (that sum to two) for the two non-common orbitals. The REKS energy is then taken to be

$$\begin{aligned} E^{REKS} = {} & \tfrac{1}{2}[n_r E^{KS}(\ldots\phi_r^2) + n_s E^{KS}(\ldots\phi_s^2)] \\ & + f(n_r,n_s)\{E^{KS}(\ldots\phi_r\phi_s) - \tfrac{1}{2}[E^{KS}(\ldots\phi_r\bar{\phi}_s) \\ & + E^{KS}(\ldots\bar{\phi}_r\phi_s)]\} \end{aligned} \qquad (13)$$

where f is a factor whose value may be chosen by analogy to CASSCF calculations or simply empirically. Comparison of REKS singlet energies to restricted-open-shell Kohn–Sham (ROKS) triplet energies then offers an alternative means to compute $2J$ values in systems with 2 unpaired spins. Moreira *et al.*[521] compared the REKS approach with different factors f to use of eqn (8) for 6 binuclear copper complexes having J values ranging from –382 to 111 cm^{-1}. They found that with eqn (8) the predicted J values correlated reasonably well with experiment, but the slopes of the correlations were 4.8, 1.6, and 0.5 for the BLYP, B3LYP, and BH&HLYP functionals, respectively [note that the slopes in this case would be one-half of the values with eqn (8) if eqn (9) were used instead]. Thus, there is considerable sensitivity in the approach to the amount of Hartree–Fock exchange included in the functional. With the REKS approach based on eqn (13), Moreira *et al.*[521] observed similar correlations and slopes of the correlations to those obtained with eqn (8) for B3LYP and BH&HLYP. The concluded that eqn (8) is the more appropriate one for use in these systems when prediction from the broken-symmetry SCF solution is undertaken (*cf.* the contrasting conclusions of Valero *et al.*[480] above with M06 results) and that improved quantitative performance of the REKS formalism will be contingent on improved understanding of how to avoid double counting the electron correlation energy by designing functionals specifically for use in the REKS approach, a point which Perez-Jimenez *et al.*[522] have explored in more detail for various antiferromagnetic solids and biradicals. Ukai *et al.*[523] have also explored the application of more general CAS-DFT approaches for computations of magnetic properties for the complexes $V(H_2O)_6^{3+}$, $V(CO)_6^{3+}$, and $[Cu(H_2O)]_2(\mu\text{-}CH_3CO_2)_4$.

Other alternatives to the broken-symmetry approach include the use of so-called spin-flip DFT, where the antiferromagnetically coupled low-spin state can be rigorously described as an excited state of a single-determinantal high-spin reference.[524] In a recent study of copper–dioxygen complexes, de la Lande *et al.*[525] observed good agreement between spin-flip singlet–triplet splittings and either experiment or multi-reference WFT predictions; they further emphasized that the spin-flip formalism permits optimization of the molecular geometry without the spin-state ambiguities associated with broken-symmetry calculations and also that analysis of the spin-flip excitations can be useful for identifying suitable active spaces for subsequent multi-reference WFT calculations. Rhee and Head-Gordon have also successfully employed spin-flip DFT to characterize molecules containing oxidized CuPCuP rings as singlet diradicals.[526]

A difficulty with spin-flip DFT as originally introduced is that, with collinear density functionals (which are used in the overwhelming majority of applications), the spin flip can only be introduced by Hartree–Fock exchange, and thus the theory can be used only with hybrid functionals. In local collinear functionals, the functional depends on the spin-up and spin-down densities, the magnitudes of their gradients, and, in meta functionals, the spin-kinetic energies or the Laplacians of the spin densities. However, as mentioned in section 3.2, noncollinear functionals also depend on the off-diagonal elements of the spin density matrix, and they induce spin-flip transitions even in the absence of Hartree–Fock exchange;[527] the resulting noncollinear spin-flip TD-DFT[527–530] is more satisfactory; so far, however, applications to systems containing transition metals are in their infancy.[531]

Another recently described alternative to broken-symmetry DFT involves the use of perturbation theory and the second derivative of the Kohn–Sham energy for a single, chosen reference state.[532] And, in somewhat older work, Cramer *et al.*[64,471] considered correcting broken-symmetry DFT energies based on application of wave function spin-projection operators to the Kohn–Sham Slater determinant. It will be interesting to observe how these various approaches perform as additional applications are reported for transition-metal containing systems.

We will not review here in detail recent developments or applications associated with the use of DFT to compute EPR and NMR spectral parameters for open-shell systems containing transition metals. Rather, we refer readers to the recent review of Neese for a thorough coverage of this subject,[452] and we note briefly a few interesting reports. Teale *et al.*[24] have recently compared NMR chemical shifts computed from GGA and hybrid functionals using the optimized effective potential (OEP) formalism. Alam *et al.*[533] predicted ^{19}F chemical shifts in fluoropolyoxotantalates and in particular the influence of Ta–F spin–orbit coupling on those shifts, and Autschbach and Zheng[534] have used two-component relativistic DFT to rationalize the influence of nonbonding Pt 5d orbitals on Pt chemical shifts in supported coordination compounds having oxidation states from II to IV. Morbec and Capelle[535] have recently emphasized the connections between spin–orbit polarization terms in spin DFT and the exchange correlation vector potential that arises in current-density functional theory, which may serve as an interesting alternative for the computation of magnetic spectral quantities. Hrobárik *et al.*[536] calculated EPR parameters for oxo-molybdenum(v) and oxo-tungsten(v) complexes by two-component relativistic calculations.

5.2 Electronic and vibrational spectroscopy

5.2.1 Electronic spectroscopy. The primary method for computing transition energies to electronically excited states within the framework of DFT is to employ a time-dependent formalism[537,538] (TD-DFT, which was introduced in section 2.3), and the strengths and limitations of that model have been amply reviewed elsewhere.[159,232,452,539–544] With respect to transition-metal complexes, a particularly troublesome feature of TD-DFT is the tendency of many functionals to significantly underestimate the energies of excited states characterized by high degrees of non-local charge transfer, although in principle this problem may be addressed by replacing the DFT exchange functional by 100% Hartree–Fock exchange,[232,545] by using certain range-separated functionals,[188,190,236] as in a recent application to charge transfer excitation in pyridine complexes with Ag_{20},[546] or by going beyond first-order response.[173] Nevertheless, linear-response TD-DFT with various functionals continues to be an especially useful one-electron model for understanding the optical spectra of transition-metal complexes. We highlight a few examples here.

Salassa *et al.*[547] have used TD-B3LYP to study the singlet and triplet excited states of Ru^{II} polypyridine complexes and to explain their photodissociation behaviors on the basis of the excited-state potential energy surfaces (a number of earlier TD-DFT studies of Ru and Os polypyridyl complexes have been reported with the goal of rationalizing their absorption spectra in the gas and condensed phases[548–554]). Jackson *et al.*[555] have employed TD-DFT to characterize the intense near UV absorptions in axially ligated Fe^{IV}═O complexes as ligand to Fe═O charge transfer transitions and thereby rationalize the strong resonance enhancement of the Fe═O stretching mode upon excitation of these transitions. Hutin *et al.*[556] characterized the unusual mixed valence excited state of a binuclear copper helicate with TD-B3LYP and TD-BP86 and further computed its circular dichroism in order to assign its absolute chirality which derived from an interesting self-sorting process during crystallization. Later, Schultz *et al.*[557] showed that this mixed valence behavior extends over all 4 copper atoms in a helicate dimer, thereby rationalizing experimental cyclic voltammetry data and indicating a potential means to construct a wrapped molecular copper wire. In addition, Bar-Nahum *et al.*[558] found TD-B98 to be especially helpful in explaining an unusual long wavelength metal to ligand charge-transfer transition occurring in a mixed valence trinuclear copper disulfide (Fig. 1).

A recent review provides an overview of DFT and TD-DFT applications to electronic spectroscopy and excited-state properties of d^6 metal carbonyls, strongly phosphorescent cyclometallated complexes, Ru^{II} photosensitizers (as used, for example, in solar cells and light switches), and isonitrile complexes of Re^{I} and Ru^{II}.[559]

Fan *et al.*[560] used spin-unrestricted TD-DFT with the BP86 density functional, a continuum solvation model, and empirical corrections to calculate circular dichroism spectra of a number of trigonal dihedral Cr^{III} d^3 complexes and compared to earlier related work.

Perala *et al.*[561] used TD-DFT and magnetically perturbed TD-DFT with statistical averaging of orbital potentials[562] to calculate ultraviolet and magnetic circular dichroism spectra

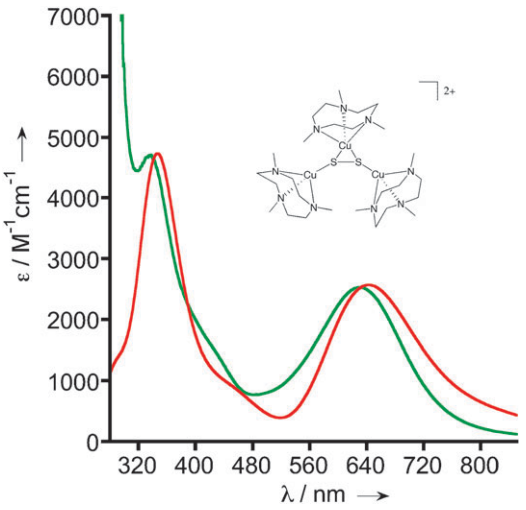

Fig. 1 Experimental (light) and computed (TD-B98, 0.2 eV offset, dark) UV/Vis spectrum for the inset trinuclear copper complex.

of MTAP (M = Ni, Zn) and ZnPc where TAP denotes tetraazaporphyrin.

Another particularly useful application of TD-DFT is for the interpretation of the optical spectra of intermediates too reactive to be readily isolated. Thus, Kunishita *et al.*[563] inferred the creation of a reactive Cu^{II} 2-hydroxy-2-hydroperoxypropane intermediate upon addition of hydrogen peroxide to a solution of a supported Cu^{I} complex in acetone based on a comparison of measured UV spectral data to those computed at the TD-B98 level, thereby rationalizing subsequent reactivity of this complex.

In the area of larger inorganic clusters, Stener *et al.*[564] have successfully reproduced and rationalized the blue shift in the optical spectra of gold nanoparticles with decreasing cluster size using scalar relativistic TD-DFT applied to clusters of 146, 44, and 6 gold atoms. Stener *et al.*[565] have also examined the optical spectroscopy of the WAu_{12} and $MoAu_{12}$ clusters at the TD-DFT level, noting that while spin–orbit coupling merely shifts the energies of the lower excitations in the former compound, it gives rise to more complex splittings in many of the excitations for the latter compound. In subsequent work, Stener *et al.*[566] added to their comparison TD-DFT results for the anionic dodecahedral clusters VAu_{12}, $NbAu_{12}$, and $TaAu_{12}$.

It is important to note that medium effects on optical spectra (solvatochromism) can be large for polar transition-metal compounds, and the inclusion of such effects in the TD-DFT model is typically most efficient when the surrounding medium is modeled as a dielectric continuum. Thus, for example, Charlot and Aukauloo[552] have assessed aqueous solvatochromic effects on the spectra of Ru^{II} polypyridine complexes using the non-equilibrium polarized continuum model[567–569] (PCM). De Angelis *et al.*[570] have employed a similar strategy combined with Car–Parrinello molecular dynamics to simulate the optical properties of dye sensitizers interacting with TiO_2 nanoparticles, such systems being critical components of modern dye-sensitized solar cells. Lundqvist *et al.*[571] used B3LYP to study the structural and optical properties of ruthenium polypyridyl complexes on TiO_2 nanoparticles. The spectra[550,572,573] and photovoltaic parameters[574] of dyes adsorbed on bulk TiO_2 surfaces were also studied with B3LYP. Abuabara *et al.*[575] studied the dynamics of interfacial electron transfer at catechol-sensitized TiO_2 with the PW91 functional.

In the cases of smaller inorganic molecules, various benchmark studies of DFT protocols compared to WFT methods have been undertaken. Ramirez-Solis *et al.*[576] have compared DFT to CASPT2 and multi-reference averaged coupled pair functional (ACPF) results for the lowest ligand-field states of $AgCl_2$, including consideration of spin–orbit effects. Considering the B97-2, B3LYP, and PBE0 functionals, they found that DFT predicted the first excited $^2\Sigma_g^+$ state to be too high in energy relative to the $^2\Pi_g$ ground state by about a factor of 2. Although improved results could be obtained by increasing the percentage of Hartree–Fock exchange in B3LYP to 42%, this led to poor prediction of molecular geometries. In general, the DFT densities were found to predict excessive delocalization of unpaired spin density in the various states, this phenomenon being attributable to self-interaction error.

In the ultra-high energy region of electronic spectroscopy, DFT has proven to be a popular tool for the interpretation of X-ray absorption spectra (XAS) in transition-metal containing systems. In the most straightforward applications, the only DFT calculation undertaken is for the ground state. Experimental pre-edge XAS intensities D_0 for ligand atoms may be interpreted according to[577]

$$D_0^{\phi_{\text{core}}\rightarrow\phi^*} = \frac{\alpha^2 h}{3n}\langle\phi_{\text{core}}|\mathbf{r}|\phi^*\rangle \qquad (14)$$

where the core electron is typically 1s, α^2 is the covalency of the light atom's valence p orbitals mixed into the acceptor orbital ϕ^* (expressed as a percentage), h is the number of holes in the acceptor orbital (or orbitals in the event of degeneracy), n is the number of absorbing atoms, and the transition dipole moment is estimated based on empirically determined linear relationships with measured edge XAS intensities into outer light-atom orbitals. Following experimental near-edge intensity measurements, eqn (14) is solved for α^2 and the covalencies so determined are compared to those computed from atomic basis orbital contributions to computed Kohn–Sham virtual orbitals. Analogous procedures may be used with metal XAS intensities. In this way, the nature of the acceptor orbitals and the ordering of the virtual manifold may in principle be established, offering insights into ligand and metal oxidation states and redox behavior.

Applying this XAS analysis approach, ligand effects on the covalency of supported Fe^{IV}=O species have been assessed,[578] the varying oxidation states of S_2 bridges in binuclear copper complexes have been characterized,[579] and the effects of different ligands and oxidation states on the properties of copper and nickel bis(dithiolene)[580] and molybdenum tris(dithiolene)[577] complexes have been rationalized.

In terms of predicting actual near-edge XAS transition energies, TD-DFT in principle provides a means to predict such one-electron excitation energies in the same fashion in which valence to valence excitations are computed. However, the total number of all possible one-electron excitations is MN where M is the number of occupied orbitals and N the number of virtual orbitals, so applying TD-DFT for *all* one-electron excitations is cumbersome. Instead, the TD-DFT process is modified so that only core orbitals are included in the linear response equations. Thus, the remaining occupied molecular orbitals do not relax with respect to the core hole, although the valence orbitals are all responsive since they are included in the calculation. While this approach tends to lead to large absolute errors, it has shown good utility in the prediction of *relative* transition energies, and has been applied to assess the covalency of metal-chloride bonds in metallocene dichlorides, both with[581] and without[582] accounting for relativistic spin–orbit effects. The inclusion[583] of spin–orbit effects using the two-component zeroth-order regular approximation (ZORA) leads to significant improvements in predicted absolute excitation energies for heavy transition metals. In addition, the TD-DFT for XAS approach has been used to characterized metal ligand covalency in oxomolybdenum compounds relevant to the sulfite oxidase active site.[584] A particularly interesting application of this method to study benzenedithiolate complexes of Ni, Pd, Pt, Cu, Co, and Au offered insights into those factors affecting the innocence or non-innocence of the benzodithiolenes.[585] Other recent studies have provided insights into the nature of relativistic and solvation effects on K-edge XAS spectra for Fe^{II} and Fe^{III} species,[586] as well as for "superoxidized" Fe^{V} and Fe^{VI} complexes.[587,588] Finally, in something of a DFT tour de force, Sarangi *et al.*[589] used both ground-state DFT and valence and near-edge TD-DFT to compare changes in bonding, UV spectra, and pre-edge XAS spectra between the wild-type blue copper active site of azurin and a mutant substituting selenocysteine for cysteine. These authors found that changes in Cu–S *vs.* Cu–Se bond distances led to very similar covalencies in the two copper–chalcogen bonds, so that spectra were minimally affected in spite of the 0.2 Å variation in bond lengths.

As an alternative method to computing electronic excitation energies, Cheng *et al.*[590] and Gilbert *et al.*[591] have both recently described an approach they call excited-state DFT (eDFT) or the maximum overlap method (MOM), where in each instance the Kohn–Sham procedure is modified so that the total energy is minimized subject to a constraint that the final density has maximal overlap with a target density. In this way densities that correspond to systems with one or more holes in low energy orbitals may in principle be constructed and their Kohn–Sham energies determined directly (as opposed to using TD-DFT). In the case of a system of non-interacting electrons, selection of a target density is trivially accomplished by swapping one or more virtual orbitals with occupied orbitals. By turning on the adiabatic coupling in small steps, Cheng *et al.*[590] found that they were able to achieve self-consistent eDFT solutions even for Rydberg states and Gilbert *et al.*[591] showed the utility of MOM for charge-transfer excited states. This work is too preliminary to have been applied to any transition-metal containing systems, but it has the potential to sidestep known problems with TD-DFT in such complexes, so we mention it here.

An interesting question in the spectroscopy and optics of metal clusters is the quenching of spin–orbit coupling as a function of geometry. This was studied using PBE for gold clusters by Castro *et al.*[592]

One key application where it is important to predict the correct spin-state splitting is multi-state reactivity. Yang *et al.*[593] used B3LYP calculations to study the gas-phase spin-forbidden addition reactions of Y^+, Zr^+, Nb^+, Mo^+, Pd^+, and Ag^+ with N_2O to form $MONN^+$, where M denotes the metal atom; the location of the crossing scheme is sensitive to the spin-state splitting. Additional examples are found in the two-state reactivity examples studied by Shaik and coworkers,[594] which are discussed briefly in section 5.3.1.6, and in the two-state triplet–singlet mechanism for olefin epoxidation and oxidation reactions studied by Morokuma and coworkers.[595]

5.2.2 Vibrational spectroscopy. The computation of vibrational frequencies is nearly always undertaken in modern practice in order to verify the nature of optimized stationary points. The comparison of computed frequencies to values measured by IR or Raman spectroscopy is also routine, and we will not address such studies here, although the

performance of various functionals on benchmark data sets is summarized above in section 4. One study focusing more specifically on an information provided by the vibrational spectrum has been described by Hebben *et al.*[596] In order to critically assess a prior suggestion[597] that homoaromatic interactions between ethylene ligands causes the geometry of $Ni(C_2H_4)_3$ to have all of its heavy atoms in a common plane, Hebben *et al.*[596] used BP86 calculations to assign in detail measured IR and Raman spectra for $Ni(C_2H_4)_3$, $Pd(C_2H_4)_3$, and $Pt(C_2H_4)_3$. From analysis of the interfragment force constants, they concluded that homoaromaticity plays no role in the structures of these species: the Ni and Pd cases are well described as Dewar–Chatt–Duncanson complexes; the Pt case includes some metallacyclopropane character. A prior study noted the high accuracy of hybrid functionals with respect to predicting the vibrational spectra of $Ni(C_2H_4)$ and $Ni(C_2H_4)^+$.[598]

Vibrational spectroscopy can be useful in assigning chirality in transition metal complexes, typically from comparison of experimental and computed vibrational circular dichroism (VCD) or Raman optical activity (ROA) spectra.[452,599–601] Some recent examples in this area include prediction of VCD[602] and ROA[603] spectra for some chiral tris(acetylacetonato) metal complexes.

Coupling optical and vibrational spectroscopies, resonance Raman and off-resonance Raman spectroscopies also play key roles in the characterization of transition-metal containing systems.[604–606] Recent advances in the direct computation of resonance Raman intensities have been reported,[452,600,601,607] and applications have included examination of the first photoexcitation step in a tetranuclear (Ru_2Pd_2) light-harvesting complex[608] and the determination that benzenedithiolate ligands need not be innocent in complexes of group 8, 9, and 10 metals.[609]

Another interesting use of computed vibrational frequencies is for the construction of molecular partition functions from which equilibrium or kinetic isotope effects (EIEs and KIEs, respectively) may be computed so as to gain improved insight into electronic structure or mechanism. We note in particular recent work of Popp *et al.*[610] which reported a computed $^{18}O/^{16}O$ KIE in good agreement with experiment for the formation of a PdO_2 adduct. Popp *et al.* found the rate-determining step to involve an end-on to side-on isomerization of the O_2 unit, which was contrary to an earlier proposal[611] that the measured KIE was consistent with a concerted 2-electron oxidation and direct side-on binding of the O_2. Roth and co-workers have also been quite active in comparing experimental and DFT-derived KIEs in transition-metal containing systems.[611–614] In recent work on O_2 binding to Cu[614] and also in rationalizing $^{18}O/^{16}O$ KIEs in horseradish peroxidase,[615] it has been emphasized that EIEs need not represent upper limits on KIEs, which had hitherto been a fairly common assumption for O_2-binding reactions in the bioinorganic community.[613]

In another interesting study making use of the full vibrational partition function, Brehm *et al.*[616] used the BP86 functional to compute the differential vibrational entropic contribution to temperature-dependent spin crossover in $[Fe(pmea)(NCS)_2]$ (pmea = {bis[(2-pyridyl)methyl]-2-(2-pyridyl)ethylamine}), providing insights into its low-spin to high-spin transition.

Carbonniere *et al.*[617] studied anharmonic effects on the vibrational spectra of d^0 transition-metal tetroxides and found B3LYP and PBE0 to offer good comparison with experiment, while BP86, OLYP, and TPSS did less well.

5.2.3 Nonlinear optical properties. Most applications of TD-DFT are carried out using the linear-response formalism in which the applied electromagnetic field is weak; this is sufficient for single-photon spectroscopy. Nonlinear optics[618,619] and two-photon spectroscopy[620] require high-order treatments or a combination of TD-DFT with a sum over states, and such treatments are beyond the scope of this review.

5.3 Structure, reactivity, and other properties

This section is divided into six subsections, focusing on coordination complexes/clusters and organometallics, solids, surfaces, systems having special relevance to heterogeneous catalysis, those having special relevance to electrocatalysis and those having special relevance to photocatalysis.

5.3.1 Coordination complexes/clusters and organometallics. We organize this subsection, which addresses coordination complexes/clusters and organometallics, by the transition-metal groups in the periodic table from left to right. In some cases this organization has the unfortunate consequence that a given type of problem is discussed in more than one subsection, but there is no completely satisfactory organizing principle for such a broad survey. Of course, certain transition metals have been the subject of considerably more theoretical attention than others, but we make an effort to identify at least one interesting application for each element insofar as this is possible. In many instances, a particular modeling study may have addressed several different transition metals, in which case we have tended to discuss it within a group that offers opportunities to compare to other, perhaps more specifically focused work. As there are a vast number of reports from which to choose, we have inevitably applied somewhat arbitrary selection principles in determining which studies to highlight below. Thus, for instance, we do not discuss full metalloenzyme studies, but we do summarize several small-molecule model studies relevant to metalloenzyme active sites. We trust that readers will understand that such choices were essential to maintaining a reasonable size for the review.

Before starting to work our way across the periodic table, we mention an especially relevant review by Ziegler and Autschbach,[621] who surveyed a large number of applications of DFT to inorganic and organometallic reaction mechanisms and kinetics. We also direct the reader to a somewhat older but very concentrated thematic issue of *Chem. Rev.* devoted to computational transition metal chemistry.[622]

5.3.1.1 Scandium, yttrium, lanthanum. We have already discussed in section 5.1 the DFT calculations of Matxain *et al.*[503] associated with the computational determination of the ground state for Sc_2.

Group 3 metallocenes have been studied extensively as catalysts for C–H bond activation, and olefin polymerization, hydroamination, and hydroalkylation.[623–632] The primary focus of these studies has been to elucidate the influence of

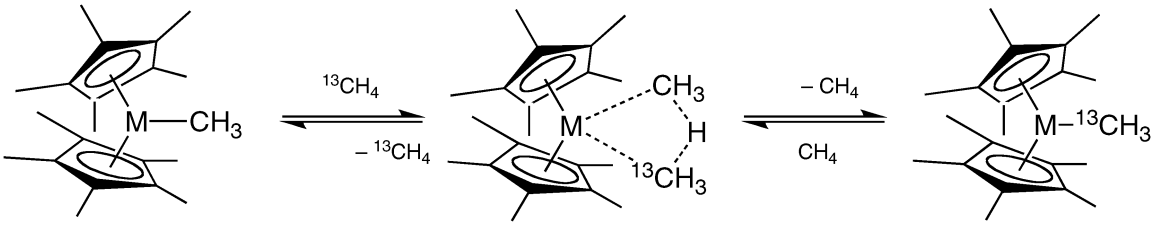

Fig. 2 Methane metathesis in a methyl group-3 metallocene.

varying degrees of ligand steric bulk and metal size on reactivity. In the case of C–H bond activation, transition-state theory rate constants computed for methane metathesis (Fig. 2) at the *m*PW1PW level were found to be in good agreement with experiment as long as important contributions from tunneling were included.[623] The utility of *ansa* ligands with respect to increasing the exposure, and thus reactivity, of the metal center, has been a particular subject of study.[627,632] Vastine and Hall[633] have examined the transition-state structures for the methane metathesis shown in Fig. 2, for the illustrated scandocene, for $[Cp^*Ir(PMe_3)(CH_3)]^+$, and for some additional systems; using atoms-in-molecules analysis[634] of the electron density they conclude that a continuum of mechanisms ranging from σ-bond metathesis (shown in Fig. 2) to oxidative addition/reductive elimination can be operative in the overall metathesis process.

Cationic alkyl complexes of Sc or Y have also been found to be effective polymerization catalysts, and Tredget *et al.*[635] used DFT to characterize the structural details of various such species, noting the general presence of stabilizing agostic interactions.

Scott *et al.*[636] have used DFT to characterize the metal–ligand binding in a novel methylidene scandium complex. In addition, the first examples of compounds containing a μ^4 bonded hydride species, the tetranuclear polyhydride clusters $[(C_5Me_4SiMe_3)_4M_4H_8]$ with M = Y and Lu, were characterized by Luo *et al.*[637] at the PW91 level, elucidating structural features obscured by significant disorder in the Lu crystal structure.

5.3.1.2 Titanium, zirconium, hafnium. In a recent study of all-inorganic metallocene analogs of the early transition metals, which have been the subject of considerable prior theoretical attention,[638–640] Mercero *et al.*[641] characterized the electronic structures of the sandwich compounds $(cAl_4)_2M^{n-}$ for M = Ti, V, Cr, Nb, Mo, Hf, Ta, and W, where *n* is 2, 1, or 0 for metals in groups 4, 5, and 6, respectively, and cAl_4 is the 4-membered ring composed entirely of aluminium atoms that is triply aromatic as a dianion. Mercero *et al.* found that the sandwich compounds of groups 5 and 6 were stable, maintained strong aromaticity in the cAl_4^{2-} rings, and were not prone to autodetachment of an electron. Introduction of an alkali cation was required to prevent such autodetachment in the case of the group 4 analogs.

Ochi *et al.*[642] studied C–H and N–H bond activation at Ti^{IV} imido complexes with B3LYP and WFT. They drew conclusions not only from energetics (energetic stability of a precursor complex) but also by analysis of the atomic populations, orbitals, and orbital interactions at stationary points.

The growth of zirconium clusters up to 15 atoms has been studied by Sheng *et al.*[643] using the PW91 functional. These authors found that cluster sizes of 7, 13, and 15 were particularly stable, and that all clusters were particularly active with respect to the dissociative chemisorption of molecular hydrogen. Joubert *et al.*[644] have studied the alkane hydrogenolysis reactivity of ZrH species supported on alumina surfaces at the PW91 level.

Mandal *et al.*[645] have characterized at the B3LYP level the olefin polymerization activities of two hybrid metallocene-nonmetallocene polynuclear complexes, in one case a binuclear (ZrTi) species and in the other a trinuclear (Zr_2Hf) species. They found that cationic zirconocene sites are more energetically favorable but that cationic titanium sites are more sterically accessible so that bimodal activity would be expected for the polymerization of small *vs.* sterically hindered alkenes. Lewin and Cramer[646] have described a multilevel quantum protocol that combines DFT for zirconocenes with small-basis-set Hartree–Fock calculations or molecular mechanics calculations using modified carbon effective core potentials to account for changes in the electron-donating strengths of alkyl-substituted metallocenes. Wondimagegn *et al.*[647,648] have use QM/MM calculations with the BP86 density functional for the QM part to suggest improved zirconocene catalysts for olefin polymerization. Morokuma has provided an historical overview of DFT studies on the activation of molecular nitrogen by homogeneous zirconium catalysts.[595]

5.3.1.3 Vanadium, niobium, tantalum. We noted in section 5.2 the TD-DFT calculations of Stener *et al.*[566] undertaken to rationalize the optical spectra of MAu_{12}^- clusters, where M = V, Nb, and Ta.

Owing to the importance of vanadium oxide catalysts in a number of heterogeneous industrial processes, a substantial amount of work has been done applying DFT to study the reactivity of small V_mO_n clusters with various species. Thus, Dong *et al.*[649,650] have studied the gas-phase oxidation of saturated and unsaturated hydrocarbons by such clusters at the B3LYP level, comparing theoretical predictions to product distributions generated in mass spectrometric experiments. In analogous work, Ma *et al.*[651] have examined the cyclotrimerization of acetylene catalyzed by VO_2, and Gracia *et al.*[652] have studied the gas-phase reaction of propyne with VO_2^+.

The VO_2^+ cation may be present in aqueous solution during the hydrothermal synthesis of vanadophosphates. To better understand its behavior in aqueous solution, Sadoc *et al.*[653]

have performed Car–Parrinello simulations using the PBE functional. They determined that a five-coordinate $VO_2^+(H_2O)_3$ species was most stable, but that strongly acidic conditions were required to prevent spontaneous deprotonation of this compound.

Because of the utility of the ^{51}V nucleus in NMR, various studies have appeared combining DFT and NMR to gain insights into geometric and electronic structural details, *e.g.*, in heptacoordinate hydroxylamido vanadium picolinate complexes[654] and oxoperoxo vanadium complexes of lactic acid.[655]

Michelini *et al.*[656] used B3LYP to calculate energies along the gas-phase reaction paths for $Nb^+(^3P)$ and $Nb^+(^5D)$ reacting with ethane to produce H_2, C_2H_4, H, or C_2H_6. Validation of available functionals for the relative energies of high-spin and low-spin insertion transition states would be valuable for this kind of calculation.

Arteaga-Müller *et al.*[657] have characterized the electronic structures of supported niobium and tantalum imido compounds in order to better rationalize their activities as catalysts for the polymerization of methyl methacrylate. Based on orbital analysis they emphasize the isolobal character of the niobium and tantalum complexes compared to mono-cyclopentadienyl zirconium complexes.

5.3.1.4 Chromium, molybdenum, tungsten. The series of supported transition-metal dimers $Pn^*_2M_2$ where Pn* is permethylpentalene ($C_8Me_6^{2-}$) and M = V, Cr, Mn, Co, and Ni has been prepared by Ashley *et al.*[658] and the character of the metal-metal bonding has been analyzed using the BP86 functional. In particular, a triple bond is observed between the two V atoms, a double bond between the two Cr atoms, a single bond between the two Mn atoms, and single bond character is maintained in the cases of Co and Ni but the coordination of the Pn* fragments to the metals is increasingly reduced from η^5 to η^3. For the Cr case, replacing the Pn* ligands with 1,4-triisopropylpentalene ligands leads to a supported metal dimer having a ground state best characterized as two antiferromagnetically coupled $S = \frac{1}{2}$ Cr atoms, but the triplet state is measured to be higher in energy by only about 0.5 kcal mol^{-1}, so that paramagnetic behavior is observed at room temperature.[659] BP86 and B3LYP calculations incorrectly predict the triplet state to be the ground state by 2–3 kcal mol^{-1}, and CASPT2 calculations of the state-energy splitting using partially relaxed DFT structures also incorrectly predict a triplet ground state but by only 0.6 kcal mol^{-1}.

The nature of bonding between bare and supported Cr_2 dimers has been extensively explored by Gagliardi and co-workers[660–665] because of substantial interest in the very high bond order between the two atoms and the significant challenge to many theoretical models posed by the nature of the bonding.[93,658,659,666–669] In experimental practice, the very high bond orders inferred for supported chromium dimers compared to iron or cobalt analogs are attributable to the tendency for the latter two metals to preferentially bond to arenes included in the ligand structure; chromium exhibits a much smaller tendency to engage in such bonding.[664]

The activity of Mo and W alkylidene complexes as catalysts for olefin polymerization has been studied by Poater *et al.*,[670] who found at the B3PW91 level that turnover efficiency was related to a balance between the stability of metallacycle intermediates in the catalytic cycle and energies required to distort the organometallic from its resting tetrahedral geometry. Haunschild *et al.*[671] used B3LYP to characterize the many possible paths for reaction of ethylene with the group 6 alkylidenes $MO_2(CH_2)(CH_3)$ for M = Cr, Mo, and W.

Caramori and Frenking[672] have carried out energy decomposition analysis at the DFT level to characterize the bonding of Mo to P, N, PO, and NO ligands.

Yan *et al.*[673] employed the BP86 functional and a continuum model of acetonitrile solvation to study alternating bond lengths in Mo-containing polyoxometallates, which they attributed to pseudo Jahn–Teller distortions involving frontier π bonding and antibonding orbitals.

Schenk *et al.*[674] have used BP86 (with occasional state-energy splittings computed using B3LYP*) to study the nitrogenase activity of the Schrock catalyst MoHIPT (HIPT = tris[(*N*-hexaisopropylterphenyl)-2-amidoethyl]amine). The local nature of the BP86 functional was critical for efficiency with the very large HIPT ligand, which was found to have a significant influence on predicted reaction energetics compared to prior studies that employed smaller model ligands.[675–682] Christian *et al.*[683] came to similar conclusions with respect to the importance of including the full ligand in rationalizing differences between the full HIPT ligand *vs.* model ligands in the Schrock and related systems. Schrock[684] has recently provided a very interesting comparison of theoretical predictions and experiment for such molybdenum-based complexes, noting that theory has proven particularly helpful in elucidating the role of added acid in the reaction mechanism. Stephan *et al.*[685] have recently detailed acid effects further in various steps relevant to catalysis. Finally, Dance[686] has summarized the implications of these and other theoretical studies with respect to the biological nitrogenase activity of the FeMo cofactor.

Leyssens *et al.*[687] examined the changes in electron density (and molecular geometry) associated with one-electron oxidations of chromium and molybdenum phosphine and amine complexes, and they noted that the changes are consistent with significant metal to phosphorus π back bonding that is not present in the analogous amine compounds. This analysis approximated the Fukui function as a full electron finite difference calculation.[688]

5.3.1.5 Manganese, technetium, rhenium. A key feature of the group 7 series is the ready accessibility of their high-spin d^5 states following oxidation by two electrons in the presence of a suitably weak ligand field. Matxain *et al.*[689] have used MPWB1K to study the endohedral Mn@Sn_{12} molecule and its dimer in order to evaluate its potential for the construction of a magnetic material. They predict that the Mn^{II} ion inside the dodecahedral Sn_{12}^{2-} cage prefers a high-spin ground state by more than 1 eV, that it has a large ionization potential, and that two such endohedral complexes associate, without reorganization to a more networked solid, with a binding energy on the order of 0.03 eV. The exchange coupling (computed using eqn (10) above) of the dimer is computed

to be -5 cm^{-1}, *i.e.*, high-spin coupled, suggesting that the monomer should be an interesting precursor from which to make potentially magnetic materials. In analogous work, Matxain *et al.*[690] considered endohedral complexes of the first 8 third-row transition metals in Z_nS_n cages for $n = 12$ and 16. In all cases, they found the endohedrally trapped species to be thermodynamically stable, and negligible spin or charge transfer was observed from the interior metal atom to the surrounding cage, such that the high-spin state of each atom was preferred, again suggesting that materials built from such encapsulated species might have interesting magnetic properties.

Manganese is also of particular interest as the transition-metal found in the active site of the oxygen evolving complex (OEC) in photosynthesis. Yamaguchi *et al.*[691] investigated the electronic structures of manganese–oxo bonds using hybrid DFT, comparing a high-valent manganese–oxo porphyrin complex to the active Mn=O bonds found in both native OEC and artificial systems. The oxygen atoms in these bonds were found to be highly electrophilic in nature and also to exhibit strong biradical character, not unlike the situation observed for other high-valent metal oxos like those found in methane monooxygenase (MMO) and cytochrome P450 (see below). Relevant to such systems, Balcells *et al.*[692] have emphasized that in oxomanganese porphyrins, only high spin states placing substantial radical character on the O atom are reactive for C–H bond activation, so that *trans* ligands stabilizing the singlet ground state relative to the high-spin states decrease reactivity.

The studies of Ashley *et al.*[658] and Balasz *et al.*[659] on various bimetallic pentalene sandwich compounds have been highlighted above in section 5.3.1.4. In addition, for the case of Mn_2 bis(1,4-triisopropylpentalene), a particularly interesting phenomenon is observed: one of the two Mn^{II} atoms is low-spin ($S = \frac{1}{2}$) and coordinated η^5, while the other is high-spin ($S = 5/2$) and coordinated η^2.[693] B3LYP calculations predict that the state having $M_S = 3$ is 1.1 kcal mol^{-1} lower in energy than that having $M_S = 2$, consistent with magnetic susceptibility measurements that suggest an $S = 3$ state lying slightly below an $S = 2$ state. With respect to the binuclear rhenium, Krapp *et al.*[694] have performed energy decomposition analysis at the DFT level to quantify the importance of σ, π, and δ bonding in $Re_2Cl_8^{2-}$.

Lundberg and Siegbahn[57] tested BLYP, HCTH, B3LYP, B3LYP*, and B98 for O–H bond energies and bond lengths in six aqua- and hydroxyl-manganese complexes. The best functional was found to be B3LYP with an MUE of 3 kcal mol^{-1}, and the least accurate was BLYP with an MUE of about 20 kcal mol^{-1}.

Jia *et al.*[695] applied B3LYP to investigate interconversions of five-coordinate monooxo Tc^{V} and six-coordinate dioxo Tc^{VI} amine oxime complexes, which involve both addition reactions and proton transfer with the aid of water molecules.

Solans-Monfort *et al.*[670] used B3PW91 to study the structural and dynamic properties of rhenium alkylidene complexes, which are of interest as olefin polymerization catalysts. Haunschild *et al.*[696] used B3LYP to characterize the many possible paths for reaction of ethylene with the group 7 alkylidenes $MO_2(CH_2)(CH_3)$ for M = Re, Tc, and Mn.

5.3.1.6 Iron, ruthenium, osmium. Because of their tremendous importance in biology and their possible extension to bio-inspired catalytic systems, the chemistry of heme- and non-heme-supported iron–oxo species has been the subject of extensive theoretical attention.[578,697–713] However, given the number of extant reviews in this area,[702,709] we will restrict our discussion of iron here primarily to polynuclear cases. Particularly informative studies addressing species containing a single iron atom, however, do merit some mention. For example, B3LYP calculations were instrumental in establishing that bis(α-diimine) complexes of single iron atoms—hitherto commonly described as high-spin Fe^0 complexes—are instead properly described as antiferromagnetically coupled bis(α-diiminate)-Fe^{II} species, the non-innocent ligands each having accepted one electron from iron into a low-energy π orbital.[714] In a detailed study, the ability of various functionals to predict the binding energy of CO, NO, and O_2 to heme-supported iron was studied by Radon and Pierloot[715] using several functionals and also the CASPT2 model. These authors found that CASPT2 provided the best agreement with experiment and that the OLYP functional was similarly accurate (*cf.* the good performance of this functional in the prediction of state energy splittings in supported iron compounds[497] in section 5.1 above), but that BP86 predicted severe overbinding and B3LYP and PBE0 severe underbinding. A prior study by Strickland and Harvey[716] focused on the same binding processes (and also considered binding of H_2O) and emphasized the contribution of a spin-crossover requirement to the kinetic barrier associated with CO binding. Mehn *et al.*[717] characterized the bonding of borohydride ligands to high- and low-spin iron compounds, finding sufficiently strong interactions with both H and B atoms to describe borohydride as an η^4 ligand. Shaik, Thiel, and their respective co-workers[594,718–734] have been especially active in characterizing the single- and two-state reactivities of various supported iron compounds, particularly for cases relevant to metalloenzymes like cytochrome P450, heme oxygenase, horseradish peroxidase (*cf.* the KIE work of Roth and Cramer[615] noted in section 5.2.2), and nitric oxide synthase, and have provided additional recent insights into mechanistic details through DFT calculations, primarily making use of the B3LYP functional. The most recent example[734] involves triplet and quintet reactivity in nonheme oxoiron(IV), which was modeled in B3LYP calculations.

In the case of polynuclear iron compounds, Reilly *et al.*[735] employed PBE to study the ground state geometries and spin multiplicities of cationic iron oxide clusters containing one or two iron atoms and up to five oxygen atoms. They compared computed reaction paths for the oxidation of CO with mass spectrometric data to assess the relative facility of CO oxidation *vs.* oxygen atom replacement by CO and found good correlation between computed barriers and observed reaction channels.

Gold/iron oxide composite nanoparticles have a number of potential biological applications based on binding magnetic nanoparticles to various substances, and there are many questions about the binding strengths. Sun *et al.*[736] showed that the PW91 functionals applied to $Au_6Fe_{13}O_8$ clusters can explain the differential binding ability of various amino acids to these nanoparticles. They also studied magnetic moments, bond distances, and gold coating energies in clusters up to size $Au_{50}Fe_{13}O_8$.

Considering biologically relevant multinuclear iron complexes, Schwarz *et al.*[737] employed BP86 to correlate predicted d orbital energy splittings with those determined from magnetic circular dichroism (MCD) for the two non-equivalent iron atoms in the active site of toluene-4-monooxygenase (T4MO) which is strongly similar to that of soluble methane monooxygenase (sMMO). Based on their calculations, which also address the energetics of different active site geometries formed from the two iron centers and anchored amino acid side chains acting as ligands, they concluded that a water molecule found to be axially bound to one of the iron centers in several sMMO X-ray crystal structures is unlikely to remain bound when the oxygenases are complexed with their respective effector proteins, T4moD and MmoB; they further conclude that complexation by these effector proteins is likely to change the orientation of a terminal glutamate ligand on one iron, thereby possibly facilitating formation of a Fe_2O_2 reactive intermediate and rationalizing the 1000-fold increase in catalytic activity of sMMO when complexed with MmoB. In separate work, Rinaldo *et al.*[738] have examined the catalytic cycle of sMMO by employing a QM/MM method in which a QM subsystem is treated with the B3LYP functional, and they suggest that the protein stabilizes a peroxo intermediate having a μ-η^2:η^2 coordination geometry and also adjusts the overall thermochemistry so as to favor products over reactants, thus emphasizing the sometime importance of including the full protein environment in the modeling of metalloenzymes.

An additional spectroscopic technique that can be useful for characterizing the electron structure of iron compounds is Mossbauer spectroscopy, and Han *et al.* have reported good agreement between experimental isomer shifts for 61 different iron sites and those computed at the PW91 level after applying a linear correction.[739] Han and Noodleman subsequently evaluated the performance of a number of other functionals for computed Mossbauer isomer shifts and found similarly good performance from OPBE and OLYP.[740,741] Based on computed isomer shifts, geometries, pK_a values, spin populations, predicted ground states, and quadrupole splittings, Han and Noodleman assign a *cis*-μ-1,2 peroxo bridging structure to intermediate state P of MMO,[740] a bis(μ-oxo) structure to intermediate Q,[741] and a *cis* to *trans* isomerization pathway connecting P to Q that is coupled to specific ligand rearrangements.[740]

A different binuclear iron site of substantial biological interest is that found in ribonucleotide reductase, where there has been substantial controversy with respect to the geometric and electronic structure of intermediate X in the catalytic cycle,[699,704,742] which includes antiferromagnetically coupled high-spin Fe^{III} and Fe^{IV} centers. Mitic *et al.*[743] have compared (i) d orbital energies computed for various hypothetical geometries at the BP86 level to splittings determined from MCD and (ii) predicted transition energies from TD-DFT and ΔSCF calculations for the same geometries to electronic spectroscopic data; based on their calculations, they conclude that the best model for intermediate X involves one bridging μ-oxo group and one bridging μ-hydroxo group. This prediction stands in contrast to a prior suggestion of a bis(μ-oxo) core based on a similar analysis,[744] illustrating the somewhat subtle spectral differences predicted for different model geometries. However, Mitic *et al.*[743] emphasize that the use of group theory to predict spectral *intensities* can offer helpful additional information for use in resolving spectral differences.

Turning to polyiron clusters involving sulfide bridges in place of oxo bridges, which have been extensively studied by DFT and indeed have served as a testing and validation ground for broken-symmetry techniques over the years,[305–306,310,460,745–751] Szilagyi and Winslow[478] have presented an interesting technical study of alternative approaches to generating broken-symmetry determinants that have an antiferromagnetic coupling of proper magnitude spin densities on different centers, noting that some electronic structure programs provide tools for doing this based on fragment constraints, while others can be induced to converge to the experimentally supported spin distribution when starting from fully ionic determinants generated by enforcing block diagonalization of the Kohn–Sham matrix in a preceding step. They note that spin densities in a series of Fe_2S_2, Fe_4S_4, and $MoFe_3S_4$ clusters are relatively insensitive to choice of correlation functional combined with B88 exchange, but are improved relative to local exchange by inclusion of 5% Hartree–Fock exchange. Such clusters are also relevant to the chemistry of nitrogenase enzymes, and Moritz *et al.*[752] have employed B3LYP* (the asterisk indicates, as explained in section 2.2, that the amount of exact exchange in the B3LYP functional is reduced from the usual 20% to 15%) to study the binding of N_2 to Sellmann-type iron(II) complexes, noting that spin-state changes associated with binding have thermodynamic and kinetic consequences on this process.

In an effort to understand the widespread distribution of Fe_4S_4 clusters in biology, Jensen *et al.*[753] have carried out BP86 calculations for MFe_3S_4 and $M_2Fe_2S_4$ clusters where M = Cr, Mn, Fe, Co, Ni, Cu, Zn, and Pd. They observe good agreement for structures and spin states in cases that are known experimentally, and note that the structures and reduction potentials of the cubic clusters are surprisingly insensitive to substitution of other transition metals, suggesting that this may be an evolutionary advantage to this motif. Jensen *et al.* also note that the modified clusters all have alternative spin states that lie closer in energy to one another than those for the all-iron case, so that spin crossover may be more facile in the mixed-metal clusters.

Li *et al.*[754] found that MR-CI calculations agree with experiment that FeO_2^- is linear, but nine of ten tested density functionals predict it to be bent, with only BH&HLYP giving a linear ground state. However, BH&HLYP predicts qualitatively incorrect results for other states.

The prediction of one-electron reduction (or oxidation) potentials for molecules containing transition-metals has been extensively explored in the recent past,[755–763] building on the good success of DFT-based models applied to predict this property in organic systems.[764–771] Recent efforts in this area include a study by Jaque *et al.*[762] examining the aqueous $Ru^{3+}|Ru^{2+}$ couple with 37 density functionals and five basis sets and further considering the effects of one or two explicit shells of solvent water (six or 18 water molecules, respectively) about the bare Ru ion in addition to continuum solvation. Jaque *et al.* concluded that at least two shells of explicit water

were necessary to approach quantitative agreement with experiment and that an important issue is a substantial degree of positive charge transfer from the metal ion to the outer-shell waters in microsolvated clusters (*cf.* the hydrated gold cation discussed below). For two explicit solvent shells, the difference in solvation energy of Ru^{3+} and Ru^{2+} varies from −6.83 to −7.45 eV, depending on the choice of density functional and basis set, showing that one must be cautious about qualitative values of calculated reduction potentials especially in articles where the sensitivity to the functional is not explored. Kritayakornupong[772,773] carried out QM/MM calculations on both Ru^{2+} and Ru^{3+} in aqueous solution. Although the QM region was treated by Hartree–Fock theory (not DFT), the simulations provide valuable insight into the solvated structures presented in the solution. For example, for Ru^{3+} the second coordination shell contains only ten water molecules.[773] Three-body corrections to a purely MM calculation were insufficient to reproduce the hydration structure of Ru^{3+}.[773] The structure of the hydration shell of Fe^{3+}(aq) was studied by Amira *et al.*,[774] and the hydrolysis of Fe^{3+} was studied by De Abreu *et al.*[775]

The relative stability of hydrated oxo *vs.* hydroxy structures has been examined by experiments and calculations for compounds with the formula $MO_2H_2^+$, where M = Fe, Co, or Ni. For M = Ni, the $(H_2O)MO^+$ structure is favored, whereas for M = Fe, the $M(OH)_2^+$ structure is favored; for M = Co, the isomers are energetically similar.[776]

In work focusing on a large number of supported Ru complexes, interesting because of their anticancer therapeutic potential, Chiorescu *et al.*[763] benchmarked various continuum solvation models in conjunction with the B3LYP functional for 80 reduction potentials in four solvents. Comparison with experimental data indicated that errors were minimized when solute cavities were constructed from Bondi's set of atomic radii—the default choices in some electronic structure programs were found to lead to errors that were larger by 70 to 140 mV.

In work aimed at predicting aqueous one-electron reduction potentials for the most common aqueous couple of *all* of the first-row transition metals, Moens *et al.*[771,777] found that the global value of the electrophilicity (a descriptor from conceptual DFT[688]) was a good predictor of reduction potentials when computed for clusters including two solvation shells about the central metal ion. Uudsemaa and Tamm[756] had previously studied this series, computing the reduction potentials directly from DFT and continuum solvation free energies, and had come to similar conclusions with respect to the importance of two solvation shells.

While not computational electrochemistry *per se*, recent experimental work measuring one-electron reduction potentials of aqueous nanodrops in the gas phase[778,779] is worth noting here because of its potential to connect more directly to the absolute half-reaction reduction potentials that are typically computed by theory. Continued comparison of theory to experiment in these instances is likely to be helpful in resolving ongoing discussion on the absolute potential of the hydrogen electrode,[778,780–785] to which the relative electrochemical scale is anchored.

We turn next to ruthenium. Grubbs Ru-based catalysts for olefin metathesis are among the most economically important catalysts invented in the past decade, especially the second-generation catalysts with *N*-heterocyclic carbene ligands like 1,3-dimesityl-4,5-dihydro-2-ylidene (H_2IMes), and substantial DFT work has been done to rationalize the influence that various factors may have on the activity of the supported ruthenium complexes.[670,786–793] Thus, for instance, Mathew *et al.*[790] have used DFT to study five different self-deactivation pathways, all based on intramolecular C–H bond activation, and suggested that increased rigidity in NHC substituents might be expected to improve catalyst stability. Benitez *et al.*[791] have used B3LYP and M06 to determine that throughout the metathesis process the olefin remains "bottom-bound" to the $(H_2IMes)(Cl)_2Ru$ catalyst and the chlorides remain *trans* to one another, so that efforts to design diastereo- and enantioselective catalysts should be undertaken within this coordination environment. In later work Benitez *et al.*[794] used the M06 functional to calculate the dissociation energy of the Ru bond to tricyclohexylphosphine (PCy_3) in a Grubbs catalyst and found excellent agreement with experiment. They found that the M06 functional leads to improved accuracy over B3LYP (by ∼0.5 kcal mol^{-1}) for relative energies of various stable intermediates and much improved accuracy (by ∼23 kcal mol^{-1}) for PCy_3, and they concluded that their calculations settle a longstanding controversy. In very recent work, Tonner and Frenking[792] have used DFT to suggest that carbodiphosphoranes might prove to be better ligands than NHCs for the design of Grubbs catalysts.

In a particularly comprehensive study, Zhao and Truhlar[793] developed a set of benchmark relative energies for key stationary points in the Grubbs second-generation olefin metathesis catalytic cycle using a composite model based on CCSD(T) calculations. To make the calculations of benchmark results feasible, small model ligands were used. They assessed spin-component-scaled MP2 approaches for computing these relative energies, where MP2 denotes second-order WFT perturbation theory, and they also examined 39 different density functionals; they found that the local M06-L functional combines good accuracy and, by virtue of being local, excellent efficiency with respect to computations on reasonably large catalysts. A number of GGA functionals incorporating the LYP correlation functional were found to perform poorly, in part because these functionals do a poor job of accounting for medium-range correlation effects that are decisive for predicting the importance of dispersion-like interactions between various ligands in the catalytic system.[789] Averaging over the entire catalytic cycle, the mean unsigned errors in kcal mol^{-1} were found to be 1.2 for hybrid M06, 2.6 for hybrid MPW1B95, 3.0 for local meta M06-L and hybrid PBE0, 4.1–4.4 for local PBE, hybrid M06-2X, and local meta TPSS, 5.7 for hybrid meta τ-HCTHh, 6.6 for the popular local BP86, 7.2–9.9 for hybrid B98, X3LYP, and B97-3, and 11.0 for the popular hybrid B3LYP.

When these methods were applied to real catalysts, with their large bulky ligands, the differences between the predictions of the various functionals were even larger.[412,789,793]

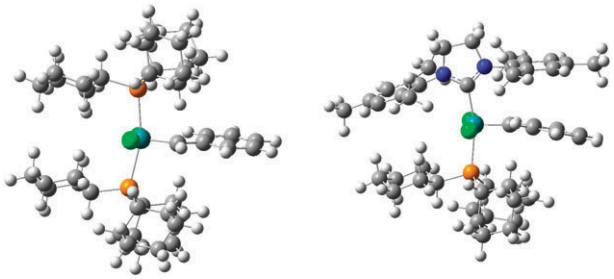

Fig. 3 Ball-and-stick depictions of Grubbs I (left) and II (right) catalysts.

Grubbs second-generation (Grubbs II) catalysts are a hundred to a thousand times more active than the first-generation (Grubbs I) Ru metathesis catalysts, and they have greater thermal and chemical stability and better functional group tolerance. However, the 14-electron catalyst is generated more slowly from the 16-electron precatalyst than was the case for the first-generation catalysts. This can be problematic because living polymerization can be thwarted if the ratio of the rate constant of chain propagation to that for chain initiation is too high.[795] The difference between the Grubbs I and Grubbs II catalysts is the substitution of one tricyclohexylphosphine (PCy_3) in a typical biphosphine Grubbs I precatalyst, $(PCy_3)_2Cl_2Ru{=}CHPh$, by an NHC in a typical Grubbs II precatalyst, $(PCy_3)(H_2IMes)Cl_2Ru{=}CHPh$. These catalysts are shown in Fig. 3.

Tsipis *et al.*[796] noted that gas-phase calculations with B3LYP and BP86 both predict that the PCy_3 bond dissociation energy of the Grubbs I precatalyst is larger than that of the Grubbs II precatalyst by 1.4–2.3 kcal mol^{-1}, whereas the experimental result[797] is that it is smaller by 3 kcal mol^{-1}, approximately independent of solvent. Zhao and Truhlar[789,793] showed that PW91, PBE0, and TPSSh also give the wrong sign (+0.4 to +1.1 kcal mol^{-1}) for the difference in bond dissociation energies but that M06-L gives −4 kcal mol^{-1} in good agreement with the experimental value of −3 kcal mol^{-1}. Zhao and Truhlar then repeated the calculation with the Ru and Cl atoms removed to find the contribution of noncovalent interactions of the bulky ligands. For B3LYP this noncovalent interaction is repulsive, but for M06-L it is attractive, and in fact it is 4.5 kcal mol^{-1} stronger for the Grubbs I precatalyst than for the Grubbs II precatalyst. Thus the difference in the bond dissociation energies is essentially completely accounted for by noncovalent attractive interactions. This is an important qualitative finding because the catalyst design literature is almost entirely focused on the electron donating ability of the ligands and their potential coordinate covalent bonding strength, with some consideration given to steric crowding, but there has been essentially no consideration of attractive noncovalent interactions.

M06-L gives a bond dissociation energy of 39–40 kcal mol^{-1} for the Grubbs II precatalyst, whereas MPW1B95 gives 30 kcal mol^{-1}, and B3LYP, BP86, TPSS, PBE, TPSSh, and PBE0 give values in the range 14–23 kcal.[789,793] The value inferred from the experiment[797] in toluene is 27 kcal mol^{-1}. After the 40 kcal mol^{-1} value was published,[789] a gas-phase experiment was published,[798] yielding the same 40 kcal mol^{-1}. This not only confirms the M06-L calculation (and also M06, which gives very similar results in this case[793]), but it shows that the older density functionals give much worse results for the large, real molecules than for the smaller model catalysts; this effect of size has also been noted in main-group chemistry[799] and is attributed to an accumulation of medium-range correlation energy in large, complex systems, with smaller effects in extended chains.[799,800] In more recent work, Stewart *et al.*[801] reported that B3LYP predicts geometries for Ru-metathesis-relevant complexes more accurately than M06-L.

In related work, Pandian *et al.*[802] successfully applied the M06 functional to the Ru-catalyzed ring closing metathesis of 1,6-heptadiene. Sieffert and Bühl[803] studied the binding enthalpy of a triphenylphosphine ligand in $Ru(CO)Cl(PPh_3)_3(CH{=}CHPh)$ with BP86, B3LYP, and the M05 and M06 families, as well as with density functionals to which an empirical MM dispersion is added. They found that BP86, B3LYP, and M05 do not reproduce the experimental results, whereas all four members of the M06 family and the empirically corrected functionals do; M05-2X was found to be intermediate. They agreed with the conclusion of Zhao and Truhlar[789,793] that noncovalent interactions make a very large contribution to the total binding enthalpy. The success of new density functionals for these noncovalent interactions allowed them to define a computationally efficient protocol for studying catalytic reactions.

In other work on ruthenium, Caramori and Frenking[804] have carried out energy decomposition analysis to characterize the bonding of NO to ground- and excited-state ruthenium tetraamine complexes. Krapp *et al.*[805] have used BP86 and CCSD(T) calculations to clarify details of the electronic structures of supported iron and ruthenium complexes coordinating naked carbon, *e.g.*, $(CO)_2(PMe_3)_2Ru(C)$. And, as noted in section 5.1, Baik and co-workers[494,495] have used B3LYP calculations to assess mechanistic details associated with oxygen formation in water catalyzed by supported diruthenium complexes, an area that continues to generate intense interest in the experimental and theoretical communities.[493,806–820] In particularly recent work, Bozoglian *et al.*[818b] have shown that M06-L correctly predicts which of two alternative pathways for water oxidation is operative for the Ru-Hbpp catalyst; B3LYP, on the other hand, makes the wrong prediction.[495]

Morokuma[595] recently reviewed his DFT studies of multi-step reactions of organometallic tri-ruthenium complexes.

Elschenbroich *et al.*[821] characterized the electronic structures of *trans*-Cl_2-(η^1-$C_5H_5P)_4M$ for M = Ru and Os and *trans*-Cl_2-(η^1-$C_5H_5As)_4Ru$, the final case being the first arsenine complex of a late transition metal to have been isolated.

Zhang *et al.*[822,823] employed B3LYP and TD-B3LYP to study the structures and spectroscopic properties of highly luminescent Os^{II} complexes.

5.3.1.7 Cobalt, rhodium, iridium. The organometallic coenzyme B_{12} and related small-molecule models have been the subject of many studies designed to probe the mechanistic details of the Co–C bond cleavage reactions critical to the

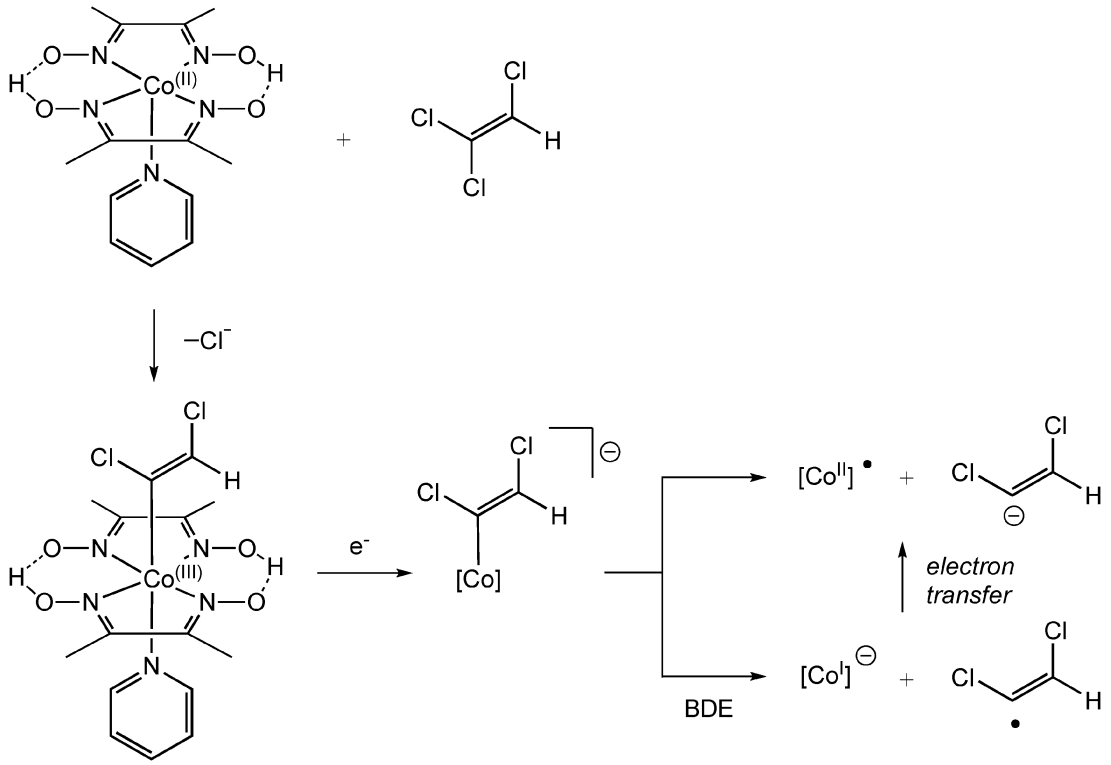

Fig. 4 Reductive dechlorination of trichloroethylene by a cobaloxime.

function of such enzymes as 5-methyltetrahydrofolate-homocysteine methyltransferase and methylmalonyl coenzyme A mutase.[824] The more recent demonstration of the efficacy of B_{12} for the reductive dechlorination of halogenated aliphatics and olefins has sparked additional interest in the design of supported cobalt species for environmental remediation.[825] For example, reaction of a pyridine-coordinated cobaloxime with trichloroethylene leads to a *cis*-1,2-dichlorovinyl organocobalt species that may undergo subsequent reductive Co–C bond cleavage (Fig. 4).[826] From a mechanistic standpoint, the final bond-cleavage event may proceed either homolytically to generate an organic radical and a Co^{I} species or heterolytically to generate an organic anion and a Co^{II} species. In biological systems involving B_{12}, the Co is supported by a corrin macrocycle and *trans* ligation is typically effected by an imidazole or benzimidazole.

Pratt and van der Donk[827] carried out extensive studies of chlorinated vinylcobalamin species at the B3LYP/6-31G(d) level and observed good correlations between computed and experimental structural data, noting in particular that the use of a corrin ring having all of its rim substituents removed compared to one with 15 methyl groups (to mimic the various side chains present in biological corrins) led to no substantial geometric differences. By computing one-electron reduction potentials for different species and analysis of the virtual orbitals involved, Pratt and van der Donk[827] and subsequently Birke *et al.*[828] suggested that reductive bond cleavage may take place *via* the "base-off" cobalamin, *i.e.*, after equilibrium dissociation of the *trans* imidazole or benzimidazole ligand. Both Pratt and van der Donk[827] and Birke *et al.*[828] also observed good correlations between one-electron reduction potentials and Co–C bond lengths in the pre-reduction complexes.

Follett *et al.*[826] carried out similar studies at the B3LYP/6-31+G(d) level for the system illustrated in Fig. 4. They too analyzed one-electron reduction potentials and, more interestingly, followed the electronic structure of reduced cobaloximes along their bond dissociation coordinates. By examining spin and charge distributions, they were able to elucidate the degrees to which different organic ligands (methyl, vinyl, and dichlorovinyl) tended to prefer the homolytic *vs.* heterolytic pathways and the influence of solvation upon those preferences.

Both Pratt and van der Donk[827] and Follett *et al.*[826] confirmed observations first reported by Jensen and Ryde[829] with respect to the computed Co–C bond dissociation energies (BDEs; see Fig. 4). In particular, the B3LYP functional consistently underestimates BDEs in both cobalamin and cobaloxime systems by 40–50 kJ mol^{-1} when the products include a doublet Co^{II} species, but B3LYP provides more accurate results when singlet Co^{I} or Co^{III} products are generated. By contrast, the local BP86 functional was found to provide near quantitative agreement with experiment, illustrating the degree to which inclusion of exact Hartree–Fock exchange can affect predicted energy differences between open- and closed-shell states. Jensen *et al.* have discussed this point in more detail with respect to dissociation energies of diatomic species formed from one transition metal atom and one non-metal atom, relating functional performance to the high- or low-spin nature of the various asymptotes.[408]

Considerable modeling attention has also been paid to Co–C bond cleavage in the enzymatic systems 5-methyltetrahydrofolate

homocysteine methyltransferase and methylmalonyl coenzyme A mutase as well. As that work has been very recently reviewed elsewhere, we refer interested readers there.[830]

Morschel *et al.*[831] have examined the influence of supporting ligands on cobalt-catalyzed Diels–Alder reactions. At the BP86 level, at least 4 different pathways are available leading to products, with low-energy intermediates not necessarily correlating with low-energy barriers for subsequent steps; once all paths are considered, the BP86 predictions for regioselection in the reaction between isoprene and phenylacetylene were found to be in good agreement with experiment.

There is substantial interest in CO_2 as a cheap C1 feedstock, so its catalytic hydrogenation is an active area of exploration. Huang *et al.*[832] have used the KMLYP functional to characterize the mechanism of hydrogenation of CO_2 by a pincer PCP–rhodium complex, noting that strongly electron-donating ligands disfavor reductive elimination of formic acid after hydrogenation (where PCP denotes phenylcyclohexylpiperidine). Hu and Boyd[833] assessed B3LYP for the reaction energy and forward and reverse barrier heights to dissociate a CO ligand in $Cl_2Rh(CO)_2^-$. The deviation of these three quantities from CCSD(T) calculations was only 1–2 kcal mol^{-1}.

In an unusual example of oxygen activation, Praetorius *et al.*[834] have characterized a singlet square planar rhodium complex in which the O_2 ligand has not oxidized the metal center. They suggest that prior examples of rhodium-O_2 complexes with very short O–O bonds that have been assigned as superoxo species may merit reassignment in light of their new results.

In the organic area, the mechanistic details associated with rhodium-catalyzed asymmetric addition of boronic acids to α,β-unsaturated 2-pyridylsulfones have been studied by Mauleon *et al.*[835] at the B3LYP level. In another recent report, Fristrup *et al.*[836] have explored the mechanism for the rhodium-catalyzed decarbonylation of aldehydes, also at the B3LYP level. Based on a comparison of computed to measured H/D KIEs, migratory extrusion of CO was established as the rate determining step for this process. Liu *et al.*[837] used B3LYP to study the mechanistic details of homogeneous rhodium catalyzed [5 + 2] cycloadditions between vinylcyclopropanes and alkynes. Orian *et al.*[838] used BLYP calculations to study end-on side-on isomerization of nitrile ligand half-sandwich five-membered rhodacycles; they analyzed the saddle points in terms of the strain energy upon activation.

The utility of Ir^{III} cyclometalated complexes in organic light-emitting diodes has given rise to many TD-DFT studies of their electronic spectral properties.[839–843] More relevant to catalysis, recent studies have appeared employing DFT (usually B3LYP) to study the mechanistic details of iridium-catalyzed allylic etherification,[844] alkene hydrosilation,[845] and C–H bond activation.[846] Ghosh *et al.*[847] successfully rationalized carbon–carbon bond forming reductive elimination rates in pincer PCP–Ir complexes having various degrees of steric bulk, noting the critical importance of non-bonded interactions (as opposed to electronic effects) affecting ligand rotations required to bring eliminating alkyl fragments into reactive conformations.

Marom and Kronik[848] compared Kohn–Sham orbital eigenvalues computed for CoPc and NiPc with the B3LYP, PBE, PBE0, and M06 functionals to experimental ultraviolet photoemission spectroscopy (UPS) data. They found poor agreement for PBE and good agreement for the other three functionals.

5.3.1.8 Nickel, palladium, platinum. Calaminici has examined the polarizability of small nickel clusters, up to 5 atoms, using a GGA functional.[849] She found that in contrast to clusters of iron or copper, the per-atom polarizability failed to increase with increasing cluster size, but instead showed more complex behavior, suggesting that experiments to better understand this situation would be of interest. Earlier work by Arvizu and Calaminici[850] established the energetics of various isomers of Ni_n, Ni_n^+, and Ni_n^-, for n up to 5, and was useful for the development of a Ni basis set optimized for cluster calculations.[370,850] Shoji *et al.*[851,852] have employed the generalization[465] of the Yamaguchi broken-symmetry method [eqn (10)] with B3LYP to compute exchange interactions in two supported Ni_9 complexes and compared this approach to the simpler Ising model, observing good agreement with experiment for predicted ground spin states and magnetic susceptibilities.

Conradie *et al.*[853] observed that the BLYP, OLYP, OPBE, and PW91 local functionals and the B3LYP and B3LYP* hybrid functionals all predict, in gas-phase calculations on the doublet d^7 states of nickel(III) tetra(*tert*-butyl)porphyrin dicyanide anion, that the ground state has the unpaired electron in a $d_{x^2-y^2}$ orbital, whereas the experimental ground state has it in a d_{z^2} orbital. They attribute the error not to inaccurate functionals but rather to neglect of the counterion effect.

Kozuch *et al.*[854] studied Pd^0L_2 and $Pd^0L_2Cl^-$ model catalysts with B3LYP calculations for cross coupling reactions with phenyl chloride as substrate. They found that the anion lowers the barrier for the oxidative addition step, and they explained this in terms of occupied orbital destabilization and unoccupied orbital stabilization.

de Jong and Bickelhaupt[855] used the BLYP functional to study oxidative addition of C–H, C–C, C–F, and C–Cl bonds to model Pd coordination complexes in order to gain insight into the competing factors of reactant strain, steric shielding, transition-state stabilization, and anion assistance in controlling these bond activation processes. They studied these factors not only at the transition state but also as functions of the reaction coordinate, and they used the Kohn–Sham orbitals and an energy decomposition scheme in their interpretation. The analysis provided considerable insight into the differences between C–C and C–Cl bond activations and C–H alternatives.

Viñes *et al.*[856] examined palladium clusters having nuclearity ranging from 38 to 225 by adopting a plane-wave approach where the individual clusters occupy the centers of unit cells having at least 1 nm of vacuum separating one cluster from another, thus permitting the efficiency of the plane-wave approach with negligible interactions between clusters and no symmetry constraints on individual clusters. They determined that scalability to bulk density-of-states behavior begins at a cluster size of about 80, with Pd_{140} and Pd_{225}

particles showing properties very similar to bulk Pd. In a separate study,[857] Viñes *et al.* showed that these larger nanoparticles also showed converged behavior with respect to their tendency to self-aggregate in linear arrays, as observed in the formation of particulate Pd nanowires.[858]

Betz *et al.*[859] have explored the relative stabilities of different *N*,*S vs. N*,*N*, *vs. S*,*S* coordination motifs in π-allyl palladium complexes supported by asymmetric bis-thiazoline ligands and their influence on reactivity. Legault *et al.*[860] employed B3LYP to rationalize regioselectivities in homogeneous palladium catalyzed sequential cross-couplings of polyhalogenated heterocycles.

Continuing in the organometallic arena, the last decade has seen substantial interest in the use of *N*-heterocyclic carbenes[861,862] (NHCs, already mentioned in section 5.3.1.6) as ligands owing to their tunable steric demands and their character as a strong σ donor to the metal center. Radius and Bickelhaupt[863] have studied the nature of σ *vs.* π bonding of NHCs to metals in the group 10 series as a function of other ligands using the extended transition state density decomposition scheme of Ziegler and Rauk.[864] Radius and Bickelhaupt emphasize that the importance of π bonding, particularly with 3rd-row transition metals, should not be discounted, and the directionality of the bonding (in terms of charge transfer) and its magnitude are quite sensitive to the nature of the remaining ligands, *e.g.*, with CO ligands being better π acceptors in this d^{10} series than NHCs (a similar sensitivity of metal–NHC π bonding to other ligands was noted in recent calculations on supported f element compounds[865,866]). Computational investigations into the nature of NHCs and their bonding to *all* transition metals have recently been reviewed by Jacobsen *et al.*[867] and a review focused exclusively on the Group 10 transition metals has also been provided by Radius and Bickelhaupt.[868] Finally, Tonner *et al.*[869] have compared the bonding of different tautomers of NHCs to phosphine ligands for complexes of group 4, 6, 8, and 11 transition metals. All of these studies need to be re-examined in light of the importance of attractive noncovalent interactions, as discussed in section 5.3.1.6.

Based on computed structural data and comparison of computed EPR spectral parameters to experiment, Harmer *et al.*[870] have proposed a novel nickel hydride intermediate that plays a key role in "reverse methanogenesis" in the enzyme methyl-coenzyme M reductase (MCR). In earlier work, Yang *et al.*[871] applied a similar protocol to identify a related methylnickel complex.

de Jong and Bickelhaupt used the BLYP functional to study carbon–halogen bond activation by oxidative addition at Pd atoms[414,872] and $PdCl^-$ model catalysts[872] and by an S_N2 mechanism involving Walden inversion at C. Solvation effects were found to change the relative favorability of the two mechanisms. The results were explained by an activation strain analysis.

The B3LYP functional has been used to study ligand effects on oxidative addition,[873] reductive elimination,[874] and carbon–carbon bond formation[875] in Pd coordination complexes.

Adams *et al.*[876] used B3PW91 calculations, either treating a small model fully quantum mechanically or employing a QM/MM approach with the UFF force field[877] to fully represent large phosphine ligands, to characterize the ability of a pentanuclear Re_2Pt_3 complex to add up to three equivalents of H_2 at room temperature. Because of the clinical importance of cisplatin as an anticancer drug, several recent DFT studies have appeared focusing on the structural details of the drug or derivatives either isolated or bound to DNA, and on the chemical consequences of binding.[878–886] For example, van der Wijst *et al.*[887] used the BP86 functional to study the influence of coordination to Pt^{II} on the relative energies of tautomers of 1-methyluracil and 1-methylthymine, finding that such coordination causes an otherwise rare tautomer to be favored in solution.

Datta *et al.*[888] used the B3LYP functional to study tunneling effects in oxidative addition of methane to a Pt complex. As in an earlier study[889] applying B3LYP to oxidative addition of methane to a model Rh complex, they found very large tunneling effects.

Gilbert and coworkers[890] used the MPW1K functional to study the intramolecular hydrogen bonds in *cis*-diamine-platinum(II) pyrophosphate complexes.

Mo and Kaxiras[891] used the PBE functional to study cyanide-transition-metal nanotubes containing Ni, Pd, or Pt. They stated that their computational parameters ensure high accuracy, but the accuracy of the PBE functional is not guaranteed.

5.3.1.9 Copper, silver, gold. Studies of the coinage metals have focused upon their activities as single-center catalysts in supported metal complexes as well as upon their structures and properties in clusters ranging from a few atoms to nanoparticles; single atoms, ions, and bulk metals have also been studied. With respect to clusters, Roldán *et al.*[892] have employed plane-wave LDA and PW91 calculations to study nanoparticles of copper and silver ranging from 38 to 146 atoms and nanoparticles of gold ranging from 38 to 225 atoms. They observed linear convergence to bulk values of predicted average nearest-neighbor interatomic distances with respect to average coordination numbers as the sizes of the nanoparticles increased. However, the reproduction of experimental bulk values was inconsistent, with PW91 being better than LDA by 5 pm for Cu, LDA better than PW91 by 7 pm for Au, and the experimental value for Ag falling precisely in between LDA and PW91, differing from each by 5 pm. Trends in cohesive energies per atom were similar, with PW91 being clearly better for Cu, but not for the heavier coinage metals. Analysis of density of states (DOS) plots for the three families of clusters indicated that beyond 80 atoms, DOS parameters were scalable to bulk values, with no special characteristics like those associated with smaller clusters.

Calaminici *et al.*[893] employed the same density functionals as Roldán *et al.* but focused in detail on neutral and anionic Cu_9. The work was motivated by significant disagreement between prior theoretical studies[894] and experiment[895] for the electron affinity of the nonameric cluster. Employing a cluster geometry search strategy[896] at the LDA level Calaminici *et al.* found six and nine minima for the neutral and anionic nonamers, respectively. While LDA energies were not found to be useful for identification of the lowest energy

structures, nor for rationalizing the measured electron affinity, energies computed at the PW91 level (for the LDA structures) provided good agreement with both vertical and adiabatic experimental data.

Shi *et al.*[897] studied the mechanism of a gold-catalyzed [1,2]-hydrogen shift whose rate is increased by water. A spotlight discussion is available.[898]

Because of their importance in heterogeneous catalysis, the properties of small gold clusters have been studied extensively, and Pyykkö has recently reviewed theoretical efforts in this area.[899,900] An unusual and interesting feature of gold anion clusters compared to their Cu and Ag congeners is that various experimental techniques[901–903] indicate that two-dimensional structures are preferred over three-dimensional isomers up to a cluster number of 12. Johansson *et al.*[904] showed very recently that DFT successfully predicts this 2D to 3D transition size provided (i) one uses the meta TPSS functional, the hybrid meta TPSSh functional, or a GGA like PBEsol that is fit (among other criteria) to yield accurate predictions of jellium surface energies, and (ii) spin–orbit contributions to cluster energies are included. They found by contrast that BP86 and PBE both are significantly biased towards 2D clusters. Other functionals that performed poorly compared to PBEsol and TPSS include LSDA, BLYP, B3LYP, and X3LYP. It was shown previously[905] that the mean absolute relative error in the exchange–correlation surface energy for jellium is much smaller (1.1%) for the TPSS and TPSSh functionals than for PBE (5%), and Johansson *et al.* emphasized this property in rationalizing why PBEsol, TPSS, and TPSSh perform better than PBE for this transition. The conclusion about the importance of fitting the jellium surface energy is very interesting in light of the discussion in section 2.5, and this issue deserves further study. Olson *et al.*[906] had previously noted poor performance of older functionals for this same problem, and had shown that large basis-set MP2 and CCSD(T) calculations gave results in good agreement with experiment. Recently it has been shown that the hybrid meta M05 and M06 functionals and the meta M06-L functional all predict the 2D to 3D transition correctly in going from Au_{11}^- to Au_{13}^-.[907] Ferrighi *et al.* reported a similar finding, almost simultaneously.[908] Several other authors have used DFT to study related structural issues in slightly larger gold clusters, from Au_5 to Au_{20},[909] Au_{14} to Au_{29},[910] Au_{15}^- to Au_{24}^-,[911] Au_{20},[912] Au_{20}^{n+},[912] Au_{20}^{n-} (with n = 1 or 2),[912] Au_{21}^- to Au_{25}^-,[913,914] and Au_{26}.[915] For example, Kryachko and Remacle, in a review,[912] noted that Au_{20} has several planar and 3D isomers, including a unique tetrahedral structure with all atoms on the surface and a "large" HOMO–LUMO gap.

Another interesting study of a gold cluster anion has been reported by Lechtken *et al.*[916] These authors studied Au_{34}^- and found that the TPSS functional predicts the lowest-energy cluster to be chiral and belong to the C_3 point group. Lechtken *et al.* then employed BP86 structures and TD-DFT with this functional to compute the electronic excitation spectrum of the neutral cluster at the anion geometry, and derive therefrom a predicted photoelectron spectrum (PES). The TD-DFT approach is more physically appropriate than using a density of states computation based on orbital energies, and Lechtken *et al.* find that only the chiral isomer predicted at the TPSS level to be lowest in energy gives a predicted PES consistent with experiment. This result is particularly intriguing since chiral clusters might be expected to carry out asymmetric catalysis. Gu *et al.*[917] also studied Au_{34}^-. They used the LSDA and PW91 functionals and found several low-energy structures with the form of a Au_4 core surrounded by 30 fluxional outer atoms.

Li *et al.*[918] carried out calculations on Au_{20} and Au_{20}^- with the PW91 functional and found that the optimum geometry is a pyramidal cluster that represents a small piece of bulk gold with four (111) faces. They found an orbital energy gap of 1.8 eV.[918] Further work on the anions Au_n^- with the PBE functional showed an evolution in shape from planar to flat cages to hollow cages to pyramidal as n increased from 13 to 20,[919,920] and a transition from pyramidal to fused planar to tubular to core/shell compact for n = 21–25.[914] Zubarev and Boldyrev analyzed the bonding in the cages with the B3PW91 functional.[921]

Torres *et al.*[922] used the PBE functional to study $Au_nO_2^+$ for n = 4–8 and $MAu_nO_2^+$ for n = 3–7 where M is a dopant atom of either Ti or Fe. The preferred geometry for adsorption of oxygen on the doped clusters is with both O atoms on the impurity. Prestianni *et al.* used B3LYP to study various adsorption sites of O_2 or CO on Au_n^{m+} with n = 1, 9, and 13 and m = 0, 1, and 3,[923] later extending this to coadsorption on Au_{13}^+,[924] coadsorption on Au_{13},[924,925] and separate and coadsorption on Au_9, Au_{13}, Au_9^+, and Au_{13}^+.[925] The latter study included reaction paths and barriers.

Metiu and coworkers[926,927] examined the binding of propene to gold and mixed gold-silver clusters and showed that it binds in an electron-donating mode and binds most strongly at sites where the LUMO protrudes. They concluded that orbital shape and orbital energy, not just low coordination number, are important for determining the catalytic properties of small gold clusters. They also noted[927] that there are numerous low-lying isomers of metal clusters, a subject mentioned above.[912,928,929] They used the local PW91 or PBE functionals to study the binding of gold clusters on TiO_2 surfaces,[930] CO adsorption on gold-doped ceria surfaces,[931] and CO oxidation on TiO_2 doped with V, Cr, Mo, W, and Mn.[932] Supported gold atoms and clusters have also been studied in other works.[933,934] See section 5.3.3 for further discussion of surface science.

Golightly *et al.*[935] used B3LYP to study diphosphine-protected Au_{11} clusters and stressed the sensitivity of the results to the precise nature of the ligand when the ligand has donor–acceptor abilities.

A troubling aspect of gold clusters is that even for Au_3 the most complete DFT calculations of the dissociation energy still show discrepancies from experiment of 5–10 kcal mol^{-1}.[936]

Ending our discussion of coinage metal clusters, Crawford *et al.*[937] have reported a particularly interesting study of a semiconductor cluster $Ag_{28}S_{26}(P(O)PhOMe)_{12}(PPh_3)_{12}$. The X-ray crystal structure of this cluster exhibits substantial disorder in its core associated with two silver atoms that can occupy any of six equivalent sites. DFT calculations at the BP86 level show that as long as the two sites occupied do not neighbor one another, essentially equivalent structures are obtained upon optimization of any given choice. By following

a constrained DFT molecular dynamics trajectory, Crawford *et al.* estimated the barrier for the concerted movement of both silver atoms into new (equivalent) positions to be about 26 kJ mol^{-1}. They suggest that this estimate may also be appropriate for cation mobility in bulk silver chalcogenides.

The largest gold cluster studied so far by DFT is the thiolate-passivated $Au_{102}(p\text{-MBA})_{44}$ where *p*-MBA is *p*-mercaptobenzoic acid.[373,938]

Moving from clusters to supported metal compounds having only one or two atoms, there has been extensive theoretical activity devoted to studying the activation of molecular oxygen by supported copper species,[487,939–942] owing to the prevalence of this theme in biological and inorganic catalysis.[487,611,939,940,943–946] Güell *et al.*[947] have studied the interaction of O_2 with atomic copper and noted that a broad range of local, hybrid, and meta-hybrid functionals all predict the ground-state geometry of the triatomic complex to involve end-on binding to O_2, a result at odds with highly correlated levels of electronic structure theory (CCSD(T) with a complete basis set,[947] CASPT2,[948] *etc.*) In addition, they found that B3LYP-like functionals required substantially different amounts of exact exchange to provide satisfactory agreement with complete basis set CCSD(T) for geometries (20%) *vs.* relative electronic state energies (90%), and they attributed this behavior to the failure of most functionals to properly balance the covalent *vs.* ionic character of the different geometries and states, noting that most DFT models significantly overestimate the first ionization potential of Cu.

In most biological and catalytic systems, however, copper is not found in its atomic form but is rather ionized prior to its interaction with O_2. From a formal oxidation-reduction standpoint, the combination of O_2 with a LCu^{I} partner (L being a generic supporting ligand environment) may occur either without change of the copper oxidation state, or with one or two electrons transferred so as to generate $LCu^{II}O_2(-)$ and $LCu^{III}O_2(2-)$ mesomers, respectively. As O_2 has a triplet electronic ground state, weakly coupled $LCu^{I}O_2$ species may also be expected to be triplets, while singlet and triplet states may have similar energies for $LCu^{II}O_2(-)$, since the d^9 Cu^{II} and superoxide radical anion may have separated biradical character, while finally $LCu^{III}O_2(2-)$ would be expected to have a singlet ground state given the closed-shell character of d^8 Cu^{III} and the peroxide dianion. Accurately modeling this spectrum of energetic possibilities is a challenge for Kohn–Sham DFT because of the varying degrees of dynamical and non-dynamical electron correlation effects in the different redox states, which can be effectively tuned by choice of ligand environment L. An additional factor influencing the electronic structure and reactivity of $LCuO_2$ complexes is the geometry of O_2 coordination; both end-on and side-on coordination geometries have been observed depending on L.[487]

Cramer *et al.*[949] computed the relative energies of the singlet and triplet states for the end-on and side-on geometries of the 7 $LCuO_2$ complexes in Fig. 5 at several different levels of electronic structure theory. They observed good agreement in predicted relative energies when comparing completely renormalized coupled-cluster calculations[950–953] (CR-CC(2,3)) and multi-reference second-order perturbation theory[954] (CASPT2) and based on such agreement benchmarked various DFT protocols against the two WFT methods. They observed that local functionals such as BLYP, *m*PWPW, and M06-L provided generally good agreement with benchmark values, but the inclusion of Hartree–Fock exchange in functionals like B3LYP, *m*PW1PW, M06, or M06-2X led to increasingly inaccurate results with increasing Hartree–Fock exchange. Interestingly, the most accurate results from the BLYP and *m*PWPW functionals were obtained when a restricted Kohn–Sham formalism was employed for the singlet states, even though the Kohn–Sham wave functions were unstable to spin-symmetry breaking. With the M06-L functional, spin purification of broken-symmetry energies provided slightly improved values for singlet energies compared to restricted Kohn–Sham energies. For the remaining functionals, errors were large irrespective of the protocol used to assign singlet state energies.

By studying the ligands in Fig. 5, Cramer *et al.*[949] were able successfully to rationalize the observed geometries and ground electronic states of a diverse array of experimentally

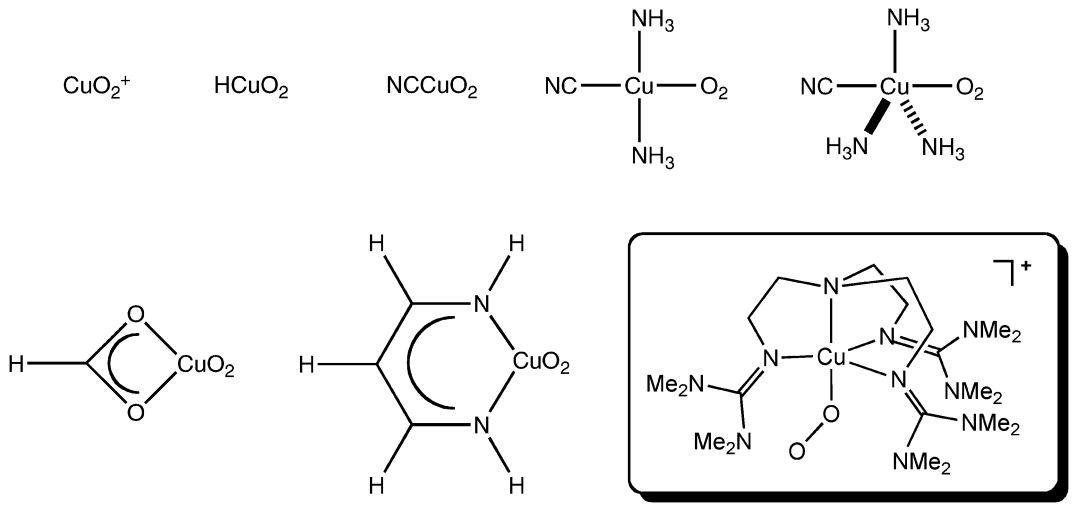

Fig. 5 Benchmark ligand systems L for comparing singlet and triplet electronic state energies for end-on and side-on $LCuO_2$ coordination geometries and $TMG_3trenCuO_2^+$ (inset).

characterized $LCuO_2$ complexes, identifying the importance of ligand stereoelectronic effects on orbital interactions between the LCu and O_2 fragments. One particular case is especially interesting, namely $TMG_3trenCuO_2^+$ (TMG_3tren = 1,1,1-tris{2-[N_2-(1,1,3,3-tetramethylguanidino)]ethyl}amine; see Fig. 5 inset). Originally reported by Schatz *et al.*,[955] the end-on nature of the O_2 coordination was assigned in part based on good agreement between observed resonance Raman O_2 stretching frequencies and those computed for a restricted singlet state at the BP86 level. The O_2 coordination geometry was later confirmed by single-crystal X-ray crystallography;[956] however, subsequent experimental work by Lanci *et al.*[614] established the electronic ground state of $TMG_3trenCuO_2^+$ to be triplet, not singlet, suggesting that the correlation in observed (triplet) and computed (singlet) O_2 stretching frequencies was coincidental. At the *m*PWPW level of theory, the triplet state is predicted to be lower in energy than the restricted singlet by 16 kcal mol^{-1}, and it is also lower than the broken-symmetry state by 7 kcal mol^{-1}, consistent with the experimental ground-state determination.[614] The *m*PWPW level of theory also provides reasonable quantitative agreement with the measured ^{18}O equilibrium isotope effect (EIE) for O_2 binding, with theory suggesting that solvation effects in acetone increase the charge transfer from LCu to the O_2 fragment, compared to the gas phase, and play a significant role in modulating the O_2 stretching frequency. De la Lande *et al.*[957] have also considered the chemistry of the $trenCuO_2^+$ system, applying a variable supplementary pseudopotential to the apical nitrogen atom to tune the oxidation potential of the supported Cu atom and examine the effects on C–H bond cleavage reaction coordinates. Gherman *et al.*[958] have examined the influence of biological ligands on O_2 coordination geometries and oxidation numbers.

The reactivity of supported $LCuO_2$ complexes has also seen substantial study at the DFT level. Thus, Aboelella *et al.*[959] examined the influence of a thioether ligand on the binding of O_2 to a Cu^I diketiminate, using BLYP and B3LYP to characterize the energetics and geometric details of the complex, as well as to explain an experimentally observed equilibrium between the monocopper complex and a bis(μ-oxo) dimer (see below for further discussion of bis(μ-oxo) copper species). Gherman *et al.*[960] used B3LYP to compare variations in oxygenation pathways, reduction potentials, and other properties when comparing diketiminate supporting ligands to anilido–imine ligands; Hill *et al.*[961] employed the same level of theory to explore the effects of ligand fluorination; and Heppner *et al.*[962] examined the possible influence of other auxiliary ligands on Cu-diketiminate-O_2 electronic structures. (In all of the studies cited in this paragraph, the poor performance of B3LYP for predicting singlet–triplet state energy splittings in $LCuO_2$ complexes was suspected and CASPT2 state energy splittings were computed instead.)

Considering a novel reaction of $LCuO_2$ species, Hong *et al.*[963] have employed M06-L to characterize the reaction path by which a supported Cu^I-α-ketocarboxylate-O_2 complex is transformed by decarboxylation of the ketocarboxylate into a highly reactive Cu=O species (best described as a triplet Cu^{II}–O(−/•) moiety) which then goes on to oxygenate a ligand phenyl ring *via* a concerted electrophilic attack on the ring. Huber *et al.*[488,964] expanded this initial study to explore ligand effects on the energetics of various steps, and moreover on computed electronic state energy differences, singlet *vs.* triplet, for all intermediates. For singlet–triplet splittings M06-L was compared to CASPT2 and RASPT2 and predictions from the DFT and WFT levels of theory were generally within 2 kcal mol^{-1} of one another irrespective of whether broken symmetry energies were used or spin purification was carried out. The starting O_2 complexes were exceptions, however, with M06-L predicting the singlet states to be substantially too high in energy, probably owing to the large nondynamical correlation associated with what amounts to a weakly perturbed singlet oxygen fragment. Comba *et al.*[965] have used B3LYP and coupled cluster methods also to study the aromatic hydroxylation activity of a Cu=O species, in this case generated from N–O homolysis of CuTMAO complexes (TMAO = trimethylamine *N*-oxide). As in the system of Hong *et al.*,[963] concerted attack of the oxo fragment on the aromatic ring is predicted by both B3LYP and coupled-cluster calculations to be favored over a stepwise H-abstraction/hydroxylation path, giving good agreement for the energetics of the reaction pathway. The critical intermediacy of a Cu=O species has also been invoked by Yoshizawa and Shiota[966] based on DFT studies, including QM/MM analyses, of the mechanism of methane to methanol conversion at the monocopper active site in particulate methane monooxygenase.

Considering the nitrogen equivalent of the Cu=O fragment, namely a copper nitrene, Comba *et al.*[967] have used B3LYP to characterize the mechanistic details of the bispidine copper catalyzed aziridination of olefins. A spin crossover is required to move from triplet reactants to singlet products. Bar-Nahum *et al.*[558] have used M06-L to determine the mechanism by which a trinuclear copper cluster reduces N_2O to N_2.

The structures and reactivities of various supported dinuclear $(LCu)_2O_2$ complexes have been the subject of many modeling studies, in part because they pose significant challenges to DFT with respect to computing relative isomer energies (Fig. 6). This challenge arises primarily from the varying degrees of open-shell *vs.* closed-shell character in singlet states depending on the oxidation states of the coupled copper atoms; when the two copper atoms are well described as d^9 Cu^{II} the usual challenges associated with multiconfigurational character in DFT arise.[413,485,486,968,969] As the modeling of $(LCu)_2O_2$ systems has been very recently reviewed,[942] we will mention only one recent addition.

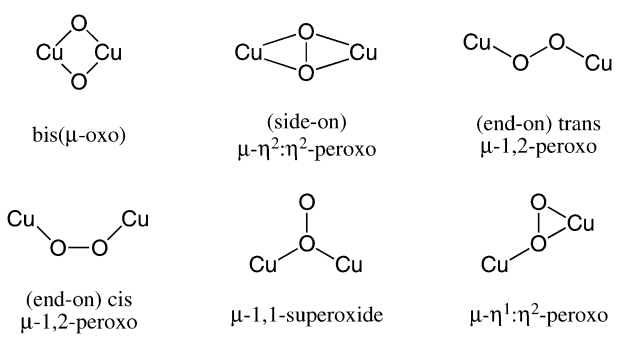

Fig. 6 Different core geometries for supported $(LCu)_2O_2$ complexes.

In particular, Sander *et al.*[970] have provided a detailed characterization of the mechanistic details associated with aromatic hydroxylation accomplished by an $(LCu)_2O_2$ complex having a μ-η^2:η^2 core.

A sometimes important reactive intermediate in the activation of molecular oxygen by copper is the hydroperoxide CuOOH. Osako *et al.*[971] employed the B98 functional to establish, by comparison of computed and experimental vibrational frequencies and EPR parameters, that a reactive intermediate originally presumed to be a Cu^{II} peroxide was instead a $Cu^{II}OOH$ species. Ghattas *et al.*,[972] based in part on B3LYP calculations, have also posited the importance of a CuOOH intermediate in the copper catalyzed conversion of 1-amino-cyclopropane carboxylic acid into ethylene by hydrogen peroxide. In acetone as solvent, the CuOOH intermediate can react with a molecule of solvent to generate a coordinated hydroxyhydroperoxypropane fragment that is itself capable of aromatic ring hydroxylation;[563] the mechanism for this process was studied by Kunishita *et al.*[973] at the *m*PWPW level.

Considering other ligands binding to copper, Periyasamy *et al.*[974] have concluded based on computed isomer energies and EPR parameters that the binding of nitric oxide to the Cu^{I} site in copper nitrite reductase is end-on, which is not consistent with current structural data, suggesting that higher resolution crystallography may be required to assess this discrepancy.

In the area of computational electrochemistry, Holland *et al.*[975] have employed DFT and continuum solvent models in the characterization of supported copper complexes that undergo quasi-reversible one-electron reductions at biologically accessible potentials that render them suitable as medical imaging agents for the study of hypoxia. As noted above, Schultz *et al.*[557] also rationalized experimental cyclic voltammetry data in multicopper helicates based on DFT calculations with continuum solvation, observing wirelike behavior in a tetranuclear system. Nazmutidinov *et al.*[976] modeled medium effects on the multi-electron reduction of Cu^{II}–Cu^{II} binuclear complexes.

Reveles *et al.*[977] have examined the nucleation of water molecules around Au^+, choosing a functional and basis set combination based on good agreement with experiment for simple water clusters. Consistent with the trend in experimental gas-phase binding energies and earlier theoretical studies, they predict that only 2 molecules of water can be considered to coordinate to the Au cation; subsequent waters form a shell that is anchored to the two ligating waters. As noted for Ru cations in section 5.3.1.6, they found significant charge transfer to the outermost water molecules in increasingly large solvation shells.

Considering supported gold compounds in homogeneous catalysis, Cheong *et al.*[978] employed B3LYP to establish the mechanism of homogeneous gold-catalyzed cycloisomerization of 1,5-allenynes to cross-conjugated trienes. Interesting, two molecules of catalyst are required to activate the alkyne. Soriano and Marco-Contelles[979] also used B3LYP and studied Pt- and Au-catalyzed the mechanisms of cycloisomerizations of enynes and propargylic esters.

Schwerdtfeger *et al.*[419] carried out accurate coupled cluster calculations on AuCO, Au_2CO, and their positive and negative ions. They used this data to test four density functionals, finding that B3LYP performs better than LSDA, BP86, and PW91. Unpublished calculations[980] show that M06-L performs about as well as B3LYP on this test.

5.3.1.10 Zinc, cadmium, mercury. Carrasco *et al.*[981] have used plane-wave PW91 calculations to study novel polymorphs of ZnO formed from the combination of low-energy $(MO)_{12}$ cage structures. The resulting nanoparticles would lead in the bulk limit to ultralow density mesoporous solids with potentially interesting properties, particularly if dopants can be introduced into the cavities. By analysis of equation of state data, Carrasco *et al.* predict that their most stable poly-cage structure should exhibit a bulk stability falling between the known wurtzite and rock-salt phases of ZnO, suggesting that it should be an ideal candidate for synthetic attention.

Cadenbach *et al.*[982] have shown the utility of alkylzinc and monocyclopentadienylzinc fragments as one electron donors to other transition metals, *e.g.*, in the unusual molybdenum complex $Mo(ZnCH_3)_9(ZnCp^*)_3$.

Bernasconi *et al.*[983] used the BLYP functional to study the dissociation of a water molecule coordinated to Zn^{2+} in aqueous solution. They observed delocalization of OH^- charge density over several water molecules in $Zn(H_2O)_5(OH)^+$.

Zn clusters have been studied by various workers. Dai *et al.*[984] used PW91, and Iokibe *et al.*[985] used LSDA, PW91, and B3LYP. Sorkin *et al.*[431] found that B3LYP and M05-2X both give reasonable results for the binding energies of small Zn clusters. Iokibe *et al.*[985] found that the bond length and cohesive energy of the clusters depends on the extent of 4s/4p mixing, in contrast to earlier transition metals where 4s/3d mixing is a key quantity.

Botticelli *et al.*[929] applied the PBE functional to investigate 13-atom Zn–Cu alloy clusters, both neural and cationic, and found special stability for icosahedral Zn_7Cu_6 clusters. However, they also found two other low-lying (within 0.2 eV of the global minimum) isomers of Zn_7Cu_6, indicating that the structure is not magic. The search for magic numbers and low-energy isomers of metal nanoparticles is an important field for future activity, as theory can characterize the rugged landscapes of such particles in a way not accessible to experiment.[928]

Tachikawa *et al.*[986] applied PW91 to calculate structures and electronic states $Zn_n(H_2O)_m$ with $n = 1$–32 and $m = 1$–3. In agreement with earlier work,[987] they found that the transition from noncovalent to covalent binding in Zn_n occurs between Zn_3 and Zn_4. This transition persists when water is bound.

Suwattanamala *et al.*[988] carried out B3LYP and PBE0 calculations on dipropoxythiacalix[4]arenes in chloroform solvent and examined the preferred metal coordination modes in their Zn^{2+} complexes by using B3LYP.

Lu *et al.*[989] have employed B3LYP and TD-B3LYP to rationalize the structure and intense fluorescence of a trinuclear cadmium coordination polymer, noting that the cadmium plays only a structural role, with the optical transitions being well described as ligand-to-ligand charge transfer in character. Fernandez *et al.*[990] used a phosphinothiol ligand designed to suppress the formation of coordination polymers and successfully isolated a series of polynuclear Zn, Cd, and

Hg compounds. These authors used B3LYP calculations to assess the nature of the bonding between the group 12 metals and their different ligands. Bonding *between* two group 12 metals has only rarely been demonstrated, but Zhu *et al.*[991] successfully synthesized dimers of the form ArMMAr for Ar = tetraisopropylterphenyl and M = Zn, Cd, or Hg and characterized the bonding at the BP86 level using energy decomposition analysis.

With respect to Hg, Wiederhold *et al.*[992] employed a combination of M06-L calculations with relativistic pseudopotentials and all-electron relativistic MP2 calculations to compute the mass-dependent and nuclear volume fractionation factors (MDF and NVF, respectively) contributing to the equilibrium partitioning of all Hg isotopes between dissolved Hg^{II} species and thiol-bound Hg^{II}, where the latter is a model for environmentally sorbed Hg^{II}. Wiederhold *et al.* observed excellent agreement with experiment for $HgCl_2$ and $Hg(OH)_2$ and found that both MDF and NVF made significant contributions to the total equilibrium isotope effects.

5.3.2 Solids. There is a wide range of solids containing transition metals. For example, transition metal oxides may be insulators, semiconductors, conductors, or superconductors, and they may have interesting magnetic, ferroelectric, antiferroelectric, and piezoelectric properties; they are important minerals and constituents of rocks, and they are also important in modern technology.[993] The literature is far too large to be fully surveyed here, but it is interesting to make some connection to other topics discussed in this review.

The LSDA already provides a good approximation for some, but not all, properties of some, but not all, transition metal solids.[994,995] GGAs do not necessarily improve the results.[996]

Kurth *et al.*[997] tested the accuracy of nine local functionals for the unit cell volumes of Cu, Pd, W, Pt, and Au. The mean unsigned errors (MUEs) are 1.0% for LSDA, 1.3–2.9% for GGAs (PBE best, followed by HCTH, RPBE, and BLYP), and 0.6–2.7% for meta-GGAs (PKZB best, followed by FT98, and VS98). Simple math shows that the percentage errors in lattice constants would be about 3 times smaller. LSDA underestimates the volumes (overbinding) whereas the GGAs and meta-GGAs usually overestimate them (underbinding). A similar trend was found for Cu, Rh, Pd, Ag, Ir, Pt, and Au with LSDA and PBE.[998] For the same five transition metals the MUEs in bulk moduli are 19% for LSDA, 8-34% for GGAs, and 6–27% for meta-GGAs.[997] The TPSS meta-GGA typically improves on PKZB for TM lattice constants but makes TM bulk moduli worse.[905]

Heyd *et al.*[999] showed that they could calculate accurate lattice constants with the screened Coulomb hybrid HSE functional. For example, the lattice constants of ZnS, ZnSe, and ZnTe are overestimated by HSE by an average of 0.7%, whereas the local PBE functional overestimates the same lattice constants by an average of 1.4%. This is important because HSE predicts much more accurate band structures (discussed below) than do local functionals.

For phonon frequencies of pure TMs, LSDA usually overestimates and PBE usually underestimates, but for thermal expansion, heat capacity, and free energy, LSDA is usually more accurate than PBE.[998] Suggestions have been made for improving the accuracy of calculated thermodynamic data of TMs and alloys by combining DFT data for temperature dependence with more accurate results for 0 K.[998] DFT has also been applied to more complex solid materials such as PbTiO3 perovskites[1000–1002] and HCP iron.[1003,1004]

Sun *et al.*[1005] used the LSDA, PBE, and WC functionals to calculate the equation of state for Pt. The Helmholtz energy was approximated as a function of lattice constants and temperature by setting it equal to a sum of three terms: the ground-state electronic energy (including core repulsion), the free energy of thermally excited electronic states, and the vibrational free energy of the lattice. Scalar relativistic effects were included, but not spin–orbit coupling. Electronic temperature effects were nonnegligible (as has also been found true recently for the free energies of Al nanoparticles[1006]).

With local functionals, the vertical HOMO–LUMO orbital energy gap is equal (to at least a good approximation) to the lowest TD-DFT excitation energy.[1007] This is also true[1007] for range-separated hybrids like HSE so that such functionals can give more accurate band gaps with the orbital-energy gap expression than do local hybrids.[999] For example, for ZnS, ZnSe, and ZnTe, HSE orbital energies underestimate the band gaps by an average of 0.27 eV (7–14%) whereas for the same three materials, the local PBE functional underestimates the band gaps by an average of 1.46 eV (41–58%).

Improvements can be obtained with the nonlocal weighted density approximation (WDA; see section 2.3); for eleven metal oxides containing transition metals (Ti, Hf, Zr, or Cu), the average error in the LSDA gaps is 2.0 eV, whereas the average error in the WDA calculations of Robertson *et al.* is 0.5 eV.[110] The error in the LSDA gap is inversely proportional to the high-frequency dielectric constant.[110,1008] The ability to calculate the gaps more accurately allows one to study interesting problems such as the charge states of interstitial hydrogens in oxides like TiO_2, $SrTiO_3$, $PbTiO_3$, ZrO_2, $SrZrO_3$, $ZrSiO_4$, HfO_2, ZnO, and CdO.[110,1009]

Grabowski *et al.*[998] calculated the free-energies and phonon dispersion curves of Rh, Ir, Pd, Pt, Ag, Au, and Cu with the LSDA and the PBE GGA. For the electronic free energy they used the finite-temperature DFT of Mermin.[1010] For phonon dispersion curves, the experimental results generally lie between those calculated by LSDA and PBE, whereas for free energies, LSDA is usually more accurate. The biggest differences between the two functionals were found for Ag and Au.

Theoretical studies are especially useful for studying materials under conditions that are hard to produce experimentally, for example, under the high-pressure conditions in the earth's mantle. Isaev *et al.*[1011] used the PBE density functional to calculate the electronic energy, including core repulsion, as a function of volume at high pressure for three phases of FeH, and they extended their calculations to free energy as a function of pressure by adding a quasiharmonic vibrational (*i.e.*, phonon) contribution to the ground-state electronic energy. Their analysis of the resulting phase diagram shows phase transitions at 37 GPa at 300 K and 50 GPa at 1000 K.

Umemoto *et al.*[1012] studied the spin state of Fe in iron-bearing magnesium silicate perovskite, $(Mg,Fe)SiO_3$, under lower-mantle conditions; this spin state is a crucial parameter

for determining key mantle properties such as elastic and seismic properties, the post-perovskite transition pressure, and electrical and thermal conductivities. Unfortunately the spin properties depend strongly on the choice of density functional (LSDA *vs.* PW91[129] or LSDA *vs.* PBE[130]). Nevertheless calculations with the LSDA and PBE functionals provide valuable insight into the effect of iron concentration, the coordination number of iron, and the nonmetalllic band structure at lower-mantle pressures.[1012]

Shi *et al.*[175] used the PW91 and sX approximations to study the cohesive energy, structural parameters, vibrational frequencies, and band structure of Au_2O and Au_2O_3. The projected density of states was analyzed to characterize the bonding, in particular the Au 5d and O 2p mixing and the ionic character. Whereas PW91 predicts Au_2O to be metallic, sX predicts a band gap of 0.8 eV.

For ZnO, the local LSDA, BLYP, PBE, and TPSS functionals predict a band gap of 0.9 eV, the local M06-L functional predicts 1.0 eV, and the hybrid HSE functional predicts 2.9 eV, in comparison to an experimental value of 3.4 eV.[999,1013,1014] The effect of Mn cluster doping on the optical properties of ZnO was studied with the PW1PW density functional.[104]

Filippetti *et al.*[1015] used ASIC-corrected (see section 2.2) LSDA calculations as well as uncorrected LSDA to study the spin-polarized band structures of the Mn-doped GaN and GaAs semiconductors. The results confirmed the LSDA picture for (Ga,Mn)As, but the results of the two kinds of calculations were very different for (Ga,Mn)N. Additional DFT calculations on this kind of half-metallic diluted magnetic semiconductor were reported by several subsequent groups.[1016–1022] Filippetti and Fiorentini[1023] applied the SIC scheme to cuprates.

Liu and Ge[1024,1025] studied hydrogen absorption in Ti-doped and Sc-doped $NaAlH_4$ with the PBE density functionals in order to better understand how transition metal doping might affect reversible hydrogen storage mechanisms.

Recent applications of linear response theory to the optical excitations of Cu, Ag, and Au are examples of improved approaches based on DFT.[1026,1027]

DFT has also been used to study spin polarization in potential materials (such as $CO_{1-x}Fe_xS_2$ alloys) for spintronics applications. An introduction to this subject is provided by Leighton *et al.*[1028]

An area of special interest for technology is the effect of external variables on spin-state orderings. In an atom, the high-spin state is often preferred, whereas crystal field splitting can stabilize a lower spin state in coordination compounds. As an example of the effect of an external variable, changing the pressure can affect the competition between high-spin (favored by electron exchange and reduced repulsion between two electrons otherwise paired in the same orbital) and low-spin (favored by crystal field splitting). A recently studied example is $SrFeO_2$, in which experiments reveal a transition at 33 GPa from an antiferromagnetic (AFM) insulator phase, in which the four-coordinate Fe^{II} is in a high-spin $S = 2$ state to a ferromagnetic (FM) metallic phase in which the four-coordinate Fe^{II} is in an intermediate-spin $S = 1$ state.[1029,1030] This was studied with the PBE0 functional, but varying the percentage X of Hartree–Fock exchange from the standard value of 25; it was found that the spin transition from the AFM $S = 2$ state is to a half-metallic FM $S = 1$ state if $X < 20$, and to a FM $S = 2$ state if $X > 20$. With $X = 15$, the calculated transition pressure is at 53 GPa.[1029] The transition was attributed to in-layer bonding interactions of Fe d orbitals with O p orbitals.

5.3.3 Surfaces and nanoparticles. Surfaces of bulk materials and nanoparticles, thin films, self-assembled monolayers, nanocrystalline coatings, and ligand-decorated materials interfaces are very important for catalysis and for technological applications such as molecular electronics, microelectronics, structural components, magnetic data storage, solar devices, and sensors. (Catalysis is mainly deferred to section 5.3.4.) In all of these applications, DFT can be used to study structural and morphological issues, reactivity and stability, and optical properties such as photoabsorption. In some cases it can also be used to calculate electrical and electron dynamical properties such as conductance and electron transfer or mesoscopic processes like sintering. Our review contains only a small subset of this burgeoning field.

Magyar *et al.*[1031] studied the geometries and magnetic properties of Au dimer, Au_{14}, and Au nanoclusters of sizes from Au_{28} to Au_{68} with B3LYP, PBE, and PBE0. They found that the clusters are magnetized primarily on their surfaces and that the Au_{14} and Au_{38} clusters are expanded as compared to the bulk geometry. They attributed the magnetism of Au nanoclusters to s–d hybridization, in contrast to another mechanism for surface magnetism in gold, in which local magnetic moments are induced by coupling to adsorbates.[1032]

Wende *et al.*[1033] used PW91 to calculate the energy of iron porphyrin molecules as a function of their distance from a face-centered cubic Co(100) magnetic substrate. At the optimum distance they also computed the spin-resolved partial densities of states in order to study the Fe–Co exchange coupling.

The rest of this subsection is primarily devoted to a sampling of the literature on adsorption; see also section 5.3.4 on heterogeneous catalysis.

Bilic *et al.*[1034] studied physisorption of benzene on Cu, Ag, and Au surfaces with the PW91 and PBE GGAs; they found that the binding energy is severely underestimated due to inaccurate treatment of correlation energy by these functionals. In related work, Café *et al.*[1035] studied monolayers of 1,10-phenanthroline on Au surfaces with the PW91 functional. Because this functional does not treat medium-range correlation accurately the binding energy of the physisorbed horizontal molecule was calculated to be only 2 kcal mol^{-1}; WFT calculations were used to estimate that the actual binding energy is much larger, 15 kcal mol^{-1}. The binding energy of the chemisorbed vertical molecule was also underestimated by PW91, which yielded an 8 kcal mol^{-1} binding energy as compared to a WFT estimate of 22 kcal mol^{-1}. Ma and Yang[1036] used B3PW91 to calculate Raman frequencies for adsorbed *p*-nitroaniline on a single Au-atom model of Au nanoparticles.

Neyman *et al.*[1037–1040] calculated the adsorption energies of all group-6 through group-11 atoms and of dimers, trimers

and tetramers of Cu, Ag, and Au (group 11) on MgO(001). For Pd absorption they obtained a binding energy of 1.4 eV with the BP86 functional and 1.1 eV with the RPBE functional, both in good agreement with the experimental value of 1.2 ± 0.2 eV. The effective adsorption energy per atom was found to be 7% less for Cu_3 than for Cu_2 and 22% less for Au_3 than for Au_2. They also studied the optical spectra of monomers and dimers.[1041] Additional studies of these systems were carried out by other workers.[1042–1046] The most recent study[1046] showed that the Au adsorption site most likely to lead to growth of a dimer (Au_2) is a neutral F_8 center. Florez *et al.* considered the effects of adsorption on that atomic spin states of the adsorbed metals and found that although spin-state splittings were reduced, high-spin states were in general not quenched upon adsorption.[1047]

Hinneman and Carter[1048] used the PBE density functional to study the adsorption of Y, Hf, and Pt on γ-Al_2O_3(0001). They found that Y and Hf form strong ionic bonds at 3-fold hollow sites, whereas Pt bonds more weakly at an on-top site without appreciable charge transfer.

The interaction of oxygen with Ag surfaces has been studied for a long time, but it is still controversial, despite the application of DFT.[1049–1052] The structures of oxide layers on other late transition metals have also been studied in detail;[425,1051,1053] the study of Rogal *et al.*[425] is particularly complete in that it uses calculated chemical potentials to compute the phase diagram of the Pd(100) surface in equilibrium and constrained equilibrium with an O_2 and CO gas phase. Jacob and coworkers[1054] analyzed the adsorption of oxygen on five different surface faces that are involved in the faceting of Ir(210), including the effect of aqueous electrolytes under electrochemical conditions.

Ge and coworkers used the PW91 density functional to study the adsorption and clustering of Pt adatoms on defect-free and defective anatase TiO_2(101).[1055,1056] They found barriers of 1.0 and 1.1 eV for Pt diffusion as required for dimer formation.

Xia *et al.*[1057] used the PW91 density functional to study surface hydration on freshly cleaved slabs of γ-manganite, MnO(OH). They found that water–water interactions dominate water–surface interactions for the density functional used.

King and coworkers[1058] used PW91 to explain the fact that water dimers diffuse more rapidly than water monomers on Pd(111) by a beautiful mechanism that they dubbed "the waltz of the water dimers". The details of their interpretation in terms of tunneling need to be checked. Another study of a similar nature is the finding that Pd_4 diffuses 200 times faster than Pd across an MgO(100) surface;[1059] on this surface, Pd_2 shows a walking (not quite waltzing) mechanism.[1059]

LSDA, PW91, PBE, and revPBE calculations predict that CO on Pt(111) preferentially adsorbs at 3-fold hollow sites, but the experimental result is preference for an on-top site.[1060,1061] This is consistent with a general trend for LSDA and GGA functionals to overly favor higher-coordination sites.[1060] Hybrid B3LYP calculations, in contrast, predict the correct preference,[1061,1062] which was attributed to the predicted HOMO–LUMO gap and the position of the HOMO and LUMO with respect to the Fermi energy.[1062] The reported contrast between the local PBE and nonlocal PBE0 functionals was particularly dramatic:[1063] PBE was said to favor the 3-fold site by 0.11 eV, and PBE0 was said to favor the on-top site by 0.13 eV, with the 2-fold bridge site intermediate for both functionals. Studies on the triatomic molecule PdCO and the tetra-atomic molecule Pd_2CO also lead to the conclusion that only hybrid functionals can qualitatively and quantitatively predict the nature of the σ-donation/π-back donation mechanism that is associated with CO binding in these cases.[326] Nevertheless the local BLYP functional does correctly predict the site preference, not only for CO/Pt(111), but also for CO/Rh(111) and CO/Cu(111).[221] The BLYP calculations also show that the HOMO–LUMO gap explanation for the site preference is not correct.[221] The PBE density functional predicts accurate CO stretching frequencies for CO adsorbed on Pt and Pt–Ru surfaces.[1064] The explanation for the frequency shifts in terms of σ donation and π back donation are very similar for adsorption at surfaces and for organometallic molecules.[326,1064] We will return to the important role of the π back-bonding orbital of CO in section 5.3.4 in discussing the adsorption of CO on Au(111).[1065]

Stroppa and Kresse[433] applied the local BLYP and PBE functionals and the nonlocal B3LYP and HSE functionals to the adsorption of CO at atop and hollow sites on the (111) surfaces of Ru, Os, Rh, Ir, Pd, Pt, and Ag. They concluded that BLYP and B3LYP are more accurate for adsorption, with PBE inaccurate, and HSE least accurate. This contradicts the previous claim[1063] that hybrid functionals solve the CO adsorption puzzle; Stroppa and Kresse conclude that the previous conclusion[1063] is an artifact of the way that pseudopotentials were employed in the previous work. Stroppa and Kresse drew general conclusions in a broad discussion that includes not only BLYP, B3LYP, PBE, and HSE but also LSDA, RPBE, PBE0, AM05 and PBEsol. One pays a price for the successful chemisorption predictions of BLYP and B3LYP, namely a poor description of the lattice constants of transition metals and a poor description of surface energies. They concluded that hybrid functionals are not a step forward for metals, which agrees with the conclusion of Schultz *et al.*[93,94] prior to the development of M05 and M06. Unfortunately M05 and M06 have not yet been put to most of the tests discussed in this section.

Lo and Ziegler[1066] carried out spin-polarized PBE calculations of CO adsorption and dissociation on the (110) surface of FeCo alloys. They then recalculated the adsorption energies with the RPBE functional and obtained values lower by 7–10 kcal mol^{-1}. Furthermore, for coverages of 0.25 monolayer and higher, the favored binding site at Fe changed from a long bridge to an on-top site, which is consistent with previous work[1067] for Fe(110), whereas the overall favored binding site at Co did not change. In related studies using the PW91 functional, they examined CO adsorption on Fe(310),[1068] and they studied adsorption and reactions of C_2 hydrocarbon fragments on Fe(100);[1069] spin polarization was included in all calculations to account for the ferromagnetic properties of bulk Fe.

Valcárcel *et al.*[1070] used the PW91 density functional to calculate the binding modes of propyne on Pd(111) and Pt(111). Wang *et al.* used the PW91 density functional to

study the adsorption of 2-methyl-2-propanethiol on reconstructed Au(111),[1071] the adsorption of CH_3S radicals on unreconstructed Au(111),[1072] and the $(22 \times \sqrt{3})$ surface reconstruction of Au(111).[1073] In the last-named study they found that the nearest-neighbor distances in the top layer are 0.09–0.16 Å shorter than the bulk nearest-neighbor distances, and the interlayer distance is increased by 0.05–0.17 Å by reconstruction. Friend and Kaxiras and coworkers[1074] also used the PW91 density functional, and they studied changes in gold surfaces induced by sulfur adsorption. They also studied structures and binding energies of chlorine adsorbed on Au, again with the PW91 density functional.[1075,1076]

Marks *et al.*[1077] studied the surface reconstruction and surface energies of $SrTiO_3$ by DFT with a limited number of functionals, and they found TPSSh to be most accurate. The results are analyzed in detail, which makes the paper particularly interesting.

Mao *et al.*[1078] calculated spin-polarized band structures with the PBE density functional for single Mn, Fe, and Co atoms on a single graphene sheet. Kaghazchi *et al.*,[1054] employing the PBE density functional, evaluated interfacial free energies of adsorbate-induced surface faces of nano-faceted Ir(210). Kuganathan and Green[1079] used the LSDA to predict the structure and conduction band of CuI in single-walled carbon nanotubes (SWNTs). Sceats and Green[1080] used LSDA and PW91 functionals to study cobaltocene and bis(benzene)chromium encapsulated in SWNTs. Friend and Kaxiras and coworkers[1081] used the PW91 density functional to study MoO_3 monolayers nanocrystals on Au(111) and their selective reduction.

Carter and Yarovsky and their coworkers used the PBE and PW91 functionals, respectively, to study a variety of adsorption, dissociation, and diffusion processes on Fe, Al/Fe, Fe/Si and sulfur-covered-Fe surfaces[1082–1090] and structure and magnetism at Cr/Fe interfaces.[1091] Yarovsky and coworkers[1092,1093] used the PW91 density functional to carry out spin-polarized direct dynamics simulations of H_2S dissociation at the (110) and (100) surfaces of Fe at temperatures from 298 K to 1800 K. The dissociation mechanism was found to change as a function of temperature.

Iokibe *et al.*[985] studied the adsorption and diffusion of Zn on Zn(001) with the PW91 density functional. Kurzweil and Baer[1094] used a novel DFT approach to study the surface plasmon absorption of Au_8 and Au_{18}. Ferrando *et al.*[1095] reviewed the application of theory to structural, optical, magnetic, thermodynamic, and kinetic properties of mixed-metal clusters and binary alloyed nanoparticles of transition metal elements.

Zhu *et al.*[1096] used hybrid GGAs to calculate quantum well states for charge transfer excitations from Au to C_{60} at the C_{60}/Au(111) interface. The experiments were later reinterpreted by Li *et al.*[1097] in terms of superatom molecular orbitals[1098,1099] of C_{60}.

Geng *et al.*[1100] and Derosa *et al.*[1101] studied adsorption of benzenethiolate at transition-metal (Pt, Cu, Ag, Au) surfaces.

Although there are no established rules for the precise usage of words like "nanoparticles" and "quantum dots", one could classify isolated molecules in a range of ascending sizes from complexes and clusters, defined as particles with diameters less than 1 nm, to nanoparticles, defined as particles with diameter greater than 1 nm but having morphology different from the bulk, up to quantum dots, often defined as having the bulk structure but exhibiting quantum confinement (of electrons or holes) in three spatial dimensions (note that systems with quantum confinement in only two or one dimensions are called quantum wires and quantum wells, respectively, or—especially if smaller—they may be called, among other possibilities, nanowires, nanotubes, nanowells, or thin films). However, these distinctions are fluid; for example, quantum dots are often called nanoparticles, but nanoparticles that do not have the bulk structure are not usually called quantum dots. Furthermore, researchers interested in catalysis are more likely to use the nanoparticle language, and those interested in electronic properties are more likely to use the quantum dot language. Some recent examples of DFT studies modeling quantum dots containing transition metals are cited to illustrate the possibilities.[1102–1105]

5.3.4 Heterogeneous catalysis. The distinctions between homogeneous and heterogeneous catalysis are blurred in many applications, such as catalysis by clusters or nanoparticles, which may be unsupported or supported on metal oxides, zeolites, or thin films, or catalysis by supported thin films, or by supported organometallic species.[856,916,1054,1106–1122] As mentioned in section 5.3.1.9, gold atoms, gold clusters, and gold nanoparticles have been especially widely studied.[856,1112,1113,1116,1119–1121,1123] Although only a fraction of this kind of work could be included in section 5.3.1, in this section we focus only on conventional heterogeneous catalysis, in particular on surfaces of metals, alloys, and oxides; see also discussions of adsorption and adsorbates on surfaces in section 5.3.3. Grönbeck,[1124] Catlow *et al.*,[1125] Cinquini *et al.*,[1126] Nørskov *et al.*,[1127,1128] and Neyman and Illas[1129] recently provided introductory overviews of DFT applied to heterogeneous catalysis, and Coquet *et al.*[1130] provided a critical review of the theory and simulation of heterogeneous gold catalysis. Two recent contributions have emphasized the nanoparticle/crystal surface distinctions for catalysis from both experimental[1131] and combined experimental/computational[1132] points of view. For example, Falsig *et al.*[1132] contrasted Au_{12} to Au(111). A review more focused on dynamical processes, especially of hydrogen, has been presented by Lanzani *et al.*[1133]

In discussing dynamical processes at surfaces, especially metal surfaces (and sometimes in discussing dynamical processes more generally), the question arises of whether the Born–Oppenheimer approximation is valid or, in contrast, whether one must invoke electronically nonadiabatic processes and the participation of electronic excited states.[1134–1160] In the surface science literature this is often called electron-hole creation or electron-hole participation (similarly, vibrational excitation of the surface is often called phonon creation). There is considerable evidence that electronically excited states play a role in some but not all processes at metal surfaces. Kroes and coworkers[1147] have offered an explanation for why electron-hole pairs are more important for H_2/Pt(111) than for NO/Au(111). In other work discussed below, it is assumed (usually implicitly) that only the ground-electronic-state potential energy surface plays a role.

A heterogeneous catalytic process with a dramatic effect on the course of world history is the Haber process for the synthesis of ammonia, originally carried out on enriched Fe and later on Ru, and this reaction is still being studied, most recently with the PW91 and RPBE density functionals.[1161–1163] It was found that the overall rate predicted by the RPBE density functional is a factor of 3 to 20 too low, as compared to experiment.[1161]

A familiar and practically important example of heterogeneous catalysis by transition metals is catalytic removal of undesirable gases from automotive exhausts. Liu *et al.*[1164] studied the selective reduction of NO by Ir under conditions of excess oxygen such as occur in lean burns. In the absence of an appropriate reductant, oxygen is found to poison the catalytic process.

Although it is not a catalytic process, the chemisorption of H_2 on metal surfaces has been a very widely studied prototype process, and much can be learned because of the possibility of carrying out more complete quantum mechanical dynamics calculations than for other reagents and the resulting possibility of obtaining accurate empirical values for barrier heights.[242] Recent papers on H_2 dissociation over W, Ru, Pt, and Cu be consulted as an entry point into this literature,[1147,1165–1171] and there is also a recent review.[1172]

The binding of CO on MgO(001) has proved to be a very difficult case, but recent work has shown that the M06-2X and M06-HF functionals can, for the first time, provide a simultaneously satisfactory description of adsorbate geometry, vibrational frequency shift, and adsorption energy.[1173] Although this system has no transition metals, it may provide a route to further progress on equally challenging problems such as the bonding and dissociation of nitrogen oxides on $Ni_xMg_{1-x}O(100)$.[1126, 1174–1180] In preliminary studies[1180] the M06 functional shows the best performance for NO binding to $Ni_xMg_{1-x}O(100)$.

Heyden *et al.*[1181–1183] used B3LYP to study nitrous oxide decomposition at iron sites in the iron-exchanged microporous ZSM-5 zeolite. Rate parameters were determined for 167 elementary steps, and the resulting reaction mechanism explained a variety of transient and steady-state experiments. This work elucidated the nuclearity of the active Fe sites during steady-state decomposition of N_2O and showed that previously invoked oxygen desorption is kinetically not relevant for this process.

Goodrow and Bell[1184] used B3LYP for methanol oxidation on isolated vanadate ($(O)_3V{=}O^{3-}$) supported on TiO_2 and showed that the difference in rate from vanadate supported on TiO_2 is not due to the influence of the support on the electronic properties of vanadate, but rather is due to the higher incidence of defects on TiO_2. Introduction of an O-vacancy in the support adjacent to vanadate lowers the apparent activation energy of the rate limiting step (transfer of an H atom from an adsorbed methoxy to a vanadyl O) from 23 to 16 kcal mol^{-1}.

Bonde *et al.*[1185] used the RPBE functional to model electrochemical oxidation of nanoparticulate MoS_2, WS_2, Co–Mo–S, and Co–W–S with special emphasis on the edge structures.

Gokhale *et al.* studied the water-gas shift reaction ($CO + H_2O \rightarrow CO_2 + H_2$) on Cu(111)[1186] and Pt(111)[394] with the PW91 functional. They found that key mechanistic determinants are the binding energies of CO, OH, and COOH and that a mechanism involving COOH is more favorable than direct oxidation of CO. Their results were used in a microkinetic model to estimate turnover rates under various conditions, and they provide an excellent example of the state of the art in complete catalytic process modeling.

Andersson *et al.*[1187] studied the dissociation of CO on Ni surfaces. They used the RPBE functional with a scheme to correct for the systematic overbinding of CO to metals with this functional. Their study included the effect of coadsorbed hydrogen and defects, and they included a COH species in their mechanism; they provided a good account of the experimental results.

Schneider and coworkers have also placed a special emphasis on using DFT to simulate catalysis under realistic conditions of oxidation environment, oxygen pressure, temperature, particle size, and catalyst composition. They attempted to quantify the conditions that lead to various adsorbate coverages. Their work is mainly concerned with CO and NO oxidation on Pt catalysts,[1188–1192] and they also used PW91 to study the influence of oxygen coverage on the structure, energetics, and electronics of the $RuO_2(110)$ surface.[1193]

Rösch, Chen, and coworkers[398,1194–1199] and other researchers[1200] used the PW91 and BP86 density functionals to study the effects of crystal faces, surface composition, and steps on a variety of decomposition steps on ZnPd, Cu, and Pd surfaces. The recent work[398] on methanol decomposition on nanocrystallites of Pd catalysts is particularly illuminating because it models some aspects of the nanocatalyst more realistically than usual, in particular as a 79-atom nanocrystallite that contains nonideal specific sites and facets that occur in real catalytic systems.[1201] Unfortunately, the cluster geometries were frozen during the calculations in an attempt to make up for deficiencies of the models and density functional.

Li *et al.*[1200] found that nuclear tunneling needs to be taken into account to predict the temperature-programmed desorption peak temperatures for β-hydride elimination of ethyl radical on Cu. Additional studies have recently been carried out using the PBE density functional.[1202] Recent experiments on Pd surfaces with Zn incorporation are consistent with earlier theoretical studies[1194–1196] but suggest that such studies should be carried out with lower concentrations of Zn.[1203]

Tang and Trout[1204] used the PW91 functional to calculate adsorption energies of SO_2 and NO on surface alloys of Pt with Ru, Ru, Ir, Ni, Pd, Cu, and Au to evaluate potential oxidation emissions catalysts.

King and coworkers studied the dissociative chemisorption of methane on Pt[1205] and subsequent dehydrogenation steps to produce CH_2, CH, and C.[391] Using PW91, they found[1205] breaking bond lengths for the transition states of the $CH_4 \rightarrow CH_3 + H$ reaction on Pt(110)-(1 × 2) and Pt(111) to be 1.48 Å and 1.54 Å, respectively, which may be compared to earlier calculations that yielded 1.37 Å (calculated[1206] by embedded diatomics-in-molecules), 1.53 Å (calculated[1207] by an embedded-cluster configuration interaction calculation), 1.59 Å (calculated[1208] by PW91), 1.47 Å (calculated[1209,1210] by

PW91), or 1.58 Å (calculated[1211] by PBE) on Ni(111) and 1.53 Å (calculated[1212] with an unspecified GGA) on Ni(100). The calculated barriers also differ, with barriers of 17,[1207] 26,[1208] 14,[1206] and 25[1211] kcal mol^{-1} on Ni(111) and barriers of 12[1205] and 21[1211] kcal mol^{-1} on Pt(111). (Liao *et al.*[1213] and Psofogiannakis *et al.*[1214] also discussed the $CH_4 \rightarrow CH_3 + H$ reaction at metal surfaces (Pt[1213,1214] and three other metals,[1213] with PB86,[1213] B3LYP,[1214] and PW91[1214]), but they approximated the metal surfaces by small (unembedded) clusters.) For CH_2 dehydrogenation, the calculated barrier height of King and coworkers,[391] 28 kcal mol^{-1}, agrees well with an experiment that was interpreted to yield 29 kcal mol^{-1}.

Further work on C–H bond activation has been reported by Li *et al.*,[1215] in this case including both metal surfaces and oxides. In particular they applied the PBE functional to study the dissociation of CH_4 on Tc(0001), Ru(0001), Pd(111), Pt(111), Cu(111), and three crystal faces of PdO. Following Nørskov and coworkers (see next paragraph) they found a linear correlation between the C–H activation barrier and the total chemisorption energy in the final dissociated state, and they discussed the heterolytic component of the dissociation process.

Nørskov and coworkers have developed a general analysis based on scaling properties[1128] and have applied it to numerous problems. In such an analysis one compares results for several different surface compositions and tries to identify a small number of key variables upon which the binding energy depends linearly. A good example is provided by the adsorption energies of hydrogen-containing compounds (CH_n, NH_n, OH_n, and SH_n) on Ru, Rh, Ir, Ni, Pd, Pt, Cu, Ag, and Au; here they identified n as the key variable, and they rationalized this by an effective medium theory similar to embedded atom theory.[1216] The finding that reaction rates vary linearly with bond energies or reaction energies is reminiscent of the Evans–Polanyi–Semenov linear correlation between activation energy and enthalpy of reaction in gas-phase kinetics.[1217,1218] Another example is provided by the analysis of the selective hydrogenation of acetylene on metallic and bimetallic surfaces; the key variables were identified as the heats of adsorption of acetylene and ethylene; and on this basis they identified NiZn alloys as potential new selective catalysts (producing ethylene in preference to ethane), and the prediction was verified experimentally.[1219] Later work based on the same principles showed how subsurface carbon and alloying Pd with Ag have similar effects on selective hydrogenation of acetylene.[1220] The compromise required in optimizing a process that correlates with two or more different properties is often presented in the form of a two-dimensional or three-dimensional "volcano" plot.[1221,1222]

Surface-catalyzed chain growth mechanisms, that is, the formation of C–C bonds, on Re, Fe, Ru, Co, and Rh were studied using the PBE functional.[1223,1224] Surface catalyzed hydrogenation has also been studied; for example, Saeys *et al.*[1225] have used BP86 to assess the mechanistic details associated with the hydrogenation of benzene to cyclohexane on Pt(111) surfaces.

Interpretation of the role of promoters on heterogeneous catalysis has long been a goal of theoretical modeling.[1226,1227] Zhang *et al.*[1065] took up the question for stabilization of CO on Au(111); they used the PBE functional to calculate charge densities of adsorbed species to interpret experimental observations of promoting effects. They found depletion of electron density from the π back-bonding orbital of CO when coadsorbed with NO_2, thereby weakening the bonding of CO to the surface. O, S, and Cl behave analogously to NO_2, and the calculations suggest that the interaction between two electronegative adsorbates need not be repulsive.

Pacchioni and coworkers[147,148] have recently provided a very pessimistic assessment of the ability of DFT to predict the energetics needed for quantitative modeling of catalytic processes in TiO_2 and at TiO_2 and NiO surfaces. The functionals on which they based their conclusions are PW91, PBE, B3PW91, B3LYP, and BH&HLYP. On the other hand, Labat *et al.*[1228,1229] noted that while it is disappointing that all functionals fail to predict accurately the relative stability of rutile and anatase, PBE0 otherwise offered a good compromise for lattice parameters and band structure.

Porous metal–organic frameworks are becoming more popular as hosts for catalytic reactions, and Choomwattana *et al.*[1230] have recently used combined QM/MM calculations with B3LYP for the QM subsystem for the Cu-catalyzed reaction of formaldehyde with propene. Kuc *et al.*[1231] concluded that PBE0 greatly underestimates the interaction energies of hydrogen molecules with the organic linkers of Zn-based metal–organic frameworks.

Various groups have applied DFT for additional studies of the structures and energetics of adsorption and heterogeneous catalytic processes, and selected references are given to illustrate recent progress.[1063,1186,1222,1232–1250]

Despite the great progress that has been made in modeling heterogeneous catalytic processes, comparison to experimental catalytic processes is still limited, not only by the quality of the density functionals (and sometimes by inadequate basis sets or noninclusion of scalar and/or vector relativistic effects), but also by the inability to simultaneously include all aspects of finite temperature, coverage, partial pressures of all species present, dopants, coadsorbents, reconstruction, local morphology, defects, and consideration of all possible pathways. Nevertheless, much has been learned and progress is accelerating. A key direction for making the calculations more and more relevant to real catalysis is the increasing use of kinetic Monte Carlo and microkinetic models in conjunction with the DFT calculations.[394,1186,1251–1266] Without inclusion of DFT input and explicit treatment of diffusion and site-specific local concentration effects (spatial effects), phenomenological models may involve "effective parameters which have only limited (if any) microscopic meaning".[1255,1259] Reuter *et al.*[1255] included dissociation, adsorption, surface diffusion, surface chemical reactions, and desorption in their KMC model of CO oxidation on RuO_2(110). Coupling to heat transfer and fluid dynamical treatments of mass transfer are in the near future.

While the microkinetic models allow improved comparison to experiment under a variety of realistic conditions involving competing pathways, better experimental isolation of preselected pathways allows more direct comparison of theory with experiment. It is hoped that the recent experimental study of size-preselected Pt clusters under high-temperature catalytic

conditions (atmospheric pressure) presages a new round of informative activity of this type.[1267,1268] In these experiments, size-preselected Pt_8–Pt_{10} clusters stabilized on high-surface area supports were used to dehydrogenate propane to propene with high efficiency and good product selectivity, and B3LYP (for clusters) and RPBE (for surfaces) calculations were used[1268] to interpret the improved catalytic properties of clusters relative to the surface in terms of the under-coordination of the Pt sites in the clusters.[1268]

Tao *et al.*[1269] have recently investigated the performance of selected density functionals for jellium surfaces and bulk jellium linear response, where jellium systems serve as a model for testing functionals.

5.3.5 Electrocatalysis. Electrochemical redox processes at metal surfaces have also been studied by DFT, but we limit ourselves here to presented some very recent references on processes occurring at Pt as a starting point into the literature of the field.[1270–1280] For more general remarks on DFT applied to electrocatalysis involving transition metals, see the recent *Faraday Discussion*.[1281,1282]

5.3.6 Photocatalysis. Doped and sensitized TiO_2 are well studied for their photocatalytic properties.[1283–1287] Although research on TiO_2 structural, electronic, optical, photocatalytic, photovoltaic, and hydrogen storage properties is still driven mainly by experiment, there are many opportunities for DFT to contribute.[570–575,930,932,1009,1014,1055,1056,1097,1184,1283–1302]

Zapol and Curtis[1303] reviewed the application of DFT to adsorption and photoexcitation of organic adsorbates on TiO_2 nanoparticles. Vittadini *et al.*[1290] reviewed theoretical studies of surface structure, stability, and reactivity of TiO_2 surface systems. Recent studies of the band structure of Mn-doped rutile TiO_2[1304] and of the nucleation, growth, and adsorption of transition metal clusters on anatase TiO_2 (101)[1305,1306] are of particular interest.

A very recent calculation[1287] employs the local PBE functional and the nonlocal B3LYP functional to calculate the spin-polarized density of states for Cr/Sb codoped TiO_2. The PBE, experimental, and B3LYP band gaps are 2.6, 3.6, and 3.9 eV, respectively, and the two calculations give different predictions for the positions of the Sb and Cr states relative to the valence and conduction bands, but the more accurate hybrid calculations allow an interpretation of why the co-doped system shows increased photostability.

Nakamura and Yamashita[1307] used a nonequilibrium Green's function method to calculate the reaction probability of the photoinduced desorption/dissociation of O_2 on Ag(110). They used the PBE density functional.

6. Concluding remarks

The application of DFT to transition metal systems has become well established, even though many studies have been carried out with less than fully reliable density functionals. Given the rapid pace of ongoing functional development and the ever increasing scope of applications, the field must be regarded as still in its infancy. There remains considerable room for improvement, and the future is likely to be exciting.

Acknowledgements

The authors are grateful to Yan Zhao for innumerable discussions, for collaboration on density functional development and applications, and for providing Fig. 3 and to Ilaria Ciofini, Ke Yang, and Yan Zhao for suggestions on improving the manuscript. This work was supported in part by the US Air Force Office of Scientific Research under grant no. FA9550-08-1-018 and the US National Science Foundation under grants CHE-0610183 and CHE07-04974.

References

1 W. Kohn, A. D. Becke and R. G. Parr, *J. Phys. Chem.*, 1996, **100**, 12974.
2 P. Hohenberg and W. Kohn, *Phys. Rev. B*, 1964, **136**, B864.
3 L. H. Thomas, *Math. Proc. Cambridge Philos. Soc.*, 1927, **23**, 542.
4 E. Fermi, *Z. Phys.*, 1928, **48**, 73.
5 W. Kohn and L. J. Sham, *Phys. Rev.*, 1965, **140**, A1133.
6 U. von Barth and L. Hedin, *J. Phys. C: Solid State Phys.*, 1972, **5**, 1629.
7 A. K. Rajagopal and J. Callaway, *Phys. Rev. B: Condens. Matter Mater. Phys.*, 1973, **7**, 1912.
8 D. R. Hartree, W. Hartree and B. Swirles, *Philos. Trans. R. Soc. London, Ser. A*, 1939, **238**, 229.
9 O. Sinanoglu and D. F. Tuan, *J. Chem. Phys.*, 1963, **38**, 1740.
10 D. G. Truhlar, *J. Comput. Chem.*, 2007, **28**, 73.
11 H. J. Silverstone and O. Sinanoglu, *J. Chem. Phys.*, 1966, **44**, 1899.
12 M. W. Schmidt and M. S. Gordon, *Annu. Rev. Phys. Chem.*, 1998, **49**, 233.
13 R. J. Deeth, *Struct. Bonding*, 2004, **113**, 37.
14 F. Neese, *JBIC, J. Biol. Inorg. Chem.*, 2006, **11**, 702.
15 P. E. M. Siegbahn and T. Borowski, *Acc. Chem. Res.*, 2006, **39**, 729.
16 L. Noodleman and W.-G. Han, *JBIC, J. Biol. Inorg. Chem.*, 2006, **11**, 674.
17 L. Bertini, M. Bruschi, L. de Gioia, P. Fantucci, C. Greco and G. Zampella, *Top. Curr. Chem.*, 2007, **268**, 1.
18 V. Polo, E. Kraka and D. Cremer, *Mol. Phys.*, 2002, **100**, 1771.
19 D. Cremer, *Mol. Phys.*, 2001, **99**, 1899.
20 A. D. Becke, A. Savin and H. Stoll, *Theor. Chem. Acc.*, 1995, **91**, 147.
21 J. P. Perdew, A. Savin and K. Burke, *Phys. Rev. A: At., Mol., Opt. Phys.*, 1995, **51**, 4531.
22 A. Görling, *J. Chem. Phys.*, 2005, **123**, 062203.
23 J. D. Talman and W. F. Shadwick, *Phys. Rev. A: At., Mol., Opt. Phys.*, 1976, **14**, 36.
24 A. M. Teale, A. J. Cohen and D. J. Tozer, *J. Chem. Phys.*, 2007, **126**, 074101.
25 A. V. Arbuznikov, M. Kaupp and H. Bahrman, *J. Chem. Phys.*, 2006, **124**, 204102.
26 A. V. Arbuznikov, *J. Struct. Chem.*, 2007, **48**, S1.
27 J. F. Janak, *Phys. Rev. B: Condens. Matter Mater. Phys.*, 1978, **18**, 7165.
28 I. G. Kaplan, *Intermolecular Interactions*, Wiley, Chichester, UK, 2006, ch. 3.
29 K. T. Tang and J. P. Toennies, *J. Chem. Phys.*, 1984, **80**, 3726.
30 K. T. Tang and J. P. Toennies, *Molecular Physics: An International Journal at the Interface Between Chemistry and Physics*, 2008, **106**, 1645.
31 J. F. Dobson, A. White and A. Rubio, *Phys. Rev. Lett.*, 2006, **96**, 073201.
32 J. Harl and G. Kresse, *Phys. Rev. B: Condens. Matter Mater. Phys.*, 2008, **77**, 045136.
33 M. Rohlfing and T. Bredow, *Phys. Rev. Lett.*, 2008, **101**, 266106.
34 Y. Zhao, N. E. Schultz and D. G. Truhlar, *J. Chem. Phys.*, 2005, **123**, 161103.
35 Y. Zhao and D. G. Truhlar, *J. Phys. Chem. A*, 2006, **110**, 5121.
36 Y. Zhao and D. G. Truhlar, *J. Chem. Theory Comput.*, 2006, **2**, 1009.
37 Y. Zhao and D. G. Truhlar, *J. Chem. Theory Comput.*, 2007, **3**, 289.
38 Y. Zhao and D. G. Truhlar, *J. Chem. Phys.*, 2006, **125**, 194101.
39 Y. Zhao and D. G. Truhlar, *Theor. Chem. Acc.*, 2008, **120**, 215.

40 C. Adamo and F. Lelj, *J. Chem. Phys.*, 1995, **103**, 10605.
41 T. Ziegler, *Chem. Rev.*, 1991, **91**, 651.
42 J. P. Perdew, in *Density Functional Theory of Molecules, Clusters, and Solids*, ed. D. E. Ellis, Kluwer, Dordrecht, 1995, p. 47.
43 W. Kohn, *Rev. Mod. Phys.*, 1999, **71**, 1253.
44 E. J. Baerends, *Theor. Chem. Acc.*, 2000, **103**, 265.
45 J. P. Perdew and S. Kurth, in *A Primer in Density Functional Theory*, ed. C. Foilhais, F. Nogueira and M. Marques, Spinger-Verlag, Berlin, 2003, p. 1.
46 U. von Barth, *Phys. Scr.*, 2004, **t109**, 9.
47 G. E. Scuseria and V. N. Staroverov, in *Theory and Applications of Computational Chemistry: The First Forty Years*, ed. C. E. Dykstra, G. Frenking, K. S. Kim and G. E. Scuseria, Elsevier, Amsterdam, 2005, p. 669.
48 F. M. Bickelhaupt and E. J. Baerends, *Rev. Comput. Chem.*, 2000, **15**, 1.
49 T. A. Wesolowski, in *Molecular Materials with Specific Applications*, ed. W. A. Sokalski, Springer, Heidelberg, 2007, p. 153.
50 J. P. Perdew, A. Ruzsinsky, J. Tao, V. N. Staroverov, G. E. Scuseria and G. I. Csonka, *J. Chem. Phys.*, 2005, **123**, 062201.
51 J. P. Perdew, A. Ruzsinszky, L. A. Constantin, J. Sun and G. I. Csonka, *J. Chem. Theory Comput.*, 2009, **5**, 902.
52 P. A. M. Dirac, *Math. Proc. Cambridge Philos. Soc.*, 1930, **26**, 376.
53 J. C. Slater, *Phys. Rev.*, 1951, **81**, 385.
54 D. M. Ceperley and B. J. Alder, *Phys. Rev. Lett.*, 1980, **45**, 566.
55 S. H. Vosko, L. Wilk and M. Nusair, *Can. J. Phys.*, 1980, **58**, 1200.
56 J. Perdew and Y. Wang, *Phys. Rev. B: Condens. Matter Mater. Phys.*, 1992, **45**, 13244.
57 J. P. Perdew, J. Tao and S. Kümmel, *ACS Symp. Ser.*, 2007, **958**, 13.
58 A. D. Becke, *Phys. Rev. A: At., Mol., Opt. Phys.*, 1988, **38**, 3098.
59 J. P. Perdew, *Phys. Rev. B: Condens. Matter Mater. Phys.*, 1986, **33**, 8822.
60 C. Lee, W. Yang and R. G. Parr, *Phys. Rev. B: Condens. Matter Mater. Phys.*, 1988, **37**, 785.
61 J. P. Perdew, in *Electronic Structure of Solids '91*, ed. P. Ziesche and H. Eschrig, Akademie Verlag, Berlin, 1991, p. 11.
62 J. P. Perdew, K. Burke and M. Enzerhof, *Phys. Rev. Lett.*, 1996, **77**, 3865.
63 C. Adamo and V. Barone, *J. Chem. Phys.*, 1998, **108**, 664.
64 M. H. Lim, S. E. Worthington, F. J. Dulles and C. J. Cramer, in *Chemical Applications of Density Functional Theory*, ed. B. B. Laird, R. B. Ross and T. Ziegler, American Chemical Society, Washington, DC, 1996, vol. 629, p. 402.
65 M. W. Nolan and G. W. Watson, *J. Chem. Phys.*, 2006, **125**, 144701.
66 T. Bally and G. N. Sastry, *J. Phys. Chem. A*, 1997, **101**, 7923.
67 C. J. Cramer and S. E. Barrows, *J. Org. Chem.*, 1998, **63**, 5523.
68 B. Braieda, P. C. Hiberty and A. Savin, *J. Phys. Chem. A*, 1998, **102**, 7872.
69 M. Sodupe, J. Bertran, L. Rodriguez-Santiago and E. J. Baerends, *J. Phys. Chem. A*, 1999, **103**, 166.
70 G. Pacchioni, F. Frigoli, D. Ricci and J. A. Weil, *Phys. Rev. B: Condens. Matter Mater. Phys.*, 2000, **63**, 054102.
71 J. L. Gavartin, P. V. Sushko and A. L. Schluger, *Phys. Rev. B: Condens. Matter Mater. Phys.*, 2003, **67**, 035108.
72 J. Poater, M. Sola, A. Rimola, L. Rodriguez-Santiago and M. Sodupe, *J. Phys. Chem. A*, 2004, **108**, 6072.
73 M. Lundberg and P. E. M. Siegbahn, *J. Chem. Phys.*, 2005, **122**, 224103.
74 F. Lechermann, A. Georges, A. Poteryaev, S. Biermann, M. Posternak, A. Yamasaki and O. K. Andersen, *Phys. Rev. B: Condens. Matter Mater. Phys.*, 2006, **74**, 125120.
75 K. Terakura, T. Oguchi, A. R. Williams and J. Kübler, *Phys. Rev. B: Condens. Matter Mater. Phys.*, 1984, **30**, 4734.
76 V. I. Anisimov, J. Zaanen and O. K. Andersen, *Phys. Rev. B: Condens. Matter Mater. Phys.*, 1991, **44**, 943.
77 V. I. Anisimov, P. Kuiper and J. Nordgren, *Phys. Rev. B: Condens. Matter Mater. Phys.*, 1994, **50**, 8257.
78 S. L. Dudarev, G. A. Bolton and S. Y. Savrasov, *Phys. Rev. B: Condens. Matter Mater. Phys.*, 1998, **57**, 1505.
79 A. D. Becke, *J. Chem. Phys.*, 1998, **109**, 2092.
80 N. M. Harrison, V. R. Saunders, R. Dovesi and W. C. Mackrodt, *Philos. Trans. R. Soc. London, Ser. A*, 1998, **356**, 75.
81 T. Bredow and A. B. Gerson, *Phys. Rev. B: Condens. Matter Mater. Phys.*, 2000, **61**, 5194.
82 O. Bengone, M. Alouani, P. Blöchl and J. Hugel, *Phys. Rev. B: Condens. Matter Mater. Phys.*, 2000, **62**, 16392.
83 J. Muscat, A. Wander and N. M. Harrison, *Chem. Phys. Lett.*, 2001, **342**, 397.
84 S. A. Gramsch, R. E. Cohen and S. Y. Savrasov, *Am. Mineral.*, 2003, **88**, 257.
85 A. Rohrbach, J. Hafner and G. Kresse, *Phys. Rev. B: Condens. Matter Mater. Phys.*, 2004, **69**, 075413.
86 X.-B. Feng and N. M. Harrison, *Phys. Rev. B: Condens. Matter Mater. Phys.*, 2004, **69**, 035114.
87 C. Franchini, V. Bayer, R. Podloucky, J. Paier and G. Kresse, *Phys. Rev. B: Condens. Matter Mater. Phys.*, 2005, **72**, 045132.
88 F. Tran, P. Blaha, K. Schwarz and P. Novak, *Phys. Rev. B: Condens. Matter Mater. Phys.*, 2006, **74**, 155108.
89 L. Wang, T. Maxisch and G. Ceder, *Phys. Rev. B: Condens. Matter Mater. Phys.*, 2006, **73**, 195107.
90 P. Novák, J. Kunes, L. Chaput and W. E. Pickett, *Phys. Status Solidi B*, 2006, **243**, 563.
91 D. Kasinathan, J. Kunei, K. Koepernik, C. V. Diaconu, R. L. Martin, I. D. Prodan, G. E. Scuseria, N. Spaldin, L. Petit, T. C. Schulthess and W. E. Pickett, *Phys. Rev. B: Condens. Matter Mater. Phys.*, 2006, **74**, 195110.
92 L. Giordano, G. Pacchioni, J. Goniakowski, N. Nilius, E. D. I. Rienks and H.-J. Freund, *Phys. Rev. Lett.*, 2008, **101**, 026102.
93 N. E. Schultz, Y. Zhao and D. G. Truhlar, *J. Phys. Chem. A*, 2005, **109**, 4388.
94 N. E. Schultz, Y. Zhao and D. G. Truhlar, *J. Phys. Chem. A*, 2005, **109**, 11127.
95 F. Furche and J. P. Perdew, *J. Chem. Phys.*, 2006, **124**, 044103.
96 P. J. Stephens, F. J. Devlin, C. F. Chabalowski and M. J. Frisch, *J. Phys. Chem.*, 1994, **98**, 11623.
97 A. D. Becke, *J. Chem. Phys.*, 1993, **98**, 5648.
98 P. J. Stephens, F. J. Devlin, C. S. Ashwar, K. L. Bak, P. R. Taylor and M. J. Frisch, in *Chemical Applications of Density Functional Theory*, ed. B. B. Laird, R. B. Ross and T. Ziegler, American Chemical Society, Washington, DC, 1996, vol. 629, p. 105.
99 C. Adamo and V. Barone, *Chem. Phys. Lett.*, 1997, **274**, 242.
100 M. Ernzerhof and G. E. Scuseria, *J. Chem. Phys.*, 1999, **110**, 5029.
101 B. J. Lynch, P. L. Fast, M. Harris and D. G. Truhlar, *J. Phys. Chem. A*, 2000, **104**, 4811.
102 M. Reiher, O. Salomon and B. A. Hess, *Theor. Chem. Acc.*, 2001, **107**, 48.
103 G. Brewer, M. J. Olida, A. M. Schmiderkamp, C. Viragh and P. Y. Zavalij, *Dalton Trans.*, 2006, 5617.
104 H. Saal, T. Bredow and M. Binnewies, *Phys. Chem. Chem. Phys.*, 2009, **11**, 3201.
105 M. Radon, M. Srebro and E. Broclawik, *J. Chem. Theory Comput.*, 2009, **5**, 1237.
106 J. A. Alonso and L. A. Girifalco, *Phys. Rev. B: Condens. Matter Mater. Phys.*, 1978, **17**, 3735.
107 J. P. A. Charlesworth, *Phys. Rev. B: Condens. Matter Mater. Phys.*, 1996, **53**, 12666.
108 M. Sadd and M. P. Teter, *Phys. Rev. B: Condens. Matter Mater. Phys.*, 1996, **54**, 13643.
109 P. P. Rushton, D. J. Tozer and S. J. Clark, *Phys. Rev. B: Condens. Matter Mater. Phys.*, 2002, **65**, 235203.
110 J. Robertson, K. Xiong and S. J. Clark, *Thin Solid Films*, 2006, **496**, 1.
111 J. Robertson, K. Xiong and S. J. Clark, *Phys. Status Solidi B*, 2006, **243**, 2054.
112 J. P. Perdew and A. Zunger, *Phys. Rev. B: Condens. Matter Mater. Phys.*, 1981, **23**, 5048.
113 A. Svane, W. M. Temmerman, Z. Szotek, J. Laegsgaard and H. Winter, *Int. J. Quantum Chem.*, 2000, **77**, 799.
114 C. Legrand, E. Suraud and P.-G. Reinhard, *J. Phys. B: At., Mol. Opt. Phys.*, 2002, **35**, 1115.
115 I. Ciofini, H. Chermette and C. Adamo, *Chem. Phys. Lett.*, 2003, **380**, 12.
116 D. M. Bylander and L. Kleinman, *Phys. Rev. B: Condens. Matter Mater. Phys.*, 1990, **41**, 7868.
117 D. Vogel, P. Krüger and J. Pollmann, *Phys. Rev. B: Condens. Matter Mater. Phys.*, 1998, **58**, 3865.

118 A. Filippetti and V. Fiorentini, *Phys. Rev. B: Condens. Matter Mater. Phys.*, 2005, **72**, 035128.
119 C. D. Pemmaraju, T. Archer, D. Sanchez-Portal and S. Sanvito, *Phys. Rev. B: Condens. Matter Mater. Phys.*, 2007, **75**, 045101.
120 A. Akande and S. Sanvito, *J. Chem. Phys.*, 2007, **127**, 034112.
121 A. I. Liechtenstein, V. I. Anisimov and J. Zaanen, *Phys. Rev. B: Condens. Matter Mater. Phys.*, 1995, **52**, R5467.
122 V. I. Anisimov, F. Aryasetiawan and A. I. Liechtenstein, *J. Phys.: Condens. Matter*, 1997, **9**, 767.
123 W. E. Pickett, S. C. Erwin and E. C. Ethridge, *Phys. Rev. B: Condens. Matter Mater. Phys.*, 1998, **58**, 1201.
124 J. Hubbard, *Proc. R. Soc. London, Ser. A*, 1963, **266**, 238.
125 H. Hsu, K. Umemoto, M. Cococcioni and R. Wentzcovitch, *Phys. Rev. B: Condens. Matter Mater. Phys.*, 2009, **79**, 125124.
126 A. Svane and O. Gunnarsson, *Phys. Rev. Lett.*, 1990, **65**, 1148.
127 Z. Szotek, W. M. Temmerman and H. Winter, *Phys. Rev. B: Condens. Matter Mater. Phys.*, 1993, **47**, 4029.
128 D. G. Isaak, R. E. Cohen, M. J. Mehl and D. J. Singh, *Phys. Rev. B: Condens. Matter Mater. Phys.*, 1993, **47**, 7720.
129 S. Stackhouse, J. P. Brodholt and G. D. Price, *Earth Planet. Sci. Lett.*, 2007, **253**, 282.
130 A. Bengtson, K. Persson and D. Morgan, *Earth Planet. Sci. Lett.*, 2008, **265**, 535.
131 M. Alfredsson, G. David Price, C. R. A. Catlow, S. C. Parker, R. Orlando and J. P. Brodholt, *Phys. Rev. B: Condens. Matter Mater. Phys.*, 2004, **70**, 165111.
132 G. Kotliar, S. Y. Savrasov, K. Haule, V. S. Oudovenko, O. Parcollet and C. A. Marianetti, *Rev. Mod. Phys.*, 2006, **78**, 865.
133 P. Ravindran, R. Vidya, P. Vajeeston, A. Kjekshus and H. Fellvåg, *J. Solid State Chem.*, 2003, **176**, 338.
134 P. Zhang, W. Luo, V. H. Crespi, M. L. Cohen and S. G. Louie, *Phys. Rev. B: Condens. Matter Mater. Phys.*, 2004, **70**, 085108.
135 F. Zhou, M. Cococcioni, C. A. Marianetti, D. Morgan and G. Ceder, *Phys. Rev. B: Condens. Matter Mater. Phys.*, 2004, **70**, 235121.
136 R. Pocha, D. Johrendt, B. Ni and M. M. Abd-Elmeguid, *J. Am. Chem. Soc.*, 2005, **127**, 8732.
137 M. Cococcioni and S. de Gironcoli, *Phys. Rev. B: Condens. Matter Mater. Phys.*, 2005, **71**, 035105.
138 H. J. Kulik, M. Cococcioni, D. A. Scherlis and N. Marzari, *Phys. Rev. Lett.*, 2006, **97**, 103001.
139 K. Leung, S. B. Rempe, P. A. Schultz, E. M. Sproviero, V. S. Batista, M. E. Chandross and C. J. Medforth, *J. Am. Chem. Soc.*, 2006, **128**, 3659.
140 K. Leung and C. J. Medforth, *J. Chem. Phys.*, 2007, **126**, 024501.
141 C. Yao, W. Guan, Z. M. Su, J. D. Feng, L. K. Yan and Z. J. Wu, *Theor. Chem. Acc.*, 2007, **117**, 115.
142 N. J. Mosey, P. Liao and E. A. Carter, *J. Chem. Phys.*, 2008, **129**, 014103.
143 H. J. Kulik and N. Marzari, *J. Chem. Phys.*, 2008, **129**, 134314.
144 S. Lany and A. Zunger, *Phys. Rev. B: Condens. Matter Mater. Phys.*, 2008, **78**, 235104.
145 M. Cococcioni, A. Dal Corso and S. de Gironcoli, *Phys. Rev. B: Condens. Matter Mater. Phys.*, 2003, **67**, 094106.
146 G. Rollmann, H. C. Herper and P. Entel, *J. Phys. Chem. A*, 2006, **110**, 10799.
147 G. Pacchioni, *J. Chem. Phys.*, 2008, **128**, 182505.
148 E. Finazzi, C. Di Valentin, G. Pacchioni and A. Selloni, *J. Chem. Phys.*, 2008, **129**, 154113.
149 F. Cinquini, L. Giordano and G. Pacchioni, *Theor. Chem. Acc.*, 2008, **120**, 575.
150 X. Y. Deng, X. Dai and Z. Fang, *Europhys. Lett.*, 2008, **83**, 37008.
151 G.-T. Wang, X. Dai and Z. Fang, *Phys. Rev. Lett.*, 2008, **101**, 066403.
152 M. Marder, *Condensed Matter Physics*, John Wiley & Sons, New York, 2000.
153 J. P. Perdew and M. Levy, *Phys. Rev. Lett.*, 1983, **51**, 1884.
154 W. Hanke and L. J. Sham, *Phys. Rev. B: Condens. Matter Mater. Phys.*, 1980, **21**, 4656.
155 L. Brus, *J. Phys. Chem.*, 1986, **90**, 2555.
156 Y. Kayanuma, *Phys. Rev. B: Condens. Matter Mater. Phys.*, 1988, **38**, 9797.
157 C. Delerue, M. Lannoo and G. Allan, *Phys. Rev. Lett.*, 2000, **84**, 2457.
158 M. S. Hybertsen and S. G. Louie, *Phys. Rev. B: Condens. Matter Mater. Phys.*, 1988, **37**, 2733.
159 G. Onida, L. Reining and A. Rubio, *Rev. Mod. Phys.*, 2002, **74**, 601.
160 F. Fuchs, J. Furthmuller, F. Bechstedt, M. Shishkin and G. Kresse, *Phys. Rev. B: Condens. Matter Mater. Phys.*, 2007, **76**, 115109.
161 P. H. Hahn, K. Seino, W. G. Schmidt, J. Furthmüller and F. Bechstedt, *Phys. Status Solidi B*, 2005, **242**, 2720.
162 L. Hedin, *Phys. Rev.*, 1965, **139**, A796.
163 S. G. Louie, in *Conceptual Foundations of Materials: A Standard Model for Ground- and Excited-State Properties*, ed. S. G. Louie and M. L. Cohen, Elsevier, Amsterdam, 2006, p. 9.
164 P. Huang and E. A. Carter, *Annu. Rev. Phys. Chem.*, 2008, **59**, 261.
165 M. Shishkin and G. Kresse, *Phys. Rev. B: Condens. Matter Mater. Phys.*, 2007, **75**, 235102.
166 P. Rinke, A. Qteis, J. Neugebauer and M. Scheffler, *Phys. Status Solidi B*, 2008, **245**, 929.
167 P. H. Hahn, W. G. Schmidt, K. Seino, M. Preuss, F. Bechstedt and J. Bernholc, *Phys. Rev. Lett.*, 2005, **94**, 037404.
168 L. E. Ramos, J. Paier, G. Kresse and F. Bechstedt, *Phys. Rev. B: Condens. Matter Mater. Phys.*, 2008, **78**, 195423.
169 S. Botti, A. Schindlmayr, R. D. Sole and L. Reisling, *Rep. Prog. Phys.*, 2007, **70**, 357.
170 A. Marini, R. D. Sole and A. Rubio, in *Time-Dependent Density Functional Theory*, ed. M. A. L. Marques, C. A. Ulrich, F. Noguiera, K. Burke and E. K. U. Gross, Springer, Berlin, 2006, p. 161.
171 L. J. Sham and W. Kohn, *Phys. Rev.*, 1966, **145**, 561.
172 L. X. Benedict, A. Puzder, A. J. Williamson, J. C. Grossman, G. Galli, J. E. Klepeis, J.-Y. Raty and O. Pankratov, *Phys. Rev. B: Condens. Matter Mater. Phys.*, 2003, **68**, 085310.
173 T. Ziegler, M. Seth, M. Krykunov, J. Autschbach and F. Wang, *THEOCHEM*, 2009, **914**, 106.
174 E. K. U. Gross and K. Burke, in *Time-Dependent Density Functional Theory*, ed. M. A. L. Marques, C. A. Ulrich, F. Noguiera, K. Burke and E. K. U. Gross, Springer, Berlin, 2006, p. 1.
175 H. Shi, R. Asahi and C. Stampfl, *Phys. Rev. B: Condens. Matter Mater. Phys.*, 2007, **75**, 205125.
176 L. J. Sham and M. Schlüter, *Phys. Rev. Lett.*, 1983, **51**, 1888.
177 R. W. Godby, M. Schlüter and L. J. Sham, *Phys. Rev. B: Condens. Matter Mater. Phys.*, 1988, **37**, 10159.
178 M. Gruning, A. Marini and A. Rubio, *Phys. Rev. B: Condens. Matter Mater. Phys.*, 2006, **74**, 161103.
179 A. J. Cohen, P. Mori-Sanchez and W. Yang, *Phys. Rev. B: Condens. Matter Mater. Phys.*, 2008, **77**, 115123.
180 A. D. Becke, *J. Chem. Phys.*, 1992, **96**, 2155.
181 R. van Leeuwen and E. J. Baerends, *Phys. Rev. A: At., Mol., Opt. Phys.*, 1994, **49**, 2421.
182 A. Dal Corso and R. Resta, *Phys. Rev. B: Condens. Matter Mater. Phys.*, 1994, **50**, 4327.
183 A. V. Arbuznikov and M. Kaupp, *Chem. Phys. Lett.*, 2003, **381**, 495.
184 P. Mori-Sanchez, A. J. Cohen and W. Yang, *J. Chem. Phys.*, 2006, **125**, 201102.
185 A. D. Becke and M. R. Roussel, *Phys. Rev. A: At., Mol., Opt. Phys.*, 1989, **39**, 3761.
186 A. D. Becke, *J. Chem. Phys.*, 1996, **104**, 1040.
187 J. Tao, J. P. Perdew, V. N. Staroverov and G. E. Scuseria, *Phys. Rev. Lett.*, 2003, **91**, 146401.
188 A. Savin, in *Recent Developments and Applications of Modern Density Functional Theory*, ed. J. Seminario, Elsevier, New York, 1996, p. 227.
189 T. Leininger, H. Stoll, H.-J. Werner and A. Savin, *Chem. Phys. Lett.*, 1997, **275**, 151.
190 H. Iikura, T. Tsuneda, T. Yanai and K. Hirao, *J. Chem. Phys.*, 2001, **115**, 3540.
191 J. Heyd, G. E. Scuseria and M. Ernzerhof, *J. Chem. Phys.*, 2003, **118**, 8207.
192 J. Heyd and G. E. Scuseria, *J. Chem. Phys.*, 2004, **120**, 7274.
193 J. Heyd and G. E. Scuseria, *J. Chem. Phys.*, 2004, **121**, 1187.
194 R. Baer and D. Neuhauser, *Phys. Rev. Lett.*, 2005, **94**, 043002.
195 E. Livshitz and R. Baer, *Phys. Chem. Chem. Phys.*, 2007, **9**, 2932.
196 T. M. Henderson, A. F. Izmaylov, G. E. Scuseria and A. Savin, *J. Chem. Phys.*, 2007, **127**, 221103.
197 J. Jaramillo, G. E. Scuseria and M. Ernzerhof, *J. Chem. Phys.*, 2003, **118**, 1068.

198 H. Bahmann, A. Rodenberg, A. V. Arbuznikov and M. Kaupp, *J. Chem. Phys.*, 2007, **126**, 011103.
199 A. V. Arbuznikov and M. Kaupp, *Chem. Phys. Lett.*, 2007, **440**, 160.
200 A. V. Arbuznikov and M. Kaupp, *J. Chem. Phys.*, 2008, **128**, 214107.
201 A. V. Krukau, G. E. Scuseria, J. P. Perdew and A. Savin, *J. Chem. Phys.*, 2008, **129**, 124103.
202 P. M. W. Gill, *Mol. Phys.*, 1996, **89**, 433.
203 Y. Zhang and W. Yang, *Phys. Rev. Lett.*, 1998, **80**, 890.
204 B. Hammer, L. B. Hansen and J. K. Nørskov, *Phys. Rev. B: Condens. Matter Mater. Phys.*, 1999, **59**, 7413.
205 L. Vitos, B. Johansson, J. Kollár and H. L. Skriver, *Phys. Rev. B: Condens. Matter Mater. Phys.*, 2000, **62**, 10046.
206 W. Kohn and A. E. Mattsson, *Phys. Rev. Lett.*, 1998, **81**, 3487.
207 N. C. Handy and A. J. Cohen, *Mol. Phys.*, 2001, **99**, 403.
208 X. Xu and W. A. Goddard, III, *Proc. Natl. Acad. Sci. U. S. A.*, 2004, **101**, 2673.
209 R. Armiento and A. E. Mattsson, *Phys. Rev. B: Condens. Matter Mater. Phys.*, 2005, **72**, 085108.
210 L. A. Constantin, J. M. Pitarke, J. F. Dobson, A. Garcia-Lekue and J. P. Perdew, *Phys. Rev. Lett.*, 2008, **100**, 036401.
211 Z. Wu and R. E. Cohen, *Phys. Rev. B: Condens. Matter Mater. Phys.*, 2006, **73**, 235116.
212 Y. Zhao and D. G. Truhlar, *Phys. Rev. B: Condens. Matter Mater. Phys.*, 2008, **78**, 197101.
213 J. P. Perdew, A. Ruzsinszky, G. I. Csonka, O. A. Vydrov, G. E. Scuseria, L. A. Constantin, X. Zhou and K. Burke, *Phys. Rev. Lett.*, 2008, **100**, 136406 and the erratum: J. P. Perdew, A. Ruzsinszky, G. I. Csonka, O. A. Vydrov, G. E. Scuseria, L. A. Constantin, X. Zhou and K. Burke, *Phys. Rev. Lett.*, 2009, **102**, 039902.
214 Y. Zhao and D. G. Truhlar, *J. Chem. Phys.*, 2008, **128**, 184109.
215 J. P. Perdew, K. Burke and M. Ernzerhof, *Phys. Rev. Lett.*, 1998, **80**, 891.
216 J. P. Perdew, A. Ruzsinszky, G. I. Csonka, O. A. Vydrov, G. E. Scuseria, L. A. Constantin, X. Zhou and K. Burke, *Phys. Rev. Lett.*, 2008, **101**, 239702.
217 A. E. Mattsson, R. Armiento and T. R. Mattsson, *Phys. Rev. Lett.*, 2008, **101**, 239701.
218 A. E. Mattsson, R. Armiento, P. A. Schultz and T. R. Mattsson, *Phys. Rev. B: Condens. Matter Mater. Phys.*, 2006, **73**, 195123.
219 A. E. Mattsson, R. Armiento, J. Paier, G. Kresse, J. M. Wills and T. R. Mattsson, *J. Chem. Phys.*, 2008, **128**, 084714.
220 S. F. Sousa, P. A. Fernandes and M. J. Ramos, *J. Phys. Chem. A*, 2007, **111**, 10439.
221 M. Alaei, H. Akbarzadeh, H. Gholizadeh and S. de Gironcoli, *Phys. Rev. B: Condens. Matter Mater. Phys.*, 2008, **77**, 085414.
222 H. L. Schmider and A. D. Becke, *J. Chem. Phys.*, 1998, **108**, 9624.
223 F. A. Hamprecht, A. J. Cohen, D. J. Tozer and N. C. Handy, *J. Chem. Phys.*, 1998, **109**, 6264.
224 P. J. Wilson, T. J. Bradley and D. J. Tozer, *J. Chem. Phys.*, 2001, **115**, 9233.
225 T. W. Keal and D. J. Tozer, *J. Chem. Phys.*, 2005, **123**, 121103.
226 Y. Zhao and D. G. Truhlar, *J. Phys. Chem. A*, 2005, **109**, 5656.
227 A. D. Becke, *J. Chem. Phys.*, 2000, **112**, 4020.
228 A. D. Boese and N. C. Handy, *J. Chem. Phys.*, 2002, **116**, 9559.
229 A. D. Boese and J. M. L. Martin, *J. Chem. Phys.*, 2004, **121**, 3405.
230 J. Krieger, J. Chen, G. J. Iafiate and A. Savin, in *Electron Correlations and Material Properties*, ed. A. Gonis and N. Kioussis, Plenum, New York, 1999, p. 463.
231 J. P. Perdew, S. Kurth, A. Zupan and P. Blaha, *Phys. Rev. Lett.*, 1999, **82**, 2544.
232 Y. Zhao and D. G. Truhlar, *J. Phys. Chem. A*, 2006, **110**, 13126.
233 Y. Zhao, N. E. Schultz and D. G. Truhlar, *J. Chem. Theory Comput.*, 2006, **2**, 364.
234 Y. Zhao and D. G. Truhlar, *J. Chem. Theory Comput.*, 2008, **4**, 1849.
235 E. A. Amin and D. G. Truhlar, *J. Chem. Theory Comput.*, 2008, **4**, 75.
236 T. Yanai, D. P. Tew and N. C. Handy, *Chem. Phys. Lett.*, 2004, **393**, 51.
237 T. Van Voorhis and G. E. Scuseria, *J. Chem. Phys.*, 1998, **109**, 400.
238 Y. Zhao and D. G. Truhlar, *J. Phys. Chem. A*, 2004, **108**, 6908.
239 E. I. Proynov, S. Sirois and D. R. Salahub, *Int. J. Quantum Chem.*, 1997, **64**, 427.
240 J. Pu and D. G. Truhlar, *J. Chem. Phys.*, 2002, **116**, 1468.
241 B. L. Kormos and C. J. Cramer, *J. Phys. Org. Chem.*, 2002, **15**, 712.
242 C. Diaz, E. Pijper, R. A. Olsen, H. F. Busnengo, D. J. Auerbach and G. J. Kroes, preprint (April 21 2009).
243 G. Lippert, J. Hutter and M. Parrinello, *Mol. Phys.*, 1997, **92**, 477.
244 J. VandeVondele, M. Krack, F. Mohamed, M. Parrinello, T. Chassaing and J. Hutter, *Comput. Phys. Commun.*, 2005, **167**, 103.
245 J. C. Phillips and L. Kleinman, *Phys. Rev.*, 1959, **116**, 287.
246 M. H. Cohen and V. Heine, *Phys. Rev.*, 1961, **122**, 1821.
247 C. F. Melius, B. D. Olafson and W. A. Goddard, *Chem. Phys. Lett.*, 1974, **28**, 457.
248 L. R. Kahn, P. Baybutt and D. G. Truhlar, *J. Chem. Phys.*, 1976, **65**, 3826.
249 P. A. Christiansen, Y. S. Lee and K. S. Pitzer, *J. Chem. Phys.*, 1979, **71**, 4445.
250 D. R. Hamann, M. Schlüter and C. Chiang, *Phys. Rev. Lett.*, 1979, **43**, 1494.
251 W. J. Stevens, H. Basch and M. Krauss, *J. Chem. Phys.*, 1984, **81**, 6026.
252 P. J. Hay and W. R. Wadt, *J. Chem. Phys.*, 1985, **82**, 270.
253 P. J. Hay and W. R. Wadt, *J. Chem. Phys.*, 1985, **82**, 284.
254 P. J. Hay and W. R. Wadt, *J. Chem. Phys.*, 1985, **82**, 299.
255 A. M. Rappe, K. M. Rabe, E. Kaxiras and J. D. Joannopoulos, *Phys. Rev. B: Condens. Matter Mater. Phys.*, 1990, **41**, 1227.
256 D. Vanderbilt, *Phys. Rev. B: Condens. Matter Mater. Phys.*, 1990, **41**, 7892.
257 N. Troullier and J. L. Martins, *Phys. Rev. B: Condens. Matter Mater. Phys.*, 1991, **43**, 1993.
258 T. V. Russo, R. L. Martin and P. J. Hay, *J. Phys. Chem.*, 1995, **99**, 17085.
259 S. Goedecker, M. Teter and J. Hutter, *Phys. Rev. B: Condens. Matter Mater. Phys.*, 1996, **54**, 1703.
260 P. Schwerdtfeger, J. R. Brown, J. K. Laerdahl and H. Stoll, *J. Chem. Phys.*, 2000, **113**, 7110.
261 J. M. L. Martin and A. Sundermann, *J. Chem. Phys.*, 2001, **114**, 3408.
262 A. Dal Corso, *Phys. Rev. B: Condens. Matter Mater. Phys.*, 2001, **64**, 235118.
263 M. Dolg, *Theor. Chem. Acc.*, 2005, **114**, 297.
264 E. Fromager, L. Visscher, L. Maron and C. Teichteil, *J. Chem. Phys.*, 2005, **123**, 164105.
265 L. E. Roy, P. J. Hay and R. L. Martin, *J. Chem. Theory Comput.*, 2008, **4**, 1029.
266 P. E. Blöchl, C. J. Först and J. Schimpl, *Bull. Mater. Sci.*, 2003, **26**, 33.
267 P. E. Blöchl, *Phys. Rev. B: Condens. Matter Mater. Phys.*, 1994, **50**, 17953.
268 G. Kresse and D. Joubert, *Phys. Rev. B: Condens. Matter Mater. Phys.*, 1999, **59**, 1758.
269 M. Valiev, E. J. Bylaska, A. Gramada and J. H. Weare, in *Reviews of Modern Quantum Chemistry*, ed. K. D. Sen, World Scientific, Singapore, 2002, vol. 2, p. 1684.
270 M. Valiev, E. J. Bylaska and J. H. Weare, *J. Chem. Phys.*, 2003, **119**, 5955.
271 J. J. Mortensen, L. B. Hansen and K. W. Jacobsen, *Phys. Rev. B: Condens. Matter Mater. Phys.*, 2005, **71**, 035109.
272 H. J. Monkhorst and J. D. Pack, *Phys. Rev. B: Condens. Matter Mater. Phys.*, 1976, **13**, 5188.
273 A. E. Mattsson, P. A. Schultz, M. P. Desjarlais, T. R. Mattsson and K. Leung, *Modell. Simul. Mater. Sci. Eng.*, 2005, **13**, R1.
274 A. Sorouri, W. M. C. Foulkes and N. D. M. Hine, *J. Chem. Phys.*, 2006, **124**, 064105.
275 M. C. Payne, M. P. Teter, D. C. Allan, T. A. Arias and J. D. Joannopoulos, *Rev. Mod. Phys.*, 1992, **64**, 1045.
276 J. L. Han, L. Z. Sun, X. D. Qu, Y. P. Chen and J. X. Zhong, *Phys. B*, 2009, **404**, 131.
277 G. Kresse and J. Hafner, *Phys. Rev. B: Condens. Matter Mater. Phys.*, 1993, **48**, 13115.
278 G. Y. Sun, J. Kurti, P. Rajczy, M. Kertesz, J. Hafner and G. Kresse, *THEOCHEM*, 2003, **624**, 37.

279 J. Paier, R. Hirschl, M. Marsman and G. Kresse, *J. Chem. Phys.*, 2005, **122**, 234102.
280 J. S. Tse, *Annu. Rev. Phys. Chem.*, 2002, **53**, 249.
281 B. I. Dunlap, J. W. D. Connolly and J. R. Sabin, *J. Chem. Phys.*, 1979, **71**, 4993.
282 O. Vahtras, J. Almlöf and M. W. Feyereisen, *Chem. Phys. Lett.*, 1993, **213**, 514.
283 M. Sierka, A. Hogekamp and R. Ahlrichs, *J. Chem. Phys.*, 2003, **118**, 9136.
284 R. Polly, H. J. Werner, F. R. Manby and P. J. Knowles, *Mol. Phys.*, 2004, **102**, 2311.
285 R. M. Wentzcovitch, *Phys. Rev. B: Condens. Matter Mater. Phys.*, 1991, **44**, 2358.
286 R. M. Wentzcovitch, J. L. Martins and G. D. Price, *Phys. Rev. Lett.*, 1993, **70**, 3947.
287 H. M. Senn and W. Thiel, *Angew. Chem., Int. Ed.*, 2009, **48**, 1198.
288 Y.-y. Ohnishi, Y. Nakao, H. Sato and S. Sakaki, *J. Phys. Chem. A*, 2008, **112**, 1946.
289 B. Wang and D. G. Truhlar, *J. Chem. Theory Comput.*, in press.
290 K. G. Dyall and K. Faegri, *Introduction to Relativistic Quantum Chemistry*, Oxford University Press, New York, USA, 2007.
291 N. Rösch, A. Matveev, V. A. Nasluzov, K. M. Neyman, L. Moskaleva and S. Krüger, in *Relativistic Electronic Structure Theory, Part 2. Applications*, ed. P. Pyykkö and P. Schwerdtfeger, Elsevier, Amsterdam, 2004, p. 656.
292 L. L. Foldy and S. A. Wouthuysen, *Phys. Rev.*, 1950, **78**, 29.
293 M. Douglas and N. M. Kroll, *Ann. Phys.*, 1974, **82**, 89.
294 B. A. Hess, *Phys. Rev. A: At., Mol., Opt. Phys.*, 1986, **33**, 3742.
295 G. Jansen and B. A. Hess, *Phys. Rev. A: At., Mol., Opt. Phys.*, 1989, **39**, 6016.
296 A. Wolf, M. Reiher and B. A. Hess, *J. Chem. Phys.*, 2002, **117**, 9215.
297 I. Malkin, O. L. Malkina, V. G. Malkin and M. Kaupp, *J. Chem. Phys.*, 2005, **123**, 244103.
298 M. Reiher, *Theor. Chem. Acc.*, 2006, **116**, 241.
299 E. van Lenthe, E. J. Baerends and J. G. Snijders, *J. Chem. Phys.*, 1994, **101**, 9783.
300 M. Mayer, S. Krüger and N. Rösch, *J. Chem. Phys.*, 2001, **115**, 4411.
301 E. van Lenthe, J. G. Snijders and E. J. Baerends, *J. Chem. Phys.*, 1996, **105**, 6505.
302 F. Wang, G. Hong and L. Li, *Chem. Phys. Lett.*, 2000, **316**, 318.
303 D. G. Fedorov, S. Koseki, M. W. Schmidt and M. S. Gordon, *Int. Rev. Phys. Chem.*, 2003, **22**, 551; B. O. Roos and P.-Å. Malmqvist, *Phys. Chem. Chem. Phys.*, 2004, **6**, 2919.
304 C. van Wüllen, *J. Comput. Chem.*, 2001, **23**, 779.
305 M. Shoji, K. Koizumi, R. Takeda, Y. Kitagawa, S. Yamanaka, M. Okumura and K. Yamaguchi, *Polyhedron*, 2007, **26**, 2335.
306 K. Yamaguchi, S. Yamanaka, M. Nishino, Y. Takano, Y. Kitagawa, H. Nagao and Y. Yoshioka, *Theor. Chem. Acc.*, 1999, **102**, 328.
307 S. Lunell, *Chem. Phys. Lett.*, 1972, **13**, 93.
308 K. Yamaguchi, Y. Yoshioka and T. Fueno, *Chem. Phys. Lett.*, 1977, **46**, 360.
309 S. Hammes-Schiffer and H. C. Andersen, *J. Chem. Phys.*, 1993, **99**, 1901.
310 S. Yamanaka, D. Yamaki, Y. Shigeta, H. Nagao, Y. Yoshioka, N. Suzuki and K. Yamaguchi, *Int. J. Quantum Chem.*, 2000, **80**, 664.
311 S. Yamanaka, D. Yamaki, Y. Shigeta, H. Nagao and K. Yamaguchi, *Int. J. Quantum Chem.*, 2001, **84**, 670.
312 D. Hobbs and J. Hafner, *J. Phys.: Condens. Matter*, 2000, **12**, 7025.
313 S. Sharma, J. K. Dewhurst, C. Ambrosch-Draxl, S. Kurth, N. Helbig, S. Pittalis, S. Shallcross, L. Nordstrom and E. K. U. Gross, *Phys. Rev. Lett.*, 2007, **98**, 196405.
314 D. Naveh and L. Kronik, *Solid State Commun.*, 2009, **149**, 177.
315 T. Oda, A. Pasquarello and R. Car, *Phys. Rev. Lett.*, 1998, **80**, 3622.
316 D. Hobbs, G. Kresse and J. Hafner, *Phys. Rev. B: Condens. Matter Mater. Phys.*, 2000, **62**, 11556.
317 P. Ruiz-Díaz, J. Dorantes-Davila and G. M. Pastor, *Eur. Phys. J. D*, 2009, **52**, 175.
318 N. Fujima and T. Oda, *Eur. Phys. J. D*, 2003, **24**, 89.
319 C. Köhler, T. Frauenheim, B. Hourahine, G. Seifert and M. Sternberg, *J. Phys. Chem. A*, 2007, **111**, 5622.
320 C. Kohl and G. F. Bertsch, *Phys. Rev. B: Condens. Matter Mater. Phys.*, 1999, **60**, 4205.
321 J. E. Peralta, G. E. Scuseria and M. J. Frisch, *Phys. Rev. B: Condens. Matter Mater. Phys.*, 2007, **75**, 125119.
322 S. Yamanaka, R. Takeda, T. Kawakami, K. Nakata, T. Sakuma, T. Takada and K. Yamaguchi, *J. Magn. Magn. Mater.*, 2004, **272–276**/Supplement 1, E255.
323 K. S. Pitzer, *Acc. Chem. Res.*, 1979, **12**, 271.
324 P. Pyykkö and J. P. Desclaux, *Acc. Chem. Res.*, 1979, **12**, 276.
325 P. Pyykkö, *Chem. Rev.*, 1988, **88**, 563.
326 N. E. Schultz, B. F. Gherman, C. J. Cramer and D. G. Truhlar, *J. Phys. Chem. B*, 2006, **110**, 24030.
327 M. Filatov, *Chem. Phys. Lett.*, 2003, **373**, 131.
328 E. Van Lenthe and E. J. Baerends, *J. Comput. Chem.*, 2003, **24**, 1142.
329 B. O. Roos, R. Lindh, P.-Å. Malmqvist, V. Veryazov and P.-O. Widmark, *J. Phys. Chem. A*, 2004, **108**, 2851.
330 R. L. A. Haiduke, L. G. M. De Macedo and A. B. F. Da Silva, *J. Comput. Chem.*, 2005, **26**, 932.
331 B. O. Roos, R. Lindh, P.-Å. Malmqvist, V. Veryazov and P.-O. Widmark, *J. Phys. Chem. A*, 2005, **109**, 6575.
332 K. Dyall, *Theor. Chem. Acc.*, 2006, **115**, 441.
333 M. J. Frisch, G. W. Trucks, H. B. Schlegel, G. E. Scuseria, M. A. Robb, J. R. Cheeseman, J. A. Montgomery, Jr., T. Vreven, K. N. Kudin, J. C. Burant, J. M. Millam, S. S. Iyengar, J. Tomasi, V. Barone, B. Mennucci, M. Cossi, G. Scalmani, N. Rega, G. A. Petersson, H. Nakatsuji, M. Hada, M. Ehara, K. Toyota, R. Fukuda, J. Hasegawa, M. Ishida, T. Nakajima, Y. Honda, O. Kitao, H. Nakai, M. Klene, X. Li, J. E. Knox, H. P. Hratchian, J. B. Cross, V. Bakken, C. Adamo, J. Jaramillo, R. Gomperts, R. E. Stratmann, O. Yazyev, A. J. Austin, R. Cammi, C. Pomelli, J. Ochterski, P. Y. Ayala, K. Morokuma, G. A. Voth, P. Salvador, J. J. Dannenberg, V. G. Zakrzewski, S. Dapprich, A. D. Daniels, M. C. Strain, O. Farkas, D. K. Malick, A. D. Rabuck, K. Raghavachari, J. B. Foresman, J. V. Ortiz, Q. Cui, A. G. Baboul, S. Clifford, J. Cioslowski, B. B. Stefanov, G. Liu, A. Liashenko, P. Piskorz, I. Komaromi, R. L. Martin, D. J. Fox, T. Keith, M. A. Al-Laham, C. Y. Peng, A. Nanayakkara, M. Challacombe, P. M. W. Gill, B. G. Johnson, W. Chen, M. W. Wong, C. Gonzalez and J. A. Pople, *GAUSSIAN 03 (Revision D.1)*, Gaussian, Inc., Wallingford, CT, 2004.
334 B. G. Johnson and M. J. Fisch, *J. Chem. Phys.*, 1994, **100**, 7429.
335 J. Zheng, M. A. Iron, B. A. Ellingson, J. C. Corchado, Y.-Y. Chuang and D. G. Truhlar, *NWChemRate 2007*, University of Minnesota, Minneapolis, 2007.
336 A. Fernandez-Ramos, B. A. Ellingson, B. C. Garrett and D. G. Truhlar, *Rev. Comput. Chem.*, 2007, **23**, 125.
337 G. Kresse and J. Furthmüller, *Phys. Rev. B: Condens. Matter Mater. Phys.*, 1996, **54**, 11169.
338 J. Hafner, *J. Comput. Chem.*, 2008, **29**, 2044.
339 P. Blaha, K. Schwarz, P. Sorantin and S. B. Trickey, *Comput. Phys. Commun.*, 1990, **59**, 399.
340 K. Schwarz and P. Blaha, *Comput. Mater. Sci.*, 2003, **28**, 259.
341 J. Paier, M. Marsman, K. Hummer, G. Kresse, I. C. Gerber and J. G. Angyan, *J. Chem. Phys.*, 2006, **124**, 154709.
342 A. Kiejna, G. Kresse, J. Rogal, A. De Sarkar, K. Reuter and M. Scheffler, *Phys. Rev. B: Condens. Matter Mater. Phys.*, 2006, **73**, 035404.
343 C. Fonseca Guerra, J. G. Snijders, G. te Velde and E. J. Baerends, *Theor. Chem. Acc.*, 1998, **99**, 391.
344 G. te Velde, F. M. Bickelhaupt, E. J. Baerends, C. F. Guerra, S. J. A. Van Gisbergen, J. G. Snijders and T. Ziegler, *J. Comput. Chem.*, 2001, **22**, 931.
345 E. J. Baerends, J. Autschbach, J. A. Berger, A. Bérces, F. M. Bickelhaupt, C. Bo, P. L. d. Boeij, P. M. Boerrigter, L. Cavallo, D. P. Chong, L. Deng, R. M. Dickson, D. E. Ellis, M. van Faassen, L. Fan, T. H. Fischer, C. Fonseca Guerra, S. J. A. van Gisbergen, A. W. Götz, J. A. Groeneveld, O. V. Gritsenko, M. Grüning, F. E. Harris, P. van den Hoek, C. R. Jacob, H. Jacobsen, L. Jensen, E. S. Kadantsev, G. v. Kessel, R. Klooster, F. Kootstra, M. V. Krykunov, E. v. Lenthe, J. N. Louwen, D. A. McCormack, A. Michalak, J. Neugebauer, V. P. Nicu, V. P. Osinga, S. Patchkovskii, P. H. T. Philipsen, D. Post, C. C. Pye, W. Ravenek, J. I. Rodriguez, P. Romaniello, P. Ros, P. R. T. Schipper, G. Schreckenbach, J. G. Snijders, M. Solà, M. Swart, D. Swerhone, G. t. Velde, P. Vernooijs,

L. Versluis, L. Visscher, O. Visser, F. Wang, T. A. Wesolowski, E. M. van Wezenbeek, G. Wiesenekker, S. K. Wolff, T. K. Woo, A. L. Yakovlev and T. Ziegler, *ADF2008*, Scientific Computing and Modeling, Amsterdam, 2008.
346 G. Wiesenekker and E. J. Baerends, *J. Phys.: Condens. Matter*, 1991, **3**, 6721.
347 G. te Velde and E. J. Baerends, *Phys. Rev. B: Condens. Matter Mater. Phys.*, 1991, **44**, 7888.
348 G. te Velde, E. J. Baerends, P. H. T. Philipsen, G. Wiesenekker, J. A. Broeneveld, J. A. Berger, P. L. de Boeij, R. Klooster, F. Kootstra, P. Romaniello, J. G. Snijders, E. S. Kadantsev and T. Ziegler, *BAND2008.1*, Scientific Computation and Modeling, Amsterdam, 2008.
349 R. A. Kendall, E. Apra, D. E. Bernholdt, E. J. Bylaska, M. Dupuis, G. I. Fann, R. J. Harrison, J. Ju, J. A. Nichols, J. Nieplocha, T. P. Straatsma, T. L. Windus and A. T. Wong, *Comput. Phys. Commun.*, 2000, **128**, 260.
350 E. Aprà, E. J. Bylaska, D. J. Dean, A. Fortunelli, F. Gao, P. S. Krstic, J. C. Wells and T. L. Windus, *Comput. Mater. Sci.*, 2003, **28**, 209.
351 M. W. Schmidt, K. K. Baldridge, J. A. Boatz, S. T. Elbert, M. S. Gordon, J. H. Jensen, S. Koseki, N. Matsunaga, K. A. Nguyen, S. Su, T. L. Windus, M. Dupuis and J. A. Montgomery, *J. Comput. Chem.*, 1993, **14**, 1347.
352 M. S. Gordon and M. W. Schmidt, in *Theory and Applications of Computational Chemistry: The First Forty Years*, ed. C. E. Dykstra, G. Frenking, K. S. Kim and G. E. Scuseria, Elsevier, Amsterdam, 2005, p. 1167.
353 M. Higashi, A. V. Marenich, R. M. Olson, A. C. Chamberlin, J. Pu, C. P. Kelly, J. D. Thompson, J. D. Xidos, J. Li, T. Zhu, G. D. Hawkins, Y.-Y. Chuang, P. L. Fast, B. J. Lynch, D. A. Liotard, D. Rinaldi, J. Gao, C. J. Cramer and D. G. Truhlar, *GAMESSPLUS version 2008-2*, University of Minnesota, Minneapolis, 2008.
354 A. V. Marenich, R. M. Olson, C. P. Kelly, C. J. Cramer and D. G. Truhlar, *J. Chem. Theory Comput.*, 2007, **3**, 2011.
355 B. Marten, K. Kim, C. Cortis, R. A. Friesner, R. B. Murphy, M. N. Ringnalda, D. Sitkoff and B. Honig, *J. Phys. Chem.*, 1996, **100**, 11775.
356 G. Karlström, R. Lindh, P.-Å. Malmqvist, B. O. Roos, U. Ryde, V. Veryazov, P. O. Widmark, M. Cossi, B. Schimmelpfennig, P. Neogrady and L. Seijo, *Comput. Mater. Sci.*, 2003, **28**, 222.
357 Y. Shao, L. F. Molnar, Y. Jung, J. Kussmann, C. Ochsenfeld, S. T. Brown, A. T. B. Gilbert, L. V. Slipchenko, S. V. Levchenko, D. P. O'Neill, R. A. DiStasio, R. C. Lochan, T. Wang, G. J. O. Beran, N. A. Besley, J. M. Herbert, C. Y. Lin, T. Van Voorhis, S. H. Chien, A. Sodt, R. P. Steele, V. A. Rassolov, P. E. Maslen, P. P. Korambath, R. D. Adamson, B. Austin, J. Baker, E. F. C. Byrd, H. Dachsel, R. J. Doerksen, A. Dreuw, B. D. Dunietz, A. D. Dutoi, T. R. Furlani, S. R. Gwaltney, A. Heyden, S. Hirata, C. P. Hsu, G. Kedziora, R. Z. Khalliulin, P. Klunzinger, A. M. Lee, M. S. Lee, W. Liang, I. Lotan, N. Nair, B. Peters, E. I. Proynov, P. A. Pieniazek, Y. M. Rhee, J. Ritchie, E. Rosta, C. D. Sherrill, A. C. Simmonett, J. E. Subotnik, H. L. Woodcock, W. Zhang, A. T. Bell, A. K. Chakraborty, D. M. Chipman, F. J. Keil, A. Warshel, W. J. Hehre, H. F. Schaefer, J. Kong, A. I. Krylov, P. M. W. Gill and M. Head-Gordon, *Phys. Chem. Chem. Phys.*, 2006, **8**, 3172.
358 H. L. Woodcock, M. Hodoscek, A. T. B. Gilbert, P. M. W. Gill, H. F. Schaefer and B. R. Brooks, *J. Comput. Chem.*, 2007, **28**, 1485.
359 R. Ahlrichs, M. Bär, M. Häser, H. Horn and C. Kölmel, *Chem. Phys. Lett.*, 1989, **162**, 165.
360 T. Helgaker, H. J. Aa. Jensen, P. Jørgensen, J. Olsen, K. Ruud, H. Ågren, A. A. Auer, K. L. Bak, V. Bakken, O. Christiansen, S. Coriani, P. Dahle, E. K. Dalskov, T. Enevoldsen, B. Fernandez, C. Hättig, K. Hald, A. Halkier, H. Heiberg, H. Hettema, D. Jonsson, S. Kirpekar, R. Kobayashi, H. Koch, K. V. Mikkelsen, P. Norman, M. J. Packer, T. B. Pedersen, T. A. Ruden, P. Salek, A. Sanchez, T. Saue, S. P. A. Sauer, B. Schimmelpfennig, K. O. Sylvester-Hvid, P. R. Taylor and O. Vahtras, *DALTON, a molecular electronic structure program, Release 2.0*, 2005, see http://www.kjemi.uio.no/software/dalton/dalton.html.
361 B. Jansik, P. Salek, D. Jonsson, O. Vahtras and H. Ågren, *J. Chem. Phys.*, 2005, **122**, 054107.
362 M. Guidon, F. Schiffmann, J. Hutter and J. VandeVondele, *J. Chem. Phys.*, 2008, **128**, 214104.
363 H.-J. Werner, P. J. Knowles, R. Lindh, F. R. Manby, M. Schütz, P. Celani, T. Korona, A. Mitrushenkov, G. Rauhut, T. B. Adler, R. D. Amos, A. Bernhardsson, A. Berning, D. L. Cooper, M. J. O. Deegan, A. J. Dobbyn, F. Eckert, E. Goll, C. Hampel, G. Hetzer, T. Hrenar, G. Knizia, C. Köppl, Y. Liu, A. W. Lloyd, R. A. Mata, A. J. May, S. J. McNicholas, W. Meyer, M. E. Mura, A. Nicklaß, P. Palmieri, K. Pflüger, R. Pitzer, M. Reiher, U. Schumann, H. Stoll, A. J. Stone, R. Tarroni, T. Thorsteinsson, M. Wang and A. Wolf, *MOLPRO 2008.1*, University College, Cardiff, 2008.
364 F. Neese, *ORCA*, Universtiy of Bonn, Germany, 2009.
365 J. M. Soler, E. Artacho, J. D. Gale, A. García, J. Junquera, P. Ordejón and D. Sánchez-Portal, *J. Phys.: Condens. Matter*, 2002, **14**, 2745.
366 D. Sánchez-Portal, P. Ordejón and E. Canadell, *Struct. Bonding*, 2004, **113**, 103.
367 E. Artacho, E. Anglada, O. Dieguez, J. D. Gale, A. Garcia, J. Junquera, R. M. Martin, P. Ordejon, J. M. Pruneda, D. Sanchez-Portal and J. M. Soler, *J. Phys.: Condens. Matter*, 2008, **20**, 064208.
368 D. R. Salahub, A. Goursot, J. Weber, A. M. Köster and A. Vela, in *Theory and Applications of Computational Chemistry: The First Forty Years*, ed. C. E. Dykstra, G. Frenking, K. S. Kim and G. E. Scuseria, Elsevier, Amsterdam, 2005, p. 1079.
369 A. M. Köster, G. Goudtner, T. Heine and A. Vela, *ALLCHEM*, Instituto Politécnico Nacional, Mexico, 2001.
370 A. M. Köster, P. Calaminici, Z. Gómez and U. Reveles, in *Reviews of Modern Quantum Chemistry*, ed. K. D. Sen, World Scientific, Singapore, 2002, p. 1439.
371 A. M. Köster, P. Calaminici, M. E. Casida, R. Flores-Moreno, G. Geudtner, A. Goursot, T. Heine, A. Ipatov, F. Janetzko, J. M. del Campo, S. Patchkovskii, J. U. Reveles, D. R. Salahub and A. Vela, *deMon2k*, 2006 (http://www.demon-software.com/public_html/), accessed October 12, 2009.
372 M. Ryzhkov, A. Ivanovskii and B. Delley, *Theor. Chem. Acc.*, 2008, **119**, 313.
373 Y. Gao, N. Shao and X. C. Zeng, *ACS Nano*, 2008, **2**, 1497.
374 X. Y. Cui, J. E. Medvedeva, B. Delley, A. J. Freeman and C. Stampfl, *Phys. Rev. B: Condens. Matter Mater. Phys.*, 2008, **78**, 245317.
375 M. A. L. Marques, A. Castro, G. F. Bertsch and A. Rubio, *Comput. Phys. Commun.*, 2003, **151**, 60.
376 A. Castro, H. Appel, M. Oliveira, C. A. Rozzi, X. Andrade, F. Lorenzen, M. A. L. Marques, E. K. U. Gross and A. Rubio, *Phys. Status Solidi B*, 2006, **243**, 2465.
377 S. Scandolo, P. Giannozzi, C. Cavazzoni, S. de Gironcoli, A. Pasquarello and S. Baroni, *Z. Kristallogr.*, 2005, **220**, 574.
378 X. Wu, A. Selloni and R. Car, *Phys. Rev. B: Condens. Matter Mater. Phys.*, 2009, **79**, 085102.
379 R. Dovesi, R. Orlando, C. Roetti, C. Pisani and V. R. Saunders, *Phys. Status Solidi B*, 2000, **217**, 63.
380 R. Dovesi, B. Civalleri, R. Orlando, C. Ruetti and V. R. Saunders, *Rev. Comput. Chem.*, 2005, **21**, 1.
381 I. Baraille, A. Loudet, S. Lacombe, H. Cardy and C. Pisani, *THEOCHEM*, 2003, **620**, 291.
382 D. Muñoz, N. M. Harrison and F. Illas, *Phys. Rev. B: Condens. Matter Mater. Phys.*, 2004, **69**, 085115.
383 G. M. Rignanese, X. Gonze, G. Jun, K. Cho and A. Pasquarello, *Phys. Rev. B: Condens. Matter Mater. Phys.*, 2004, **69**, 184301.
384 M. Levy and T. Pagnier, *Sens. Actuators, B*, 2007, **126**, 204.
385 J. W. Zwanziger and M. Torrent, *Appl. Magn. Reson.*, 2008, **33**, 447.
386 A. Mellouki, L. Kalarasse, B. Bennecer and F. Kalarasse, *Comput. Mater. Sci.*, 2009, **44**, 876.
387 Y. Imai, M. Mukaida and T. Tsunoda, *Thin Solid Films*, 2001, **381**, 176.
388 J. W. Medlin and M. D. Allendorf, *J. Phys. Chem. B*, 2003, **107**, 217.
389 K. Refson, S.-H. Park and G. Sposito, *J. Phys. Chem. B*, 2003, **107**, 13376.
390 S. J. Clark, M. D. Segall, C. J. Pickard, P. J. Hasnip, M. J. Probert, K. Refson and M. C. Payne, *Z. Kristallogr.*, 2005, **220**, 567.
391 M. A. Petersen, S. J. Jenkins and D. A. King, *J. Phys. Chem. B*, 2004, **108**, 5920.

392 B. Hinnemann and J. K. Nørskov, *J. Am. Chem. Soc.*, 2003, **125**, 1466.
393 F. Abild-Pedersen, O. Lytken, J. Engbaek, G. Nielsen, I. Chorkendorff and J. K. Nørskov, *Surf. Sci.*, 2005, **590**, 127.
394 L. C. Grabow, A. A. Gokhale, S. T. Evans, J. A. Dumesic and M. Mavrikakis, *J. Phys. Chem. C*, 2008, **112**, 4608.
395 A. V. Postnikov, G. Bihlmayer and S. Blügel, *Comput. Mater. Sci.*, 2006, **36**, 91.
396 S. Y. Savrasov, *Z. Kristallogr.*, 2005, **220**, 555.
397 A. Umetani, E. Nagoshi, T. Kubodera and M. Matoba, *Phys. B*, 2008, **403**, 1356.
398 I. V. Yudanov, A. V. Matveev, K. M. Neyman and N. Rösch, *J. Am. Chem. Soc.*, 2008, **130**, 9342.
399 J. R. Chelikowsky, N. Troullier and Y. Saad, *Phys. Rev. Lett.*, 1994, **72**, 1240.
400 J. L. Fattebert and J. Bernholc, *Phys. Rev. B: Condens. Matter Mater. Phys.*, 2000, **62**, 1713.
401 J. L. Fattebert and F. Gygi, *Phys. Rev. B: Condens. Matter Mater. Phys.*, 2006, **73**, 115124.
402 C. J. Barden, J. C. Rienstra-Kiracofe and H. F. Schaefer, III, *J. Chem. Phys.*, 2000, **113**, 690.
403 C. Diedrich, A. Luchow and S. Grimme, *J. Chem. Phys.*, 2005, **122**, 021101.
404 M. C. Holthausen, *J. Comput. Chem.*, 2005, **26**, 1505.
405 N. E. Schultz, Y. Zhao and D. G. Truhlar, *J. Comput. Chem.*, 2008, **29**, 185.
406 Y. Zhao and D. G. Truhlar, *J. Chem. Phys.*, 2006, **124**, 224105.
407 V. Karttunen, M. Linnolahti, T. Pakkanen, J. Maaranen and P. Pitkänen, *Theor. Chem. Acc.*, 2007, **118**, 899.
408 K. P. Jensen, B. O. Roos and U. Ryde, *J. Chem. Phys.*, 2007, **126**, 014103.
409 S. Goel and A. E. Masunov, *J. Chem. Phys.*, 2008, **129**, 214302.
410 F. S. Legge, G. L. Nyberg and J. B. Peel, *J. Phys. Chem. A*, 2001, **105**, 7905.
411 F. Wang and L. M. Li, *J. Comput. Chem.*, 2004, **25**, 669.
412 Y. Zhao and D. G. Truhlar, *Acc. Chem. Res.*, 2008, **41**, 157.
413 J. N. Harvey, *Annu. Rep. Prog. Chem., Sect. C*, 2006, **102**, 203.
414 G. T. de Jong and F. M. Bickelhaupt, *J. Chem. Theory Comput.*, 2006, **2**, 322.
415 M. M. Quintal, A. Karton, M. A. Iron, A. D. Boese and J. M. L. Martin, *J. Phys. Chem. A*, 2006, **110**, 709.
416 S. Li, J. M. Hennigan, D. A. Dixon and K. A. Peterson, *J. Phys. Chem. A*, 2009, **113**, 7861.
417 N. J. Mayhall, K. Raghavachari, P. C. Redfern and L. A. Curtiss, *J. Phys. Chem. A*, 2009, **113**, 5170.
418 Q. Ge, C. Song and L. Wang, *Comput. Mater. Sci.*, 2006, **35**, 247.
419 P. Schwerdtfeger, M. Lein, R. P. Krawczyk and C. R. Jacob, *J. Chem. Phys.*, 2008, **128**, 124302.
420 G. T. de Jong, D. P. Geerke, A. Diefenbach and F. Matthias Bickelhaupt, *Chem. Phys.*, 2005, **313**, 261.
421 A. Ikeda, Y. Nakao, H. Sato and S. Sakaki, *J. Phys. Chem. A*, 2007, **111**, 7124.
422 S. Li and D. A. Dixon, *J. Phys. Chem. A*, 2007, **111**, 11908.
423 S. Zhao, Z.-H. Li, W.-N. Wang, Z.-P. Liu, K.-N. Fan, Y. Xie and H. F. Schaefer III, *J. Chem. Phys.*, 2006, **124**, 184102.
424 F. Stevens, I. Carmichael, F. Callens and M. Waroquier, *J. Phys. Chem. A*, 2006, **110**, 4846.
425 J. Rogal, K. Reuter and M. Scheffler, *Phys. Rev. B: Condens. Matter Mater. Phys.*, 2007, **75**, 205433.
426 P. Song, W. Guan, C. Yao, Z. Su, Z. Wu, J. Feng and L. Yan, *Theor. Chem. Acc.*, 2007, **117**, 407.
427 J. S. Sears and C. D. Sherrill, *J. Phys. Chem. A*, 2008, **112**, 6741.
428 J. S. Sears and C. D. Sherrill, *J. Phys. Chem. A*, 2008, **112**, 3466.
429 A. Ghosh, E. Gonzalez, E. Tangen and B. O. Roos, *J. Phys. Chem. A*, 2008, **112**, 12792.
430 A. Ghosh and P. R. Taylor, *Curr. Opin. Chem. Biol.*, 2003, **7**, 113.
431 A. Sorkin, D. G. Truhlar and E. A. Amin, *J. Chem. Theory Comput.*, **5**, 1254.
432 J. Paier, M. Marsman and G. Kresse, *J. Chem. Phys.*, 2007, **127**, 024103.
433 A. Stroppa and G. Kresse, *New J. Phys.*, 2008, **10**, 063020.
434 A. Matveev, M. Staufer, M. Mayer and N. Rösch, *Int. J. Quantum Chem.*, 1999, **75**, 863.
435 R. J. Deeth and N. Fey, *J. Comput. Chem.*, 2004, **25**, 1840.
436 G. I. Csonka, J. P. Perdew, A. Ruzsinszky, P. H. T. Philipsen, S. Lebegue, J. Paier, O. A. Vydrov and J. G. Angyan, *Phys. Rev. B: Condens. Matter Mater. Phys.*, 2009, **79**, 155107.
437 P. Haas, F. Tran and P. Blaha, *Phys. Rev. B: Condens. Matter Mater. Phys.*, 2009, **79**, 085104.
438 M. Ropo, K. Kokko and L. Vitos, *Phys. Rev. B: Condens. Matter Mater. Phys.*, 2008, **77**, 195445.
439 F. Tran, R. Laskowski, P. Blaha and K. Schwarz, *Phys. Rev. B: Condens. Matter Mater. Phys.*, 2007, **75**, 115131.
440 D. Rinaldo, L. Tian, J. N. Harvey and R. A. Friesner, *J. Chem. Phys.*, 2008, **129**, 164108.
441 M. Bühl, C. Reimann, D. A. Pantazis, T. Bredow and F. Neese, *J. Chem. Theory Comput.*, 2008, **4**, 1449.
442 J. Handzlik, *Chem. Phys. Lett.*, 2009, **469**, 140.
443 C. Mosch, C. Koukounas, N. Bacalis, A. Metropoulos, A. Gross and A. Mavridis, *J. Phys. Chem. C*, 2008, **112**, 6924.
444 J. J. Zheng, Y. Zhao and D. G. Truhlar, *J. Chem. Theory Comput.*, 2009, **5**, 808.
445 M. Reiher, *Faraday Discuss.*, 2007, **135**, 97.
446 W. Heisenberg, *Z. Phys.*, 1928, **49**, 619.
447 P. A. M. Dirac, *Proc. R. Soc. London, Ser. A*, 1929, **123**, 714.
448 J. H. Van Vleck, *Rev. Mod. Phys.*, 1945, **17**, 27.
449 J. C. Slater, *Rev. Mod. Phys.*, 1953, **25**, 199.
450 I. Ciofini and C. A. Daul, *Coord. Chem. Rev.*, 2003, **238–239**, 187.
451 J. N. Harvey, *Struct. Bonding*, 2004, **112**, 151.
452 F. Neese, *Coord. Chem. Rev.*, 2009, **253**, 526.
453 L. Noodleman and E. R. Davidson, *Chem. Phys.*, 1986, **109**, 131.
454 F. Neese, *J. Phys. Chem. Solids*, 2004, **65**, 781.
455 E. R. Davidson and A. E. Clark, *Int. J. Quantum Chem.*, 2005, **103**, 1.
456 S. Pittalis, S. Kurth and E. K. U. Gross, *J. Chem. Phys.*, 2006, **125**, 084105.
457 T. Ziegler, A. Rauk and E. J. Baerends, *Theor. Chim. Acta*, 1977, **43**, 261.
458 L. Noodleman, *J. Chem. Phys.*, 1981, **74**, 5737.
459 A. J. Cohen, P. Mori-Sánchez and W. Yang, *Science*, 2008, **321**, 792.
460 J.-M. Mouesca, J. L. Chen, L. Noodleman, D. Bashford and D. A. Case, *J. Am. Chem. Soc.*, 1994, **116**, 11898.
461 S. Sinnecker, F. Neese, L. Noodleman and W. Lubitz, *J. Am. Chem. Soc.*, 2004, **126**, 2613.
462 E. Ruiz, J. Cano, S. Alvarez and P. Alemany, *J. Comput. Chem.*, 1999, **20**, 1391.
463 K. Yamaguchi, F. Jensen, A. Dorigo and K. N. Houk, *Chem. Phys. Lett.*, 1988, **149**, 537.
464 T. Soda, Y. Kitagawa, T. Onishi, Y. Takano, Y. Shigeta, H. Nagao, Y. Yoshioka and K. Yamaguchi, *Chem. Phys. Lett.*, 2000, **319**, 223.
465 M. Shoji, K. Koizumi, Y. Kitagawa, T. Kawakami, S. Yamanaka, M. Okumura and K. Yamaguchi, *Chem. Phys. Lett.*, 2006, **432**, 343.
466 J. Pople, P. Gill and N. Handy, *Int. J. Quantum Chem.*, 1995, **56**, 303.
467 J. Baker, A. Scheiner and J. Andzelm, *Chem. Phys. Lett.*, 1993, **216**, 380.
468 J. Wang, L. A. Eriksson, R. J. Boyd, Z. Shi and B. G. Johnson, *J. Phys. Chem.*, 1994, **98**, 1844.
469 C. J. Cramer, F. J. Dulles and D. E. Falvey, *J. Am. Chem. Soc.*, 1994, **116**, 9787.
470 C. J. Cramer, F. J. Dulles, J. W. Storer and S. E. Worthington, *Chem. Phys. Lett.*, 1994, **218**, 387.
471 C. J. Cramer, F. J. Dulles, D. J. Giesen and J. Almlöf, *Chem. Phys. Lett.*, 1995, **245**, 165.
472 J. Wang, A. D. Becke and J. V. H. Smith, *J. Chem. Phys.*, 1995, **102**, 3477.
473 J. Gräfenstein, E. Kraka, M. Filatov and D. Cremer, *Int. J. Mol. Sci.*, 2002, **3**, 360.
474 D. Cremer, M. Filatov, V. Polo, E. Kraka and S. Shaik, *Int. J. Mol. Sci.*, 2002, **3**, 604.
475 J. Gräfenstein and D. Cremer, *Mol. Phys.*, 2001, **99**, 981.
476 V. N. Staroverov and E. R. Davidson, *Chem. Phys. Lett.*, 2001, **340**, 142.
477 H. Carmen, Y. Lian and R. Markus, *J. Comput. Chem.*, 2006, **27**, 1223.
478 R. K. Szilagyi and M. A. Winslow, *J. Comput. Chem.*, 2006, **27**, 1385.
479 A. Sorkin, M. A. Iron and D. G. Truhlar, *J. Chem. Theory Comput.*, 2008, **4**, 307.

480 R. Valero, R. Costa, I. Moreira, D. G. Truhlar and F. Illas, *J. Chem. Phys.*, 2008, **128**, 114103.
481 C. Adamo, V. Barone, A. Bencini, F. Totti and I. Ciofini, *Inorg. Chem.*, 1999, **38**, 1996.
482 E. Ruiz, S. Alvarez, J. Cano and V. Polo, *J. Chem. Phys.*, 2005, **123**, 164110.
483 C. Adamo, V. Barone, A. Bencini, R. Broer, M. Filatov, N. M. Harrison, F. Illas, J. P. Malrieu and I. D. R. Moreira, *J. Chem. Phys.*, 2006, **124**, 107101.
484 J. L. Lewin, D. E. Heppner and C. J. Cramer, *JBIC, J. Biol. Inorg. Chem.*, 2007, **12**, 1221.
485 C. J. Cramer, A. Kinal, M. Wloch, P. Piecuch and L. Gagliardi, *J. Phys. Chem. A*, 2006, **110**, 11557.
486 C. J. Cramer, M. Wloch, P. Piecuch, C. Puzzarini and L. Gagliardi, *J. Phys. Chem. A*, 2006, **110**, 1991.
487 C. J. Cramer and W. B. Tolman, *Acc. Chem. Res.*, 2007, **40**, 601.
488 S. M. Huber, M. Z. Ertem, F. Aquilante, L. Gagliardi, W. B. Tolman and C. J. Cramer, *Chem.–Eur. J.*, 2009, **15**, 4886.
489 P. Å. Malmqvist, K. Pierloot, A. R. Moughal Shahi, C. J. Cramer and L. Gagliardi, *J. Chem. Phys.*, 2008, **128**, 204109.
490 P. Rivero, I. D. R. Moreira, F. Illas and G. E. Scuseria, *J. Chem. Phys.*, 2008, **129**, 184110.
491 A. Roth, J. Becher, C. Herrmann, H. Gorls, G. Vaughan, M. Reiher, D. Klemm and W. Plass, *Inorg. Chem.*, 2006, **45**, 10066.
492 N. Marom and L. Kronik, *Appl. Phys. A: Mater. Sci. Process.*, 2009, **95**, 165.
493 E. R. Batista and R. L. Martin, *J. Am. Chem. Soc.*, 2007, **129**, 7224.
494 X. Yang and M. H. Baik, *J. Am. Chem. Soc.*, 2004, **126**, 13222.
495 X. Yang and M. H. Baik, *J. Am. Chem. Soc.*, 2006, **128**, 7476.
496 T. R. Weaver, T. J. Meyer, S. A. Adeyemi, G. M. Brown, R. P. Eckberg, W. E. Hatfield, E. C. Johnson, R. W. Murray and D. Untereker, *J. Am. Chem. Soc.*, 1975, **97**, 3039.
497 K. Pierloot and S. Vancoillie, *J. Chem. Phys.*, 2008, **128**, 034104.
498 M. Swart, *J. Chem. Theory Comput.*, 2008, **4**, 2057.
499 C. Rong, S. Lian, D. Yin, B. Shen, A. Zhong, L. Bartolotti and S. Liu, *J. Chem. Phys.*, 2006, **125**, 174102.
500 J. L. Carreon-Macedo and J. N. Harvey, *Phys. Chem. Chem. Phys.*, 2006, **8**, 93.
501 J. Song, E. Apr·, Y. G. Khait, M. R. Hoffmann and K. Kowalski, *Chem. Phys. Lett.*, 2006, **428**, 277.
502 F. Neese, *J. Inorg. Biochem.*, 2006, **100**, 716.
503 J. M. Matxain, E. Rezabal, X. Lopez, J. M. Ugalde and L. Gagliardi, *J. Chem. Phys.*, 2008, **128**, 194315.
504 C. Herrmann, L. Yu and M. Reiher, *J. Comput. Chem.*, 2006, **27**, 1223.
505 C. Herrmann, M. Reiher and B. A. Hess, *J. Chem. Phys.*, 2005, **122**, 034102.
506 A. E. Clark and E. R. Davidson, *J. Chem. Phys.*, 2001, **115**, 7382.
507 I. Mayer, *Chem. Phys. Lett.*, 2007, **440**, 357.
508 O. Hubner, K. Fink and W. Klopper, *Phys. Chem. Chem. Phys.*, 2007, **9**, 1911.
509 M. Podewitz, C. Herrmann, A. Malassa, M. Westerhausen and M. Reiher, *Chem. Phys. Lett.*, 2008, **451**, 301.
510 P. H. Dederichs, S. Blügel, R. Zeller and H. Akai, *Phys. Rev. Lett.*, 1984, **53**, 2512.
511 Q. Wu and T. V. Voorhis, *Phys. Rev. A: At., Mol., Opt. Phys.*, 2005, **72**, 024502.
512 Q. Wu, C.-L. Cheng and T. Van Voorhis, *J. Chem. Phys.*, 2007, **127**, 164119.
513 S. Difley, D. Beljonne and T. Van Voorhis, *J. Am. Chem. Soc.*, 2008, **130**, 3420.
514 I. Rudra, Q. Wu and T. Van Voorhis, *Inorg. Chem.*, 2007, **46**, 10539.
515 J. R. Schmidt, N. Shenvi and J. C. Tully, *J. Chem. Phys.*, 2008, **129**, 114110.
516 H. Fliegl, K. Fink, W. Klopper, C. E. Anson, A. K. Powell and R. Clerac, *Phys. Chem. Chem. Phys.*, 2009, **11**, 3900.
517 I. Ciofini, F. Illas and C. Adamo, *J. Chem. Phys.*, 2004, **120**, 3811.
518 M. Filatov and S. Shaik, *Chem. Phys. Lett.*, 1999, **304**, 429.
519 F. Illas, I. D. R. Moreira, J. M. Bofill and M. Filatov, *Theor. Chem. Acc.*, 2006, **116**, 587.
520 A. Kazaryan, J. Heuver and M. Filatov, *J. Phys. Chem. A*, 2008, **112**, 12980.
521 I. d. P. R. Moreira, R. Costa, M. Filatov and F. Illas, *J. Chem. Theory Comput.*, 2007, **3**, 764.
522 A. J. Pérez-Jiménez, J. M. Pérez-Jordá, I. d. P. R. Moreira and F. Illas, *J. Comput. Chem.*, 2007, **28**, 2559.
523 T. Ukai, K. Nakata, S. Yamanaka, T. Takada and K. Yamaguchi, *Mol. Phys.*, 2007, **105**, 2667.
524 Y. H. Shao, M. Head-Gordon and A. I. Krylov, *J. Chem. Phys.*, 2003, **118**, 4807.
525 A. de la Lande, V. Moliner and O. Parisel, *J. Chem. Phys.*, 2007, **126**, 035102.
526 Y. M. Rhee and M. Head-Gordon, *J. Am. Chem. Soc.*, 2008, **130**, 3878.
527 F. Wang and T. Ziegler, *J. Chem. Phys.*, 2004, **121**, 12191.
528 F. Wang and T. Ziegler, *J. Chem. Phys.*, 2005, **122**, 074109.
529 F. Wang and T. Ziegler, *Int. J. Quantum Chem.*, 2006, **106**, 2545.
530 O. Vahtras and Z. Rinkevicius, *J. Chem. Phys.*, 2007, **126**, 114101.
531 A. V. Soldatova, J. Kim, A. Rosa, G. Ricciardi, M. E. Kenney and M. A. J. Rodgers, *Inorg. Chem.*, 2008, **47**, 4275.
532 J. E. Peralta and V. Barone, *J. Chem. Phys.*, 2008, **129**, 194107.
533 T. M. Alam, J. S. Clawson, F. o. Bonhomme, S. G. Thoma, M. A. Rodriguez, S. Zheng and J. Autschbach, *Chem. Mater.*, 2008, **20**, 2205.
534 J. Autschbach and S. Zheng, *Magn. Reson. Chem.*, 2008, **46**, S45.
535 J. M. Morbec and K. Capelle, *Int. J. Quantum Chem.*, 2008, **108**, 2433.
536 P. Hrobárik, O. L. Malkina, V. G. Malkin and M. Kaupp, *Chem. Phys.*, 2009, **356**, 229.
537 E. Runge and E. K. U. Gross, *Phys. Rev. Lett.*, 1984, **52**, 997.
538 R. Bauernschmitt and R. Ahlrichs, *Chem. Phys. Lett.*, 1996, **256**, 454.
539 R. Van Leeuwen, *Int. J. Mod. Phys. B*, 2001, **15**, 1969.
540 K. Burke, M. Petersilka and E. K. U. Gross, in *Recent Advances in Density Functional Methods*, ed. P. Fantucci and A. Bencini, World Scientific, Singapore, 2002, vol. 3, p. 67.
541 R. J. Deeth, *Faraday Discuss.*, 2003, **124**, 379.
542 M. A. L. Marques and E. K. U. Gross, *Annu. Rev. Phys. Chem.*, 2004, **55**, 427.
543 A. Dreuw and M. Head-Gordon, *Chem. Rev.*, 2005, **105**, 4009.
544 P. Elliot, F. Furche and K. Burke, *Rev. Comput. Chem.*, 2009, **26**, 91.
545 N. C. Handy, *Mol. Phys.*, 2004, **102**, 2399.
546 V. Arcisauskaite, J. Kongsted, T. Hansen and K. V. Mikkelsen, *Chem. Phys. Lett.*, 2009, **470**, 285.
547 L. Salassa, C. Garino, G. Salassa, R. Gobetto and C. Nervi, *J. Am. Chem. Soc.*, 2008, **130**, 9590.
548 J. F. Guillemoles, V. Barone, L. Joubert and C. Adamo, *J. Phys. Chem. A*, 2002, **106**, 11354.
549 P. P. Lainé, I. Ciofini, P. Ochsenbein, E. Amouyal, C. Adamo and F. Bedioui, *Chem.–Eur. J.*, 2005, **11**, 3711.
550 M. K. Nazeeruddin, F. De Angelis, S. Fantacci, A. Selloni, G. Viscardi, P. Liska, S. Ito, B. Takeru and M. Gratzel, *J. Am. Chem. Soc.*, 2005, **127**, 16835.
551 P. P. Lainé, F. Loiseau, S. Campagna, I. Ciofini and C. Adamo, *Inorg. Chem.*, 2006, **45**, 5538.
552 M. F. Charlot and A. Aukauloo, *J. Phys. Chem. A*, 2007, **111**, 11661.
553 M. Marcaccio, F. Paolucci, C. Fontanesi, G. Fioravanti and S. Zanarini, *Inorg. Chim. Acta*, 2007, **360**, 1154.
554 M. Abrahamsson, M. Jager, R. J. Kumar, T. Osterman, P. Persson, H. C. Becker, O. Johansson and L. Hammarstrom, *J. Am. Chem. Soc.*, 2008, **130**, 15533.
555 T. A. Jackson, J. U. Rohde, M. S. Seo, C. V. Sastri, R. DeHont, A. Stubna, T. Ohta, T. Kitagawa, E. Munck, W. Nam and L. Que, *J. Am. Chem. Soc.*, 2008, **130**, 12394.
556 M. Hutin, C. J. Cramer, L. Gagliardi, A. R. Moughal Shahi, G. Bernardinelli, R. Cerny and J. R. Nitschke, *J. Am. Chem. Soc.*, 2007, **129**, 8774.
557 D. Schultz, F. Biaso, A. R. M. Shahi, M. Geoffroy, K. Rissanen, L. Gagliardi, C. J. Cramer and J. R. Nitschke, *Chem.–Eur. J.*, 2008, **14**, 7180.
558 I. Bar-Nahum, A. K. Gupta, S. M. Huber, M. Z. Ertem, C. J. Cramer and W. B. Tolman, *J. Am. Chem. Soc.*, 2009, **131**, 2812.
559 A. Vlček Jr and S. Záliš, *Coord. Chem. Rev.*, 2007, **251**, 258.
560 J. Fan, M. Seth, J. Autschbach and T. Ziegler, *Inorg. Chem.*, 2008, **47**, 11656.

561 G. A. Peralta, M. Seth, H. Zhekova and T. Ziegler, *Inorg. Chem.*, 2008, **47**, 4185.
562 P. R. T. Schipper, O. V. Gritsenko, S. J. A. van Gisbergen and E. J. Baerends, *J. Chem. Phys.*, 2000, **112**, 1344.
563 A. Kunishita, J. Teraoka, J. D. Scanlon, T. Matsumoto, M. Suzuki, C. J. Cramer and S. Itoh, *J. Am. Chem. Soc.*, 2007, **129**, 7248.
564 M. Stener, A. Nardelli, R. De Francesco and G. Fronzoni, *J. Phys. Chem. C*, 2007, **111**, 11862.
565 M. Stener, A. Nardelli and G. Fronzoni, *J. Chem. Phys.*, 2008, **128**, 134307.
566 M. Stener, A. Nardelli and G. Fronzoni, *Chem. Phys. Lett.*, 2008, **462**, 358.
567 M. Caricato, B. Mennucci, J. Tomasi, F. Ingrosso, R. Cammi, S. Corni and G. Scalmani, *J. Chem. Phys.*, 2006, **124**, 124520.
568 G. Scalmani, M. J. Frisch, B. Mennucci, J. Tomasi, R. Cammi and V. Barone, *J. Chem. Phys.*, 2006, **124**, 094107.
569 B. Mennucci, *Theor. Chem. Acc.*, 2006, **116**, 31.
570 F. De Angelis, S. Fantacci and A. Sgamellotti, *Theor. Chem. Acc.*, 2007, **117**, 1093.
571 M. J. Lundqvist, M. Nilsing, S. Lunell, B. Akermark and P. Persson, *J. Phys. Chem. B*, 2006, **110**, 20513.
572 P. Persson, M. J. Lundqvist, R. Ernstorfer, W. A. Goddard and F. Willig, *J. Chem. Theory Comput.*, 2006, **2**, 441.
573 M. Nilsing, P. Persson, S. Lunell and L. Ojamae, *J. Phys. Chem. C*, 2007, **111**, 12116.
574 F. De Angelis, S. Fantacci, A. Selloni, M. Gratzel and M. K. Nazeeruddin, *Nano Lett.*, 2007, **7**, 3189.
575 S. G. Abuabara, L. G. C. Rego and V. S. Batista, *J. Am. Chem. Soc.*, 2005, **127**, 18234.
576 A. Ramirez-Solis, R. Poteau and J. P. Daudey, *J. Chem. Phys.*, 2006, **124**, 034307.
577 A. L. Tenderholt, R. K. Szilagyi, R. H. Holm, K. O. Hodgson, B. Hedman and E. I. Solomon, *Inorg. Chem.*, 2008, **47**, 6382.
578 A. Decker, J. U. Rohde, E. J. Klinker, S. D. Wong, L. Que and E. I. Solomon, *J. Am. Chem. Soc.*, 2007, **129**, 15983.
579 R. Sarangi, J. T. York, M. E. Helton, K. Fujisawa, K. D. Karlin, W. B. Tolman, K. O. Hodgson, B. Hedman and E. I. Solomon, *J. Am. Chem. Soc.*, 2008, **130**, 676.
580 R. Sarangi, S. DeBeer George, D. J. Rudd, R. K. Szilagyi, X. Ribas, C. Rovira, M. Almeida, K. O. Hodgson, B. Hedman and E. I. Solomon, *J. Am. Chem. Soc.*, 2007, **129**, 2316.
581 M. Casarin, P. Finetti, A. Vittadini, F. Wang and T. Ziegler, *J. Phys. Chem. A*, 2007, **111**, 5270.
582 S. A. Kozimor, P. Yang, E. R. Batista, K. S. Boland, C. J. Burns, C. N. Christensen, D. L. Clark, S. D. Conradson, P. J. Hay, J. S. Lezama, R. L. Martin, D. E. Schwarz, M. P. Wilkerson and L. E. Wolfsberg, *Inorg. Chem.*, 2008, **47**, 5365.
583 G. Fronzoni, M. Stener, P. Decleva, F. Wang, T. Ziegler, E. van Lenthe and E. J. Baerends, *Chem. Phys. Lett.*, 2005, **416**, 56.
584 G. Fronzoni, M. Stener, A. Reduce and P. Decleva, *J. Phys. Chem. A*, 2004, **108**, 8467.
585 K. Ray, S. D. George, E. I. Solomon, K. Wieghardt and F. Neese, *Chem.–Eur. J.*, 2007, **13**, 2783.
586 S. DeBeer George, T. Petrenko and F. Neese, *J. Phys. Chem. A*, 2008, **112**, 12936.
587 J. F. Berry, S. D. George and F. Neese, *Phys. Chem. Chem. Phys.*, 2008, **10**, 4361.
588 J. F. Berry, E. Bill, E. Bothe, S. D. George, B. Mienert, F. Neese and K. Wieghardt, *Science*, 2006, **312**, 1937.
589 R. Sarangi, S. I. Gorelsky, L. Basumallick, H. J. Hwang, R. C. Pratt, T. D. P. Stack, Y. Lu, K. O. Hodgson, B. Hedman and E. I. Solomon, *J. Am. Chem. Soc.*, 2008, **130**, 3866.
590 C.-L. Cheng, Q. Wu and T. Van Voorhis, *J. Chem. Phys.*, 2008, **129**, 124112.
591 A. T. B. Gilbert, N. A. Besley and P. M. W. Gill, *J. Phys. Chem. A*, 2008, **112**, 13164.
592 A. Castro, M. A. L. Marques, A. H. Romero, M. J. T. Oliveira and A. Rubio, *J. Chem. Phys.*, 2008, **129**, 144110.
593 X.-Y. Yang, Y.-C. Wang, Z.-Y. Geng and Z.-Y. Liu, *Chem. Phys. Lett.*, 2006, **430**, 265.
594 S. Shaik, H. Hirao and D. Kumar, *Acc. Chem. Res.*, 2007, **40**, 532.
595 K. Morokuma, *Bull. Chem. Soc. Jpn.*, 2007, **80**, 2247.
596 N. Hebben, H.-J. Himmel, G. Eickerling, C. Herrmann, M. Reiher, V. Herz, M. Presnitz and W. Scherer, *Chem.–Eur. J.*, 2007, **13**, 10078.
597 R. Herges and A. Papafilippopoulos, *Angew. Chem., Int. Ed.*, 2001, **40**, 4671.
598 B. D. Alexander and T. J. Dines, *J. Phys. Chem. A*, 2004, **108**, 146.
599 V. W. Jurgensen and K. Jalkanen, *Phys. Biol.*, 2006, **3**, S63.
600 S. Sinnecker and F. Neese, *Top. Curr. Chem.*, 2007, **268**, 47.
601 C. Herrmann and M. Reiher, *Top. Curr. Chem.*, 2007, **268**, 85.
602 H. Sato, T. Taniguchi, K. Monde, S.-I. Nishimura and A. Yamagishi, *Chem. Lett.*, 2006, **35**, 364.
603 S. Luber and M. Reiher, *Chem. Phys.*, 2008, **346**, 212.
604 B. B. Johnson and W. L. Peticolas, *Annu. Rev. Phys. Chem.*, 1976, **27**, 465.
605 A. Warshel, *Annu. Rev. Biophys. Bioeng.*, 1977, **6**, 273.
606 R. J. H. Clark and B. Stewart, *Struct. Bonding*, 1979, **36**, 1.
607 F. Neese, T. Petrenko, D. Ganyushin and G. Olbrich, *Coord. Chem. Rev.*, 2007, **251**, 288.
608 C. Herrmann, J. Neugebauer, M. Presselt, U. Uhlemann, M. Schmitt, S. Rau, J. Popp and M. Reiher, *J. Phys. Chem. B*, 2007, **111**, 6078.
609 T. Petrenko, K. Ray, K. E. Wieghardt and F. Neese, *J. Am. Chem. Soc.*, 2006, **128**, 4422.
610 B. V. Popp, J. E. Wendlandt, C. R. Landis and S. S. Stahl, *Angew. Chem., Int. Ed.*, 2007, **46**, 601.
611 V. V. Smirnov, D. W. Brinkley, M. P. Lanci, K. D. Karlin and J. P. Roth, *J. Mol. Catal. A: Chem.*, 2006, **251**, 100.
612 M. P. Lanci and J. P. Roth, *J. Am. Chem. Soc.*, 2006, **128**, 16006.
613 J. P. Roth and J. P. Klinman, in *Isotope Effects in Chemistry and Biology*, ed. A. Kohen and H.-H. Limbach, CRC Press, Boca Raton, 2006, p. 645.
614 M. P. Lanci, V. V. Smirnov, C. J. Cramer, E. V. Gauchenova, J. Sundermeyer and J. P. Roth, *J. Am. Chem. Soc.*, 2007, **129**, 14697.
615 J. P. Roth and C. J. Cramer, *J. Am. Chem. Soc.*, 2008, **130**, 7802.
616 G. Brehm, M. Reiher, B. Le Guennic, M. Leibold, S. Schindler, F. W. Heinemann and S. Schneider, *J. Raman Spectrosc.*, 2006, **37**, 108.
617 P. Carbonniere, I. Ciofini, C. Adamo and C. Pouchan, *Chem. Phys. Lett.*, 2006, **429**, 52.
618 B. Insuasty, C. Atienza, C. Seoane, N. Martin, J. Garin, J. Orduna, R. Alcala and B. Villacampa, *J. Org. Chem.*, 2004, **69**, 6986.
619 L. Fang, G. Yang, Y. Qiu and Z. Su, *Theor. Chem. Acc.*, 2008, **119**, 329.
620 O. Rubio-Pons, Y. Luo and H. Agren, *J. Chem. Phys.*, 2006, **124**, 094310.
621 T. Ziegler and J. Autschbach, *Chem. Rev.*, 2005, **105**, 2695.
622 E. R. Davidson, *Chem. Rev.*, 2000, **100**, 351.
623 E. C. Sherer and C. J. Cramer, *Organometallics*, 2003, **22**, 1682.
624 N. Barros, O. Eisenstein, L. Maron and T. D. Tilley, *Organometallics*, 2006, **25**, 5699.
625 N. Barros, O. Eisenstein and L. Maron, *Dalton Trans.*, 2006, 3052.
626 N. L. Woodrum and C. J. Cramer, *Organometallics*, 2006, **25**, 68.
627 J. L. Lewin, N. L. Woodrum and C. J. Cramer, *Organometallics*, 2006, **25**, 5906.
628 L. Perrin, O. Eisenstein and L. Maron, *New J. Chem.*, 2007, **31**, 549.
629 P. A. Hunt, *Dalton Trans.*, 2007, 1743.
630 V. L. Cruz, S. Martinez, J. Martinez-Salazar and J. Sancho, *Macromolecules*, 2007, **40**, 7413.
631 M. Zimmermann, F. Estler, E. Herdtweck, K. W. Tornroos and R. Anwander, *Organometallics*, 2007, **26**, 6029.
632 N. Barros, O. Eisenstein, L. Maron and T. D. Tilley, *Organometallics*, 2008, **27**, 2252.
633 B. A. Vastine and M. B. Hall, *J. Am. Chem. Soc.*, 2007, **129**, 12068.
634 R. F. W. Bader, *Chem. Rev.*, 1991, **91**, 893.
635 C. S. Tredget, E. Clot and P. Mountford, *Organometallics*, 2008, **27**, 3458.
636 J. Scott, H. Fan, B. F. Wicker, A. R. Fout, M.-H. Baik and D. J. Mindiola, *J. Am. Chem. Soc.*, 2008, **130**, 14438.
637 Y. Luo, J. Baldamus, O. Tardif and Z. Hou, *Organometallics*, 2005, **24**, 4362.
638 M. Lein, J. Frunzke, A. Timoshkin and G. Frenking, *Chem.–Eur. J.*, 2001, **7**, 4155.

639 E. Urnezius, W. W. Brennessel, C. J. Cramer, J. E. Ellis and P. v. R. Schleyer, *Science*, 2002, **295**, 832.
640 M. Lein, J. Frunzke and G. Frenking, *Inorg. Chem.*, 2003, **42**, 2504.
641 J. M. Mercero, E. Formoso, J. M. Matxain, L. A. Eriksson and J. M. Ugalde, *Chem.–Eur. J.*, 2006, **12**, 4495.
642 N. Ochi, Y. Nakao, H. Sato and S. Sakaki, *J. Am. Chem. Soc.*, 2007, **129**, 8615.
643 X.-f. Sheng, G.-f. Zhao and L.-l. Zhi, *J. Phys. Chem. C*, 2008, **112**, 17828.
644 J. Joubert, F. Delbecq, C. Thieuleux, M. Taoufik, F. Blanc, C. Coperet, J. Thivolle-Cazat, J.-M. Basset and P. Sautet, *Organometallics*, 2007, **26**, 3329.
645 S. K. Mandal, P. M. Gurubasavaraj, H. W. Roesky, G. Schwab, D. Stalke, R. B. Oswald and V. Dolle, *Inorg. Chem.*, 2007, **46**, 10158.
646 J. L. Lewin and C. J. Cramer, *J. Phys. Chem. A*, 2008, **112**, 12754.
647 T. Wondimagegn, D. Wang, A. Razavi and T. Ziegler, *Organometallics*, 2008, **27**, 6434.
648 T. Wondimagegn, D. Wang, A. Razavi and T. Ziegler, *Organometallics*, 2009, **28**, 1383.
649 F. Dong, S. Heinbuch, Y. Xie, J. J. Rocca, E. R. Bernstein, Z.-C. Wang, K. Deng and S.-G. He, *J. Am. Chem. Soc.*, 2008, **130**, 1932.
650 F. Dong, S. Heinbuch, Y. Xie, E. R. Bernstein, J. J. Rocca, Z.-C. Wang, X.-L. Ding and S.-G. He, *J. Am. Chem. Soc.*, 2009, **131**, 1057.
651 Y.-P. Ma, W. Xue, Z.-C. Wang, M.-F. Ge and S.-G. He, *J. Phys. Chem. A*, 2008, **112**, 3731.
652 L. Gracia, V. Polo, J. R. Sambrano and J. Andres, *J. Phys. Chem. A*, 2008, **112**, 1808.
653 A. Sadoc, S. Messaoudi, E. Furet, R. Gautier, E. Le Fur, L. le Polles and J.-Y. Pivan, *Inorg. Chem.*, 2007, **46**, 4835.
654 K. J. Ooms, S. E. Bolte, J. J. Smee, B. Baruah, D. C. Crans and T. Polenova, *Inorg. Chem.*, 2007, **46**, 9285.
655 L. L. G. Justino, M. L. Ramos, F. Nogueira, A. J. F. N. Sobral, C. F. G. C. Geraldes, M. Kaupp, H. D. Burrows, C. Fiolhais and V. M. S. Gil, *Inorg. Chem.*, 2008, **47**, 7317.
656 M. Michelini, I. Rivalta and E. Sicilia, *Theor. Chem. Acc.*, 2008, **120**, 395.
657 R. o. Arteaga-Müller, J. Sánchez-Nieves, J. Ramos, P. Royo and M. E. G. Mosquera, *Organometallics*, 2008, **27**, 1417.
658 A. E. Ashley, R. T. Cooper, G. G. Wildgoose, J. C. Green and D. O'Hare, *J. Am. Chem. Soc.*, 2008, **130**, 15662.
659 G. Balazs, F. G. N. Cloke, L. Gagliardi, J. C. Green, A. Harrison, P. B. Hitchcock, A. R. Moughal Shahi and O. T. Summerscales, *Organometallics*, 2008, **27**, 2013.
660 F. Ferrante, L. Gagliardi, B. E. Bursten and A. P. Sattelberger, *Inorg. Chem.*, 2005, **44**, 8476.
661 M. Brynda, L. Gagliardi, P. O. Widmark, P. P. Power and B. O. Roos, *Angew. Chem., Int. Ed.*, 2006, **45**, 3804.
662 B. O. Roos, A. C. Borin and L. Gagliardi, *Angew. Chem., Int. Ed.*, 2007, **46**, 1469.
663 I. Infante, L. Gagliardi and G. E. Scuseria, *J. Am. Chem. Soc.*, 2008, **130**, 7459.
664 G. La Macchia, L. Gagliardi, P. P. Power and M. Brynda, *J. Am. Chem. Soc.*, 2008, **130**, 5104.
665 M. Brynda, L. Gagliardi and B. O. Roos, *Chem. Phys. Lett.*, 2009, **471**, 1.
666 K. Andersson, B. O. Roos, P. A. Malmqvist and P. O. Widmark, *Chem. Phys. Lett.*, 1994, **230**, 391.
667 C. W. Bauschlicher and H. Partridge, *Chem. Phys. Lett.*, 1994, **231**, 277.
668 H. Stoll and H. J. Werner, *Mol. Phys.*, 1996, **88**, 793.
669 K. E. Edgecombe and A. D. Becke, *Chem. Phys. Lett.*, 1995, **244**, 427.
670 A. Poater, X. Solans-Monfort, E. Clot, C. Coperet and O. Eisenstein, *J. Am. Chem. Soc.*, 2007, **129**, 8207.
671 R. Haunschild and G. Frenking, *J. Organomet. Chem.*, 2008, **693**, 737.
672 G. F. Caramori and G. Frenking, *Theor. Chem. Acc.*, 2008, **120**, 351.
673 L. Yan, X. López, J. J. Carbó, R. Sniatynsky, D. C. Duncan and J. M. Poblet, *J. Am. Chem. Soc.*, 2008, **130**, 8223.
674 S. Schenk, B. Le Guennic, B. Kirchner and M. Reiher, *Inorg. Chem.*, 2008, **47**, 3634.
675 D. V. Khoroshun, D. G. Musaev and K. Morokuma, *Mol. Phys.*, 2002, **100**, 523.
676 Z. X. Cao, Z. H. Zhou, H. L. Wan and Q. N. Zhang, *Int. J. Quantum Chem.*, 2005, **103**, 344.
677 M. Reiher, B. Le Guennic and B. Kirchner, *Inorg. Chem.*, 2005, **44**, 9640.
678 D. C. Graham, G. J. O. Beran, M. Head-Gordon, G. Christian, R. Stranger and B. F. Yates, *J. Phys. Chem. A*, 2005, **109**, 6762.
679 M. Holscher and W. Leitner, *Eur. J. Inorg. Chem.*, 2006, 4407.
680 F. Studt and F. Tuczek, *J. Comput. Chem.*, 2006, **27**, 1278.
681 D. V. Khoroshun, D. G. Musaev and K. Morokuma, *J. Comput. Chem.*, 2007, **28**, 423.
682 A. Magistrato, A. Robertazzi and P. Carloni, *J. Chem. Theory Comput.*, 2007, **3**, 1708.
683 G. Christian, R. Stranger and B. F. Yates, *Chem.–Eur. J.*, 2009, **15**, 646.
684 R. R. Schrock, *Angew. Chem., Int. Ed.*, 2008, **47**, 5512.
685 G. C. Stephan, C. Sivasankar, F. Studt and F. Tuczek, *Chem.–Eur. J.*, 2008, **14**, 644.
686 I. Dance, *Chem.–Asian J.*, 2007, **2**, 936.
687 T. Leyssens, D. Peeters, A. G. Orpen and J. N. Harvey, *New J. Chem.*, 2005, **29**, 1424.
688 P. Geerlings, F. D. Proft and W. Langenaeker, *Chem. Rev.*, 2003, **103**, 1793.
689 J. M. Matxain, M. Piris, E. Formoso, J. M. Mercero, X. Lopez and J. M. Ugalde, *ChemPhysChem*, 2007, **8**, 2096.
690 J. M. Matxain, E. Formoso, J. M. Mercero, M. Piris, X. Lopez and J. M. Ugalde, *Chem.–Eur. J.*, 2008, **14**, 8547.
691 K. Yamaguchi, S. Yamanaka, H. Isobe, M. Shoji, K. Koizumi, Y. Kitagawa, T. Kawakami and M. Okumura, *Polyhedron*, 2007, **26**, 2216.
692 D. Balcells, C. Raynaud, R. H. Crabtree and O. Eisenstein, *Inorg. Chem.*, 2008, **47**, 10090.
693 G. Balazs, F. G. N. Cloke, A. Harrison, P. B. Hitchcock, J. Green and O. T. Summerscales, *Chem. Commun.*, 2007, 873.
694 A. Krapp, M. Lein and G. Frenking, *Theor. Chem. Acc.*, 2008, **120**, 313.
695 H.-M. Jia, D.-C. Fang, Y. Feng, J.-Y. Zhang, W.-B. Fan and L. Zhu, *Theor. Chem. Acc.*, 2008, **121**, 271.
696 R. Haunschild and G. Frenking, *J. Organomet. Chem.*, 2008, **693**, 3627.
697 A. Ghosh, J. Almlöf and L. Que, *J. Phys. Chem.*, 1994, **98**, 5576.
698 K. Yoshizawa, T. Ohta, T. Yamabe and R. Hoffmann, *J. Am. Chem. Soc.*, 1997, **119**, 12311.
699 E. I. Solomon, T. C. Brunold, M. I. Davis, J. N. Kemsley, S. K. Lee, N. Lehnert, F. Neese, A. J. Skulan, Y. S. Yang and J. Zhou, *Chem. Rev.*, 2000, **100**, 235.
700 E. I. Solomon, A. Decker and N. Lehnert, *Proc. Natl. Acad. Sci. U. S. A.*, 2003, **100**, 3589.
701 A. Ghosh, E. Tangen, H. Ryeng and P. R. Taylor, *Eur. J. Inorg. Chem.*, 2004, 4555.
702 M. M. Abu-Omar, A. Loaiza and N. Hontzeas, *Chem. Rev.*, 2005, **105**, 2227.
703 A. Decker and E. I. Solomon, *Curr. Opin. Chem. Biol.*, 2005, **9**, 152.
704 S. V. Kryatov, E. V. Rybak-Akimova and S. Schindler, *Chem. Rev.*, 2005, **105**, 2175.
705 A. Bassan, T. Borowski, C. J. Schofield and P. E. M. Siegbahn, *Chem.–Eur. J.*, 2006, **12**, 8835.
706 M. J. Park, J. Lee, Y. Suh, J. Kim and W. Nam, *J. Am. Chem. Soc.*, 2006, **128**, 2630.
707 C. D. Brown, M. L. Neidig, M. B. Neibergall, J. D. Lipscomb and E. I. Solomon, *J. Am. Chem. Soc.*, 2007, **129**, 7427.
708 W. H. Harman and C. J. Chang, *J. Am. Chem. Soc.*, 2007, **129**, 15128.
709 W. Nam, *Acc. Chem. Res.*, 2007, **40**, 522.
710 M. L. Neidig, C. D. Brown, K. M. Light, D. G. Fujimori, E. M. Nolan, J. C. Price, E. W. Barr, J. M. Bollinger, C. Krebs, C. T. Walsh and E. I. Solomon, *J. Am. Chem. Soc.*, 2007, **129**, 14224.
711 M. Y. M. Pau, M. I. Davis, A. M. Orville, J. D. Lipscomb and E. I. Solomon, *J. Am. Chem. Soc.*, 2007, **129**, 1944.
712 L. Que, *Acc. Chem. Res.*, 2007, **40**, 493.
713 C. B. Bell, S. D. Wong, Y. M. Xiao, E. J. Klinker, A. L. Tenderholt, M. C. Smith, J. U. Rohde, L. Que, S. P. Cramer and E. I. Solomon, *Angew. Chem., Int. Ed.*, 2008, **47**, 9071.

714 N. Muresan, C. C. Lu, M. Ghosh, J. C. Peters, M. Abe, L. M. Henling, T. Weyhermoller, E. Bill and K. Wieghardt, *Inorg. Chem.*, 2008, **47**, 4579.
715 M. Radón and K. Pierloot, *J. Phys. Chem. A*, 2008, **112**, 11824.
716 N. Strickland and J. N. Harvey, *J. Phys. Chem. B*, 2007, **111**, 841.
717 M. P. Mehn, S. D. Brown, T. K. Paine, W. W. Brennessel, C. J. Cramer, J. C. Peters and L. Que, *Dalton Trans.*, 2006, 1347.
718 S. Shaik, S. P. de Visser, F. Ogliaro, H. Schwarz and D. Schröder, *Curr. Opin. Chem. Biol.*, 2002, **6**, 556.
719 A. Altun, S. Shaik and W. Thiel, *J. Am. Chem. Soc.*, 2007, **129**, 8978.
720 E. Derat, S. Shaik, C. Rovira, P. Vidossich and M. Alfonso-Prito, *J. Am. Chem. Soc.*, 2007, **129**, 6346.
721 C. Hazan, D. Kumar, S. P. de Visser and S. Shaik, *Eur. J. Inorg. Chem.*, 2007, 2966.
722 C. Li, L. Zhang, C. Zhang, H. Hirao, W. Wu and S. Shaik, *Angew. Chem., Int. Ed.*, 2007, **46**, 8168.
723 C. V. Sastri, J. Lee, K. Oh, Y. J. Lee, J. Lee, T. A. Jackson, K. Ray, H. Hirao, W. Shin, J. A. Halfen, J. Kim, L. Que, S. Shaik and W. Nam, *Proc. Natl. Acad. Sci. U. S. A.*, 2007, **104**, 19181.
724 S. Shaik, H. Hirao and D. Kumar, *Nat. Prod. Rep.*, 2007, **24**, 533.
725 Y. Wang, D. Kumar, C. L. Yang, K. L. Han and S. Shaik, *J. Phys. Chem. B*, 2007, **111**, 7700.
726 H. Chen, H. Hirao, E. Derat, I. Schlichting and S. Shaik, *J. Phys. Chem. B*, 2008, **112**, 9490.
727 H. Chen, Y. Moreau, E. Derat and S. Shaik, *J. Am. Chem. Soc.*, 2008, **130**, 1953.
728 K. B. Cho, H. Hirao, H. Chen, M. A. Carvajal, S. Cohen, E. Derat, W. Thiel and S. Shaik, *J. Phys. Chem. A*, 2008, **112**, 13128.
729 S. N. Dhuri, M. S. Seo, Y. M. Lee, H. Hirao, Y. Wang, W. Nam and S. Shaik, *Angew. Chem., Int. Ed.*, 2008, **47**, 3356.
730 H. Hirao, L. Que, W. Nam and S. Shaik, *Chem.–Eur. J.*, 2008, **14**, 1740.
731 S. Shaik, D. Kumar and S. P. de Visser, *J. Am. Chem. Soc.*, 2008, **130**, 10128.
732 D. Q. Wang, J. J. Zheng, S. Shaik and W. Thiel, *J. Phys. Chem. B*, 2008, **112**, 5126.
733 K. B. Cho, M. A. Carvajal and S. Shaik, *J. Phys. Chem. B*, 2009, **113**, 336.
734 E. J. Klinker, S. Shaik, H. Hirao and L. Que, *Angew. Chem., Int. Ed.*, 2009, **48**, 1291.
735 N. M. Reilly, J. U. Reveles, G. E. Johnson, J. M. del Campo, S. N. Khanna, A. M. Koster and A. W. Castleman, *J. Phys. Chem. C*, 2007, **111**, 19086.
736 Q. Sun, Reddy M. Marquez, P. Jena, C. Gonzalez and Q. Wang, *J. Phys. Chem. C*, 2007, **111**, 4159.
737 J. K. Schwartz, P.-p. Wei, K. H. Mitchell, B. G. Fox and E. I. Solomon, *J. Am. Chem. Soc.*, 2008, **130**, 7098.
738 D. Rinaldo, D. M. Philipp, S. J. Lippard and R. A. Friesner, *J. Am. Chem. Soc.*, 2007, **129**, 3135.
739 W. G. Han, T. Q. Liu, T. Lovell and L. Noodleman, *J. Comput. Chem.*, 2006, **27**, 1292.
740 W. G. Han and L. Noodleman, *Inorg. Chem.*, 2008, **47**, 2975.
741 W. G. Han and L. Noodleman, *Inorg. Chim. Acta*, 2008, **361**, 973.
742 M. Torrent, D. G. Musaev, H. Basch and K. Morokuma, *J. Comput. Chem.*, 2002, **23**, 59.
743 N. Mitic, M. D. Clay, L. Saleh, J. M. Bollinger and E. I. Solomon, *J. Am. Chem. Soc.*, 2007, **129**, 9049.
744 W.-G. Han, T. Liu, T. Lovell and L. Noodleman, *Inorg. Chem.*, 2006, **45**, 8533.
745 L. Noodleman and D. A. Case, *Adv. Inorg. Chem.*, 1992, **38**, 423.
746 L. Noodleman, C. Y. Peng, D. A. Case and J.-M. Mouesca, *Coord. Chem. Rev.*, 1995, **144**, 199.
747 E. Ruiz, A. Rodriguez-Fortea, J. Cano, S. Alvarez and P. Alemany, *J. Comput. Chem.*, 2003, **24**, 982.
748 R. A. Torres, T. Lovell, L. Noodleman and D. A. Case, *J. Am. Chem. Soc.*, 2003, **125**, 1923.
749 M. Shoji, K. Koizumi, Y. Kitagawa, S. Yamanaka, M. Okumura and K. Yamaguchi, *Int. J. Quantum Chem.*, 2007, **107**, 609.
750 S. Niu and T. Ichiye, *Theor. Chem. Acc.*, 2007, **117**, 275.
751 L. Noodleman, T. Lovell, T. Liu, F. Himo and R. A. Torres, *Curr. Opin. Chem. Biol.*, 2002, **6**, 259.
752 G. Moritz, M. Reiher and B. A. Hess, *Theor. Chem. Acc.*, 2005, **114**, 76.
753 K. P. Jensen, B. L. Ooi and H. E. M. Christensen, *J. Phys. Chem. A*, 2008, **112**, 12829.
754 Z. H. Li, Y. Gong, K. N. Fan and M. F. Zhou, *J. Phys. Chem. A*, 2008, **112**, 13641.
755 M. H. Baik and R. A. Friesner, *J. Phys. Chem. A*, 2002, **106**, 7407.
756 M. Uudsemaa and T. Tamm, *J. Phys. Chem. A*, 2003, **107**, 9997.
757 J. Blumberger, L. Bernasconi, I. Tavernelli, R. Vuilleumier and M. Sprik, *J. Am. Chem. Soc.*, 2004, **126**, 3928.
758 J. Blumberger and M. Sprik, *J. Phys. Chem. B*, 2004, **108**, 6529.
759 J. Blumberger, Y. Tateyama and M. Sprik, *Comput. Phys. Commun.*, 2005, **169**, 256.
760 Y. Tateyama, J. Blumberger, M. Sprik and I. Tavernelli, *J. Chem. Phys.*, 2005, **122**, 234505.
761 J. Blumberger and M. Sprik, *Theor. Chem. Acc.*, 2006, **115**, 113.
762 P. Jaque, A. V. Marenich, C. J. Cramer and D. G. Truhlar, *J. Phys. Chem. C*, 2007, **111**, 5783.
763 I. Chiorescu, D. V. Deubel, V. B. Arion and B. K. Keppler, *J. Chem. Theory Comput.*, 2008, **4**, 499.
764 P. Winget, E. J. Weber, C. J. Cramer and D. G. Truhlar, *Phys. Chem. Chem. Phys.*, 2000, **2**, 1231.
765 E. V. Patterson, C. J. Cramer and D. G. Truhlar, *J. Am. Chem. Soc.*, 2001, **123**, 2025.
766 C. Fontanesi, R. Benassi, R. Giovanardi, M. Marcaccio, F. Paolucci and S. Roffia, *J. Mol. Struct.*, 2002, **612**, 277.
767 A. Lewis, J. A. Bumpus, D. G. Truhlar and C. J. Cramer, *J. Chem. Ed.*, 2004, **81**, 596; erratum, 2007, **84**, 934.
768 P. Winget, C. J. Cramer and D. G. Truhlar, *Theor. Chem. Acc.*, 2004, **112**, 217.
769 S. Bhattacharyya, M. T. Stankovich, D. G. Truhlar and J. L. Gao, *J. Phys. Chem. A*, 2007, **111**, 5729.
770 J. L. Hodgson, M. Namazian, S. E. Bottle and M. L. Coote, *J. Phys. Chem. A*, 2007, **111**, 13595.
771 J. Moens, P. Jaque, F. De Proft and P. Geerlings, *J. Phys. Chem. A*, 2008, **112**, 6023.
772 C. Kritayakornupong and S. Hannongbua, *Chem. Phys.*, 2007, **332**, 95.
773 C. Kritayakornupong, *Chem. Phys. Lett.*, 2007, **441**, 226.
774 S. Amira, D. Spångberg, V. Zelin, M. Probst and K. Hermansson, *J. Phys. Chem. B*, 2005, **109**, 14235.
775 H. A. De Abreu, L. Guimaraes and H. A. Duarte, *J. Phys. Chem. A*, 2006, **110**, 7713.
776 D. Schröder, S. O. Souvi and E. Alikhani, *Chem. Phys. Lett.*, 2009, **470**, 162.
777 J. Moens, G. Roos, P. Jaque, F. D. Proft and P. Geerlings, *Chem.–Eur. J.*, 2007, **13**, 9331.
778 R. D. Leib, W. A. Donald, J. T. O'Brien, M. F. Bush and E. R. Williams, *J. Am. Chem. Soc.*, 2007, **129**, 7716.
779 W. A. Donald, R. D. Leib, J. T. O'Brien, M. F. Bush and E. R. Williams, *J. Am. Chem. Soc.*, 2008, **130**, 3371.
780 S. Trasatti, *Pure Appl. Chem.*, 1986, **58**, 955.
781 M. D. Tissandier, K. A. Cowen, W. Y. Feng, E. Gundlach, M. H. Cohen, A. D. Earhart, J. V. Coe and T. R. Tuttle, *J. Phys. Chem. A*, 1998, **102**, 7787.
782 D. M. Camaioni and C. A. Schwerdtfeger, *J. Phys. Chem. A*, 2005, **109**, 10795.
783 C. P. Kelly, C. J. Cramer and D. G. Truhlar, *J. Phys. Chem. B*, 2006, **110**, 16066.
784 C. P. Kelly, C. J. Cramer and D. G. Truhlar, *J. Phys. Chem. B*, 2007, **111**, 408.
785 W. R. Fawcett, *Langmuir*, 2008, **24**, 9868.
786 A. Correa and L. Cavallo, *J. Am. Chem. Soc.*, 2006, **128**, 13352.
787 C. E. Webster, *J. Am. Chem. Soc.*, 2007, **129**, 7490.
788 B. F. Straub, *Adv. Synth. Catal.*, 2007, **349**, 204.
789 Y. Zhao and D. G. Truhlar, *Org. Lett.*, 2007, **9**, 1967.
790 J. Mathew, N. Koga and C. H. Suresh, *Organometallics*, 2008, **27**, 4666.
791 D. Benitez, E. Tkatchouk and W. A. Goddard, *Chem. Commun.*, 2008, 6194.
792 R. Tonner and G. Frenking, *Chem. Commun.*, 2008, 1584.

793 Y. Zhao and D. G. Truhlar, *J. Chem. Theory Comput.*, 2009, **5**, 324.
794 D. Benitez, E. Tkatchouk and W. A. Goddard, *Organometallics*, 2009, **28**, 2643.
795 C. W. Bielawski and R. H. Grubbs, *Prog. Polym. Sci.*, 2007, **32**, 1.
796 A. C. Tsipis, A. G. Orpen and J. N. Harvey, *Dalton Trans.*, 2005, 2849.
797 M. S. Sanford, J. A. Love and R. H. Grubbs, *J. Am. Chem. Soc.*, 2001, **123**, 6543.
798 S. Torker, D. Merki and P. Chen, *J. Am. Chem. Soc.*, 2008, **130**, 4808.
799 S. Grimme, *Angew. Chem., Int. Ed.*, 2006, **45**, 4460.
800 Y. Zhao and D. G. Truhlar, *Org. Lett.*, 2006, **8**, 5753.
801 I. C. Stewart, D. Benitez, D. J. O'Leary, E. Tkatchouk, M. W. Day, W. A. Goddard and R. H. Grubbs, *J. Am. Chem. Soc.*, 2009, **131**, 1931.
802 S. Pandian, I. H. Hillier, M. A. Vincent, N. A. Burton, I. W. Ashworth, D. J. Nelson, J. M. Percy and G. Rinaudo, *Chem. Phys. Lett.*, 2009, **476**, 37.
803 N. Sieffert and M. Bühl, *Inorg. Chem.*, 2009, **48**, 4622.
804 G. F. Caramori and G. Frenking, *Organometallics*, 2007, **26**, 5815.
805 A. Krapp, K. K. Pandey and G. Frenking, *J. Am. Chem. Soc.*, 2007, **129**, 7596.
806 F. Liu, T. Cardolaccia, B. J. Hornstein, J. R. Schoonover and T. J. Meyer, *J. Am. Chem. Soc.*, 2007, **129**, 2446.
807 T. A. Betley, Y. Surendranath, M. V. Childress, G. E. Alliger, R. Fu, C. C. Cummins and D. G. Nocera, *Philos. Trans. R. Soc. London, Ser. B*, 2008, **363**, 1293.
808 T. A. Betley, Q. Wu, T. Van Voorhis and D. G. Nocera, *Inorg. Chem.*, 2008, **47**, 1849.
809 C. W. Cady, R. H. Crabtree and G. W. Brudvig, *Coord. Chem. Rev.*, 2008, **252**, 444.
810 J. L. Cape and J. K. Hurst, *J. Am. Chem. Soc.*, 2008, **130**, 827.
811 J. J. Concepcion, J. W. Jurss, J. L. Templeton and T. J. Meyer, *Proc. Natl. Acad. Sci. U. S. A.*, 2008, **105**, 17632.
812 Y. V. Geletii, B. Botar, P. Kgerler, D. A. Hillesheim, D. G. Musaev and C. L. Hill, *Angew. Chem., Int. Ed.*, 2008, **47**, 3896.
813 N. A. Ketterer, H. J. Fan, K. J. Blackmore, X. F. Yang, J. W. Ziller, M. H. Baik and A. F. Heyduk, *J. Am. Chem. Soc.*, 2008, **130**, 4364.
814 F. Liu, J. J. Concepcion, J. W. Jurss, T. Cardolaccia, J. L. Templeton and T. J. Meyer, *Inorg. Chem.*, 2008, **47**, 1727.
815 J. T. Muckerman, D. E. Polyansky, T. Wada, K. Tanaka and E. Fujita, *Inorg. Chem.*, 2008, **47**, 1787.
816 E. Poverenov, I. Efremenko, A. I. Frenkel, Y. Ben-David, L. J. W. Shimon, G. Leitus, L. Konstantinovski, J. M. L. Martin and D. Milstein, *Nature*, 2008, **455**, 1093.
817 Y. L. Pushkar, J. Yano, K. Sauer, A. Boussac and V. K. Yachandra, *Proc. Natl. Acad. Sci. U. S. A.*, 2008, **105**, 1879.
818 (*a*) I. Romero, M. Rodriguez, C. Sens, J. Mola, M. R. Kollipara, L. Francas, E. Mas-Marza, L. Escriche and A. Llobet, *Inorg. Chem.*, 2008, **47**, 1824; (*b*) F. Bozoglian, S. Romain, M. Z. Ertem, T. K. Todorova, C. Sens, J. Mola, M. Rodriguez, I. Romero, J. Benet-Buchholz, X. Fontrodona, C. J. Cramer, L. Gagliardi and A. Llobet, *J. Am. Chem. Soc.*, DOI: 10.1021/ja9036127.
819 W. M. C. Sameera and J. E. McGrady, *Dalton Trans.*, 2008, 6141.
820 J. M. Saveant, *Chem. Rev.*, 2008, **108**, 2348.
821 C. Elschenbroich, J. Six, K. Harms, G. Frenking and G. Heydenrych, *Eur. J. Inorg. Chem.*, 2008, 3303.
822 J.-P. Zhang, X. Zhou, T. Liu, F.-Q. Bai, H.-X. Zhang and A.-C. Tang, *Theor. Chem. Acc.*, 2008, **121**, 123.
823 J.-P. Zhang, X. Zhou, F.-Q. Bai, H.-X. Zhang and A.-C. Tang, *Theor. Chem. Acc.*, 2009, **122**, 31.
824 *Vitamin B_{12} and B_{12}-Proteins*, ed. B. Kräutler, D. Arigoni and B. T. Golding, Wiley-VCH, Berlin, 1998.
825 G. Glod, W. Angst, C. Holliger and R. P. Schwarzenbach, *Environ. Sci. Technol.*, 1997, **31**, 253.
826 A. D. Follett, K. A. McNabb, A. A. Peterson, J. D. Scanlon, C. J. Cramer and K. McNeill, *Inorg. Chem.*, 2007, **46**, 1645.
827 D. A. Pratt and W. A. van der Donk, *J. Am. Chem. Soc.*, 2005, **127**, 384.
828 R. L. Birke, Q. Huang, T. Spataru and D. K. Gosser, *J. Am. Chem. Soc.*, 2006, **128**, 1922.
829 K. P. Jensen and U. Ryde, *J. Phys. Chem. A*, 2003, **107**, 7539.
830 K. P. Jensen and U. Ryde, *Coord. Chem. Rev.*, 2009, **253**, 769.
831 P. Morschel, J. Janikowski, G. Hilt and G. Frenking, *J. Am. Chem. Soc.*, 2008, **130**, 8952.
832 K.-W. Huang, J. H. Han, C. B. Musgrave and E. Fujita, *Organometallics*, 2007, **26**, 508.
833 Z. Hu and R. J. Boyd, *J. Chem. Phys.*, 2000, **113**, 9393.
834 J. M. Praetorius, D. P. Allen, R. Y. Wang, J. D. Webb, F. Grein, P. Kennepohl and C. M. Crudden, *J. Am. Chem. Soc.*, 2008, **130**, 3724.
835 P. Mauleon, I. Alonso, M. R. Rivero and J. C. Carretero, *J. Org. Chem.*, 2007, **72**, 9924.
836 P. Fristrup, M. Kreis, A. Palmelund, P.-O. Norrby and R. Madsen, *J. Am. Chem. Soc.*, 2008, **130**, 5206.
837 P. Liu, P. H.-Y. Cheong, Z.-X. Yu, P. A. Wender and K. N. Houk, *Angew. Chem., Int. Ed.*, 2008, **47**, 3939.
838 L. Orian, W.-J. v. Zeist and F. M. Bickelhaupt, *Organometallics*, 2008, **27**, 4028.
839 Q. Zhao, T. Cao, F. Li, X. Li, H. Jing, T. Yi and C. Huang, *Organometallics*, 2007, **26**, 2077.
840 D. Di Censo, S. Fantacci, F. De Angelis, C. Klein, N. Evans, K. Kalyanasundaram, H. J. Bolink, M. Gratzel and M. K. Nazeeruddin, *Inorg. Chem.*, 2008, **47**, 980.
841 T. Liu, B.-H. Xia, X. Zhou, H.-X. Zhang, Q.-J. Pan and J.-S. Gao, *Organometallics*, 2007, **26**, 143.
842 S. J. Lee, K.-M. Park, K. Yang and Y. Kang, *Inorg. Chem.*, 2009, **48**, 1030.
843 T. Liu, B.-H. Xia, X. Zhou, Q.-C. Zheng, Q.-J. Pan and H.-X. Zhang, *Theor. Chem. Acc.*, 2008, **121**, 155.
844 M. Kimura and Y. Uozumi, *J. Org. Chem.*, 2007, **72**, 707.
845 E. Calimano and T. D. Tilley, *J. Am. Chem. Soc.*, 2008, **130**, 9226.
846 D. H. Ess, S. M. Bischof, J. Oxgaard, R. A. Periana and W. A. Goddard, *Organometallics*, 2008, **27**, 6440.
847 R. Ghosh, T. J. Emge, K. Krogh-Jespersen and A. S. Goldman, *J. Am. Chem. Soc.*, 2008, **130**, 11317.
848 N. Marom and L. Kronik, *Appl. Phys. A: Mater. Sci. Process.*, 2009, **95**, 159.
849 P. Calaminici, *J. Chem. Phys.*, 2008, **128**, 164317.
850 G. L. Arvizu and P. Calaminici, *J. Chem. Phys.*, 2007, **126**, 194102.
851 M. Shoji, K. Koizumi, T. Hamamoto, Y. Kitagawa, S. Yamanaka, M. Okumura and K. Yamaguchi, *Chem. Phys. Lett.*, 2006, **421**, 483.
852 M. Shoji, Y. Kitagawa, T. Kawakami, S. Yamanaka, M. Okumura and K. Yamaguchi, *J. Phys. Chem. A*, 2008, **112**, 4020.
853 J. Conradie, T. Wondimagegn and A. Ghosh, *J. Phys. Chem. B*, 2008, **112**, 1053.
854 S. Kozuch, C. Amatore, A. Jutand and S. Shaik, *Organometallics*, 2005, **24**, 2319.
855 G. T. de Jong and F. M. Bickelhaupt, *ChemPhysChem*, 2007, **8**, 1170.
856 F. Viñes, F. Illas and K. M. Neyman, *J. Phys. Chem. A*, 2008, **112**, 8911.
857 F. Viñes, F. Illas and K. M. Neyman, *Angew. Chem., Int. Ed.*, 2007, **46**, 7094.
858 Z. Shi, S. Wu and J. A. Szpunar, *Nanotechnology*, 2006, **17**, 2161.
859 A. Betz, L. Yu, M. Reiher, A.-C. Gaumont, P.-A. Jaffres and M. Gulea, *J. Organomet. Chem.*, 2008, **693**, 2499.
860 C. Y. Legault, Y. Garcia, C. A. Merlic and K. N. Houk, *J. Am. Chem. Soc.*, 2007, **129**, 12664.
861 F. E. Hahn, *Angew. Chem., Int. Ed.*, 2006, **45**, 1348.
862 F. E. Hahn and M. C. Jahnke, *Angew. Chem., Int. Ed.*, 2008, **47**, 3122.
863 U. Radius and F. M. Bickelhaupt, *Organometallics*, 2008, **27**, 3410.
864 T. Ziegler and A. Rauk, *Inorg. Chem.*, 1979, **18**, 1755.
865 L. Gagliardi and C. J. Cramer, *Inorg. Chem.*, 2006, **45**, 9442.

866 H. Nakai, X. Hu, L. N. Zakharov, A. L. Rheingold and K. Meyer, *Inorg. Chem.*, 2004, **43**, 855.
867 H. Jacobsen, A. Correa, A. Poater, C. Costabile and L. Cavallo, *Coord. Chem. Rev.*, 2009, **253**, 687.
868 U. Radius and F. M. Bickelhaupt, *Coord. Chem. Rev.*, 2009, **253**, 678.
869 R. Tonner, G. Heydenrych and G. Frenking, *Chem.–Asian J.*, 2007, **2**, 1555.
870 J. Harmer, C. Finazzo, R. Piskorski, S. Ebner, E. C. Duin, M. Goenrich, R. K. Thauer, M. Reiher, A. Schweiger, D. Hinderberger and B. Jaun, *J. Am. Chem. Soc.*, 2008, **130**, 10907.
871 N. Yang, M. Reiher, M. Wang, J. Harmer and E. C. Duin, *J. Am. Chem. Soc.*, 2007, **129**, 11028.
872 G. T. de Jong and F. M. Bickelhaupt, *J. Chem. Theory Comput.*, 2007, **3**, 514.
873 R. Fazaeli, A. Ariafard, S. Jamshidi, E. S. Tabatabaie and K. A. Pishro, *J. Organomet. Chem.*, 2007, **692**, 3984.
874 A. Ariafard and B. F. Yates, *J. Organomet. Chem.*, 2009, **694**, 2075.
875 V. P. Ananikov, D. G. Musaev and K. Morokuma, *Eur. J. Inorg. Chem.*, 2007, 5390.
876 R. D. Adams, B. Captain, C. Beddie and M. B. Hall, *J. Am. Chem. Soc.*, 2007, **129**, 986.
877 A. K. Rappé, C. J. Casewit, K. S. Colwell, W. A. Goddard and W. M. Skiff, *J. Am. Chem. Soc.*, 1992, **114**, 10024.
878 J. Raber, C. B. Zhu and L. A. Eriksson, *J. Phys. Chem. B*, 2005, **109**, 11006.
879 D. V. Deubel, *J. Am. Chem. Soc.*, 2006, **128**, 1654.
880 J. K. C. Lau and D. V. Deubel, *J. Chem. Theory Comput.*, 2006, **2**, 103.
881 T. Song and P. Hu, *J. Chem. Phys.*, 2006, **125**, 091101.
882 Y. Mantri, S. J. Lippard and M. H. Baik, *J. Am. Chem. Soc.*, 2007, **129**, 5023.
883 T. Matsui, Y. Shigeta and K. Hirao, *J. Phys. Chem. B*, 2007, **111**, 1176.
884 S. P. Oldfield, M. D. Hall and J. A. Platts, *J. Med. Chem.*, 2007, **50**, 5227.
885 S. M. Fiuza, A. M. Amado, M. P. M. Marques and L. A. E. Batista de Carvalho, *J. Phys. Chem. A*, 2008, **112**, 3253.
886 P. D. Dans, A. Crespo, D. o. A. Estrin and E. L. Coitiño, *J. Chem. Theory Comput.*, 2008, **4**, 740.
887 T. van der Wijst, C. Fonseca Guerra, M. Swart, F. M. Bickelhaupt and B. Lippert, *Chem.–Eur. J.*, 2009, **15**, 209.
888 A. Datta, D. A. Hrovat and W. T. Borden, *J. Am. Chem. Soc.*, 2008, **130**, 2726.
889 J. Espinosa-García, J. C. Corchado and D. G. Truhlar, *J. Am. Chem. Soc.*, 1997, **119**, 9891.
890 R. J. Mishur, C. Zheng, T. M. Gilbert and R. N. Bose, *Inorg. Chem.*, 2008, **47**, 7972.
891 Y. Mo and E. Kaxiras, *Small*, 2007, **3**, 1253.
892 A. Roldán, F. Viñes, F. Illas, J. Ricart and K. Neyman, *Theor. Chem. Acc.*, 2008, **120**, 565.
893 P. Calaminici, A. M. Koster and Z. Gomez-Sandoval, *J. Chem. Theory Comput.*, 2007, **3**, 905.
894 K. Jug, B. Zimmermann, P. Calaminici and A. M. Koster, *J. Chem. Phys.*, 2002, **116**, 4497.
895 D. G. Leopold, J. Ho and W. C. Lineberger, *J. Chem. Phys.*, 1987, **86**, 1715.
896 J. U. Reveles and A. M. Köster, *J. Comput. Chem.*, 2004, **25**, 1109.
897 F.-Q. Shi, X. Li, Y. Xia, L. Zhang and Z.-X. Yu, *J. Am. Chem. Soc.*, 2007, **129**, 15503.
898 H. Garcia, http://pubs.acs.org/JACSbeta/jvi/issue3.html. Accessed October 12, 2009.
899 P. Pyykkö, *Inorg. Chim. Acta*, 2005, **358**, 4113.
900 P. Pyykkö, *Chem. Soc. Rev.*, 2008, **37**, 1967.
901 F. Furche, R. Ahlrichs, P. Weis, C. Jacob, S. Gilb, T. Bierweiler and M. M. Kappes, *J. Chem. Phys.*, 2002, **117**, 6982.
902 H. Hakkinen, B. Yoon, U. Landman, X. Li, H.-J. Zhai and L.-S. Wang, *J. Phys. Chem. A*, 2003, **107**, 6168.
903 X. Xing, B. Yoon, U. Landman and J. H. Parks, *Phys. Rev. B: Condens. Matter Mater. Phys.*, 2006, **74**, 165423.
904 M. P. Johansson, A. Lechtken, D. Schooss, M. M. Kappes and F. Furche, *Phys. Rev. A: At., Mol., Opt. Phys.*, 2008, **77**, 053202.
905 V. N. Staroverov, G. E. Scuseria, J. Tao and J. P. Perdew, *Phys. Rev. B: Condens. Matter Mater. Phys.*, 2004, **69**, 075102.
906 R. M. Olson, S. Varganov, M. S. Gordon, H. Metiu, S. Chretien, P. Piecuch, K. Kowalski, S. A. Kucharski and M. Musial, *J. Am. Chem. Soc.*, 2005, **127**, 1049.
907 M. Mantina, R. Valero and D. G. Truhlar, *J. Chem. Phys.*, 2009, **131**, 064706.
908 L. Ferrighi, B. Hammer and G. K. H. Madsen, *J. Am. Chem. Soc.*, 2009, **131**, 10605.
909 L. Xiao and L. Wang, *Chem. Phys. Lett.*, 2004, **392**, 452.
910 L. Barrio, P. Liu, J. A. Rodriguez, J. M. Campos-Martin and J. L. G. Fierro, *J. Chem. Phys.*, 2006, **125**, 164715.
911 B. Yoon, P. Koskinen, B. Huber, O. Kostko, B. v. Issendorff, H. Häkkinen, M. Moseler and U. Landman, *ChemPhysChem*, 2007, **8**, 157.
912 E. S. Kryachko and F. Remacle, *Int. J. Quantum Chem.*, 2007, **107**, 2922.
913 M. Sterrer, T. Risse, U. M. Pozzoni, L. Giordano, M. Heyde, H.-P. Rust, G. Pacchioni and H.-J. Freund, *Phys. Rev. Lett.*, 2007, **98**, 096107.
914 S. Bulusu, X. Li, L.-S. Wang and X. C. Zeng, *J. Phys. Chem. C*, 2007, **111**, 4190.
915 W. Fa and J. Dong, *J. Chem. Phys.*, 2006, **124**, 114310.
916 A. Lechtken, D. Schooss, J. R. Stairs, M. N. Blom, F. Furche, N. Morgner, O. Kostko, B. v. Issendorff and M. M. Kappes, *Angew. Chem., Int. Ed.*, 2007, **46**, 2944.
917 X. Gu, S. Bulusu, X. Li, X. C. Zeng, J. Li, X. G. Gong and L.-S. Wang, *J. Phys. Chem. C*, 2007, **111**, 8228.
918 J. Li, X. Li, H.-J. Zhai and L.-S. Wang, *Science*, 2003, **299**, 864.
919 S. Bulusu, X. Li, L.-S. Wang and X. C. Zeng, *Proc. Natl. Acad. Sci. U. S. A.*, 2006, **103**, 8326.
920 W. Huang, S. Bulusu, R. Pal, X. C. Zeng and L.-S. Wang, *ACS Nano*, 2009, **3**, 1225.
921 D. Y. Zubarev and A. I. Boldyrev, *J. Phys. Chem. A*, 2009, **113**, 866.
922 M. B. Torres, E. M. Fernández and L. C. Balbás, *J. Phys. Chem. A*, 2008, **112**, 6678.
923 A. Prestianni, A. Martorana, F. Labat, I. Ciofini and C. Adamo, *J. Phys. Chem. B*, 2006, **110**, 12240.
924 A. Prestianni, A. Martorana, I. Ciofini, F. Labat and C. Adamo, *J. Phys. Chem. C*, 2008, **112**, 18061.
925 A. Prestianni, A. Martorana, F. Labat, I. Ciofini and C. Adamo, *THEOCHEM*, 2009, **903**, 34.
926 S. Chretien, M. S. Gordon and H. Metiu, *J. Chem. Phys.*, 2004, **121**, 3756.
927 S. Chretien, M. S. Gordon and H. Metiu, *J. Chem. Phys.*, 2004, **121**, 9931.
928 Z. H. Li, A. W. Jasper and D. G. Truhlar, *J. Am. Chem. Soc.*, 2007, **129**, 14899.
929 J. Botticelli, R. Fournier and M. Zhang, *Theor. Chem. Acc.*, 2008, **120**, 583.
930 S. Chretien and H. Metiu, *J. Chem. Phys.*, 2007, **127**, 084704.
931 M. Nolan, V. S. Verdugo and H. Metiu, *Surf. Sci.*, 2008, **602**, 2734.
932 H. Y. Kim, H. M. Lee, R. G. S. Pala, V. Shapovalov and H. Metiu, *J. Phys. Chem. C*, 2008, **112**, 12398.
933 N. Lopez, T. V. W. Janssens, B. S. Clausen, Y. Xu, M. Mavrikakis, T. Bligaard and J. K. Nørskov, *J. Catal.*, 2004, **223**, 232; T. Janssens, B. Clausen, B. Hvolbæk, H. Falsig, C. Christensen, T. Bligaard and J. Nørskov, *Top. Catal.*, 2007, **44**, 15.
934 Y. Chen, P. Hu, M.-H. Lee and H. Wang, *Surf. Sci.*, 2008, **602**, 1736.
935 A. A. Rusakov, E. Rykova, G. E. Scuseria and A. Zaitsevskii, *J. Chem. Phys.*, 2007, **127**, 164322.
936 J. S. Golightly, L. Gao, A. W. Castleman, D. E. Bergeron, J. W. Hudgens, R. J. Magyar and C. A. Gonzalez, *J. Phys. Chem. C*, 2007, **111**, 14625.
937 N. R. M. Crawford, C. Schrodt, A. Rothenberger, W. Shi and R. Ahlrichs, *Chem.–Eur. J.*, 2008, **14**, 319.
938 Y. Li, G. Galli and F. o. Gygi, *ACS Nano*, 2008, **2**, 1896.
939 E. A. Lewis and W. B. Tolman, *Chem. Rev.*, 2004, **104**, 1047.
940 S. Itoh, *Curr. Opin. Chem. Biol.*, 2006, **10**, 115.
941 M. Rolff and F. Tuczek, *Angew. Chem., Int. Ed.*, 2008, **47**, 2344.

942 B. F. Gherman and C. J. Cramer, *Coord. Chem. Rev.*, 2009, **253**, 723.
943 T. Punniyamurthy, S. Velusamy and J. Iqbal, *Chem. Rev.*, 2005, **105**, 2329.
944 B. Isabel, M. A. Carrondo and F. L. Peter, *JBIC, J. Biol. Inorg. Chem.*, 2006, **11**, 539.
945 J. P. Klinman, *J. Biol. Chem.*, 2006, **281**, 3013.
946 J. M. Bollinger and C. Krebs, *Curr. Opin. Chem. Biol.*, 2007, **11**, 151.
947 M. Güell, J. M. Luis, L. Rodriguez-Santiago, M. Sodupe and M. Solà, *J. Phys. Chem. A*, 2009, **113**, 1308.
948 J.-y. Hasegawa, K. Pierloot and B. O. Roos, *Chem. Phys. Lett.*, 2001, **335**, 503.
949 C. J. Cramer, J. R. Gour, A. Kinal, M. Wtoch, P. Piecuch, A. R. Moughal Shahi and L. Gagliardi, *J. Phys. Chem. A*, 2008, **112**, 3754.
950 P. Piecuch and M. Włoch, *J. Chem. Phys.*, 2005, **123**, 224105.
951 P. Piecuch, M. Włoch, J. R. Gour and A. Kinal, *Chem. Phys. Lett.*, 2006, **418**, 467.
952 M. Włoch, M. Lodriguito, P. Piecuch and J. R. Gour, *Mol. Phys.*, 2006, **104**, 2149.
953 M. Włoch, J. R. Gour and P. Piecuch, *J. Phys. Chem. A*, 2007, **111**, 11359.
954 K. Andersson, P.-Å. Malmqvist, B. O. Roos, A. J. Sadlej and K. Wolinski, *J. Phys. Chem.*, 1990, **94**, 5483.
955 M. Schatz, V. Raab, S. P. Foxon, G. Brehm, S. Schneider, M. Reiher, M. C. Holthausen, J. Sundermeyer and S. Schindler, *Angew. Chem., Int. Ed.*, 2004, **43**, 4360.
956 C. Wurtele, E. Gaoutchenova, K. Harms, M. C. Holthausen, J. Sundermeyer and S. Schindler, *Angew. Chem., Int. Ed.*, 2006, **45**, 3867.
957 A. De La Lande, H. Gerard and O. Parisel, *Int. J. Quantum Chem.*, 2008, **108**, 1898.
958 B. F. Gherman, D. E. Heppner, W. B. Tolman and C. J. Cramer, *JBIC, J. Biol. Inorg. Chem.*, 2006, **11**, 197.
959 N. W. Aboelella, B. F. Gherman, L. M. R. Hill, J. T. York, N. Holm, V. G. Young, C. J. Cramer and W. B. Tolman, *J. Am. Chem. Soc.*, 2006, **128**, 3445.
960 B. F. Gherman, W. B. Tolman and C. J. Cramer, *J. Comput. Chem.*, 2006, **27**, 1950.
961 L. M. R. Hill, B. F. Gherman, N. W. Aboelella, C. J. Cramer and W. B. Tolman, *Dalton Trans.*, 2006, 4944.
962 D. E. Heppner, B. F. Gherman, W. B. Tolman and C. J. Cramer, *Dalton Trans.*, 2006, 4773.
963 S. Hong, S. M. Huber, L. Gagliardi, C. J. Cramer and W. B. Tolman, *J. Am. Chem. Soc.*, 2007, **129**, 14190.
964 S. M. Huber, A. R. Moughal Shahi, F. Aquilante, C. J. Cramer and L. Gagliardi, *J. Chem. Theory Comput.*, DOI: 10.1021/ct900282m.
965 P. Comba, S. Knoppe, B. Martin, G. Rajaraman, C. Rolli, B. Shapiro and T. Stork, *Chem.–Eur. J.*, 2008, **14**, 344.
966 K. Yoshizawa and Y. Shiota, *J. Am. Chem. Soc.*, 2006, **128**, 9873.
967 P. Comba, C. L. Lang, C. L. de Laorden, A. Muruganantham, G. Rajaraman, H. Wadepold and M. Zajaczkowski, *Chem.–Eur. J.*, 2008, **14**, 5313.
968 C. J. Cramer, B. A. Smith and W. B. Tolman, *J. Am. Chem. Soc.*, 1996, **118**, 11283.
969 M. Flock and K. Pierloot, *J. Phys. Chem. A*, 1999, **103**, 95.
970 O. Sander, A. Henss, C. Nather, C. Wurtele, M. C. Holthausen, S. Schindler and F. Tuczek, *Chem.–Eur. J.*, 2008, **14**, 9714.
971 T. Osako, S. Nagatomo, T. Kitagawa, C. J. Cramer and S. Itoh, *JBIC, J. Biol. Inorg. Chem.*, 2005, **10**, 581.
972 W. Ghattas, M. Giorgi, Y. Mekmouche, T. Tanaka, A. Rockenbauer, M. Reglier, Y. Hitomi and A. J. Simaan, *Inorg. Chem.*, 2008, **47**, 4627.
973 A. Kunishita, J. D. Scanlon, H. Ishimaru, K. Honda, T. Ogura, M. Suzuki, C. J. Cramer and S. Itoh, *Inorg. Chem.*, 2008, **47**, 8222.
974 G. Periyasamy, M. Sundararajan, I. H. Hillier, N. A. Burton and J. J. W. McDouall, *Phys. Chem. Chem. Phys.*, 2007, **9**, 2498.
975 J. P. Holland, P. J. Barnard, D. Collison, J. R. Dilworth, R. Edge, J. C. Green, J. M. Heslop, E. J. L. McInnes, C. G. Salzmann and A. L. Thompson, *Eur. J. Inorg. Chem.*, 2008, 3549.
976 R. R. Nazmutdinov, N. V. Roznyatovskaya, D. V. Glukhov, I. Manyurov, V. M. Mazin, G. A. Tsirlina and M. Probst, *Inorg. Chem.*, 2008, **47**, 6659.
977 J. U. Reveles, P. Calaminici, M. R. Beltran, A. M. Koster and S. N. Khanna, *J. Am. Chem. Soc.*, 2007, **129**, 15565.
978 P. H.-Y. Cheong, P. Morganelli, M. R. Luzung, K. N. Houk and F. D. Toste, *J. Am. Chem. Soc.*, 2008, **130**, 4517.
979 E. Soriano and J. Marco-Contelles, *Acc. Chem. Res.*, 2009, **42**, 1026.
980 M. Mantina and D. G. Truhlar, 2009, unpublished calculations.
981 J. Carrasco, F. Illas and S. T. Bromley, *Phys. Rev. Lett.*, 2007, **99**, 235502.
982 T. Cadenbach, T. Bollermann, C. Gemel, I. Fernandez, M. von Hopffgarten, G. Frenking and R. A. Fischer, *Angew. Chem., Int. Ed.*, 2008, **47**, 9150.
983 L. Bernasconi, E. J. Baerends and M. Sprik, *J. Phys. Chem. B*, 2006, **110**, 11444.
984 Y. Dai and E. Blaisten-Barojas, *J. Phys. Chem. A*, 2008, **112**, 11052.
985 K. Iokibe, K. Azumi and H. Tachikawa, *J. Phys. Chem. C*, 2007, **111**, 13510.
986 H. Tachikawa, K. Iokibe, K. Azumi and H. Kawabata, *Phys. Chem. Chem. Phys.*, 2007, **9**, 3978.
987 H. J. Flad, F. Schautz, Y. X. Wang, M. Dolg and A. Savin, *Eur. Phys. J. D*, 1999, **6**, 243.
988 A. Suwattanamala, A. Magalhães and J. Gomes, *Theor. Chem. Acc.*, 2007, **117**, 431.
989 Z. Lu, L. Wen, Z. Ni, Y. Li, H. Zhu and Q. Meng, *Cryst. Growth Des.*, 2007, **7**, 268.
990 P. Fernández, A. Sousa-Pedrares, J. Romero, J. A. García-Vázquez, A. Sousa and P. Pérez-Lourido, *Inorg. Chem.*, 2008, **47**, 2121.
991 Z. Zhu, M. Brynda, R. J. Wright, R. C. Fischer, W. A. Merrill, E. Rivard, R. Wolf, J. C. Fettinger, M. M. Olmstead and P. P. Power, *J. Am. Chem. Soc.*, 2007, **129**, 10847.
992 J. G. Wiederhold, C. J. Cramer, K. Daniel, I. Infante, B. Bourdon and R. Kretzschmar, *Geochim. Cosmochim. Acta*, 2009, **73**, A1438.
993 C. M. Rignanese, *J. Phys.: Condens. Matter*, 2005, **17**, R357.
994 W. E. Pickett, *Comments Solid State Phys.*, 1985, **12**, 1.
995 K. B. Hathaway, H. J. F. Jansen and A. J. Freeman, *Phys. Rev. B: Condens. Matter Mater. Phys.*, 1985, **31**, 7603.
996 A. García, C. Elsässer, J. Zhu, S. G. Louie and M. L. Cohen, *Phys. Rev. B: Condens. Matter Mater. Phys.*, 1992, **46**, 9829.
997 S. Kurth, J. P. Perdew and P. Blaha, *Int. J. QuantumChem.*, 1999, **75**, 889.
998 B. Grabowski, T. Hickel and J. Neugebauer, *Phys. Rev. B: Condens. Matter Mater. Phys.*, 2007, **76**, 024309.
999 J. Heyd, J. E. Peralta, G. E. Scuseria and R. L. Martin, *J. Chem. Phys.*, 2005, **123**, 174101.
1000 S. Piskunov, E. Heifets, R. I. Eglitis and G. Borstel, *Comput. Mater. Sci.*, 2004, **29**, 165.
1001 P. Baettig, C. F. Schelle, R. LeSar, U. V. Waghmare and N. A. Spaldin, *Chem. Mater.*, 2005, **17**, 1376.
1002 S. M. Hosseini, T. Movlasooy and A. Kompany, *Phys. B*, 2007, **391**, 316.
1003 C. M. S. Gannarelli, D. Alfé and M. J. Gillan, *Phys. Earth Planet. Interiors*, 2005, **152**, 67.
1004 D. F. Johnson and E. A. Carter, *J. Chem. Phys.*, 2008, **128**, 104703.
1005 T. Sun, K. Umemoto, Z. Wu, J.-C. Zheng and R. M. Wentzcovitch, *Phys. Rev. B: Condens. Matter Mater. Phys.*, 2008, **78**, 024304.
1006 Z. H. Li, D. Bhatt, N. E. Schultz, J. I. Siepmann and D. G. Truhlar, *J. Phys. Chem. C*, 2007, **111**, 16227.
1007 A. F. Izmaylov and G. E. Scuseria, *J. Chem. Phys.*, 2008, **129**, 034101; E. N. Brothers, A. F. Izmaylov, J. O. Normand, V. Barone and G. E. Scuseria, *J. Chem. Phys.*, 2008, **129**, 11102.
1008 V. Fiorentini and A. Baldereschi, *Phys. Rev. B: Condens. Matter Mater. Phys.*, 1995, **51**, 17196.
1009 K. Xiong, J. Robertson and S. J. Clark, *J. Appl. Phys.*, 2007, **102**, 083701.
1010 N. D. Mermin, *Phys. Rev.*, 1965, **137**, A1441.
1011 E. I. Isaev, N. V. Skorodumova, R. Ahuja, Y. K. Vekilov and B. Johansson, *Proc. Natl. Acad. Sci. U. S. A.*, 2007, **104**, 9168.

1012 K. Umemoto, R. M. Wentzcovitch, Y. G. Yu and R. Requist, *Earth Planet. Sci. Lett.*, 2008, **276**, 198.
1013 J. Uddin and G. E. Scuseria, *Phys. Rev. B: Condens. Matter Mater. Phys.*, 2006, **74**, 245115.
1014 Y. Zhao and D. G. Truhlar, *J. Chem. Phys.*, 2009, **130**, 074103.
1015 A. Filippetti, N. A. Spaldin and S. Sanvito, *Chem. Phys.*, 2005, **309**, 59.
1016 M. Peressi, A. Debernardi, S. Picozzi, F. Antoniella and A. Continenza, *Comput. Mater. Sci.*, 2005, **33**, 125.
1017 C. Tablero, *Phys. Rev. B: Condens. Matter Mater. Phys.*, 2005, **72**, 035213.
1018 P. Boguslawski and J. Bernholc, *Phys. Rev. B: Condens. Matter Mater. Phys.*, 2005, **72**, 115208.
1019 T. Jungwirth, J. Sinova, J. Masek, J. Kucera and A. H. MacDonald, *Rev. Mod. Phys.*, 2006, **78**, 809.
1020 C. Tablero, *J. Chem. Phys.*, 2007, **126**, 164703.
1021 X. Y. Cui, B. Delley, A. J. Freeman and C. Stampfl, *Phys. Rev. B: Condens. Matter Mater. Phys.*, 2007, **76**, 045201.
1022 J. A. Chan, J. Z. Liu, H. Raebiger, S. Lany and A. Zunger, *Phys. Rev. B: Condens. Matter Mater. Phys.*, 2008, **78**, 184109.
1023 A. Filippetti and V. Fiorentini, *J. Magn. Magn. Mater.*, 2007, **310**, 1648.
1024 J. Liu and Q. Ge, *J. Phys. Chem. B*, 2006, **110**, 25863.
1025 J. Liu and Q. Ge, *J. Alloys Compd.*, 2007, **446–447**, 267.
1026 P. Romaniello and P. L. de Boeij, *J. Chem. Phys.*, 2005, **122**, 164303.
1027 J. A. Berger, P. Romaniello, R. van Leeuwen and P. L. de Boeij, *Phys. Rev. B: Condens. Matter Mater. Phys.*, 2006, **74**, 245117.
1028 C. Leighton, M. Manno, A. Cady, J. W. Freeland, L. Wang, K. Umemoto, R. M. Wentzcovitch, T. Chen, C. L. Chien, P. L. Kuhns, M. J. R. Hoch, A. P. Reyes, W. G. Moulton, E. D. Dahlberg, J. Checkelsky and J. Eckert, *J. Phys.: Condens. Matter*, 2007, **19**, 315219.
1029 T. Kawakami, Y. Tsujimoto, H. Kageyama, X.-Q. Chen, C. L. Fu, C. Tassel, A. Kitada, S. Suto, K. Hirama, Y. Sekiya, Y. Makino, T. Okada, T. Yagi, N. Hayashi, K. Yoshimura, S. Nasu, R. Podloucky and M. Takano, *Nat. Chem.*, 2009, **1**, 371.
1030 M.-H. Whangbo and J. Köhler, *Nat. Chem.*, 2009, **1**, 351.
1031 R. J. Magyar, V. Mujica, M. Marquez and C. Gonzalez, *Phys. Rev. B: Condens. Matter Mater. Phys.*, 2007, **75**, 144421.
1032 C. Gonzalez, Y. Simon-Manso, M. Marquez and V. Mujica, *J. Phys. Chem. B*, 2006, **110**, 687.
1033 H. Wende, M. Bernien, J. Luo, C. Sorg, N. Ponpandian, J. Kurde, J. Miguel, M. Piantek, X. Xu, P. Eckhold, W. Kuch, K. Baberschke, P. M. Panchmatia, B. Sanyal, P. M. Oppeneer and O. Eriksson, *Nat. Mater.*, 2007, **6**, 516.
1034 A. Bilic, J. R. Reimers, N. S. Hush, R. C. Hoft and M. J. Ford, *J. Chem. Theory Comput.*, 2006, **2**, 1093.
1035 P. F. Cafe, A. G. Larsen, W. Yang, A. Bilic, I. M. Blake, M. J. Crossley, J. Zhang, H. Wackerbarth, J. Ulstrup and J. R. Reimers, *J. Phys. Chem. C*, 2007, **111**, 17285.
1036 W. Ma and Y. Fang, *J. Nanopart. Res.*, 2006, **8**, 761.
1037 K. M. Neyman, C. Inntam, V. A. Nasluzov, R. Kosarev and N. Rösch, *Appl. Phys. A: Mater. Sci. Process.*, 2004, **78**, 823.
1038 C. Inntam, L. V. Moskaleva, K. M. Neyman, V. A. Nasluzov and N. Rösch, *Appl. Phys. A: Mater. Sci. Process.*, 2006, **82**, 181.
1039 C. Inntam, L. V. Moskaleva, I. V. Yudanov, K. M. Neyman and N. Rösch, *Chem. Phys. Lett.*, 2006, **417**, 515.
1040 K. M. Neyman, C. Inntam, L. V. Moskaleva and N. Rösch, *Chem.–Eur. J.*, 2007, **13**, 277.
1041 S. I. Bosko, L. V. Moskaleva, A. V. Matveev and N. Rösch, *J. Phys. Chem. A*, 2007, **111**, 6870.
1042 E. Florez, F. Mondragón, T. N. Truong and P. Fuentealba, *Surf. Sci.*, 2007, **601**, 656.
1043 G. Bacaro and A. Fortunelli, *New J. Phys.*, 2007, **9**, 22.
1044 V. Bonacic-Koutecky, C. Bürgel, L. Kronik, A. E. Kuznetsov and R. Mintric, *Eur. Phys. J. D*, 2007, **45**, 471.
1045 M. Sterrer, T. Risse, L. Giordano, M. Heyde, N. Nilius, H.-P. Rust, G. Pacchioni and H.-J. Freund, *Angew. Chem., Int. Ed.*, 2007, **46**, 8703.
1046 R. Caballero, C. Quintanar, A. M. Köster, S. N. Khanna and J. U. Reveles, *J. Phys. Chem. C*, 2008, **112**, 14919.
1047 E. Florez, F. Mondragón, P. Fuentealba and F. Illas, *Phys. Rev. B: Condens. Matter Mater. Phys.*, 2008, **78**, 075426.
1048 B. Hinnemann and E. A. Carter, *J. Phys. Chem. C*, 2007, **111**, 7105.
1049 A. Michaelides, K. Reuter and M. Scheffler, *J. Vac. Sci. Technol., A*, 2005, **23**, 1487.
1050 J. L. C. Fajín, M. N. l. D. S. Cordeiro and J. R. B. Gomes, *Surf. Sci.*, 2008, **602**, 424.
1051 C. Stampfl, A. Soon, S. Piccinin, H. Shi and H. Zhang, *J. Phys.: Condens. Matter*, 2008, **20**, 184021.
1052 B. Akdim, S. Hussain and R. Pachter, in *Lecture Notes in Computer Science (Computational Science—ICCS 2008, Part II)*, Springer-Verlag, Berlin, 2008, vol. 5102, p. 353.
1053 H. Zhang, A. Soon, B. Delley and C. Stampfl, *Phys. Rev. B: Condens. Matter Mater. Phys.*, 2008, **78**, 045436.
1054 P. Kaghazchi, F. C. Simeone, K. A. Suliman, L. A. Kibler and T. Jacob, *Faraday Discuss.*, 2009, **140**, 69.
1055 Y. Han, C.-j. Liu and Q. Ge, *J. Phys. Chem. B*, 2006, **110**, 7463.
1056 Y. Han, C.-j. Liu and Q. Ge, *J. Phys. Chem. C*, 2007, **111**, 16397.
1057 S. Xia, G. Pan, Z.-L. Cai, Y. Wang and J. R. Reimers, *J. Phys. Chem. C*, 2007, **111**, 10427.
1058 V. A. Ranea, A. Michaelides, R. Ramírez, P. L. de Andres, J. A. Vergés and D. A. King, *Phys. Rev. Lett.*, 2004, **92**, 136104.
1059 L. Xu, G. Henkelman, C. T. Campbell and H. Jónsson, *Surf. Sci.*, 2006, **600**, 1351.
1060 P. J. Feibelman, B. Hammer, J. K. Nørskov, F. Wagner, M. Scheffler, R. Stumpf, R. Watwe and J. Dumesic, *J. Phys. Chem. B*, 2001, **105**, 4018.
1061 K. Doll, *Surf. Sci.*, 2004, **573**, 464.
1062 M. Neef and K. Doll, *Surf. Sci.*, 2006, **600**, 1085.
1063 Y. Wang, S. de Gironcoli, N. S. Hush and J. R. Reimers, *J. Am. Chem. Soc.*, 2007, **129**, 10402.
1064 I. Dabo, A. Wieckowski and N. Marzari, *J. Am. Chem. Soc.*, 2007, **129**, 11045.
1065 T. Zhang, Z.-P. Liu, S. M. Driver, S. J. Pratt, S. J. Jenkins and D. A. King, *Phys. Rev. Lett.*, 2005, **95**, 266102.
1066 J. M. H. Lo and T. Ziegler, *J. Phys. Chem. C*, 2008, **112**, 3679.
1067 D. E. Jiang and E. A. Carter, *Surf. Sci.*, 2004, **570**, 167.
1068 J. M. H. Lo and T. Ziegler, *J. Phys. Chem. C*, 2008, **112**, 3692.
1069 J. M. H. Lo and T. Ziegler, *J. Phys. Chem. C*, 2007, **111**, 13149.
1070 A. Valcárcel, A. Clotet, J. M. Ricart and F. Illas, *Chem. Phys.*, 2005, **309**, 33.
1071 Y. Wang, N. S. Hush and J. R. Reimers, *J. Phys. Chem. C*, 2007, **111**, 10878.
1072 Y. Wang, N. S. Hush and J. R. Reimers, *J. Am. Chem. Soc.*, 2007, **129**, 14532.
1073 Y. Wang, N. S. Hush and J. R. Reimers, *Phys. Rev. B: Condens. Matter Mater. Phys.*, 2007, **75**, 233416.
1074 S. Y. Quek, M. M. Biener, J. Biener, J. Bhattacharjee, C. M. Friend, U. V. Waghmare and E. Kaxiras, *J. Phys. Chem. B*, 2006, **110**, 15663.
1075 W. Gao, T. A. Baker, L. Zhou, D. S. Pinnaduwage, E. Kaxiras and C. M. Friend, *J. Am. Chem. Soc.*, 2008, **130**, 3560.
1076 T. A. Baker, C. M. Friend and E. Kaxiras, *J. Chem. Phys.*, 2008, **129**, 104702.
1077 L. D. Marks, A. N. Chiaramonti, F. Tran and P. Blaha, *Surf. Sci.*, 2009, **603**, 2179.
1078 Y. Mao, J. Yuan and J. Zhang, *J. Phys.: Condens. Matter*, 2008, **20**, 115209.
1079 N. Kuganathan and J. C. Green, *Chem. Commun.*, 2008, 2432.
1080 E. L. Sceats and J. C. Green, *Phys. Rev. B: Condens. Matter Mater. Phys.*, 2007, **75**, 245441.
1081 S. Y. Quek, M. M. Biener, J. Biener, C. M. Friend and E. Kaxiras, *Surf. Sci.*, 2005, **577**, L71.
1082 D. E. Jiang and E. A. Carter, *Surf. Sci.*, 2005, **583**, 60.
1083 D. E. Jiang and E. A. Carter, *J. Phys. Chem. B*, 2005, **109**, 20469.
1084 D. E. Jiang and E. A. Carter, *J. Phys. Chem. B*, 2006, **110**, 22213.
1085 M. J. S. Spencer, I. K. Snook and I. Yarovsky, *J. Phys. Chem. B*, 2004, **108**, 10965.
1086 M. J. S. Spencer, I. K. Snook and I. Yarovsky, *J. Phys. Chem. B*, 2005, **109**, 9604.
1087 M. J. S. Spencer, I. K. Snook and I. Yarovsky, *J. Phys. Chem. B*, 2005, **109**, 10204.
1088 M. J. S. Spencer, I. K. Snook and I. Yarovsky, *J. Phys. Chem. B*, 2006, **110**, 956.
1089 S. G. Nelson, M. J. S. Spencer, I. K. Snook and I. Yarovsky, *Surf. Sci.*, 2005, **590**, 63.

1090 N. Todorova, M. J. S. Spencer and I. Yarovsky, *Surf. Sci.*, 2007, **601**, 665.
1091 D. F. Johnson, D. E. Jiang and E. A. Carter, *Surf. Sci.*, 2007, **601**, 699.
1092 M. J. S. Spencer and I. Yarovsky, *J. Phys. Chem. C*, 2007, **111**, 16372.
1093 M. J. S. Spencer, N. Todorova and I. Yarovsky, *Surf. Sci.*, 2008, **602**, 1547.
1094 Y. Kurzweil and R. Baer, *Phys. Rev. B: Condens. Matter Mater. Phys.*, 2006, **73**, 075413.
1095 R. Ferrando, J. Jellinek and R. L. Johnston, *Chem. Rev.*, 2008, **108**, 845.
1096 X. Y. Zhu, G. Dutton, D. P. Quinn, C. D. Lindstrom, N. E. Schultz and D. G. Truhlar, *Phys. Rev. B: Condens. Matter Mater. Phys.*, 2006, **74**, 241401.
1097 B. Li, J. Zhao, K. Onda, K. D. Jordan, J. Yang and H. Petek, *Science*, 2006, **311**, 1436.
1098 M. Feng, J. Zhao and H. Petek, *Science*, 2008, **320**, 359.
1099 Y. Pavlyukh and J. Berakdar, *Chem. Phys. Lett.*, 2009, **468**, 313.
1100 W. T. Geng, J. Nara and T. Ohno, *Thin Solid Films*, 2004, **464–465**, 379.
1101 P. A. Derosa, A. G. Zacarias and J. M. Seminario, in *Reviews of Modern Quantum Chemistry*, ed. K. D. Sen, World Scientific, Singapore, 2002, p. 1537.
1102 Z. A. Schelly, *Colloids Surf., B*, 2007, **56**, 281.
1103 M. Walter, P. Frondelius, K. Honkala and H. Hakkinen, *Phys. Rev. Lett.*, 2007, **99**, 096102.
1104 E. Badaeva, Y. Feng, D. R. Gamelin and X. Li, *New J. Phys.*, 2008, **10**, 055013.
1105 H. Zeng, R. R. Vanga, D. S. Marynick and Z. A. Schelly, *J. Phys. Chem. B*, 2008, **112**, 14422.
1106 I. V. Yudanov, K. M. Neyman and N. Rösch, *Phys. Chem. Chem. Phys.*, 2004, **6**, 116.
1107 K. M. Neyman, G. N. Vayssilov and N. Rösch, *J. Organomet. Chem.*, 2004, **689**, 4384.
1108 H. Grönbeck and P. Broqvist, *Phys. Rev. B: Condens. Matter Mater. Phys.*, 2005, **71**, 073408.
1109 L. M. Liu, B. McAllister, H. Q. Ye and P. Hu, *J. Am. Chem. Soc.*, 2006, **128**, 4017.
1110 E. A. Ivanova Shor, V. A. Nasluzov, A. M. Shor, G. N. Vayssilov and N. Rösch, *J. Phys. Chem. C*, 2007, **111**, 12340.
1111 M. Yang, K. A. Jackson and J. Jellinek, *J. Chem. Phys.*, 2006, **125**, 144308.
1112 F. Cinquini, L. Giordano, G. Pacchioni, A. M. Ferrari, C. Pisani and C. Roetti, *Phys. Rev. B: Condens. Matter Mater. Phys.*, 2006, **74**, 165403.
1113 S. K. Brayshaw, J. C. Green, N. Hazasi and A. S. Weller, *Dalton Trans.*, 2007, 1781.
1114 M. Castro, *Chem. Phys. Lett.*, 2007, **435**, 322.
1115 M. Baron, D. Stacchiola, S. Ulrich, N. Nilius, S. Shaikhutdinov, H. J. Freund, U. Martinez, L. Giordano and G. Pacchioni, *J. Phys. Chem. C*, 2008, **112**, 3405.
1116 G. Pacchioni, S. Sicolo, C. D. Valentin, M. Chiesa and E. Giamello, *J. Am. Chem. Soc.*, 2008, **130**, 8690.
1117 D. Bandyopadhyay, *J. Appl. Phys.*, 2008, **104**, 084308.
1118 D. Bandyopadhyay and M. Kumar, *Chem. Phys.*, 2008, **353**, 170.
1119 S. Alayoglu, A. V. Nilekar, M. Mavrikakis and B. Eichhorn, *Nat. Mater.*, 2008, **7**, 333.
1120 V. Simic-Milosevic, M. Heyde, N. Nilius, T. KoÃànig, H. P. Rust, M. Sterrer, T. Risse, H. J. Freund, L. Giordano and G. Pacchioni, *J. Am. Chem. Soc.*, 2008, **130**, 7814.
1121 H.-J. Freund and G. Pacchioni, *Chem. Soc. Rev.*, 2008, **37**, 2224.
1122 L. C. Grabow and M. Mavrikakis, *Angew. Chem., Int. Ed.*, 2008, **47**, 7390.
1123 M. Gruber, G. Heimel, L. Romaner, J.-L. Bredas and E. Zojer, *Phys. Rev. B: Condens. Matter Mater. Phys.*, 2008, **77**, 165411.
1124 H. Grönbeck, *Top. Catal.*, 2004, **28**, 59.
1125 C. R. A. Catlow, S. A. French, A. A. Sokol and J. M. Thomas, *Philos. Trans. R. Soc. London, Ser. A*, 2005, **363**, 913.
1126 F. Cinquini, C. Valentin, E. Finazzi, L. Giordano and G. Pacchioni, *Theor. Chem. Acc.*, 2007, **117**, 827.
1127 J. N. Nørskov, M. Scheffler and H. Toulhoat, *MRS Bull.*, 2006, **31**, 669.
1128 J. K. Nørskov, T. Bligaard, B. Hvolbaek, F. Abild-Pedersen, I. Chorkendorff and C. H. Christensen, *Chem. Soc. Rev.*, 2008, **37**, 2163.
1129 K. M. Neyman and F. Illas, *Catal. Today*, 2005, **105**, 2.
1130 R. Coquet, K. L. Howard and D. J. Willock, *Chem. Soc. Rev.*, 2008, **37**, 2046.
1131 G. A. Somorjai and J. Y. Park, *Angew. Chem., Int. Ed.*, 2008, **47**, 9212.
1132 H. Falsig, B. Hvolbaek, I. S. Kristensen, T. Jiang, T. Bligaard, C. H. Christensen and J. K. Nørskov, *Angew. Chem., Int. Ed.*, 2008, **47**, 4835.
1133 G. Lanzani, R. Martinazzo, G. Materzanini, I. Pino and G. Tantardini, *Theor. Chem. Acc.*, 2007, **117**, 805.
1134 B. Kasemo, E. Tornqvist, J. K. Nørskov and B. I. Lundqvist, *Surf. Sci.*, 1979, **89**, 554.
1135 M. Persson and B. Hellsing, *Phys. Rev. Lett.*, 1982, **49**, 662.
1136 S. E. Wonchoba, W.-P. Hu and D. G. Truhlar, in *Theoretical and Computational Approaches to Interface Phenomena*, ed. H. L. Sellers and J. T. Golab, Plenum, New York, 1994, p. 1.
1137 J. T. Kindt, J. C. Tully, M. Head-Gordon and M. A. Gomez, *J. Chem. Phys.*, 1998, **109**, 3629.
1138 H. Nienhaus, H. S. Bergh, B. Gergen, A. Majumdar, W. H. Weinberg and E. W. McFarland, *Phys. Rev. Lett.*, 1999, **82**, 446.
1139 J. C. Tully, *Annu. Rev. Phys. Chem.*, 2000, **51**, 153.
1140 B. Gergen, H. Nienhaus, W. H. Weinberg and E. W. McFarland, *Science*, 2001, **294**, 2521.
1141 H. Nienhaus, *Surf. Sci. Rep.*, 2002, **45**, 1.
1142 J. W. Gadzuk, *J. Phys. Chem. B*, 2002, **106**, 8265.
1143 J. R. Trail, M. C. Graham, D. M. Bird, M. Persson and S. Holloway, *Phys. Rev. Lett.*, 2002, **88**, 166802.
1144 G. Katz, R. Kosloff and Y. Zeiri, *J. Chem. Phys.*, 2004, **120**, 3931.
1145 X. Z. Ji and G. A. Somorjai, *J. Phys. Chem. B*, 2005, **109**, 22530.
1146 J. Behler, B. Delley, S. Lorenz, K. Reuter and M. Scheffler, *Phys. Rev. Lett.*, 2005, **94**, 036104.
1147 P. Nieto, E. Pijper, D. Barredo, G. Laurent, R. A. Olsen, E.-J. Baerends, G.-J. Kroes and D. Farias, *Science*, 2006, **312**, 86.
1148 A. C. Luntz, M. Persson and G. O. Sitz, *J. Chem. Phys.*, 2006, **124**, 091101.
1149 N. Shenvi, S. Roy, P. Parandekar and J. Tully, *J. Chem. Phys.*, 2006, **125**, 154703.
1150 M. Lindenblatt and E. Pehlke, *Phys. Rev. Lett.*, 2006, **97**, 216101.
1151 D. Krix, R. Nunthel and H. Nienhaus, *Phys. Rev. B: Condens. Matter Mater. Phys.*, 2007, **75**, 073410.
1152 I. Rahinov, R. Cooper, C. Yuan, X. Yang, D. J. Auerbach and A. M. Wodtke, *J. Chem. Phys.*, 2008, **129**, 214708.
1153 N. H. Nahler, J. D. White, J. LaRue, D. J. Auerbach and A. M. Wodtke, *Science*, 2008, **321**, 1191.
1154 D. M. Bird, M. S. Mizielinski, M. Lindenblatt and E. Pehlke, *Surf. Sci.*, 2008, **602**, 1212.
1155 M. Tomellini, *J. Phys.: Condens. Matter*, 2008, **20**, 135002.
1156 J. I. Juaristi, M. Alducin, R. D. Muino, H. F. Busnengo and A. Salin, *Phys. Rev. Lett.*, 2008, **100**, 116102.
1157 R. Cooper, I. Rahinov, C. Yuan, X. Yang, D. J. Auerbach and A. M. Wodtke, *J. Vac. Sci. Technol., A*, 2009, **27**, 907.
1158 S. N. Maximoff and M. P. Head-Gordon, *Proc. Natl. Acad. Sci. U. S. A.*, 2009, **106**, 11460.
1159 N. Shenvi, S. Roy and J. C. Tully, *J. Chem. Phys.*, 2009, **130**, 174107.
1160 M. Timmer and P. Kratzer, *Phys. Rev. B: Condens. Matter Mater. Phys.*, 2009, **79**, 165407.
1161 K. Honkala, A. Hellman, I. N. Remediakis, A. Logadottir, A. Carlsson, S. Dahl, C. H. Christensen and J. K. Nørskov, *Science*, 2005, **307**, 555.
1162 A. Hellman, E. J. Baerends, M. Biczysko, T. Bligaard, C. H. Christensen, D. C. Clary, S. Dahl, R. van Harrevelt, K. Honkala, H. Jonsson, G. J. Kroes, M. Luppi, U. Manthe, J. K. Nørskov, R. A. Olsen, J. Rossmeisl, E. Skulason, C. S. Tautermann, A. J. C. Varandas and J. K. Vincent, *J. Phys. Chem. B*, 2006, **110**, 17719.

1163 C. S. Tautermann, Y. K. Sturdy and D. C. Clary, *J. Catal*., 2006, **244**, 199; C. S. Tautermann and D. C. Clary, *Phys. Chem. Chem. Phys*., 2006, **8**, 1437.
1164 Z.-P. Liu, S. J. Jenkins and D. A. King, *J. Am. Chem. Soc*., 2004, **126**, 10746.
1165 J. K. Vincent, R. A. Olsen, G.-J. Kroes, M. Luppi and E.-J. Baerends, *J. Chem. Phys*., 2005, **122**, 044701.
1166 C. Crespos, H. D. Meyer, R. C. Mowrey and G. J. Kroes, *J. Chem. Phys*., 2006, **124**, 074706.
1167 H. L. Abbott and I. Harrison, *J. Chem. Phys*., 2006, **125**, 024704.
1168 G. J. Kroes, E. Pijper and A. Salin, *J. Chem. Phys*., 2007, **127**, 164722.
1169 I. M. N. Groot, H. Ueta, M. J. T. C. van der Niet, A. W. Kleyn and L. B. F. Juurlink, *J. Chem. Phys*., 2007, **127**, 244701.
1170 H. F. Busnengo and A. E. Martinez, *J. Phys. Chem. C*, 2008, **112**, 5579.
1171 R. A. Olsen, D. A. McCormack, M. Luppi and E. J. Baerends, *J. Chem. Phys*., 2008, **128**, 194715.
1172 A. C. Luntz, *Surf. Sci*., 2009, **603**, 1557.
1173 R. Valero, J. R. B. Gomes, D. G. Truhlar and F. Illas, *J. Chem. Phys*., 2008, **129**, 124710.
1174 C. Di Valentin, G. Pacchioni, T. Bredow, D. Dominguez-Ariza and F. Illas, *J. Chem. Phys*., 2002, **117**, 2299.
1175 D. Dominguez-Ariza, F. Illas, T. Bredow, C. D. Valentin and G. Pacchioni, *Mol. Phys*., 2003, **101**, 241.
1176 M. Chiesa, M. C. Paganini, E. Giamello, C. D. Valentin and G. Pacchioni, *J. Mol. Catal. A: Chem*., 2003, **204–205**, 779.
1177 G. Pacchioni, C. D. Valentin, D. Dominguez-Ariza, F. Illas, T. Bredow, T. Kluner and V. Staemmler, *J. Phys.: Condens. Matter*, 2004, **16**, S2497.
1178 A. Scagnelli, C. D. Valentin and G. Pacchioni, *Surf. Sci*., 2006, **600**, 386.
1179 A. Rohrbach and J. Hafner, *Phys. Rev. B: Condens. Matter Mater. Phys*., 2005, **71**, 045405.
1180 R. Valero, J. R. B. Gomes, D. G. Truhlar and F. Illas, to be published.
1181 N. Hansen, A. Heyden, A. T. Bell and F. J. Keil, *J. Phys. Chem. C*, 2007, **111**, 2092.
1182 A. Heyden, B. Peters, A. T. Bell and F. J. Keil, *J. Phys. Chem. B*, 2005, **109**, 1857.
1183 A. Heyden, N. Hansen, A. T. Bell and F. J. Keil, *J. Phys. Chem. B*, 2006, **110**, 17096.
1184 A. Goodrow and A. T. Bell, *J. Phys. Chem. C*, 2008, **112**, 13204.
1185 J. Bonde, P. G. Moses, T. F. Jaramillo, J. K. Nørskov and I. Chorkendorff, *Faraday Discuss*., 2009, **140**, 219.
1186 A. A. Gokhale, J. A. Dumesic and M. Mavrikakis, *J. Am. Chem. Soc*., 2008, **130**, 1402.
1187 M. P. Andersson, F. Abild-Pedersen, I. N. Remediakis, T. Bligaard, G. Jones, J. Engbaek, O. Lytken, S. Horch, J. H. Nielsen, J. Sehested, J. R. Rostrup-Nielsen, J. K. Nørskov and I. Chorkendorff, *J. Catal*., 2008, **255**, 6.
1188 Y. Xu, W. A. Shelton and W. F. Schneider, *J. Phys. Chem. B*, 2006, **110**, 16591.
1189 R. B. Getman and W. F. Schneider, *J. Phys. Chem. C*, 2007, **111**, 389.
1190 R. B. Getman, Y. Xu and W. F. Schneider, *J. Phys. Chem. C*, 2008, **112**, 9559.
1191 A. D. Smeltz, R. B. Getman, W. F. Schneider and F. H. Ribeiro, *Catal. Today*, 2008, **136**, 84.
1192 Y. Xu, R. B. Getman, W. A. Shelton and W. F. Schneider, *Phys. Chem. Chem. Phys*., 2008, **10**, 6009.
1193 H. Y. Wang and W. F. Schneider, *J. Chem. Phys*., 2007, **127**, 064706.
1194 Z.-X. Chen, K. M. Neyman, K. H. Lim and N. Rösch, *Langmuir*, 2004, **20**, 8068.
1195 Z.-X. Chen, K. H. Lim, K. M. Neyman and N. Rösch, *J. Phys. Chem. B*, 2005, **109**, 4568.
1196 K. H. Lim, Z.-X. Chen, K. M. Neyman and N. Rösch, *J. Phys. Chem. B*, 2006, **110**, 14890.
1197 K. H. Lim, L. V. Moskaleva and N. Rösch, *ChemPhysChem*, 2006, **7**, 1802.
1198 Y. Cao and Z.-X. Chen, *Surf. Sci*., 2006, **600**, 4572.
1199 Q.-L. Tang and Z.-X. Chen, *J. Chem. Phys*., 2007, **127**, 104707.
1200 X. Li, A. J. Gellman and D. S. Sholl, *J. Chem. Phys*., 2007, **127**, 144710.
1201 G. Pacchioni, http://pubs.acs.org/JACSbeta/issue3.html, accessed Jan. 16, 2009.
1202 A. S. Y. Foo and K. H. Lim, *Catal. Lett*., 2009, **127**, 113.
1203 E. Jeroro and J. M. Vohs, *J. Am. Chem. Soc*., 2008, **130**, 10199.
1204 H. Tang and B. L. Trout, *J. Phys. Chem. B*, 2006, **110**, 6856.
1205 A. T. Anghel, D. J. Wales, S. J. Jenkins and D. A. King, *Phys. Rev. B: Condens. Matter Mater. Phys*., 2005, **71**, 113410.
1206 S. E. Wonchoba and D. G. Truhlar, *J. Phys. Chem. B*, 1998, **102**, 6842.
1207 H. Yang and J. L. Whitten, *J. Chem. Phys*., 1992, **96**, 5529.
1208 P. Kratzer, B. Hammer and J. K. Nørskov, *J. Chem. Phys*., 1996, **105**, 5595.
1209 S. Nave and B. Jackson, *J. Chem. Phys*., 2007, **127**, 224702.
1210 S. Nave and B. Jackson, *Phys. Rev. Lett*., 2007, **98**, 173003.
1211 S. Nave and B. Jackson, *J. Chem. Phys*., 2009, **130**, 054701.
1212 W. Z. Lai, D. Q. Xie and D. H. Zhang, *Surf. Sci*., 2005, **594**, 83.
1213 M.-S. Liao, C.-T. Au and C.-F. Ng, *Chem. Phys. Lett*., 1997, **272**, 445.
1214 G. Psofogiannakis, A. St-Amant and M. Ternan, *J. Phys. Chem. B*, 2006, **110**, 24593.
1215 H.-Y. Li, Y.-L. Guo, Y. Guo, G.-Z. Lu and P. Hu, *J. Chem. Phys*., 2008, **128**, 051101.
1216 F. Abild-Pedersen, J. Greeley, F. Studt, J. Rossmeisl, T. R. Munter, P. G. Moses, E. Skulason, T. Bligaard and J. K. Nørskov, *Phys. Rev. Lett*., 2007, **99**, 016105.
1217 N. N. Semenov, *Some Problems in Chemical Kinetics and Reactivity*, Princeton University Press, Princeton, NJ, 1958.
1218 M. G. Evans and M. Polanyi, *Trans. Faraday Soc*., 1938, **34**, 11.
1219 F. Studt, F. Abild-Pedersen, T. Bligaard, R. Z. Sørensen, C. H. Christensen and J. K. Nørskov, *Science*, 2008, **320**, 1320.
1220 F. Studt, F. Abild-Pedersen, T. Bligaard, R. Z. Sørensen, C. H. Christensen and J. K. Nørskov, *Angew. Chem., Int. Ed*., 2008, **47**, 9299.
1221 G. Jones, J. G. Jakobsen, S. S. Shim, J. Kleis, M. P. Andersson, J. Rossmeisl, F. Abild-Pedersen, T. Bligaard, S. Helveg, B. Hinnemann, J. R. Rostrup-Nielsen, I. Chorkendorff, J. Sehested and J. K. Nørskov, *J. Catal*., 2008, **259**, 147.
1222 J. Cheng and P. Hu, *J. Am. Chem. Soc*., 2008, **130**, 10868.
1223 J. Cheng, P. Hu, P. Ellis, S. French, G. Kelly and C. M. Lok, *J. Phys. Chem. C*, 2008, **112**, 6082.
1224 J. Cheng, P. Hu, P. Ellis, S. French, G. Kelly and C. M. Lok, *J. Catal*., 2008, **257**, 221.
1225 M. Saeys, M. F. Reyniers, M. Neurock and G. B. Marin, *J. Phys. Chem. B*, 2005, **109**, 2064.
1226 D. M. Bird, *Faraday Discuss*., 1998, **110**, 335.
1227 D. G. Truhlar, *Faraday Discuss*., 1998, **110**, 521.
1228 F. Labat, P. Baranek, C. Domain, C. Minot and C. Adamo, *J. Chem. Phys*., 2007, **126**, 154703.
1229 F. Labat, P. Baranek and C. Adamo, *J. Chem. Theory Comput*., 2008, **4**, 341.
1230 S. Choomwattana, T. Maihom, P. Khongpracha, M. Probst and J. Limtrakul, *J. Phys. Chem. C*, 2008, **112**, 10855.
1231 A. Kuc, T. Heine, G. Seifert and H. Duarte, *Theor. Chem. Acc*., 2008, **120**, 543.
1232 F. Abild-Pedersen, O. Lytken, J. Engbaek, G. Nielsen, I. Chorkendorff and J. K. Nørskov, *Surf. Sci*., 2005, **590**, 127.
1233 J. Zhang, M. B. Vukmirovic, Y. Xu, M. Mavrikakis and R. R. Adzic, *Angew. Chem., Int. Ed*., 2005, **44**, 2132.
1234 S. Kandol and J. Greeley, *Catal. Today*, 2006, **111**, 52.
1235 A. Kokalj, N. Bonini, S. de Gironcoli, C. Sbraccia, G. Fratesi and S. Baroni, *J. Am. Chem. Soc*., 2006, **128**, 12448.
1236 D. Torres, S. Gonz·lez, K. M. Neyman and F. Illas, *Chem. Phys. Lett*., 2006, **422**, 412.
1237 D. Loffreda, F. Delbecq, F. Vigne and P. Sautet, *J. Am. Chem. Soc*., 2006, **128**, 1316.
1238 C. Morin, D. Simon and P. Sautet, *Surf. Sci*., 2006, **600**, 1339.
1239 M. C. Valero, P. Raybaud and P. Sautet, *J. Phys. Chem. B*, 2006, **110**, 1759.
1240 A. Salameh, J. Joubert, A. Baudouin, W. Lukens, F. Delbecq, P. Sautet, J. M. Basset and C. Coperet, *Angew. Chem., Int. Ed*., 2007, **46**, 3870.
1241 Z. Gu and P. B. Balbuena, *J. Phys. Chem. C*, 2007, **111**, 17388.
1242 S. Sharifzadeh, P. Huang and E. Carter, *J. Phys. Chem. C*, 2008, **112**, 4649.
1243 Z. Gu and P. B. Balbuena, *J. Phys. Chem. C*, 2008, **112**, 5057.

1244 Y. Pluntke, L. A. Kibler and D. M. Kolb, *Phys. Chem. Chem. Phys.*, 2008, **10**, 3684.
1245 Y. Ma and P. B. Balbuena, *J. Phys. Chem. C*, 2008, **112**, 14520.
1246 J. R. Croy, S. Mostafa, L. Hickman, H. Heinrich and B. R. Cuenya, *Appl. Catal., A*, 2008, **350**, 207.
1247 F. o. Delbecq and F. Zaera, *J. Am. Chem. Soc.*, 2008, **130**, 14924.
1248 R. Callejas-Tovar and P. B. Balbuena, *Surf. Sci.*, 2008, **602**, 3531.
1249 F. Tian and A. B. Anderson, *J. Phys. Chem. C*, 2008, **112**, 18566.
1250 Y. Gilman, P. B. Allen and M. S. Hybertsen, *J. Phys. Chem. C*, 2008, **112**, 3314.
1251 K.-i. Aika, Y. Ogata, K. Takeishi, K. Urabe and T. Onishi, *J. Catal.*, 1988, **114**, 200.
1252 C. G. M. Hermse, A. P. van Bavel, A. P. J. Jansen, L. A. M. M. Barbosa, P. Sautet and R. A. van Santen, *J. Phys. Chem. B*, 2004, **108**, 11035.
1253 S. Kandoi, J. Greeley, M. Sanchez-Castillo, S. Evans, A. Gokhale, J. Dumesic and M. Mavrikakis, *Top. Catal.*, 2006, **37**, 17.
1254 J. Greeley and M. Mavrikakis, *J. Am. Chem. Soc.*, 2004, **126**, 3910.
1255 K. Reuter, D. Frenkel and M. Scheffler, *Phys. Rev. Lett.*, 2004, **93**, 116105.
1256 L. D. Kieken, M. Neurock and D. Mei, *J. Phys. Chem. B*, 2005, **109**, 2234.
1257 A. B. Mhadeshwar and D. G. Vlachos, *J. Phys. Chem. B*, 2005, **109**, 16819.
1258 P. Raybaud, *Appl. Catal., A*, 2007, **322**, 76.
1259 B. Temel, H. Meskine, K. Reuter, M. Scheffler and H. Metiu, *J. Chem. Phys.*, 2007, **126**, 204711.
1260 O. R. Inderwildi, S. J. Jenkins and D. A. King, *J. Am. Chem. Soc.*, 2007, **129**, 1751.
1261 H. Falsig, T. Bligaard, J. Rass-Hansen, A. Kustov, C. Christensen and J. Nørskov, *Top. Catal.*, 2007, **45**, 117.
1262 O. R. Inderwildi, S. J. Jenkins and D. A. King, *J. Am. Chem. Soc.*, 2008, **130**, 2213.
1263 N. V. Petrova and I. N. Yakovkin, *Eur. Phys. J. B*, 2008, **63**, 17.
1264 J. Assmann, V. Narkhede, N. A. Breuer, M. Muhler, A. P. Seitsonen, M. Knapp, D. Crihan, A. Farkas, G. Mellau and H. Over, *J. Phys.: Condens. Matter*, 2008, **20**, 184017.
1265 J. Rogal, K. Reuter and M. Scheffler, *Phys. Rev. B: Condens. Matter Mater. Phys.*, 2008, **77**, 155410.
1266 M. Rieger, J. Rogal and K. Reuter, *Phys. Rev. Lett.*, 2008, **100**, 016105.
1267 G. Pacchioni, *Nat. Mater.*, 2009, **8**, 167.
1268 S. Vajda, M. J. Pellin, J. P. Greeley, C. L. Marshall, L. A. Curtiss, G. A. Ballentine, J. W. Elam, S. Catillon-Mucherie, P. C. Redfern, F. Mehmood and P. Zapol, *Nat. Mater.*, 2009, **8**, 213.
1269 J. Tao, J. P. Perdew, L. M. Almeida, C. Fiolhais and S. Kummel, *Phys. Rev. B: Condens. Matter Mater. Phys.*, 2008, **77**, 245107.
1270 J. Rossmeisl, J. K. Nørskov, C. D. Taylor, M. J. Janik and M. Neurock, *J. Phys. Chem. B*, 2006, **110**, 21833.
1271 V. Stamenkovic, B. S. Mun, K. J. J. Mayrhofer, P. N. Ross, N. M. Markovic, J. Rossmeisl, J. Greeley and J. K. Nørskov, *Angew. Chem., Int. Ed.*, 2006, **45**, 2897.
1272 E. Skulason, G. S. Karlberg, J. Rossmeisl, T. Bligaard, J. Greeley, H. Jonsson and J. K. Nørskov, *Phys. Chem. Chem. Phys.*, 2007, **9**, 3241.
1273 G. S. Karlberg, T. F. Jaramillo, E. Skulason, J. Rossmeisl, T. Bligaard and J. K. Nørskov, *Phys. Rev. Lett.*, 2007, **99**, 126101.
1274 M. B. Vukmirovic, J. Zhang, K. Sasaki, A. U. Nilekar, F. Uribe, M. Mavrikakis and R. R. Adzic, *Electrochim. Acta*, 2007, **52**, 2257.
1275 A. Nilekar, Y. Xu, J. Zhang, M. Vukmirovic, K. Sasaki, R. Adzic and M. Mavrikakis, *Top. Catal.*, 2007, **46**, 276.
1276 M. Janik, C. Taylor and M. Neurock, *Top. Catal.*, 2007, **46**, 306.
1277 L. L. Wang and D. D. Johnson, *J. Phys. Chem. C*, 2008, **112**, 8266.
1278 P. Ferrin, A. U. Nilekar, J. Greeley, M. Mavrikakis and J. Rossmeisl, *Surf. Sci.*, 2008, **602**, 3424.
1279 M. Subhramannia and V. K. Pillai, *J. Mater. Chem.*, 2008, **18**, 5858.
1280 Y. Gohda, S. Schnur and A. Groß, *Faraday Discuss.*, 2009, **140**, 233.
1281 M. T. M. Koper, *Faraday Discuss.*, 2009, **140**, 11.
1282 D. J. Schiffrin, *Faraday Discuss.*, 2009, **140**, 439.
1283 F. De Angelis, A. Tilocca and A. Selloni, *J. Am. Chem. Soc.*, 2004, **126**, 15024.
1284 C. Di Valentin, E. Finazzi, G. Pacchioni, A. Selloni, S. Livraghi, A. M. Czoska, M. C. Paganini and E. Giamello, *Chem. Mater.*, 2008, **20**, 3706.
1285 A. M. Czoska, S. Livraghi, M. Chiesa, E. Giamello, S. Agnoli, G. Granozzi, E. Finazzi, C. D. Valentin and G. Pacchioni, *J. Phys. Chem. C*, 2008, **112**, 8951.
1286 K. Yang, Y. Dai, B. Huang and M.-H. Whangbo, *Chem. Mater.*, 2008, **20**, 6528.
1287 C. Di Valentin, G. Pacchioni, H. Onishi and A. Kudo, *Chem. Phys. Lett.*, 2009, **469**, 166.
1288 X. Chen and S. S. Mao, *Chem. Rev.*, 2007, **107**, 2891.
1289 J. Zhao, B. Li, K. D. Jordan, J. Yang and H. Petek, *Phys. Rev. B: Condens. Matter Mater. Phys.*, 2006, **73**, 195309.
1290 A. Vittadini, M. Casarin and A. Selloni, *Theor. Chem. Acc.*, 2007, **117**, 663.
1291 L. K. Dash, F. Bruneval, V. Trinite, N. Vast and L. Reining, *Comput. Mater. Sci.*, 2007, **38**, 482.
1292 G. Teobaldi, W. A. Hofer, O. Bikondoa, C. L. Pang, G. Cabailh and G. Thornton, *Chem. Phys. Lett.*, 2007, **437**, 73.
1293 W. R. Duncan, C. F. Craig and O. V. Prezhdo, *J. Am. Chem. Soc.*, 2007, **129**, 8528.
1294 K. Yang, Y. Dai and B. Huang, *Chem. Phys. Lett.*, 2008, **456**, 71.
1295 W. R. Duncan and O. V. Prezhdo, *J. Am. Chem. Soc.*, 2008, **130**, 9756.
1296 J. Graciani, L. J. Alvarez, J. A. Rodriguez and J. F. Sanz, *J. Phys. Chem. C*, 2008, **112**, 2624.
1297 P. R. McGill and H. Idriss, *Surf. Sci.*, 2008, **602**, 3688.
1298 D. P. Hagberg, J.-H. Yum, H. Lee, F. De Angelis, T. Marinado, K. M. Karlsson, R. Humphry-Baker, L. Sun, A. Hagfeldt, M. Grätzel and M. K. Nazeeruddin, *J. Am. Chem. Soc.*, 2008, **130**, 6259.
1299 A. Vittadini and M. Casarin, *Theor. Chem. Acc.*, 2008, **120**, 551.
1300 T. Marinado, D. P. Hagberg, M. Hedlund, T. Edvinsson, E. M. J. Johansson, G. Boschloo, H. Rensmo, T. Brinck, L. C. Sun and A. Hagfeldt, *Phys. Chem. Chem. Phys.*, 2009, **11**, 133.
1301 H. Perron, C. Domain, J. Roques, R. Drot, E. Simoni and H. Catalette, *Theor. Chem. Acc.*, 2007, **117**, 565.
1302 S. Li and D. A. Dixon, *J. Phys. Chem. A*, 2008, **112**, 6646.
1303 P. Zapol and L. A. Curtiss, *J. Comput. Theor. Nanosci.*, 2007, **4**, 222.
1304 G. Shao, *J. Phys. Chem. C*, 2008, **112**, 18677.
1305 X.-Q. Gong, A. Selloni, O. Dulub, P. Jacobson and U. Diebold, *J. Am. Chem. Soc.*, 2008, **130**, 370.
1306 J. Zhang, M. Zhang, Y. Han, W. Li, X. Meng and B. Zong, *J. Phys. Chem. C*, 2008, **112**, 19506.
1307 H. Nakamura and K. Yamashita, *J. Chem. Phys.*, 2005, **122**, 194706.

